SYNTHESIS, CHARACTERIZATION, STRUCTURE AND BIOLOGICAL APPLICATIONS OF ORGANOTIN(IV) COMPLEXES OF 5-[(*E*)-2-(ARYL)-1-DIAZENYL]QUINOLIN-8-OL

A THESIS SUBMITTED IN PARTIAL FULFILMENT OF THE REQUIREMENTS FOR THE DEGREE OF DOCTOR OF PHILOSOPHY

BY

ARCHANA MIZAR

DEPARTMENT OF CHEMISTRY

SCHOOL OF PHYSICAL SCIENCES

NORTH-EASTERN HILL UNIVERSITY

SHILLONG-793022

2009

DEDICATED

TO

MY PARENTS,

BROTHERS & SISTERS

DEPARTMENT OF CHEMISTRY

NORTH-EASTERN HILL UNIVERSITY, NEHU PERMANENT CAMPUS, UMSHING
SHILLONG 793 022 (INDIA)

CERTIFICATE

This is to certify that the research work presented in the thesis entitled "Synthesis, Characterization, Structure and Biological Applications of Organotin(IV) Complexes of 5-[(*E*)-2-(aryl)-1-diazenyl]quinolin-8-ol" is carried out by Miss Archana Mizar under the Department of Chemistry, School of Physical Sciences, North-Eastern Hill University, Shillong. The work embodied in the thesis does not form the basis for the award of any previous degree, diploma, fellowship or any other similar title and that it represents entirely an independent work on the part of the candidate.

Dr. B. Myrboh

Professor and Head
Department of Chemistry
North-Eastern Hill University
Shillong 793 022

Head
Department of Chemistry
North-Eastern Hill University
Shillong- 793022.

Date: 4/06/2009

Place: Shillong

S. Ba.

Chemistry.

DECLARATION

I hereby, declare that the thesis entitled "Synthesis, Characterization, Structure and Biological Applications of Organotin(IV) Complexes of 5-[(*E*)-2-(aryl)-1-diazenyl]quinolin-8-ol" is the result of the work carried out by me under the supervision of Dr. T. S. Basu Baul, Department of Chemistry, School of Physical Sciences, North-Eastern Hill University, Shillong for the award of Doctor of Philosophy in Chemistry. The contents of the thesis did not form the basis of the award of any previous degree to me or to anybody else. The work presented in the thesis is original and the outcome of some useful results has been published in the international journals.

To the best of my knowledge the thesis has not been submitted for any degree to this university or any other university.

Archana Mizar

Archana Mizar

Department of Chemistry
North Eastern Hill University
Shillong.

Abbreviation

Å	Angstrom (X-ray)
asym	asymmetric
br	broad (NMR)
Bz	benzyl
COSY	Correlation spectroscopy (NMR)
J	coupling constant (NMR)
d	doublet (NMR)
dd	doublet of doublet (NMR)
d_{calcd}	density calculated (X-ray)
DFT	density functional theory
ESI-MS	Electrospray ionization mass spectrometry
GOF	Goodness of fit (X-ray)
gs	gradient selected (NMR)
HMBC	Heteronuclear multiple bond connectivity (NMR)
HMQC	Heteronuclear multiple quantum correlation(NMR)
HSQC	Hetronuclear single quantum correlation (NMR)
Hz	Hertz (NMR)
ID	inhibition dose
IS (δ)	Isomer shift (Mössbauer)
LC	Lethal concentration
Γ	line widths (Mössbauer)
Me	methyl
μ	absorption coefficient (X-ray)
m	multiplet (NMR)
M.p.	melting point
^{n}Bu	n-butyl
PA	proton affinity
Ph	phenyl
QS (Δ)	quadrupole splitting (Mössbauer)
QSAR	Quantitative structure-activity relationship
sym	symmetric
^{t}Bu	t-butyl
t	triplet (NMR)

V	volume (X-ray)
Z	formula unit per unit cell (X-ray)

PREFACE

The thesis entitled "Synthesis, Characterization, Structure and Biological Applications of Organotin(IV) complexes of 5-[(*E*)-2-(aryl)-1-diazenyl]quinolin-8-ol" has aimed to explore the chemistry of organotin(IV) complexes with some arylazoquinolin-8-ol ligands.

The sequence of the chapters reflects the preparation of various ligands and subsequent reactions with organotin precursors and their characterization with the help of analytical and spectroscopic data. The solid state structures of some representative complexes were determined using single crystal X-ray crystallography. The work has been divided in six chapters.

Chapter 1

This is a general introductory chapter which highlights a brief account of the chemistry and structural possibilities of organotin(IV) complexes of azo ligands. This is followed by biological applications.

Chapter 2

The ligands used for synthesizing various organotin(IV) compounds are described in Chapter 2. The 5-[(*E*)-2-(aryl)-1-diazenyl]quinolin-8-ol ($L^{1\text{-}9}H$) (Fig. 1) and substituted benzoic acid ($L^{11}H'$, $L^{12}H'$ and $L^{14}H'$) (Fig. 2) have been characterized by IR and NMR spectroscopy along with the elemental analysis. The crystal structures of two ligands 5-[(*E*)-2-(4-ethoxyphenyl)-1-diazenyl]quinolin-8-ol ($L^{8}H$) and methyl 2-{[(*E*)-8-oxo-5,8-dihydroquinolin-5-ylidene]hydrazino}benzoate ($L^{9}H$) are reported in this chapter. Further, the geometries of the unsubstituted ligand ($L^{1}H$) and *para*-substituted ligands, *viz.*, $L^{2}H$–$L^{8}H$ were optimized using the density functional theory (DFT) method.

Chapter 3

Triphenyltin(IV) complexes derived from 5-[(*E*)-2-(aryl)-1-diazenyl]quinolin-8-ol ligands are described in Chapter 3. The triphenyltin(IV) complexes were prepared by reacting the sodium salts of the ligands (LNa, generated in situ from Na and anhydrous methanol) with the Ph_3SnCl in 1:1 molar ratios in anhydrous benzene. The triphenyltin(IV) complexes of 5-[(*E*)-2-(aryl)-1-diazenyl]quinolin-8-ols ($L^{1\text{-}4}H$ and $L^{7\text{-}8}H$) (**1-6**) have been characterized by IR, ^{1}H, ^{13}C, ^{119}Sn NMR and ^{119}Sn Mössbauer spectroscopic techniques. The crystal structures of four compounds, *viz.*, $Ph_3SnL^{1}.0.5C_6H_6$ (**1**), Ph_3SnL^{2} (**2**), $Ph_3SnL^{7}.C_6H_6$ (**5**), and $Ph_3SnL^{8}.0.5\ C_6H_6$ (**6**)

are reported. Compounds **1**, **2**, **5** and **6** represent the first examples of structurally characterized triphenyltin(IV) compounds containing the ligand quinolin-8-olate.

Chapter 4

Chapter 4 reports the preparations of several diorganotin(IV) bis-5-[(*E*)-2-(aryl)-1-diazenyl)quinolin-8-olates of the type R_2SnL_2 where R = ^{n}Bu, Ph and Bz, and a systematic approach was employed to determine the structures using ^{1}H-, ^{13}C-, ^{119}Sn- NMR, ESI-MS, IR and ^{119}Sn Mössbauer spectroscopic techniques in combination with X-ray diffraction. The crystal structures of four di-*n*-butyltin compounds, *viz.*, ^{n}Bu$_2$Sn(L^4)$_2$ (**9**), ^{n}Bu$_2$Sn(L^5)$_2$.0.5C$_6$H$_6$ (**10**), ^{n}Bu$_2$Sn(L^7)$_2$ (**12**), and ^{n}Bu$_2$Sn(L^8)$_2$ (**13**); three diphenyltin(IV) compounds, *viz.*, Ph$_2$Sn(L^1)$_2$.C$_3$H$_6$O (**14**), Ph$_2$Sn(L^4)$_2$ (**17**) and Ph$_2$Sn(L^5)$_2$ (**18**) and three dibenzyltin(IV) compounds, *viz.*, Bz$_2$Sn(L^4)$_2$ (**21**), Bz$_2$Sn(L^5)$_2$ (**22**) and Bz$_2$Sn(L^7)$_2$ (**24**) are discussed.

Chapter 5

The dimeric mixed ligand di-*n*-butyltin(IV) complexes of composition [^{n}Bu$_2$Sn(L^7)(L$^{10\text{-}14}$)]$_2$ (**27-31:** where L^{10} = benzene carboxylate (**27**), L^{11} = 2-[(*E*)-2-(2-hydroxy-5-methylphenyl)-1-diazenyl]benzoate (**28**), L^{12} = 5-[(*E*)-2-(4-methylphenyl)-1-diazenyl]-2-hydroxybenzoate (**29**), L^{13} = 2-{(*E*)-4-hydroxy-3-[(*E*)-4-chlorophenyliminomethyl]-phenyldiazenyl}benzoate (**30**) and L^{14} = 2-[(*E*)-(3-formyl-4-hydroxyphenyl)-diazenyl]benzoate (**31**) constitute the subject matter of Chapter 5. The complexes (**26-31**) have been achieved by the reactions of ^{n}Bu$_2$SnCl(L^7) (**26**), where L^7 = acid residue of 5-[(*E*)-2-(4-methoxyphenyl)-1-diazenyl]quinolin-8-ol, with various substituted benzoic acids in refluxing toluene, in the presence of triethylamine. All complexes (**26-31**) have been characterized by elemental analyses, IR, ^{1}H, ^{13}C and ^{117}Sn NMR and ^{119}Sn Mössbauer spectroscopy and their structures were determined by X-ray crystallography, complemented by ^{117}Sn CP-MAS NMR spectroscopy studies in the solid state.

Chapter 6

The concluding Chapter 6 deals with the *in vitro* cytotoxicity studies of a series of di-*n*-butyltin(IV) complexes, *viz.*, ^{n}Bu$_2$Sn(L^4)$_2$ (**9**), ^{n}Bu$_2$Sn(L^5)$_2$.0.5C$_6$H$_6$ (**10**), ^{n}Bu$_2$Sn(L^6)$_2$ (**11**), ^{n}Bu$_2$Sn(L^7)$_2$ (**12**), ^{n}Bu$_2$Sn(L^8)$_2$ (**13**), ^{n}Bu$_2$SnCl(L^7) (**26**) against seven well characterized human tumour cell lines *viz.*, WIDR (colon cancer), M19 MEL (melanoma), A498 (renal cancer), IGROV (ovarian cancer) and H226 (non-small cell lung cancer), MCF7 (breast cancer) and EVSA-T (breast cancer). The results were compared with the standard drugs which are used

clinically. The basicity of the two quinolinolato donor N and O atoms of the ligands are also discussed in relation to the cytotoxicity data.

Acknowledgements

First of all , I would like to express my heartfelt thanks to my teacher, philosopher and research supervisor **Dr. T.S. Basu Baul**, Deptt of Chemistry NEHU Shillong for offering me the opportunity and ample resources to pursue this research project. His untiring dedication and constant encouragement has been very inspiring. He has played the most significant role and contributed tremendously to shape my career.

I owe my sincere gratitude to **Prof. B. Myrboh**, Head, Department of Chemistry, North Eastern Hill University, and all other Teaching and Non-teaching staffs for their valueable help and cooperation.

I 'm also thankful to **Dr. A.K. Chandra, Prof. Claudio Pettinari, Prof. Fabio Marchetti** and **Prof. Riccardo Pettinari** for timely help and discussion.

I gratefully acknowledge my collaborators, **Dr. Anthony Linden, Prof. George Eng, Dr. Dick de Vos, Prof. Eleonora Rivarola, Prof. Michal Holčapek, Prof. A. Lyčka, Prof. Ulli Englert, Prof. Rudolph Willem. Prof. Ray Butcher, Prof. Edward R.T. Tiekink** for their valueable contributions.

I extend my thanks to the **Directors** and **Technicians** of RSIC, Shillong and IISc. Bangalore for providing the spectral and analytical services.

I would like to thank **Dr. Swarnali Basu Baul** for her warm affection and encouragement.

Financial assistance from **IUC-Department of Atomic Energy, Calcutta, Department of Science and Technology, New Delhi, UGC Fellowship, Indo-Italian Fellowship** are greatly acknowledged.

My warm thanks are due to my friends and labmates **Pradip Das, Dr. K. Surjit Singh, Dr. Cheerfulman Masharing, Dr. Wandondor Rynjah, Anup Paul, Sajal Kundu, Samira Amir, Afzal Hussain, Dr D.D. Kachare , Ivan, Adele , Carrado** and **Dr. Debajani Basumatary.**

I 'm greatly indebted to my **parents, brother's** and **sister's** for their continous love , patience, inspiration, altruistic sacrifices and support throughout the course of my study and made me achieve this goal.

Above all I give all thanks and glory to **My Lord** for strengthening me now and always

Archana Mizar.

Dated: 4/06/09.

ARCHANA MIZAR

CONTENTS

	Pages
Abbreviation	v-vi
Preface	vii-ix

CHAPTER 1

A BRIEF REVIEW OF ORGANOTIN(IV) COMPLEXES OF AZO LIGANDS

1.1. Introduction	1
1.2. Organotin(IV) complexes of azo ligand systems	1-15
1.3. Biological activity of organotin(IV) complexes of azo ligand systems	15-18
References	19-21

CHAPTER 2

5-[(*E*)-2-(ARYL)-1-DIAZENYL]QUINOLIN-8-OLS AS LIGANDS: SYNTHESIS AND STRUCTURAL CHARACTERIZATION

2.1. Introduction	22
2.2. Ligands used in present study ($L^{1\text{-}14}H$)	23-25
2.3. Synthesis of ligands	25
2.4. Spectroscopic characterization	25-29
2.5. X-ray crystallography	29-33
2.6. Optimized structures of ligands	33-35
2.7. Experimental	36-40
References	41-42

CHAPTER 3

TRIPHENYLTIN(IV) COMPLEXES OF 5-[(*E*)-2-(ARYL)-1-DIAZENYL]QUINOLIN-8-OL: SYNTHESIS, SPECTROSCOPIC CHARACTERIZATION AND X-RAY CRYSTALLOGRAPHY

3.1. Introduction 43

3.2. ~~Synthesis of~~ Synthesis of triphenyltin(IV) complexes 43-44

3.3. Spectroscopic characterization and X-ray crystallography of triphenyltin(IV) complexes 44-56

3.4. Structural précis of the triphenyltin(IV) complexes 56-57

3.5. Experimental 57-60

References 61-62

CHAPTER 4

DIORGANOTIN(IV) COMPLEXES OF 5-[(*E*)-2-(ARYL)-1-DIAZENYL]QUINOLIN-8-OL: SYNTHESIS, SPECTROSCOPIC CHARACTERIZATION AND X-RAY CRYSTALLOGRAPHY

4.1. Introduction 63-64

4.2. Synthesis of diorganotin(IV) complexes of 5-[(*E*)-2-(aryl)-1-diazenyl]-quinolin- 8-ol 64-65

4.3. Spectroscopic characterization and X-ray crystallography of diorganotin(IV) complexes 65-98

4.3.1. Di-n-butyltin(IV) complexes, $^{n}Bu_2Sn(L)_2$ (where L = L^{2-8})

4.3.2. Diphenyltin(IV) complexes $Ph_2Sn(L)_2$ (where L = $L^{1-5, 8}$)

4.3.3. Dibenzyltin(IV) complexes $Bz_2Sn(L)_2$ (where L = L^{3-8})

4.4. Structural précis of the diorganotin(IV) complexes 98-99

4.5. Experimental 100-107

References 108-110

CHAPTER 5

SYNTHESIS, SPECTROSCOPIC AND X-RAY CHARACTERIZATION OF DI-*n*-BUTYLTIN(IV) COMPLEXES OF 5-[(*E*)-2-(4-METHOXYPHENYL)-1-DIAZENYL]-QUINOLIN-8-OL AND BENZOIC ACID DERIVATIVES: EN ROUTE TO ELEGANT SELF-ASSEMBLY VIA MODULATION OF THE TIN COORDINATION GEOMETRY

5.1. Introduction 111-112

5.2. Synthesis of mixed ligand di-*n*-butyltin(IV) complexes 112

5.3. Spectroscopic characterization and X-ray crystallography of chlorobutyltin(IV) complex $^{n}Bu_2SnCl(L^7)$ and mixed ligand di-*n*-butyltin(IV) complexes $[^{n}Bu_2Sn(L^7)(L^{10\text{-}14})]_2$ 112-134

5.4. Structural précis of the di-*n*-butyltin(IV) complexes of 5-[(*E*)-2-(4-methoxyphenyl)- 1-diazenyl]quinolin-8-ol and benzoic acid derivatives 134-139

5.5. Experimental 139-143

References 144-145

CHAPTER 6

EVALUATION OF *IN VITRO* CYTOTOXIC ACTIVITY OF DI-n-BUTYLTIN(IV) 5-[(*E*)-2-(ARYL)-1-DIAZENYL]QUINOLIN- 8-OLATES AGAINST HUMAN TUMOUR CELL LINES

6.1. Introduction 146-147

6.2. Synthesis and characterization of di-*n*-butyltin(IV) complexes 147

6.3. Quantum chemical calculations and Biological applications 147-151

6.4. Experimental 152-153

References 154-155

List of Publications

Chapter 1

A Brief Review of Organotin(IV) Complexes of Azo Ligands

CONTENTS

CHAPTER 1

A BRIEF REVIEW OF ORGANOTIN(IV) COMPLEXES OF AZO LIGANDS

1.1. Introduction	1
1.2. Organotin(IV) complexes of azo ligand systems	1-15
1.3. Biological activity of organotin(IV) complexes of azo ligand systems	15-18
References	19-21

1.1 Introduction

One of the most fascinating features of modern chemistry is the ever increasing academic and commercial interest enjoyed by metal complexes of organic compounds. Their importance is well known in many fields including catalysis, biology and the technology of dyes and pigments, where considerable progress has been made during the past few decades. Further, the use of tin compounds in a large variety of applications is well known and organotin(IV) carboxylates are well represented in this context, having uses in industry and agriculture [1-3]. In addition, an area of current interest involves the screening of organotin(IV) compounds for potential anti-tumour activity and focuses upon results obtained in the past decade or so, as well as upon other therapeutic applications of tin compounds [4]. A number of early reviews recording advances in the screening for antitumour potential of organotins are available [5-10]. In spite of many applications, organotin(IV) compounds of azo-ligand systems are extremely limited and are discussed in following section.

1.2 Organotin(IV) complexes of azo ligand systems

The organotin(IV) complexes derived from azo ligands (Fig. 1.1) have been reported by Majee and Banerjee [11]. This type of ligands is well suited for the preparation of a variety of interesting organotin complexes because the ligands i.e. arylazobenzoic acids with a wide variety of nuclear substituents can be easily prepared by diazotization of the amino benzoic acid followed by coupling with suitable aryl moiety and have a very favourable steric arrangement for the complexation. In this context, a series of triorganotin(IV) derivatives of arylazobenzoic acids were prepared and investigated spectroscopically [11,12] which offered interesting structural possibilities. Their UV spectra recorded in non-polar solvents exhibited a large bathochromic shifts and such shifts were predicted for N→Sn co-ordination (Fig. 1.2). These interaction was found to be absent in co-ordinating solvents as the weak N→Sn bond is replaced by a donor solvent molecule (S) as shown in Fig. 1.3.

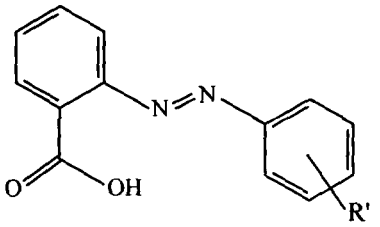

Fig. 1.1

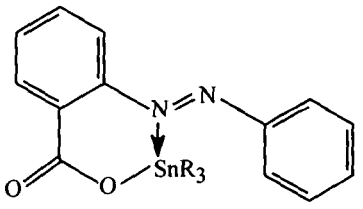

Fig. 1.2

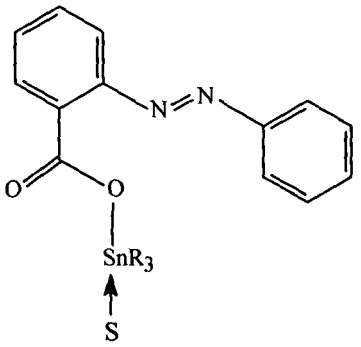

Fig. 1.3

Further, when the aryl group contains a donor group in the *ortho-* position of the coupling moiety, the arylazobenzoato moiety was postulated to function as a terdentate ligand (Fig. 1.4). In view of this, structures of triphenyltin(IV)/ tricyclohexyltin(IV) complexes of *o*-(2-hydroxy-5-methylphenylazo)benzoic acid (Fig.1.5) and triphenyltin(IV) complexes of *o*-(2-hydroxy-naphthylazo)benzoic acid (Fig. 1.6) have been studied by ^{119}Sn Mössbauer spectroscopy. In addition, triphenyltin(IV) complexes of *o*-(4-dimethylaminophenylazo)benzoic and *o*-(4-hydroxynaphthylazo)benzoic were also investigated (Figs. 1.7 and 1.8).

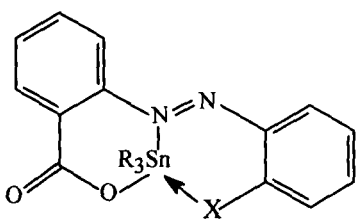

(X = -OH or $-NH_2$)

Fig. 1.4

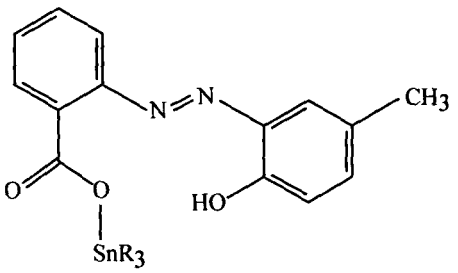

(R = Ph or cHex)

Fig. 1.5

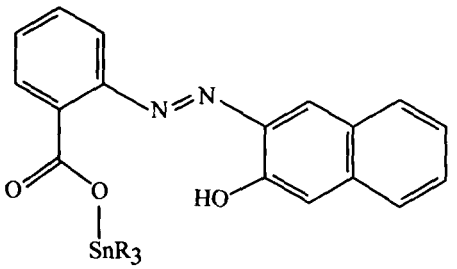

(R = Ph)

Fig. 1.6

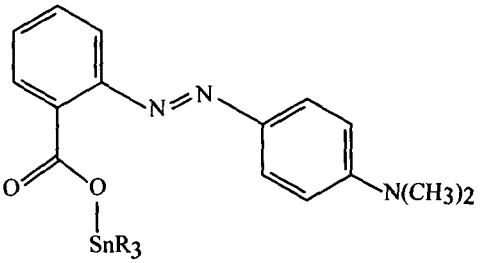

(R = Ph)

Fig. 1.7

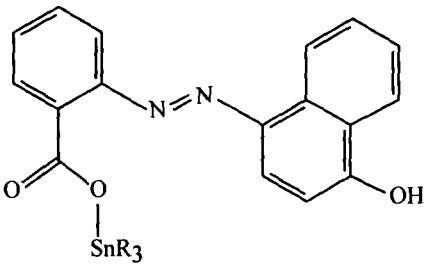

(R = Ph)

Fig. 1.8

A few years later, the crystal structure of the triphenyltin(IV) *o*-(2-hydroxy-5-methylphenylazo)benzoate was determined in the hope that the complex would constitute the first example of a six-coordinated triorganotin(IV) compound. Crystals of the triphenyltin(IV) *o*-(2-hydroxy-5-methylphenylazo) benzoate (see Fig.1.5; R = Ph) comprise discrete molecular units, in which the carboxylato group functions as an anisobidentate chelating ligand [Sn-O(I): 2.070(5), Sn...O(2): 2.463(7) Å], thus rendering the tin atom five co-ordinated (Fig. 1.9). The unit-cell projection of the compound reveals that there is no intermolecular carboxylato-bridging. The geometry at the tin atom is intermediate between tetrahedral and *cis*-trigonal bipyramidal, in which the carboxylato ligand spans equatorial and axial sites. The two C–O bond distances of the carbonyl group are as expected unequal [C-O(1): 1.296(8); C-O(2): 1.224(8) Å]. The structure of the triphenyltin(IV) *o*-(2-hydroxy-5-methylphenylazo)benzoate complex as shown in Fig. 1.9 is, therefore, the first characterized example of a truly monomeric triorganotin carboxylate [13]. It is interesting to note that, in spite of the bulky phenyl groups attached to tin and the very large steric demands of the arylazobenzoato group which prevent intermolecular bridging, the carboxyl group prefers to function as a chelating ligand giving the five- coordinated structure rather than as a unidentate ligand.

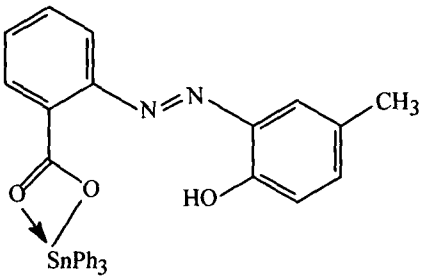

Fig. 1.9

Recently, a series of triorganotin(IV) complexes of formulation R_3SnO_2CR' where R = Me, Et, ^{n}Bu, Ph and cHex and $R'CO_2$ residue of *o*-(2-hydroxy-5-methylphenylazo)benzoic acid, has been investigated in detail [14]. Among these, the structure of triphenyltin(IV) compound was investigated earlier by Harrison *et. al* [13]. The triphenyltin(IV) compound was again synthesized and upon recrystallization from acetone/methanol (1/9) solution afforded an acetone solvated product. The structure of triphenyltin(IV) *o*-(2-hydroxy-5-methylphenylazo)benzoate acetone solvate (2/1) [15] resembles closely that of the unsolvated form as shown in Fig. 1.9 [13]. The Sn atom exists in a distorted tetrahedral geometry with Sn-O(1) being 2.079(5) Å (cf 2.070(5) Å in the unsolvated form). The Sn...O(2) separation is 2.656(5) Å and is responsible for the expansion of the C-Sn-C angle to 116.9(3)°. There are no close interaction between the solvent acetone molecule and the compound. The same coordination geometry has been reflected in tricyclohexyltin(IV) compound as shown in Fig. 1.9 for triphenyltin(IV) analogue, and with the range of angles subtended at tin being 96.7(2)-120.1(2)°. The Sn...O(2) separation is 2.759(4) Å [14]. On the other hand, trialkyltin(IV) compounds (R = Me, Et, ^{n}Bu) are polymers [14] and comprise distorted *trans*-R_3SnO_2 trigonal bipyramidal geometries (Fig. 1.10). The carboxylate ligand is bidentate bridging; however, the Sn-O bonds are not equivalent. The disparity in the Sn-O bond distances, [O(1)-Sn-O(2)], increases in the order Me (0.323 Å) < Et (0.350 Å) < ^{n}Bu (0.415 Å). The intramolecular Sn...O(2) separations are 3.175(4), 3.18(1), and 3.245(3) Å for Me, Et, ^{n}Bu, respectively.

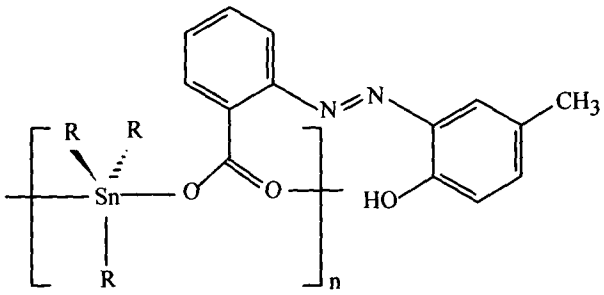

(R = Me, Et or ^{n}Bu)

Fig. 1.10

The different behaviour, among various triorganotin(IV) compounds, has been ascribed to the steric demands of the tin-bound substituents. A fair correlation was found between the difference in ^{117}Sn chemical shift between the solution and solid states and, the carbonyl oxygen-tin distance of the triorganotin(IV) compounds, only when the data of triphenyltin(IV) compound, are omitted. This indicated that the mesomeric effect of the phenyl group does not express its influence to the same extent in the solid and solution states, unlike the inductive effects. The crystal structures of the complexes were correlated with other spectroscopic data. By contrast, a good correlation including triphenyltin(IV) compound was found between the ^{119}Sn Mössbauer quadrupole splitting and the difference in ^{117}Sn chemical shift between the solution and solid states.

Trimethyltin(IV)- [14] and triethyltin(IV)- [17] complexes of *p*-(2-hydroxy-5-methylphenylazo)benzoic acid were also investigated crystallographically. Both the structures are polymeric owing to the presence of bidentate bridging carboxylate ligands. The intramolecular separation of 2.139(3) Å is shorter than the intermolecular Sn...O(2) distance of 2.497(3) Å in Me_3Sn compound. In Et_3Sn compound, the carboxylate ligands form disparate Sn-O(1) and Sn...O(2) distances of 2.149(4) Å and 2.586(4) Å, respectively. The structures of Me_3Sn and Et_3Sn resemble closely to that found for the *ortho-* analogue as shown in Fig. 1.10 [14] and structures conform to a common motif, i.e. *trans*-C_3SnO_2.

The influence of molecular geometry in halodiorganotin(IV) complexes of the *o*-(2-hydroxy-5-methylphenylazo)benzoic acid was also studied [18]. The crystal and molecular structures of three compounds were presented in which the carboxylate residue has been kept constant and the R_2Sn moiety has been altered such that R = Me, ^{t}Bu and Ph. The crystallographic study show that two distinct motifs are adopted owing to different modes of coordination of the carboxylate ligands. The chlorodimethyltin(IV) complex is dimeric with the two tin atoms being

bridged by two $^{-}O_2CR'$ anions each of which coordinates a tin atom via one of the carboxylate oxygen atom and the second tin atom via the phenoxide oxygen atom and the complex exists in a zwitterionic form. The tin atom geometry is trigonal bipyramidal, *trans*-O_2SnC_2Cl (Fig. 1.11). By contrast to the dimeric structure for chlorodimethyltin(IV) complex, the structures of chlorodi-t-butyltin(IV) and chlorodiphenyltin(IV) complexes are monomeric with the tin atoms in *cis*-O_2SnC_2Cl trigonal bipyramidal geometries (Fig. 1.12). The $^{-}O_2CR'$ anion coordinates the tin atom via the caboxylate oxygen atoms only.

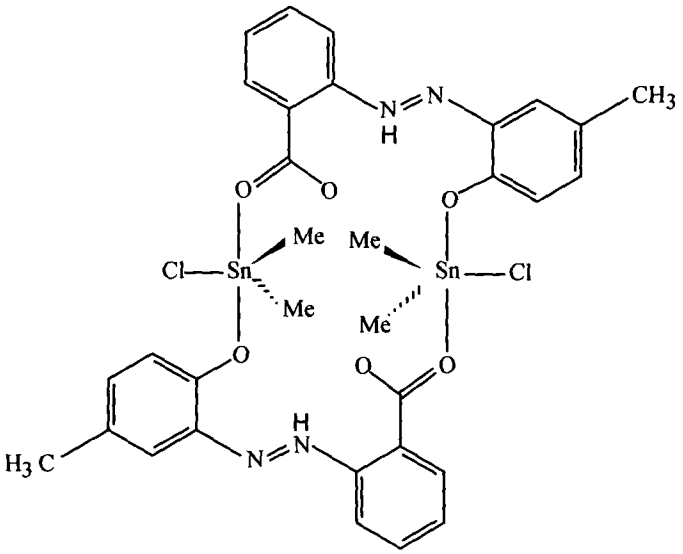

(R = Me)

Fig. 1.11

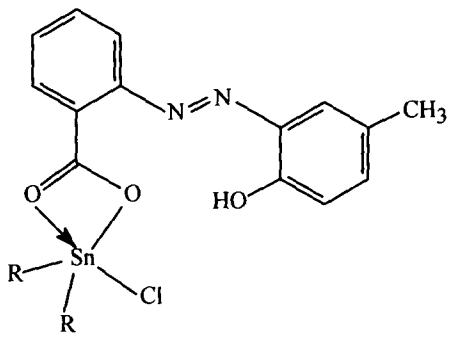

(R = ^{t}Bu or Ph)

Fig. 1.12

The crystal and molecular structures of two more compounds of the general formula $R_2Sn(O_2CR')_2$ are also reported where R = ^{t}Bu and Ph [19] (Fig. 1.13). For the R = ^{t}Bu

compound, the tin atom exists in a skew-trapezoidal bipyramidal geometry in which the trapezoidal plane is defined by two asymmetrically chelating carboxylate ligands and the organic residues lie over the weaker Sn...O interactions. A similar coordination geometry is found in the R = Ph compound which was isolated as a di-chloroform solvate. The chloroform molecules exert an influence on the molecular geometry in that a conformational change in the carboxylate ligand is induced in order to facilitate the formation of intermolecular hydrogen bonds.

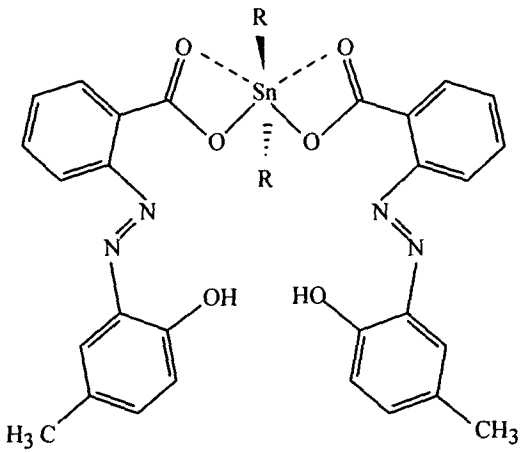

(R = ^{t}Bu or Ph)

Fig. 1.13

Systematic variations in the Sn-ligand parameters in these and related compounds are correlated with the varying Lewis acidity at the tin centres. The replacement of one carboxylate ligand in [^{t}Bu$_2$Sn(O$_2$CR')$_2$] by a chloride, i.e. yielding [^{t}Bu$_2$Sn(O$_2$CR')Cl] [18], results in a significant contraction of the Sn-O(2) distance to 2.402(3) Å while maintaining the primary Sn-O(1) interaction constant at 2.105(3) Å. The comparable distances for the [Ph$_2$Sn(O$_2$CR')Cl] structure are 2.365(3) Å and 2.090(3) Å, respectively [18]. These results are correlated with the enhanced Lewis acidity of the tin centre in the respective R$_2$SnCl moieties. For the R = Ph, substituting a carboxylate ligand in [Ph$_2$Sn(O$_2$CR')$_2$] with a phenyl group leading to [Ph$_3$Sn(O$_2$CR')] [15] results in Sn-O(1) and Sn-O(2) of 2.079(5) Å and 2.656(5) Å, respectively, a result consistent with the reduced Lewis acidity of the tin atom in Ph$_3$Sn compared with Ph$_2$Sn. The Lewis acidity of the tin center was found to decreases in the order Ph$_3$Sn < Ph$_2$Sn < Ph$_2$SnCl and ^{t}Bu$_2$Sn< ^{t}Bu$_2$SnCl for the phenyltin and tert-butyltin compounds, respectively.

More recently, a comprehensive study of organotin(IV) complexes was carried out involving 5-(arylazo)salicylic acid from the point of view of structural motifs and biological applications. A series of triphenyltin(IV) complexes of 5-(arylazo)salicylic acid has provided X-

ray quality crystals in which the ligand aryl residue has been varied (aryl = phenyl- [20], 2-methylphenyl- [20], 3-methylphenyl- [20], 4-methylphenyl- [21], 4-methoxyphenyl- [20] and 4-chlorophenyl- [22]), and Ph_3Sn was held constant. The solid state structures of these triphenyltin(IV) complexes were evaluated using ^{119}Sn Mössbauer and X-ray crystallography. The triphenyltin(IV) complexes adopt a monomeric distorted tetrahedral configuration defined by a C_3O donor set where the carboxylate ligand coordinating in a monodentate mode (Fig. 1.14). The relatively small variations observed for the geometric parameters across the series of triphenyltin(IV) complexes indicated that the variable substitution in the aryl residue has little influence on the tin geometry.

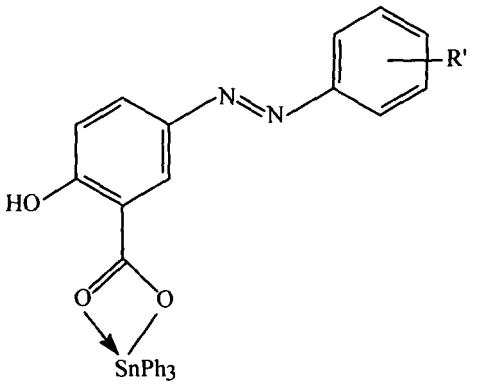

(R' = H, 2-Me, 3-Me, 4-Me, 4-OMe or 4-Cl)

Fig. 1.14

Further, one of the triphenyltin(IV) complex (tetrahedral) was subjected to the reactivity study towards 2,2'-bipyridine to ascertain the ability of 2,2'-bipyridine to coordinate to the Sn-complex and the resultant changes in the molecular architecture. The crystal structure of the product revealed that the 2,2'-bipyridine moiety does not coordinate to the Sn atom, but forms a cyclic tetrameric adduct of formula $[Ph_3SnO_2CR'(H_2O)]_2.bipy_2$ ($^-O_2CR'$= 5-(2-methylphenylazo)salicylate) through hydrogen bonding between the water ligand of $Ph_3SnO_2CR'(H_2O)$ and the 2,2'-bipyridine N atoms (Fig. 1.15) [21].

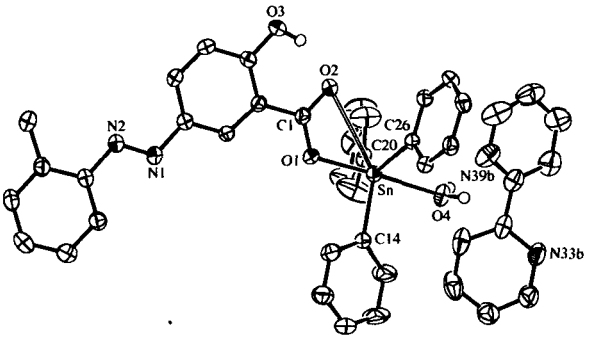

(a)

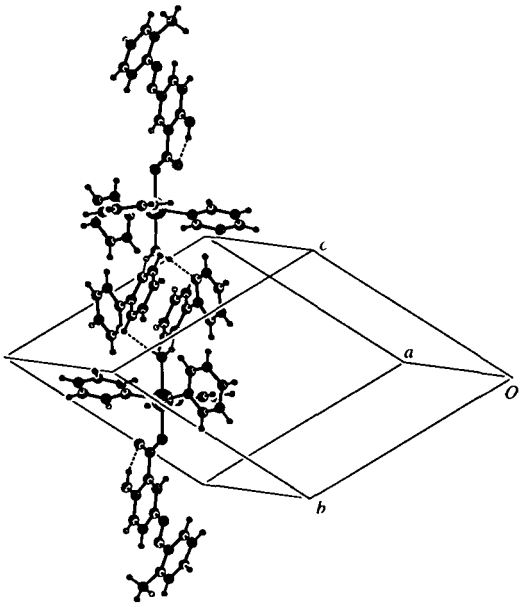

(b)

Fig.1.15 (a) The molecular structure of $Ph_3SnO_2CR'(H_2O)$.bipy (b) The hydrogen-bonded tetrameric motif in the molecular structure of $Ph_3SnO_2CR'(H_2O)$.bipy, consisting of two $Ph_3SnO_2CR'(H_2O)$.bipy and two bipy molecules.

The trialkyltin(IV) complexes, *viz.*, Me_3 [22], $^nBu_3$ [20,22] were investigated by ^{119}Sn Mössbauer and ^{119}Sn NMR spectroscopy. ^{119}Sn Mössbauer spectroscopy shows that these complexes are polymeric and feature a *trans*-trigonal bipyramidal geometry with a planar SnR_3 unit and two apical carboxylate oxygen atoms derived from bidentate bridging carboxylate ligands. These trialkyltin complexes dissociate in solution to a tetrahedral species as indicated by ^{119}Sn NMR data.

In addition, a series of di-n-butyltin complexes involving 5-(arylazo)salicylic acid have been studied in great detail in view of possible biological applications. A systematic investigation of the structures of the di-n-butyltin complexes of 5-(arylazo)salicylic acid was carried out. The

carboxylate residue was varied by virtue of changes to the aryl group (aryl = phenyl- [23], 2-methylphenyl- [24], 3-methylphenyl- [23], 4-methylphenyl- [23], 4-bromophenyl- [23] and 4-chlorophenyl- [25]), and the $^{n}Bu_2$ was held constant. In general, the crystallographic results indicated that the complexes adopt a skew-trapezoidal bipyramidal arrangement around the tin atom (Fig. 1.16).

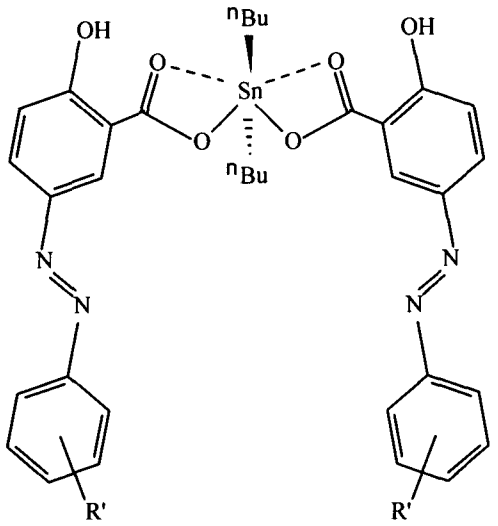

(R' = H, 2-Me, 3-Me, 4-Me, 4-Br or 4-Cl)

Fig. 1.16

In addition, there are weak bridging intermolecular Sn...O contacts in di-n-butyltin(IV) complexes when carboxylate residue is phenyl-, 2-methylphenyl- or 3-methylphenyl- but not in substituents at 4-position (e.g. 4-methylphenyl-, 4-bromophenyl- and 4-chlorophenyl-), where one of the hydroxyl oxygen atoms from a neighbouring molecule coordinates weakly with the Sn atom, thereby completing a seventh coordination site in the extended Sn coordination sphere (Fig. 1.17).

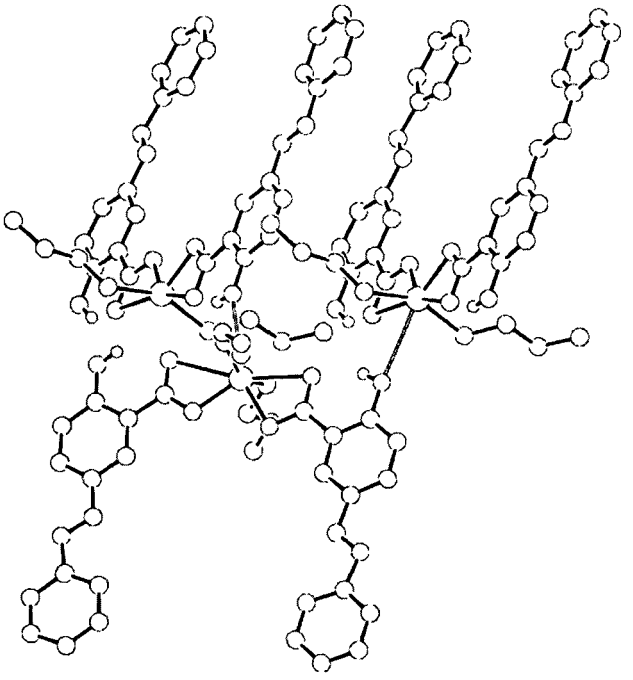

Fig.1.17 Three segments of the chain structure formed by the weak Sn···O interaction (open bonds) in di-n-butyltin(IV) complex when carboxylate residue is phenyl.

The Sn...O distance is 3.080(2) and 3.439(2) Å in di-n-butyltin(IV) complexes when carboxylate residue is phenyl-, 2-methylphenyl- or 3-methylphenyl-. The values are significantly shorter than the sum of the van der Walls radii of the Sn and O atoms. This interaction links the molecules into polymeric chains or head-to-head dimeric units as shown in Fig 1.18.

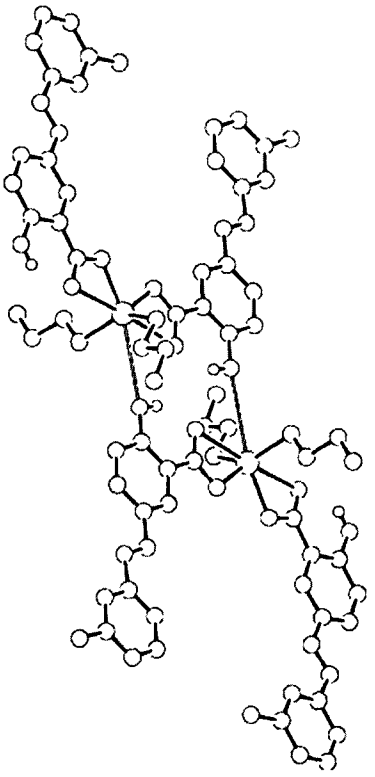

Fig.1.18 The dimeric unit formed by the weak Sn···O interaction in di-n-butyltin(IV) complexes when carboxylate residue is 3-methylphenyl.

The crystal structures of these complexes were correlated with ^{117}Sn CP MAS NMR and ^{119}Sn Mössbauer data, while their solution behaviour was evaluated using ^{119}Sn NMR in non coordinating solvents.

Another interesting report is diorganotin(IV) complexes containing mixed arylazobenzoates of composition $[R_2Sn(O_2CR')(O_2CR'')]$ where R = ^{n}Bu or Me and $^-O_2CR'$and $^-O_2CR''$ are two different 5-(arylazo)salicylates. A full characterization of the structures of the complexes in the solid state was accomplished by single crystal X-ray crystallography [26]. The complexes were found to adopt the usual dicarboxylato structural type with a skew-trapezoidal bipyramidal arrangement around the tin atom as shown in Fig. 1.16.

A sterically congested organotin(IV) complex was obtained by the reaction of sodium 4-(4'-dimethylaminophenylazo)benzoate and {[2-(dimethylaminomethyl)phenyl](diphenyl)}tin chloride [27]. The crystal structure of the complex revealed that the tin atom exists in a slightly distorted trans-trigonal bipyramidal geometry defined by three *ipso*-carbon atoms of the phenyl groups in equatorial positions, with the intramolecularly bound nitrogen atom for the $CH_2N(CH_3)_2$ group and the oxygen atom of the carboxylate groups in apical positions (Fig. 1.19).

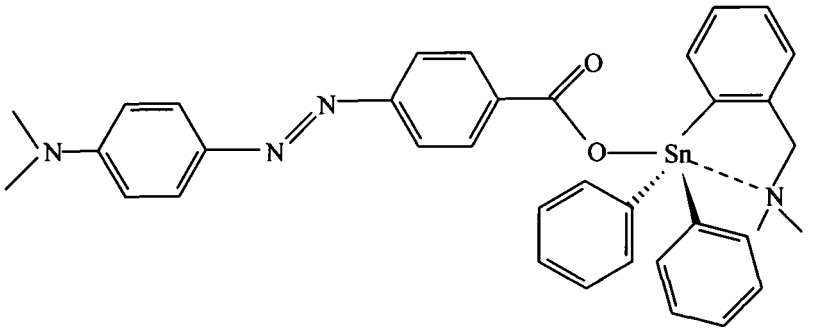

Fig.1.19

As a part of a wider study designed to ascertain the reason(s) for the structural variation found in these systems, the reactivity of a few triorganotin(IV) was studied with a new ligand system e.g. 5-(2'-carboxyphenylazo)salicylaldehyde. The molecular structure of $[Ph_3Sn(O_2CR')(OH_2)]$ (Fig. 1.20) [28] reveals that the carboxylate group coordinate to the tin atom via one of the oxygen atoms only (Sn-O = 2.161(5) Å. The tin atom is also coordinated by a water molecule (Sn-O =2.527(5) Å) and exists in a trigonal bipyramidal geometry with the three phenyl groups in equatorial positions; the O-Sn-O axial angle is 176.3(2)°. The lattice is stabilized by H-bonding contacts as well as charge-transfer interactions. A brief report of a polymeric trimethyltin(IV) compound $[Me_3Sn(O_2CR')]_n$ is also there in the literature [29]. The tin atom in this compound is fivefold-coordinated, existing in a distorted trigonal bipyramidal geometry (Fig. 1.21). The trigonal plane is defined by the three methyl groups and the axial positions by symmetry related oxygen atoms; Sn-O(1) = 2.174(6) Å, Sn-O(2)' = 2.448(7) Å and the tin atom lies 0.1246(7) Å out of the plane in the direction of the more strongly bound O(1) atom.

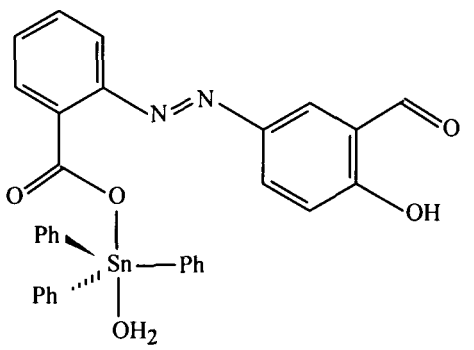

Fig.1.20

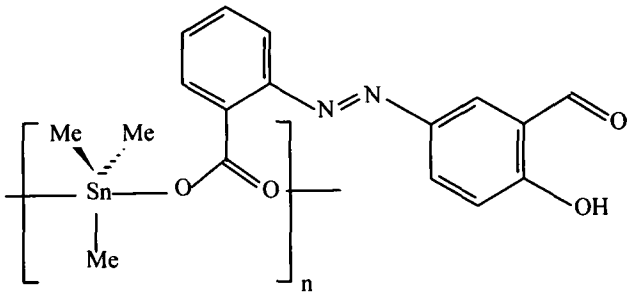

Fig.1.21

A series of adducts of tin(IV) derivatives with 2,2'-azopyridine (AZPy) has been studied [30,31] by Mössbauer and X-ray photoelectronic spectroscopies and the crystal and molecular structure of $SnMe_2Br_2$.AZPy has been determined. The linear correlation of the Mössbauer parameter isomer shift with partial atomic charge on tin suggests the occurrence of a single homologous series of isostructural adducts. The correlation of the Mössbauer parameter quadrupole splitting and C-Sn-C bond angle permits their calculation in $SnMe_2X_2AZPy$ adducts (X = Cl, Br). The N_{1s} binding energies, obtained by XPS data, pointed out two slightly different values for both pyridinic and azo-group nitrogens. The crystallographic studies of the $SnMe_2Br_2AZPy$ adduct shows a new structure in which the Sn atom is seven-coordinated [31].

On the other hand, functionally substituted 5-azoxines, hereafter 5-[(*E*)-2-(aryl)-1-diazenyl]quinolin-8-ol, are long known as analytical reagents for qualitative detection of metal ions [32-34]. This class of azo-dyes forms complexes in solution with a wide variety of metals [34] and the studies concern mainly the azo-hydrazone tautomeric equilibria [35-37], bacteriocidal properties [38,39], determination of trace elements by flame atomic absorption spectrometry [40] and derivative spectrophotometry [41] and binding to bovine serum albumin [42]. Later, these reagents have attracted the attention of several workers in recent years and consequently, some of the earlier publications have dealt with the coordinating behavior of such reagents towards organotin [43-45], transition metals [46], mixed organotin transition metals [46], mercury [47, 48], and uranium [49]. Among these, 5-[(*E*)-2-(aryl)-1-diazenyl]quinolin-8-ol forms di/tri-organotin complexes similar to the well-known organotin oxinates [43-45], but polyfunctional 5-(2'-carboxyphenylazo)-8-quinolinol forms three classes of compounds, *viz.*, the carboxylates, quinolinolates and binuclear complexes (mixed carboxylates-quinolinolates $R_2Sn(LSnR'_3)_2$ and $R_3SnLSnR_3$) (R = Ph, ^{n}Bu, ^{n}Oct, Me; R' = Ph, ^{n}Bu) [44]. The carboxylates, R_3SnLH, are 5-coordinate complexes similar to other triorganotin arylazobenzoates while the quinolinolates, $R_2Sn(LH)_2$, closely resemble the corresponding organotin oxinates. Unlike the oxinates, $R_2Sn(LH)_2$ type complexes can be made water soluble by treatment with aqueous

$NaHCO_3$ whereby $R_2Sn(LNa)_2$ type complexes are formed. The binuclear complexes $R_2Sn(LSnR_3)_2$ contain five- and six-coordinate organotin groups in the same ligand. The tentative structures of the complexes were proposed on the basis of IR, UV–Vis, ^1H NMR and ^{119m}Sn Mössbauer spectroscopic techniques.

Further work in this area involving 5-[(*E*)-2-(aryl)-1-diazenyl]quinolin-8-ol and related systems constitute the subject matter of the thesis and are described in the forth coming chapters.

1.3 Biological activity of organotin(IV) complexes of azo ligand systems

Triorganotin(IV) *o*-(arylazo)benzoates [50] (Fig.1.22) were screened *in vitro* for their biological activity against several microorganisms. These complexes were found to exhibit considerable activity against *Staphylococcus aureus, Bacillus Cereus, Sarcina lutea, Bacillus pumilus, Micrococcus flovus,* and *Bacillus subtitis.*

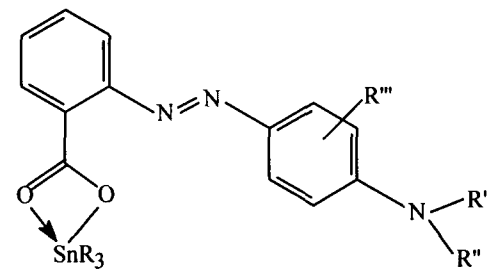

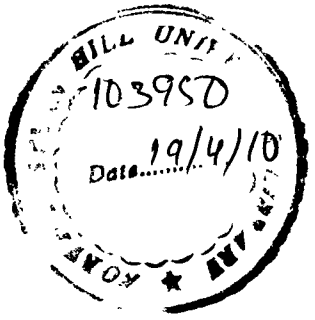

Fig. 1.22

The activity were correlated on the nature of aryl R', R'', R'''-substituents. The significant inhibition of bacterial growth by triorganotin *o*-(arylazo)benzoates compared to corresponding *o*-(arylazo)benzoic acid was explained and mechanism was proposed for arresting bacterial growth. The enzymatic proteins in their relatively rigid planar peptide structure possess carbonyl group capable of forming metal-oxygen bond with the stannyl groups of organotin carboxylate and this bond formation is further augmented by the nearby β- azoic nitrogen and stannyl carboxylate carbonyl oxygens which form bifurcated hydrogen bonds with the peptide N-H groups (N-H....N = 2.97 Å, N-H....O = 3.29 Å), thus, enhancing the electron density on the peptide oxygen.

Organotin(IV) complexes of 5-(arylazo)salicylic acid have been studied in great detail for evaluating their biological properties. A series of organotin(IV) complexes of formulations $^nBu_2Sn(O_2CR')_2$, Ph_3SnO_2CR' and $^nBu_3SnO_2CR'$ ($^-O_2CR'$ = substituted 5-(arylazo)salicylate)

were subjected to toxicities studies against second larval instar of *Aedes aegypti* mosquito larvae [25]. The results indicate that all the triorganotin(IV) compounds have activities of an order of magnitude higher than for the diorganotin(IV) derivative. The LC_{50} values (concentration at which the test compounds killed 50% of the tested organisms) for the triorganotin(IV) compounds ranged from 0.53 to 3.50 mg l^{-1}. Also, the data indicated that the tri-n-butyltin(IV) compounds were more effective than the phenyl derivatives. Although the triorganotin(IV) compounds, are not as effective as organophosphorus insecticides [51] in their larvicial effects, their advantages lie in their biodegradability and lack of known resistance by this species of mosquitoes.

In addition, a representative di-n-butyltin(IV) compound of formulation $^{n}Bu_2Sn(O_2CR')_2$ ($^{-}O_2CR'$ = substituted 5-(arylazo)salicylate), was tested across a panel of human cell lines *viz.*, WIDR (colon cancer), M19 MEL (melanoma), A498 (renal cancer), IGROV (ovarian cancer) and H226 (non-small cell lung cancer), MCF7 (breast cancer), EVSA-T (breast cancer) to establish the activity [23]. The data clearly show that the di-n-butyltin(IV) compound is more active *in vitro* than cisplatin and etoposide against all seven human cancer cell lines.

The toxicity studies of tri-n-butyltin(IV) complexes of formulation $^{n}Bu_3SnO_2CR'$($^{-}O_2CR'$ = substituted 5-(arylazo)salicylate) and the parent 5-(arylazo)salicylic acid were evaluated by using sea urchin early developmental stages as recommended model organisms for toxicity tests [52]. The present report also throw light on the effects of new organotin compounds towards two species of sea urchin, *Paracentrotus lividus* and *Sphaerechinus granularis*, in order to compare variation in the impact incidence of contaminant exposure among different species. Biological activity tests of the tri-n-butyltin(IV) complexes demonstrated that the (i) embryos exposed to the tri-n-butyltin(IV) complexes at 10^{-5} and 10^{-7} M solutions presented blocks and strong developmental anomalies. (ii) embryos treated with free 5-(arylazo)salicylic acid at 10^{-5} M concentration stopped to develop at the blastula stage. At 10^{-7} M, they developed regularly as the control. (iii) embryos treated with tri-n-butyltin(IV) chloride (positive control) did not develop any more. (iv) sensitivity of *S. granularis* embryos was like that of *P. lividus*. The developmental anomalies can be seen in Figs. 1.23 and 1.24.

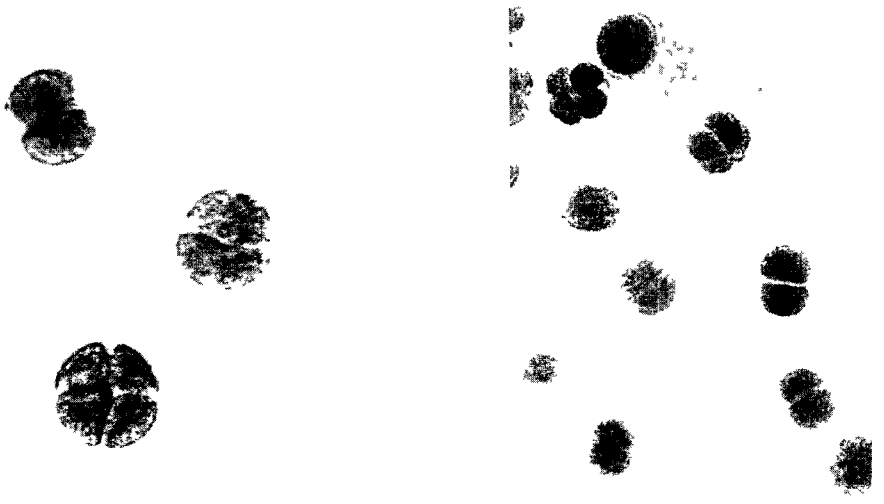

(a) (b)

Fig. 1.23 Sea urchin control embryos and treated embryos with tri-n-butyltin(IV) compounds. Anomalous embryos exposed to tri-n-butyltin(IV) compounds solutions did not show any significant difference under optical microscopy: *P. lividus* (a) and *S. granularis* (b) anomalous embryos, after incubation in 10^{-5} M solution of the compound for 48 h. The blastomeres are of different sizes and are blocked at the two to four- cell stages.

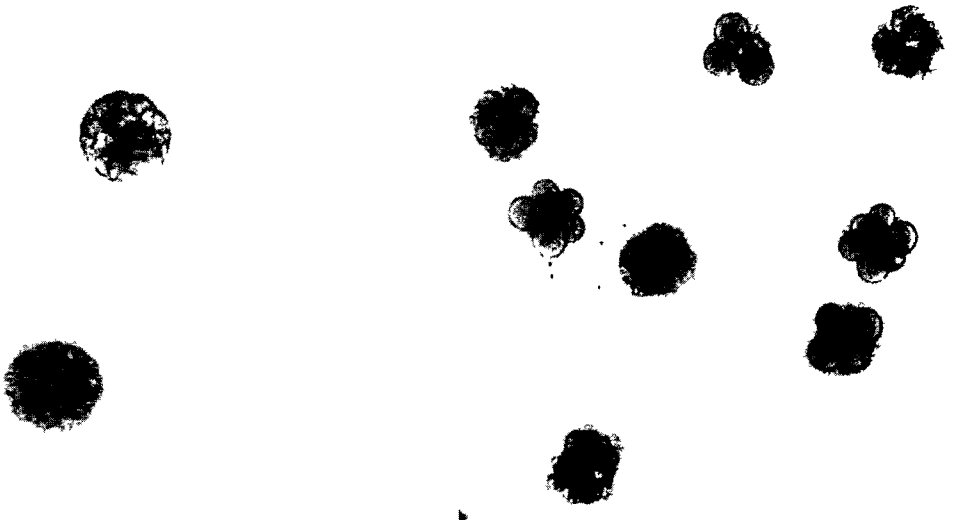

(a) (b)

Fig. 1.24 Sea urchin control embryos and treated embryos with tri-n-butyltin(IV) compounds. Anomalous embryos exposed to tri-n-butyltin(IV) compounds solutions did not show any significant difference under optical microscopy: *P. lividus* (a) and *S. granularis* (b) anomalous embryos, after incubation in 10^{-7} M solution of the compound for 48 h and arrested anomalous embryos.

In conclusion, the tri-n-butyltin(IV) compounds induced high embryonic mortality in *P. lividus* and *S. granularis;* and were as toxic as tri-n-butyltin(IV) chloride independently of the presence of the ligands.

From the foregoing description of the structural chemistry of organotin(IV) complexes, it is clear that there exists a rich diversity in Sn atom geometry and coordination modes of the azo-ligands themselves. Such complexes are likely to find wide application in biology, medicine etc.

References

[1] A.G. Davies, P.J. Smith, in: G. Wilkinson, F.G.A. Stone, E.W. Abel (Eds.), Comprehensive Organometallic Chemistry, Vol. 2, Pergamon Press, Oxford, 1982, Ch. 11.

[2] C.J. Evans, S. Karpel, Organotin Compounds in Modern Technology, J. Organomet. Chem. Library, Vol. 16, Elsevier, Amsterdam, 1985.

[3] I. Omae, Organotin Chemistry, J. Organomet. Chem. Library, Vol. 21, Elsevier, Amsterdam, 1989.

[4] M. Gielen, E.R.T. Tiekink, in: M. Gielen, E.R.T. Tiekink (Eds.), Metallotherapeutic Drug and Metal-Based Diagnostic Agents: ^{50}Sn Tin Compounds and Their Therapeutic Potential, Wiley, 2005, pp. 421-439.

[5] F. Huber, R. Barbieri, in: N.F. Cardarelli (Eds.), Tin as a Vital Nutrient: Implications in Cancer Prophylaxis and other Physiological Processess, CRC Press, Boca Ration, 1986, pp. 175-187.

[6] A.J. Crowe, Drugs of the Future **12** (1987) 255.

[7] L.R. Sherman, F. Huber, Appl. Organomet. Chem. **2**, (1988) 65.

[8] A.K. Saxena, F. Huber, Coord. Chem. Rev. **95** (1989) 109.

[9] A.J. Crowe, in: M. Gielen (Eds.), Tin Compounds and their Potential as Pharmaceutical Agents, NATO ASI Series, Vol. H37, Springer-Verlag, Berlin, 1990, pp. 69-114.

[10] J.M. Tsangaris, D.R. Williams, Appl. Organomet. Chem. **6** (1992) 3.

[11] B. Majee, S. Banerjee, J. Organometal. Chem. **139**, 39 (1977).

[12] B. Majee, S. Banerjee, J. Organometal. Chem. **140**, 151 (1977).

[13] P.G. Harrison, K. Lambert, T.J. King, B. Majee, J. Chem. Soc., Dalton Trans. 363 (1983).

[14]R. Willem, I. Verbruggen, M. Gielen, M. Biesemans, B. Mahieu, T.S. Basu Baul, E.R.T.Tiekink, Organometallics **17** (1998) 5758.

[15] T.S. Basu Baul, E.R.T. Tiekink, Z. Kristallogr. **211** (1996) 489.

[16] T.S. Basu Baul, E.R.T. Tiekink, Acta Crystallogr. C **52** (1996) 1428.

[17] T.S. Basu Baul, E.R.T. Tiekink, Z. Kristallogr. NCS **212** (1997) 365.

[18] T.S. Basu Baul, E.R.T. Tiekink, Z. Kristallogr. **213** (1998) 62.

[19] T.S. Basu Baul, E.R.T. Tiekink, Z. Kristallogr. **214** (1999) 566.

[20] T.S. Basu Baul, S. Dhar, S.M. Pyke, E.R.T. Tiekink, E. Rivarola, R. Butcher, F.E. Smith, J. Organomet. Chem. **633** (2001) 7.

[21] T.S. Basu Baul, W. Rynjah, E. Rivarola, A. Linden, J. Organomet. Chem. **690** (2005) 613.

[22] T.S. Basu Baul, S. Dhar, N. Kharbani, S.M. Pyke, R. Butcher, F.E. Smith, Main Group Met. Chem. **22** (1999) 413.

[23] T.S. Basu Baul, W. Rynjah, R. Willem, M. Biesemans, I. Verbruggen, M. Holčapek, D. de Vos, A. Linden, J. Organomet. Chem. **689** (2004) 4691.

[24] T.S. Basu Baul, S. Dhar, E.R.T. Tiekink, Main Group met. Chem. **24** (2001) 293.

[25] T.S. Basu Baul, S. Dhar, E. Rivarola, F.E. Smith, R. Butcher, X. Song, M. McCain, G. Eng, Appl. Organomet. Chem. **17** (2003) 261.

[26] T.S. Basu Baul, W. Rynjah, E. Rivarola, C. Pettinari, A. Linden, J. Organomet. Chem. **690** (2005) 1413.

[27] A. Ruzicka, A. Lycka, R. Jambor, P. Novak, I. Cisarova, M. Holcapek, M. Erben, J. Holecek, Appl. Organomet. Chem. **17** (2003) 168.

[28] T.S. Basu Baul, S.M. Pyke, K.K. Sarma, E.R.T. Tiekink, Main Group met. Chem. **19** (1996) 807.

[29] T.S. Basu Baul, E.R.T. Tiekink, Z. Kristallogr. NCS **212** (1997) 363.

[30] E. Rivarola, A. Silvestri, G. Alonzo, R. Barbieri, R. H. Herber, Inorg. Chim. Acta **99** (1985) 87.

[31] M. Camalli, F. Caruso, G. Mattogno, E. Rivarola, Inorg. Chim. Acta **170** (1990) 225.

[32] J. Matheus, Ber. **21** (1888) 1642.

[33] F.J. Welcher, Organic Analytical Reagents, vol. 1, Van Nostrand, London, 1947.

[34] V.M. Ivanov, T.F. Rudometkina, Zh. Anal. Khim. **33** (1978) 2426.

[35] Y. Matsunaga, Bull. Chem. Soc.(Japan) **44** (1971) 878.

[36] G.M. Badger and R.G. Buttery, J. Chem. Soc. (1956) 614.

[37] E. Sawicki, J. Chem. Soc. (1956) 743.

[38] R.N. Shreve, R. Bennett, J. Am. Chem. Soc. **65** (1943) 2243.

[39] T. Matsuo, A. Musashi, Y. Naito, J. Pharm. Soc. (Japan), **72** (1952) 1456.

[40] R. Saran, T.S. Basu Baul, P. Srinivas, D.T. Khathing, Anal. Lett. **25** (1992) 1545.

[41] R. Saran, T.S. Basu Baul, Talanta **41** (1994) 1537.

[42] B. Pal, P.K. Bajpai, T.S. Basu Baul, Spectrochim. Acta **56** (2000) 2453.

[43] K.D. Ghuge, P. Umapathy, M.P. Gupta, D.N. Sen, Inorg. Nucl. Chem. **43** (1981) 653.

[44] T.S. Basu Baul, T.K. Chattopadhyay, B. Majee, Polyhedron **2** (1983) 635.

[45] B.K. Deb, A.K. Ghosh, Can. J. Chem. **65** (1987) 1241.

[46] T.S. Basu Baul, T.K. Chattopadhyay, B. Majee, Ind. J. Chem. A **23** (1984) 470.

[47] E. El-Sawi, F.A. Moti, S. El-Messary, Bull. Soc. Chim. (Belg.) **94** (1985) 69.

[48] T.S. Basu Baul, T.K. Sinha, R. Saran, Synth. React. Inorg. Met.-Org. Chem. **25** (1995) 615.

[49] T.S. Basu Baul, D. Dey, Synth. React. Inorg. Met.-Org. Chem. **19** (1989) 101.

[50] B.B. Maji, S. Pain, G. Biswas, K.L. Ghatak, S.N. Ganguly, A. Banerjee, Indian Acad. Sci. (Chem. Sci.) **105** (1993) 183.

[51] S.C. Rawlins, J.O.H. Wan, J. Am. Mosq. Control Assoc. **11** (1995) 59.

[52] T.S. Basu Baul, W. Rynjah, K.S. Singh, C. Pellerito, P. D'Agati, L. Pellerito, Appl. Organomet. Chem. **19** (2005) 1189.

Chapter 2

5-[(*E*)-2-(aryl)-1-diazenyl]quinolin-8-ols as Ligands: Synthesis and Structural Characterization

CONTENTS

CHAPTER 2

5-[(*E*)-2-(ARYL)-1-DIAZENYL]QUINOLIN-8-OLS AS LIGANDS: SYNTHESIS AND STRUCTURAL CHARACTERIZATION

2.1. Introduction	22
2.2. Ligands used in present study ($L^{1-14}H$)	23-25
2.3. Synthesis of ligands	25
2.4. Spectroscopic characterization	25-29
2.5. X-ray crystallography	29-33
2.6. Optimized structures of ligands	33-35
2.7. Experimental	36-40
References	41-42

2.1. Introduction

The usefulness of the 5-[(*E*)-2-(aryl)-1-diazenyl]quinolin-8-ols are described in the preceding Chapter. These ligands can form complexes with a wide variety of metals and various techniques such as IR, UV–Vis, ^{1}H NMR and ^{119m}Sn Mössbauer and magnetic moment measurements have been utilized to indicate the mode of coordination [1-8]. Nevertheless, no systematic efforts were made to characterize these ligands except for characterizing a few of them by electronic absorption, IR and resonance Raman spectroscopy [9] and recently a compound i.e. 5-[(2-ethoxyphenyl)-1-diazenyl]quinolin-8-ol by single crystal X-ray crystallography [10], in an unconnected instance. Consequently, an effort was made to characterize 5-[(*E*)-2-(aryl)-1-diazenyl]quinolin-8-ol systems from a detailed NMR analysis and couple of them were also analyzed by single crystal X-ray crystallography (see the following Sections).

Two types of ligands, *viz.*, (i) 5-[(*E*)-2-(aryl)-1-diazenyl]quinolin-8-ol ($L^{1\text{-}9}H$) and (ii) substituted benzoic acids ($L^{10\text{-}14}H'$) are described in Table 2.1. The details of their synthesis are presented in Section 2.6 while their NMR data are summarized in Section 2.4. It should be mentioned herein that the ligands $L^{10\text{-}14}H'$ were only used for synthesizing mixed ligand organotin(IV) complexes (refer to Chapter 5).

2.2. Ligands used in present study ($L^{1-14}H$)

The ligands and their systematic names are given in Table 2.1.

Table 2.1: Ligands, their names and abbreviation

Ligand	Name	Abbreviation[a]
(a) 5-[(*E*)-2-(aryl)-1-diazenyl]quinolin-8-ol ligands ($L^{1-9}H$)		
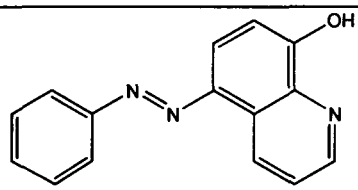	5-[(*E*)-2-(phenyl)-1-diazenyl]-quinolin -8-ol	**L^1H**
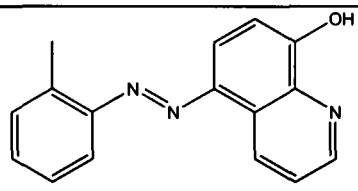	5-[(*E*)-2-(2-methylphenyl)-1-diazenyl]quinolin-8-ol	**L^2H**
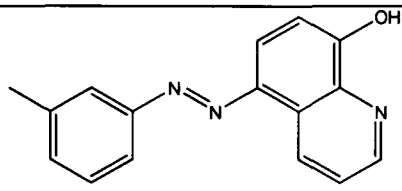	5-[(*E*)-2-(3-methylphenyl)-1-diazenyl]quinolin-8-ol	**L^3H**
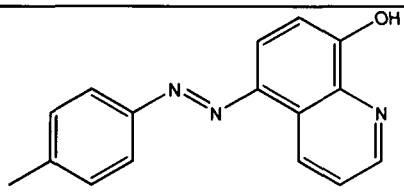	5-[(*E*)-2-(4-methylphenyl)-1-diazenyl]quinolin-8-ol	**L^4H**
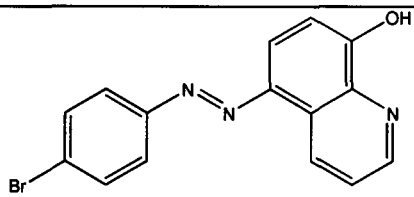	5-[(*E*)-2-(4-bromophenyl)-1-diazenyl]quinolin-8-ol	**L^5H**
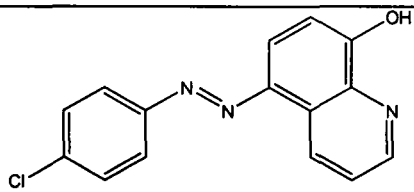	5-[(*E*)-2-(4-chlorophenyl)-1-diazenyl]quinolin-8-ol	**L^6H**

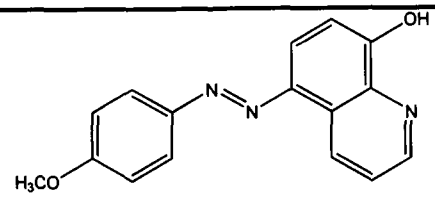	5-[(*E*)-2-(4-methoxyphenyl)-1-diazenyl]quinolin-8-ol	**L^7H**
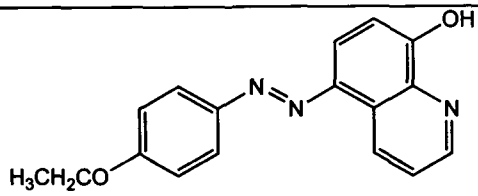	5-[(*E*)-2-(4-ethoxyphenyl)-1-diazenyl]quinolin-8-ol	**L^8H**
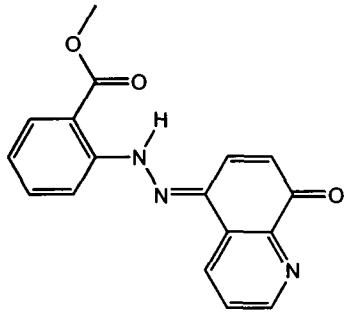	Methyl 2-{[(*E*)-8-oxo-5,8-dihydro-quinolin-5-ylidene]hydrazino}-benzoate	**L^9H**
(b) Ligands used for synthesizing mixed ligand complexes ($L^{10\text{-}14}H'$)		
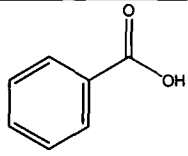	Benzene carboxylic acid	**$L^{10}H'$**
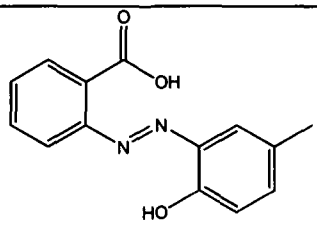	2-[(*E*)-2-(2-hydroxy-5-methyl-phenyl)-1-diazenyl]benzoic acid	**$L^{11}H'$**
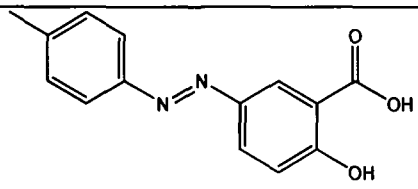	5-[(*E*)-2-(4-methylphenyl)-1-diazenyl]-2-hydroxybenzoic acid	**$L^{12}H'$**

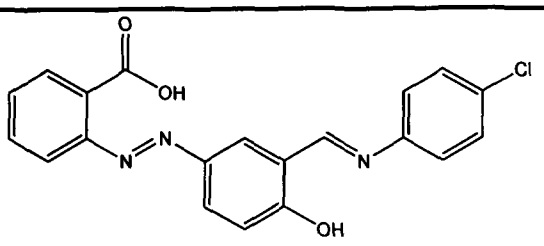	2-{(*E*)-4-hydroxy-3-[(*E*)-4-chloro-phenyliminomethyl]phenyldiazenyl} benzoic acid	$L^{13}H'$
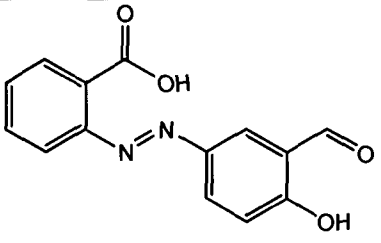	2-[(*E*)-2-(3-formyl-4-hydroxy-phenyl)-1-diazenyl]benzoic acid	$L^{14}H'$

[a]H and H' refer to the replaceable protons in the ligands $L^{1-9}H$ and $L^{10-14}H'$, respectively.

2.3. Synthesis of ligands

The 5-[(*E*)-2-(aryl)-1-diazenyl]quinolin-8-ol ($L^{1-9}H$) and substituted benzoic acid ($L^{11}H'$, $L^{12}H'$ and $L^{14}H'$) ligands were prepared by the diazo-coupling reactions between the appropriate anilines and 8-hydroxyquinoline, *p*-cresol, salicylic acid and salicylaldehyde, respectively, in alkaline medium under cold conditions. On the other hand, $L^{13}H'$ was prepared by condensation of $L^{14}H'$ and *p*-chloroaniline in anhydrous toluene-ethanol mixture at reflux temperature.

The basic ligand frameworks are shown in Table 2.1, along with their abbreviations. The details of their synthesis are presented in Section 2.6 while their characterization data are summarized below.

2.4. Spectroscopic characterization

The ^{1}H and ^{13}C NMR signals of $L^{1-8}H$ [11-13] and $L^{11-14}H'$ [14-17] were assigned by the use of correlated spectroscopy (COSY), heteronuclear single-quantum correlation (HMQC) and heteronuclear multiple-bond connectivities (HMBC) experiments using gradient coherence selection and also by examining the spin-spin splitting pattern of the signals. The ^{1}H NMR integration values were completely consistent with the formulation of the products. The number of ^{13}C signals corresponds with the proposed formulations of the products. The basic ligand

frame-work is shown in Figs. 2.1- 2.2 along with the abbreviations and numbering schemes for spectroscopic analyses. The detailed spectral features are shown below:

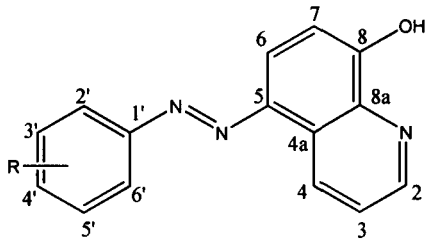

[Abbreviations: L^1H: X = H; L^2H: 2'-CH_3; L^3H: 3'-CH_3; L^4H: 4'-CH_3; L^5H: 4'-Br; L^6H: 4'-Cl; L^7H: 4'-OCH_3; L^8H: 4'-OCH_2CH_3; L^9H: 2'-$COOCH_3$]

Fig. 2.1 Generic structure of 5-[(*E*)-2-(aryl)-1-diazenyl]quinolin-8-ol ligands ($L^{1\text{-}8}H$) and the numbering proposal

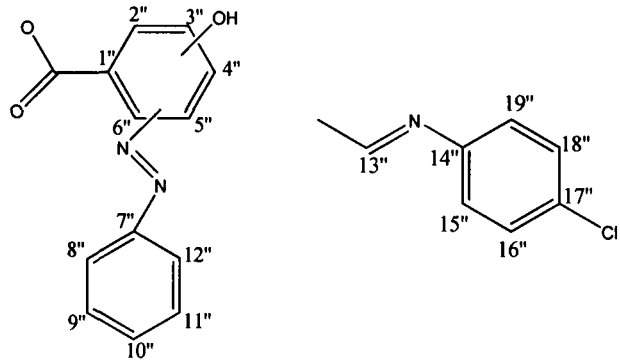

Fig. 2.2 Structures of the substituted benzoic acid ligands ($L^{10\text{-}14}H'$) and the numbering proposal

2.4.1. 5-[(E)-2-(phenyl)-1-diazenyl]quinolin-8-ol (L^1H)

^1H NMR ($CDCl_3$, 500 MHz); δ_H: 9.31 [dd, 1H, H4], 8.88 [d, 1H, H2], 8.06 [d, 1H, H6], 7.99 [d, 2H, H2'and H6'], 7.62 [m, 1H, H3], 7.54 [m, 2H, H3'and H5'], 7.48 [m, 1H, H4'], 7.27 [d, 1H, H7] ppm. The signal for the phenol was exchanged due to presence of water in the solvent. ^{13}C NMR ($CDCl_3$); δ_C: 155.4 [C8], 153.2 [C1'], 148.4 [C2], 139.9 [C5], 137.7 [C8a], 132.9 [C4], 130.6 [C4'], 129.1 [C3'and C5'], 127.3 [C4a], 122.81 [C2'and C6'], 122.80 [C3], 115.5 [C6], 109.9 [C7] ppm.

2.4.2. 5-[(E)-2-(2-methylphenyl)-1-diazenyl]quinolin-8-ol (L^2H)

^{1}H NMR ($CDCl_3$, 500 MHz); δ_H: 9.33 [dd, 1H, H4], 8.87 [dd, 1H, H2], 8.03 [d, 1H, H6], 7.74 [d, 1H, H6'], 7.61 [m, 1H, H3], 7.36 [d, 2H, H4'and H5'], 7.30 [m, 1H, H3'], 7.27 [d, 1H, H7], 2.77 [s, 3H, CH_3] ppm.. The signal for the phenol was exchanged due to presence of water in the solvent. ^{13}C NMR ($CDCl_3$); δ_C: 155.2 [C8], 151.2 [C1'], 148.4 [C2], 140.4 [C5], 137.9 [C2'], 137.7 [C8a], 133.0 [C4], 131.5 [C3'], 130.6 [C4'], 127.2 [C4a], 126.4 [C5'], 122.8 [C3], 115.8 [C6'], 115.6 [C6], 109.9 [C7], 17.7 [CH_3] ppm.

2.4.3. 5-[(E)-2-(3-methylphenyl)-1-diazenyl]quinolin-8-ol (L^3H)

^{1}H NMR ($CDCl_3$, 500 MHz); δ_H: 9.30 [dd, 1H, H4], 8.86 [dd, 1H, H2], 8.03 [d, 1H, H6], 7.79 [d, 2H, H2'and 6'], 7.60 [m, 1H, H3], 7.41 [d, 1H, H5'], 7.28 [d, 1H, H4'], 7.26 [d, 1H, H7], 2.48 [s, 3H, CH_3] ppm. The signal for the phenol was exchanged due to the presence of water in the solvent. ^{13}C NMR ($CDCl_3$); δ_C: 155.3 [C8], 153.2 [C1'], 148.4 [C2], 139.9 [C5], 138.9 [C3'], 137.7 [C8a], 132.9 [C4], 131.4 [C4'], 128.9 [C5'], 127.2 [C4a], 123.2 [C2'], 122.7 [C3], 120.2 [C6'], 115.4 [C6], 110.0 [C7], 21.4 [CH_3] ppm.

2.4.4. 5-[(E)-2-(4-methylphenyl)-1-diazenyl]quinolin-8-ol (L^4H)

^{1}H NMR ($CDCl_3$, 500 MHz); δ_H: 9.29 [dd, 1H, H4], 8.86 [dd, 1H, H2], 8.03 [d, 1H, H6], 8.01 [m, 2H, H2'and H6'], 7.59 [m, 1H, H3], 7.32 [m, 2H, H3'and H5'], 7.26 [d, 1H, H7], 2.44 [s, 3H, CH_3] ppm. The signal for the phenol was exchanged due to the presence of water in the solvent. ^{13}C NMR ($CDCl_3$); δ_C: 155.1 [C8], 151.3 [C1'], 148.3 [C2], 141.1 [C4'], 139.9 [C5], 137.7 [C8a], 132.9 [C4], 129.7 [C3'and C5'], 127.2 [C4a], 122.8 [C2'and C6'], 122.6 [C3], 115.2 [C6], 109.9 [C7], 21.5 [CH_3] ppm.

2.4.5. 5-[(E)-2-(4-bromophenyl)-1-diazenyl]quinolin-8-ol (L^5H)

^{1}H NMR (DMSO-d_6, 500 MHz); δ_H: 9.34 [dd, 1H, H4], 9.04 [dd, 1H, H2], 8.05 [d, 1H, H6], 7.99 [m, 2H, H2'and H6'], 7.67 [m, 2H, H3'and H5'], 7.82 [m, 1H, H3], 7.25 [d, 1H, H7] ppm. The signal for the phenol was exchanged due to the presence of water in the solvent. ^{13}C NMR (DMSO-d_6); δ_C: 158.1 [C8], 151.5 [C1'], 149.1 [C2], 138.7 [C5], 137.9 [C8a], 132.5

[C3'and C5'], 131.9 [C4], 127.6 [C4a], 124.4 [C2'and C6'], 124.1 [C4'], 123.4 [C3], 115.2 [C6], 111.8 [C7] ppm.

2.4.6. 5-[(E)-2-(4-chlorophenyl)-1-diazenyl]quinolin-8-ol (L^6H)

^{1}H NMR (DMSO-d_6, 500 MHz); δ_H: 9.33 [dd, 1H, H4], 9.02 [dd, 1H, H2], 8.04 [d, 1H, H6], 8.04 [m, 2H, H2'and H6'], 7.79 [m, 1H, H3], 7.68 [m, 2H, H3'and H5'], 7.25 [d, 1H, H7] ppm. The signal for the phenol was exchanged due to the presence of water in the solvent. ^{13}C NMR (DMSO-d_6); δ_C: 157.8 [C8], 151.3 [C1'], 149.0 [C2], 138.8 [C4'], 138.0 [C5], 135.2 [C8a], 131.8 [C4], 129.5 [C3'and C5'], 127.5 [C4a], 124.1 [C2'and C6'], 123.3 [C3], 115.4 [C6], 111.6 [C7] ppm.

2.4.7. 5-[(E)-2-(4-methoxyphenyl)-1-diazenyl]quinolin-8-ol (L^7H)

^{1}H NMR ($CDCl_3$, 500 MHz); δ_H: 9.29 [dd, 1H, H4], 8.87 [dd, 1H, H2], 8.02 [d, 1H, H6], 7.98 [m, 2H, H2'and H6'], 7.60 [m, 1H, H3], 7.27 [d, 1H, H7], 7.05 [m, 2H, H3'and H5'], 3.91 [s, 3H, CH_3] ppm. The signal for the phenol was exchanged due to the presence of water in the solvent. ^{13}C NMR ($CDCl_3$); δ_C: 161.9 [C8], 154.8 [C1'], 148.4 [C2], 147.5 [C4'], 140.2 [C5], 137.8 [C8a], 132.9 [C4], 127.1 [C4a], 124.6 [C3'and C5'], 122.6 [C3], 115.1 [C6], 114.3 [C2'and C6'], 109.9 [C7], 55.6 [CH_3] ppm.

2.4.8. 5-[(E)-2-(4-ethoxyphenyl)-1-diazenyl]quinolin-8-ol (L^8H)

^{1}H NMR ($CDCl_3$, 500 MHz); δ_H: 9.29 [dd, 1H, H4], 8.84 [dd, 1H, H2], 8.01 [d, 1H, H6], 7.93 [m, 2H, H2'and H6'], 7.58 [m, 1H, H3], 7.23 [d, 1H, H7], 6.99 [m, 2H, H3'and H5'], 4.12 [q, 2H, O$CH_2$$CH_3$], 1.48 [t, 3H, OCH_2CH_3] ppm. The signal for the phenol was exchanged due to the presence of water in the solvent. ^{13}C NMR ($CDCl_3$); δ_C: 161.2 [C8], 154.7 [C1'], 148.4 [C2], 147.4 [C4'], 140.0 [C5], 137.7 [C8a],132.9 [C4], 124.6 [C3'and C5'], 127.0 [C4a], 114.6 [C2'and C6'], 122.6 [C3], 114.5 [C6], 110.0 [C7], 63.6 [OCH_2CH_3], 14.8 [OCH_2CH_3] ppm.

2.4.9. 2-[(E)-2-(2-hydroxy-5-methylphenyl)-1-diazenyl]benzoic acid ($L^{11}H'$), 5-[(E)-2-(4-methylphenyl)-1-diazenyl]-2-hydroxybenzoic acid ($L^{12}H'$), 2-{(E)-4-hydroxy-3-[(E)-4-chlorophenyliminomethyl]phenyldiazenyl}benzoic acid ($L^{13}H'$) and 2-[(E)-2-(3-formyl-4-hydroxy-phenyl)-1-diazenyl]benzoic acid ($L^{14}H'$)

Ligands ($L^{11\text{-}14}H'$) used for preparing mixed ligand complexes were characterized by ^{1}H, ^{13}C NMR and the values correspond well with those reported previously [14-17].

2.5. X-ray crystallography

Crystals of the 5-[(*E*)-2-(4-ethoxyphenyl)-1-diazenyl]quinolin-8-ol ($L^{8}H$) and methyl 2-{[(*E*)-8-oxo-5,8-dihydroquinolin-5-ylidene]hydrazino}benzoate ($L^{9}H$) suitable for an X-ray crystal structure determination were obtained from benzene ($L^{8}H$) and ethylacetate/methanol mixture ($L^{9}H$) by slow evaporation of the solvent at room temperature. The crystal structures of two of the ligands ($L^{8}H$ and $L^{9}H$) have been determined. The data collection and refinement parameters for $L^{8}H$ and $L^{9}H$ are given in Table 2.2, while their selected geometric parameters are collected in Table 2.3. The structures of the ligands $L^{8}H$ and $L^{9}H$ are discussed in sequel:

2.5.1. Crystal structure of 5-[(E)-2-(4-ethoxyphenyl)-1-diazenyl]quinolin-8-ol ($L^{8}H$) [12]

The ligand $L^{8}H$ exists as the *trans*-isomer. In the solid state, both intra and intermolecular H bonds occur. The intramolecular hydrogen bond between the hydroxy H and the N atom (O···N = 2.755(2) Å, O–H···N = 115°) can be assigned the graph set symbol $S_1^1(5)$ [18], whereas the intermolecular H bond (O···N = 2.865(2) Å ,O–H···N = 137°) corresponds to the formation of a $R_2^2(10)$ ring and links neighboring molecules around inversion centres to dimers (Fig. 2.3).

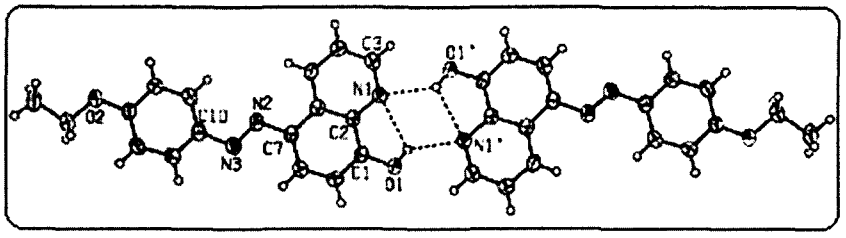

Fig. 2.3 View of the molecule of $L^{8}H$ showing the atom-labelling scheme (50% probability ellipsoids).

The same hydrogen bond pattern is observed for the isomer 5-[(2-ethoxyphenyl)-1-diazenyl]quinolin-8-ol described by Chen *et al.* [10].

Table 2.2: Crystallographic data and structure refinement parameters for the ligands (L^8H-L^9H)

	L^8H	L^9H
Empirical formula	$C_{17}H_{15}N_3O_2$	$C_{17}H_{13}N_3O_3$
Formula weight	293.32	307.30
Crystal size (mm)	0.4 × 0.3 × 0.1	0.35 × 0.13 × 0.05
Crystal shape	Plate	Prism
Temperature (K)	223(2)	98(2)
Crystal system	Monoclinic	Monoclinic
Space group	$P2_1/c$	$C2/c$
a (Å)	10.5775(14)	26.695(3)
b (Å)	11.1957(12)	8.2513(9)
c (Å)	12.7553(14)	13.5873(16)
β(°)	107.840(11)	116.589(5)
V (Å^3)	1437.9(3)	2676.3(5)
Z	4	8
D_x (g cm^{-3})	1.355	1.525
μ (mm^{-1})	0.091	0.11
Reflections measured	11496	7939
Independent reflections (R_{int})	2959 (0.076)	2329(0.024)
Reflections with $I > 2\sigma(I)$	1668	2165
Number of parameters	200	209
$R(F)$ ($I > 2\sigma(I)$ reflns)	0.0530	0.062
$wR(F^2)$ (all data)	0.1213	0.132
GOF(F^2)	1.00	1.36
max, min $\Delta\rho$ (e/Å^3)	0.167, -0.160	0.24, -0.23

Table 2.3: Selected bond lengths (Å) and angles (°) for L^8H and L^9H

L^8H		L^9H	
O(1)-C(1)	1.352(2)	O(1)-C(1)	1.209(3)
N(1)-C(2)	1.366(2)	N(1)-C(9)	1.341(3)
N(1)-C(3)	1.312(3)	N(1)-C(8)	1.320(3)
N(2)-N(3)	1.262(2)	N(2)-N(3)	1.327(3)
C(7)-N(2)-N(3)-C(10)	-179.24(18)	C(4)-N(2)-N(3)-C(10)	178.5(2)

2.5.2. Crystal structure of Methyl 2-{[(E)-8-oxo-5,8-dihydro-quinolin-5-ylidene]hydrazino}-benzoate (L^9H) [13]

In contrast to the structure of L^8H (see Section 2.5.1), the crystal structure of L^9H shows (Fig. 2.4) to exist as the phenylhydrazone tautomer, rather than in azo form as described by Sawicki [19].

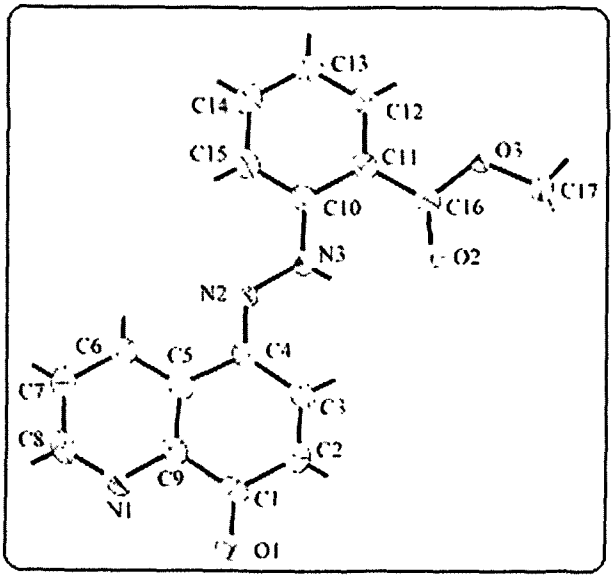

Fig. 2.4 Molecular structure of L^9H showing the atom-labelling scheme (50% probability ellipsoids)

The non-H atoms in L^9H are effectively co-planar and the dihedral angle between the N1/C1–C9 and C10–C15 ring plane is 1.33 (10)°. An intramolecular N3–H···O2 hydrogen bond contributes to the stability of the observed conformation; an intramolecular C12–H···O3

interaction is also noted. Intermolecular C8–H···O1 interactions lead to the formation of supramolecular chains aligned along the *b*-axis (Fig. 2.5, Table 2.4). These stack side-by-side to form layers and interactions between these layers are of the type C–H···O and C–H···N and involves the methyl groups (Fig. 2.6). A very closely related molecule characterized in the tautomeric form shown in Fig. 2.4 has been observed for dibenzyltin(IV) structure [20].

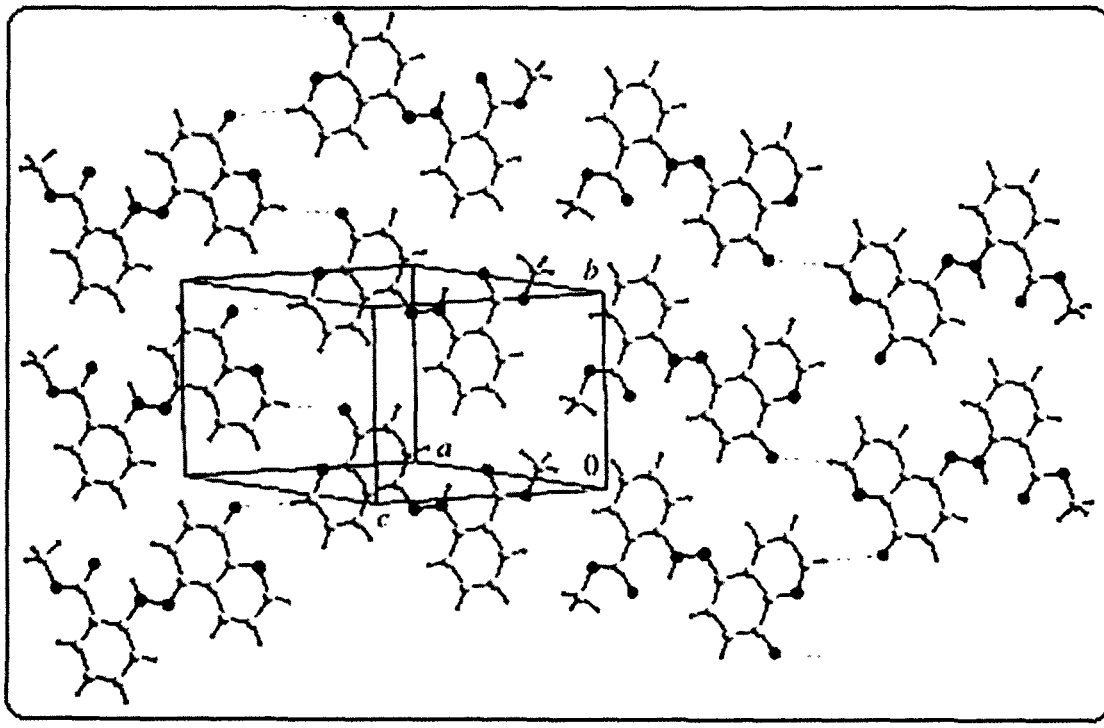

Fig. 2.5 View of the supramolecular chain in L^9H mediated by hydrogen bonds

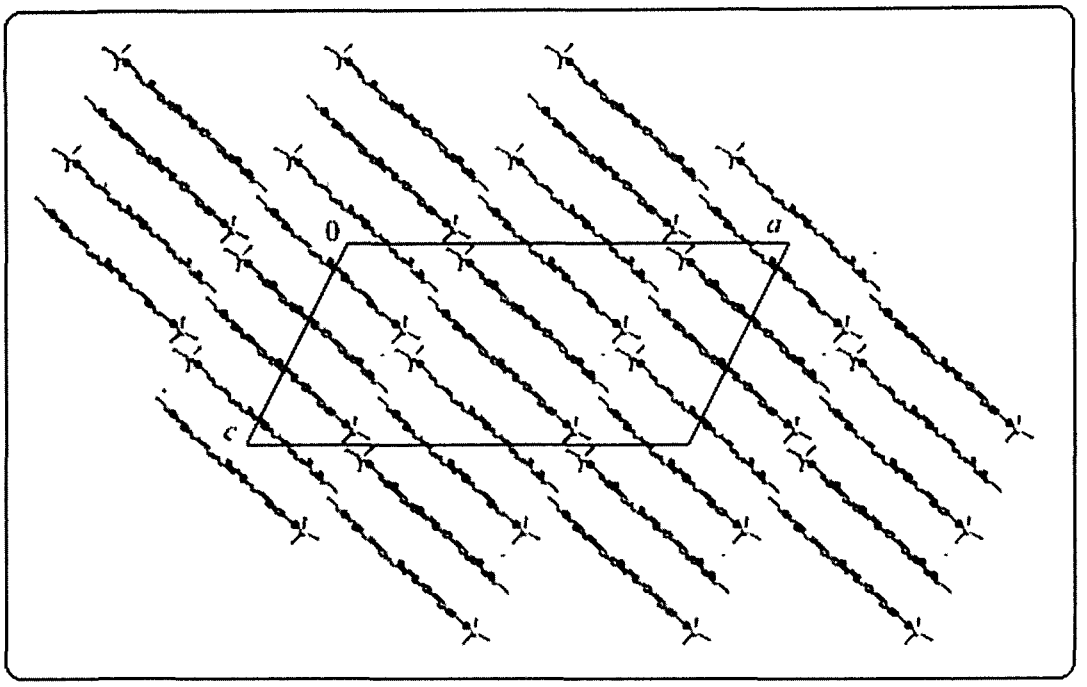

Fig. 2.6 Unit cell packing diagram in L^9H highlighting the stacking of layers

Table 2.4: Hydrogen bonding geometry (Å, °) for L^9H.

D-H···A	D-H	H···A	D···A	D-H···A
N(3)-H3N···O(2)	0.88	1.96	2.633(3)	132
C(12)-H(12)···O(3)	0.95	2.32	2.662(3)	101
C(8)-H(8)···O(1^{i})	0.95	2.51	3.425(3)	161
C(17)-H(17B)···O(1^{ii})	0.98	2.49	3.227(4)	132
C(17)-H(17C)···N(1^{iii})	0.98	2.59	3.379(3)	138

Symmetry codes: (i) -x +1/2, y-1/2, -z-1/2; (ii) x +1/2, -y +5/2, z +1/2; (iii) -x +1, y, -z +1/2.

2.6. Optimized structures of ligands (Quantum chemical calculations)

The optimized structures for the ligands (L^1H and L^2H- L^8H) are shown in Fig. 2.7 while the geometrical parameters for L^1H, L^2H–L^8H are listed in Table 2.5.

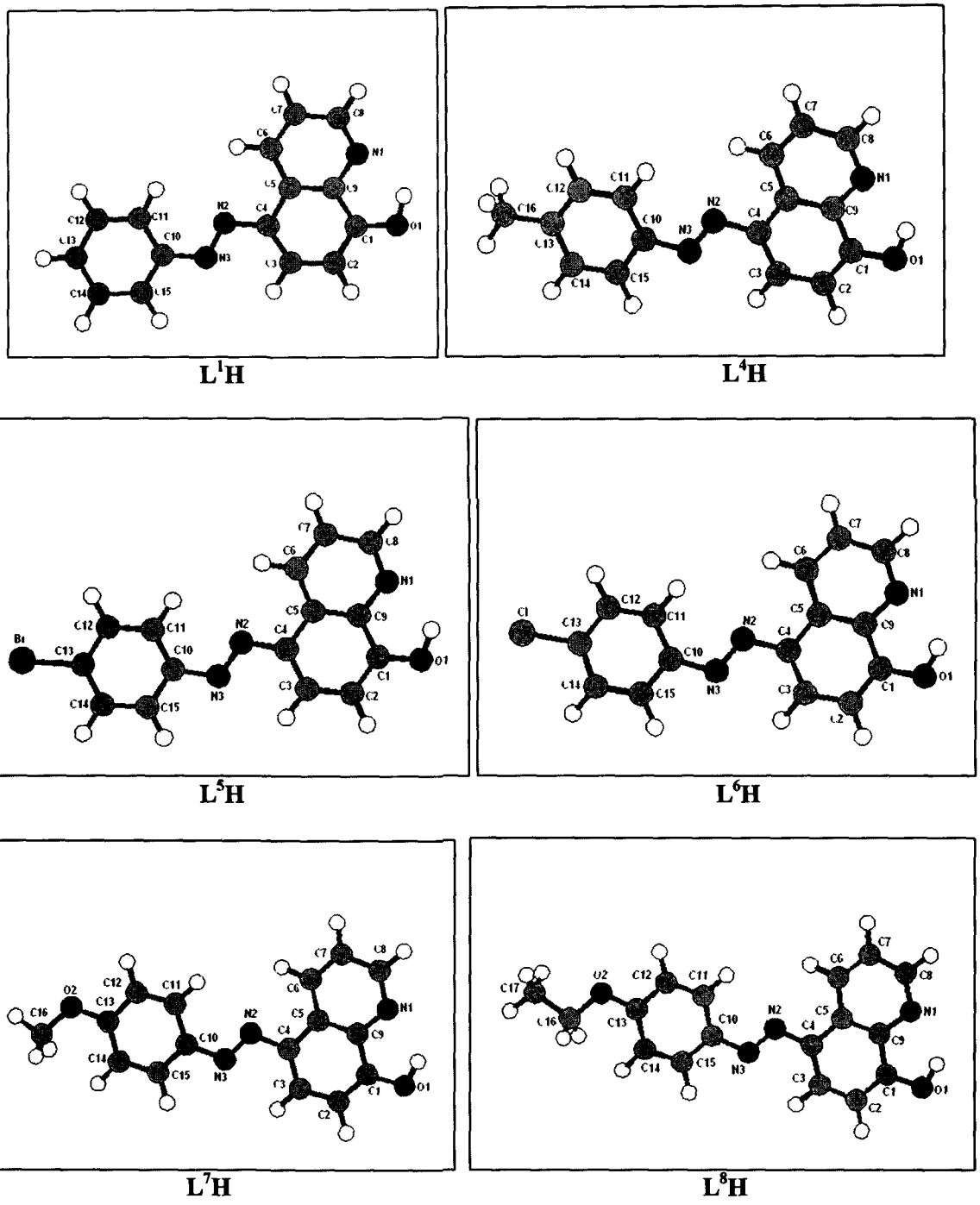

Fig. 2.7 Structures of ligands (L^1H, L^4H-L^8H) obtained after full geometry optimization at DFT level (see text).

Table 2.5: Selected bond lengths (Å), angles (°), and torsion angles (°) for optimized structures B3LYP/6-31G(d)) of ligands (L^1H, L^4H–L^8H)[a]

Bond lengths (Å) / angles (°)	**L^1H**	**L^4H**	**L^5H**	**L^6H**	**L^7H**	**L^8H (Calc)**	**L^8H (Expt.)[b]**
O(1)-C(1)	1.344	1.344	1.343	1.343	1.345	1.345	1.352(2)
O(2)-C(13)	-	1.509[c]	-	-	1.361	1.359	1.362(3)
O(2)-C(16)	-	-	-	-	1.420	1.429	1.429(2)
N(1)-C(8)	1.319	1.319	1.319	1.319	1.319	1.319	1.312(3)
N(1)-C(9)	1.360	1.344	1.360	1.360	1.360	1.361	1.366(2)
N(2)-N(3)	1.265	1.265	1.266	1.266	1.266	1.266	1.262(2)
N(2)-C(4)	1.405	1.406	1.403	1.403	1.406	1.406	1.422(3)
N(3)-C(10)	1.415	1.413	1.413	1.413	1.408	1.408	1.418(3)
C(1)-C(2)	1.387	1.387	1.387	1.387	1.386	1.386	1.367(3)
C(1)-C(9)	1.431	1.430	1.431	1.431	1.430	1.429	1.419(3)
O(1)-H	0.984	0.984	0.984	0.984	0.984	0.984	-
C(9)-N(1)-C(8)	117.8	118.0	117.8	117.8	117.8	117.8	116.97(19)
O(1)-C(1)-C(9)	118.4	118.4	118.4	118.4	118.4	121.8	120.86(19)
C(4)-N(2)-N(3)-C(10)	-179.8	-179.	180.0	179.9	180.0	-179.9	-179.24(18)

[a] Refer to Fig.2.7 for numbering scheme.
[b] Data obtained from crystal structure.
[c] C(13)-C(16) distance.

The X-ray experimental geometric parameters for L^8H are also included in Table 2.5 along with calculated values for comparison. The calculated values agree well with the experimental data. Most of the geometric parameters are found to be insensitive to the nature of the substituents. However, the substituents can have a strong effect on the basicity of donor atoms, as discussed later (see Chapter 6).

2.7. Experimental

2.7.1. Synthesis of ligands

2.7.1.1. Preparation of 5-[(E)-2-(phenyl)-1-diazenyl]quinolin-8-ol (L^1H) [12]

Aniline (5.0 g, 53.7 mmol) was mixed with HCl (16 ml) and water (16 ml) and digested in a water bath for an hour. The hydrochloride was cooled to 5°C and diazotized with ice-cold aqueous $NaNO_2$ solution (3.7 g, 53.6 mmol, 25 ml). A cold solution of 8-hydroxyquinoline (7.78 g, 53.6 mmol), previously dissolved in 10% NaOH solution (5 g, 50 ml), was then added to the cold diazonium salt solution with vigorous stirring. A yellow colour developed almost immediately and the stirring is continued for 1 h. The reaction mixture was kept overnight in a refrigerator followed by 2 h at room temperature. The precipitate was filtered, washed several times with water to remove the soluble starting materials, and dried in air. The crude product was washed with hexane to remove any tarry materials and recrystallized from methanol to yield yellow precipitate of L^1H (5.75 g, 42.9%), M.p.: 182-183 °C. Anal. Found: C, 72.35; H, 4.57; N, 16.90. Calc. for $C_{15}H_{11}N_3O$: C, 72.28; H, 4.45; N, 16.86%.

The other 5-[(*E*)-2-(aryl)-1-diazenyl]quinolin-8-ols, *viz.*, L^2H-L^8H were prepared analogously with appropriate anilines and their analytical data are presented below:

2.7.1.2. Preparation of 5-[(E)-2-(2-methylphenyl)-1-diazenyl]quinolin-8-ol (L^2H) [12]

Recrystallized from a mixture of methanol and benzene to give brown crystalline product in 69.4% yield. M.p.: 184-185 °C. Anal. Found: C, 73.10; H, 4.97; N, 16.21. Calc. for $C_{16}H_{13}N_3O$: C, 72.99; H, 4.98; N, 15.96%.

2.7.1.3. Preparation of 5-[(E)-2-(3-methylphenyl)-1-diazenyl]quinolin-8-ol (L^3H) [12]

Recrystallized from a mixture of methanol and benzene to give brown crystalline product in 64.8% yield; M.p.: 159-60 °C. Anal. Found: C, 73.20; H, 5.03; N, 16.20. Calc. for $C_{16}H_{13}N_3O$: C, 72.99; H, 4.98; N, 15.96%.

2.7.1.4. Preparation of 5-[(E)-2-(4-methylphenyl)-1-diazenyl]quinolin-8-ol (L^4H) [12]

Recrystallized from chloroform to give brick red micro-crystalline product in 63% yield; M.p.: 188-189 °C. Anal Found: C, 72.88; H, 5.01; N, 15.86. Calc. for $C_{16}H_{13}N_3O$: C, 72.99; H, 4.98; N, 15.96%.

2.7.1.5. Preparation of 5-[(E)-2-(4-bromophenyl)-1-diazenyl]quinolin-8-ol (L^5H) [12]

Recrystallized from a mixture of ethanol and benzene to give yellowish brown precipitate in 65.5% yield; M.p.: 210-211 °C. Anal. Found: C, 55.23; H, 3.12; N, 12.86. Calc. for $C_{15}H_{10}BrN_3O$: C, 54.99; H, 3.07; N, 12.80%.

2.7.1.6. Preparation of 5-[(E)-2-(4-chlorophenyl)-1-diazenyl]quinolin-8-ol (L^6H) [11]

Recrystallized from a mixture of ethanol and benzene to give a yellowish brown precipitate in 59.1% yield; M.p.: 220-221°C. Anal. Found: C, 63.40; H, 3.40; N, 14.86. Calc. for $C_{15}H_{10}ClN_3O$: C, 63.50; H, 3.50; N, 14.81%.

2.7.1.7. Preparation of 5-[(E)-2-(4-methoxyphenyl)-1-diazenyl]quinolin-8-ol (L^7H) [11]

Recrystallized from methanol to give a brownish yellow precipitate in 44.1% yield; M.p.: 170-171 °C. Anal. Found: C, 68.70; H, 4.70; N, 15.21. Calc. for $C_{16}H_{13}N_3O_2$: C, 68.75; H, 4.60; N, 15.05%.

2.7.1.8. Preparation of 5-[(E)-2-(4-ethoxyphenyl)-1-diazenyl]quinolin-8-ol (L^8H) [12]

Recrystallized from chloroform to give dark brown microcrystalline product in 64.6% yield; M.p.:180-181 °C. Anal. Found: C, 69.50; H, 5.11; N, 14.52. Calc. for $C_{17}H_{15}N_3O_2$: C, 69.61; H, 5.15; N, 14.33%.

2.7.1.9. Preparation of Methyl 2-{[(E)-8-oxo-5,8-dihydro-quinolin-5-ylidene]hydrazino}-benzoate (L^9H) [13]

Methyl anthranilate (5.0 g, 33.1 mmol) was mixed with HCl (11 ml) and water (11 ml) and digested in a water bath for 1 h. The hydrochloride was cooled to 278 K and diazotized with ice-cold aqueous $NaNO_2$ solution (5.0 g, 72.45 mmol, 25 ml). A cold solution of quinolin-8-ol (5.0 g, 34 .4 mmol), previously dissolved in methanol solution (70 ml), was then added to the cold diazonium salt solution with stirring maintaining the temperature around 0 °C. A light-orange colour developed and the stirring was continued for 1 h. A saturated solution of potassium acetate was then added to neutralize the hydrochloric acid, thereupon a deep-red precipitate appeared and stirring was continued for an additional hour. The reaction mixture was kept overnight in a refrigerator followed by 2 h at room temperature. The precipitate was filtered, washed several times with water to remove soluble starting materials, and dried in air. The crude product was washed with hexane to remove tarry materials, dried *in vacuo* and recrystallization from a methanol solution afforded orange microcrystalline compound in 53.6% (5.67 g) yield.

M.p.: 242-244 °C. Anal. Found: C, 48.59; H, 2.80; N, 8.68. Calc. for $C_{13}H_9BrN_2O_3$: C, 48.63; H, 2.83; N, 8.72 %.

2.7.1.10. Preparation of 2-[(E)-2-(2-hydroxy-5-methylphenyl)-1-diazenyl]benzoic acid ($L^{11}H'$) [14]

Recrystallized from methanol to give brown precipitate in 50% yield. M.p.: 188-190 °C. Anal. Found: C, 65.26; H, 4.60; N, 10.89. Calc. for $C_{14}H_{12}N_2O_3$: C, 65.62; H, 4.72; N, 10.93 %.

2.7.1.11. Preparation of 5-[(E)-2-(4-methylphenyl)-1-diazenyl]-2-hydroxybenzoic acid ($L^{12}H$) [15]

Recrystallized from methanol to give yellow precipitate in 50% yield. M.p.: 217-218 °C. Anal. Found: C, 65.88; H, 4.67; N, 10.82. Calc. for $C_{14}H_{12}N_2O_3$: C, 65.62; H, 4.72; N, 10.93 %.

2.7.1.12. Preparation of 2-{(E)-4-hydroxy-3-[(E)-4-chlorophenyliminomethyl]phenyldiazenyl}-benzoic acid ($L^{13}H$) [16]

Recrystallized from ethanol to give orange precipitate in 62% yield. M.p.: 225-226 °C. Anal. Found: C, 63.82; H, 11.88; N, 8.68. Calc. for $C_{20}H_{14}ClN_3O_3$: C, 63.25; H, 3.72; N, 11.6 %.

2.7.1.13. Preparation of 2-[(E)-2-(3-formyl-4-hydroxy-phenyl)-1-diazenyl]benzoic acid ($L^{14}H$) [17]

Recrystallized from toluene to give yellow precipitate in 50% yield. M.p.: 177-79 °C. Anal. Found: C, 62.10; H, 3.80; N, 10.68. Calc. for $C_{14}H_{10}N_2O_4$: C, 62.22; H, 3.73; N, 10.37 %.

2.7.2. Chemicals used for the preparations

Oxine (Merck) and benzoic acid (Aldrich) were used as such while substituted anilines (reagent grade) were either recrystallized or distilled prior to use. All the solvents used in the reactions were of AR grade and dried using standard literature procedures.

2.7.3. Physical measurements

Carbon, hydrogen and nitrogen analyses were performed with a Perkin-Elmer 2400 series II instrument. IR spectra in the range 4000-400 cm^{-1} were obtained on a BOMEM DA-8 FT-IR spectrophotometer with samples investigated as KBr disc. The two-dimensional experiments for the ligands were performed on a Bruker Avance 500 spectrometer equipped with a triple

($^1H/^{13}C$/broadband) 5 mm inverse probe operating at 500.13 and 125.76 MHz, respectively. The ^1H and ^{13}C chemical shifts were referred to Me_4Si set at 0.00 ppm, respectively.

2.7.4. X-ray crystallography

Crystals of the ligands suitable for an X-ray crystal-structure determination were obtained from benzene (L^8H) and ethylacetate/ methanol mixture (L^9H) by slow evaporation of the solvent at room temperature.

The intensity data for L^8H was measured on a Nonius CAD4 diffractometer at 223(2) K while L^9H was measured on a Rigaku AFC12K SATURN724 diffractometer at 98(2) K using Mo Kα raditaion (λ = 0.71073 Å). Crystal data, data collection parameters and convergence results are listed in Table 2.2. Views of the structures are shown in Figs. 2.3 (for L^8H) and 2.4 (for L^9H).

The structure of L^8H solved by direct methods with the help of the SHELXS-97 [21] while the structure of L^9H was solved by direct methods by using SIR92 [22] and refined on reflection intensities F^2 using the SHELXL-97 program [23]. In the final least-squares refinements, all non-hydrogen atoms were refined with anisotropic displacement parameters, and hydrogen atoms were placed in idealized positions and included as riding on the corresponding atoms.

2.7.5. Quantum chemical calculations

The geometries of the unsubstituted ligand (L^1H) and *para*-substituted ligands, *viz.*, L^2H–L^8H were optimized using the B3LYP [24] density functional theory (DFT) method with the 6-31G(d) basis set. Harmonic frequency calculations were performed at all the stationary points to characterize its nature and to ensure that the optimized structure corresponds to a global minimum. The optimized structures of an unsubstituted ligand (L^1H) and *para*-substituted ligand (L^2H–L^8H) are shown in Fig. 2.7 while the geometric parameters for L^1H, L^2H–L^8H are listed in Table 2.5. The basicity of the N(1) atom of the ligand and the O(1) atom of the corresponding anion generated after removal of the H-atom of the O(1)H group is estimated from the proton affinity of the N(1) atom [PA (N(1))] and the O(1) atom [PA (O(1))]. The PA for a base (B) is defined as the negative of the enthalpy (H) change for the reaction:

$$B + H \rightarrow BH^+$$

Therefore, at any finite temperature (T) the PA can be estimated from the expression:

$$PA = H(B) + H(H^+) - H(BH^+)$$

At 0 K, $H(H^+)$ can be taken as zero and H(B) = E(B), where E(B) is the energy of base B at 0 K. In the present calculations, the PA values at 0 K were estimated simply from the total energies

calculated at the B3LYP/6-311G(d,p)//6-31G(d) level: PA(N(1)) = E(L–H) – E(L–H–NH^+) and PA(O(1)) = E(L–O^-) – E(L–H). In the present study, the main aim is to calculate relative PA values for the ligands and for this purpose, the B3LYP method [25,26] was used which is known to produce reliable PA values. Gaussian-03 program was used for all the electronic structure calculations [27].

References

[1] V.M. Ivanov, T.F. Rudometkina, Zh. Anal. Khim. **33** (1978) 2426.

[2] K.D. Ghuge, P. Umapathy, M.P. Gupta, D.N. Sen, Inorg. Nucl. Chem. **43** (1981) 653.

[3] T.S. Basu Baul, T.K. Chattopadhyay, B. Majee, Polyhedron **2** (1983) 635.

[4] B.K. Deb, A.K. Ghosh, Can. J. Chem. **65** (1987) 1241.

[5] T.S. Basu Baul, T.K. Chattopadhyay, B. Majee, Ind. J. Chem. A **23** (1984) 470.

[6] E. El-Sawi, F.A. Moti, S. El-Messary, Bull. Soc. Chim. (Belg.) **94** (1985) 69.

[7] T.S. Basu Baul, T.K. Sinha, R. Saran, Synth. React. Inorg. Met.-Org. Chem. **25** (1995) 615.

[8] T.S. Basu Baul, D. Dey, Synth. React. Inorg. Met.-Org. Chem. **19** (1989) 101.

[9] P.K. Bajpai, B. Pal, T.S. Basu Baul, J. Raman Spectrosc. **26** (1995) 351.

[10] X.-F. Chen, X.-H. Zhu, J.J. Vittal, X.-Z. You, Acta Crystallogr. C **55** (1999), IUC 9900095.

[11] T.S. Basu Baul, A. Mizar, X. Song, G. Eng, R. Willem, M.Biesemans, I. Verbruggen, R. Butcher, J. Organomet. Chem. **691** (2006) 2605.

[12] T.S. Basu Baul, A. Mizar, A. Lyčka, E. Rivarola, R. Jiràsko, M.Holčapek, D. de Vos, J. Organomet. Chem. **691** (2006) 3416.

[13] T.S. Basu Baul, A. Mizar, E. R. T. Tiekink, Acta Crystallogr. E **63** (2007) o4256.

[14] R. Willem, I. Verbruggen, M. Gielen, M. Biesemans, B. Mahieu, T.S. Basu Baul, E.R.T. Tiekink, Organometallics **17** (1998) 5758.

[15] T.S. Basu Baul, S. Dhar, S.M. Pyke, E.R.T. Tiekink, E. Rivarola, R. Butcher, F.E. Smith, J. Organomet. Chem. **633** (2001) 7.

[16] T.S. Basu Baul, K.S. Singh, X. Song, A. Zapata, G. Eng, A. Lyčka, A. Linden, J. Organomet. Chem. **689** (2004) 4702.

[17] T.S. Basu Baul, S.M. Pyke, K.K. Sarma, E.R.T. Tiekink, Main Group Met. Chem. **19** (1996) 807.

[18] M.C. Etter, J.C. MacDonald, J. Bernstein, Acta Crystallogr. B **46** (1990) 256.

[19] E. Sawicki, J. Org. Chem. **22** (1957) 743.

[20] T.S. Basu Baul, K.S. Singh, A. Lyčka, M. Holčapek, A. Linden, J. Organomet. Chem. **690** (2005) 1581.

[21] G.M. Sheldrick, SHELXL97, Program for Structure Solution, University of Göttingen, Germany, 1997.

[22] A. Altomare, M. Cascarano, C. Giacovazzo, A. Guagliardi, M.C. Burla, G. Polidori, M. Camalli, J. Appl. Cryst. **27** (1994) 435.

[23] G.M. Sheldrick, SHELXL97, Program for the Refinement of Crystal Structures, University of Göttingen, Germany, 1997.

[24] C. Lee, W. Yang, R.G. Parr, Phys. Rev.B **37** (1988) 785.

[25] A.K. Chandra, D.Michalska, R.Wysokinsky, T. Zeegers-Huyskens, J. Phys. Chem. Sect. A **108** (2004) 9593.

[26] A.K. Chandra, T. Zeegers-Huyskens, J. Org. Chem. **68** (2003) 3618.

[27] M.J. Frisch et al., Gaussian 03, Revision D.01, Gaussian, Inc., Wallingford, CT, 2004.

Chapter 3

Triphenyltin(IV) Complexes of 5-[(*E*)-2-(aryl)-1-diazenyl]quinolin-8-ol: Synthesis, Spectroscopic Characterization and X-ray Crystallography

CONTENTS

CHAPTER 3

TRIPHENYLTIN(IV) COMPLEXES OF 5-[(*E*)-2-(ARYL)-1-DIAZENYL]QUINOLIN-8-OL: SYNTHESIS, SPECTROSCOPIC CHARACTERIZATION AND X-RAY CRYSTALLOGRAPHY

3.1. Introduction	43
3.2. Synthesis of ~~Synthesis of~~ triphenyltin(IV) complexes	43-44
3.3. Spectroscopic characterization and X-ray crystallography of triphenyltin(IV) complexes	44-56
3.4. Structural précis of the triphenyltin(IV) complexes	56-57
3.5. Experimental	57-60
References	61-62

3.1. Introduction

The chemical, biological and pharmaceutical properties of organotin(IV) complexes have been extensively studied and in this perspective, the structure-antitumour activity relations have also been studied for triorganotin(IV) oxinates and thiooxinates [1]. Because of the important applications, the structures of this class of compounds have received considerable attention and some of the earlier publications have dealt with the coordinating behavior of 5-[(*E*)-2-(aryl)-1-diazenyl]-quinolin-8-ol towards triorganotin [2-5]. Various techniques such as IR, UV–Vis, ^{1}H NMR and ^{119}Sn Mössbauer spectroscopic techniques have been utilized to indicate the mode of coordination. There has been some disagreement concerning the structure of Ph_3SnL, both four- [6] and five-co-ordinate [7] structures having been assigned on the basis of ^{119}Sn Mössbauer from the magnitude of the quadrupole splitting. Finally it was concluded that Ph_3SnL is five coordinate where two phenyl groups and a nitrogen atom are in equatorial positions while a phenyl group and an oxygen atom from the quinolin-8-olate ligand takes up the apical positions [7]. Nevertheless, there is no report on structural characterization of Ph_3SnL by X-ray crystallographic technique.

The present chapter reports the synthesis of a series of triphenyltin(IV) 5-[(*E*)-2-(aryl)-1-diazenyl]-quinolin-8-olate ligand system (Refer to Chapter 2 for specific ligands $L^{1\text{-}4}H$ and $L^{7\text{-}8}H$) which is aimed at the evaluation of the bonding mode(s) of the triphenyltin(IV) complexes from a detailed analysis of their IR, NMR (^{1}H, ^{13}C, ^{119}Sn) and ^{119}Sn Mössbauer spectra. Further, in the course of studies in this area, a series of triphenyltin(IV) complexes provided X-ray quality crystals which have been chosen in the quest to determine the complete stereochemical analyses of the triphenyltin(IV) complexes. The crystal and molecular structures of four triphenyltin(IV) complexes, viz., $Ph_3SnL^1.0.5C_6H_6$ (**1**), Ph_3SnL^2 (**2**), $Ph_3SnL^5.C_6H_6$ (**5**), and $Ph_3SnL^6.0.5C_6H_6$ (**6**) are also reported. Compounds **1**, **2**, **5** and **6** represent the first examples of structurally characterized triphenyltin(IV) compounds containing the ligand quinolin-8-olate which are described in the subsequent section.

3.2. Synthesis of triphenyltin(IV) complexes

Various synthetic methodologies were tried to obtain a variety of triorganotin(IV) derivatives of 5-[(*E*)-2-(aryl)-1-diazenyl]quinolin-8-ols (LH) such as $^{n}Bu_3SnL$, Bz_3SnL and Ph_3SnL,

however, in most of the instances either a viscous mass or a disproportionated products were obtained. For examples, LH react with $(^nBu_3Sn)_2O$ in anhydrous toluene (or in absence of solvent) in a 2:1 molar ratio to give compounds of the formulation $^nBu_3SnL$ as confirmed from ^1H NMR spectra. In both the cases, the product was obtained as dark-red viscous mass which could not be crystallized. On the other hand, the reactions of Bz_3SnCl with LNa (generated in situ from Na and MeOH) in an equimolar ratio in anhydrous benzene were also attempted with the expectation of obtaining the corresponding $Bz_3Sn(IV)$ derivatives. Instead, the work-up of the reaction mixture yielded crystals of the debenzylated products of composition $Bz_2Sn(L)_2$ as confirmed from their melting point, microanalytical, spectroscopic and crystallographic data (see Chapter 4 for details). Attempted reactions of the LH with Bz_3SnOH in anhydrous toluene also afforded the same debenzylated products. However, the triphenyltin(IV) complexes were prepared by reacting the sodium salts of the ligands (LNa, generated in situ from Na and anhydrous methanol) with the Ph_3SnCl in 1:1 molar ratios in anhydrous benzene (see below) by following procedure similar to that described by Clark *et al.* [8]. The synthetic details and characterization data for the complexes are presented in Section 3.5.2 while their spectroscopic data are summarized in Section 3.3. The complexes could be isolated by fractional crystallization with high purity in moderate yield (28–54%). The complexes are crystalline in nature, stable in air and soluble in all common organic solvents.

$$LNa + Ph_3SnCl \xrightarrow[\text{Conditions: Stir / Reflux, 3 h}]{\text{Benzene}} Ph_3SnL + NaCl$$

3.3. Spectroscopic characterization and X-ray crystallography of triphenyltin(IV) complexes

This Section deals with the spectroscopic characterization and X-ray crystallography of triphenyltin(IV) complexes of 5-[(*E*)-2-(aryl)-1-diazenyl]quinolin-8-ols ($L^{1\text{-}4}H$ and $L^{7\text{-}8}H$). The specific ligands used herein are described in Chapter 2.

3.3.1. Triphenyltin(IV) complexes of $L^{1\text{-}4}H$ and $L^{7\text{-}8}H$ ($Ph_3SnL^{1\text{-}4}$ and $Ph_3SnL^{7\text{-}8}$)

The triphenyltin(IV) complexes of 5-[(*E*)-2-(aryl)-1-diazenyl]quinolin-8-ols ($L^{1\text{-}4}H$ and $L^{7\text{-}8}H$) (**1-6**) have been characterized by IR, ^1H, ^{13}C, ^{119}Sn NMR and ^{119}Sn Mössbauer spectroscopic techniques. The crystal structures of four compounds, *viz.*, $Ph_3SnL^1.0.5C_6H_6$ (**1**), Ph_3SnL^2 (**2**), $Ph_3SnL^7.C_6H_6$ (**5**), and $Ph_3SnL^8.0.5\ C_6H_6$ (**6**) are reported.

3.3.1.1. Infrared and ^{119}Sn Mössbauer data

The ν(OH) in L^1H–L^4H, L^7H and L^8H occurs at around 3380 cm^{-1} as broad band which is assigned due to the presence of intermolecular H-bonding interactions involving the O–H–N bonds which is found to be absent in the triphenyltin(IV) complexes, **1–6,** confirming bonding through the O-atom of the ligand [9,10]. A strong band at around 1235 cm^{-1} in the ligands is found to be shifted to around 1250 cm^{-1} in the complexes, is assigned to the ν(C(aryl)O) (i.e. C8-O).

The ^{119}Sn Mössbauer data, i.e. isomer shift (δ), quadrupole splittings (Δ) and the line widths at half-peak height (Γ) for the triphenyltin complexes (**1–6**) are given in Table 3.1. In general, the complexes displayed a doublet with δ and Δ values in the range 1.04–1.11 and 1.92–2.12, mm s^{-1}, respectively. The δ values found (1.04–1.11 mm s^{-1}) are typical of quadrivalent organotin derivatives [11]. The Ph_3SnL_2 (L = electronegative ligands, e.g., O, N and halogen) type compounds may exists in one of the three isomeric forms (**I–III**, Scheme 3.1) and they can be readily distinguished by the Δ values.

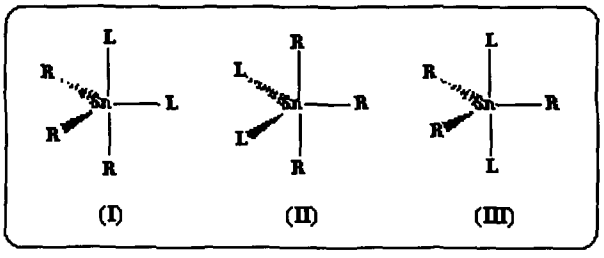

Scheme 3.1 Possible isomeric forms (**I-III**) in Ph_3SnL_2 type compounds.

On the basis of point charge treatment, the calculated Δ values for five-coordinate trigonal bipyramid Ph_3SnL_2 type compounds were ca. 1.65, 2.85 mm s^{-1} and 3.28 mm s^{-1} and these were assigned for the *facial*-(**I**), *equatorial*-(**III**) and *meridional*-R_3 (**II**) geometries,

Table 3.1 ^{119}Sn Mössbauer parameters (mm s^{-1}) and ^{119}Sn-NMR data (δ, ppm) for the triphenyltin(IV) complexes

Complex[a]	^{119}Sn Mössbauer data[b]				^{119}Sn-NMR data[c]
	δ	Δ	Γ_1	Γ_2	
$Ph_3SnL^1.0.5C_6H_6$ (1)	1.09	1.99	0.82	0.82	−183.9
Ph_3SnL^2 (2)	1.11	2.12	0.83	0.83	−184.5
Ph_3SnL^3 (3)	1.11	2.03	0.83	0.83	−184.3
Ph_3SnL^4 (4)	1.08	1.99	0.80	0.80	−184.1
$Ph_3SnL^7.C_6H_6$ (5)	1.06	1.92	0.89	0.89	−186.1
$Ph_3SnL^8.0.5\ C_6H_6$ (6)	1.04	1.95	0.86	0.86	−185.4

[a]Complex numbers are in parentheses.
[b]Parameters: δ, isomer shifts; Δ, quadrupole splitting; Γ_1 and Γ_2: line widths.
[c]In $CDCl_3$ solution.

respectively [12]. The observed Δ values for complexes are in the range 1.92–2.12 mm s^{-1} and the values are greater than for the *facial*-structure (**I**) and smaller for the *equatorial*-structure (**III**). Thus, it may be inferred that the complexes (**1–6**) adopt preferably a structure (**I**) and somewhat larger values reflect the possible distortion from the ideal proposed configuration. The Δ value of 1.75 mm s^{-1} for Ph_3SnOx (Ox = quinolin-8-olate) [7,13,14] also falls at the limit specified for *facial*-R_3 trigonal-bipyramidal geometry [11]. The larger Δ values observed in the triphenyltin 5-[(*E*)-2-(aryl)-1-diazenyl]quinolin-8-olate (**1–6**) compared to Ph_3SnOx could be ascribed to the coordination of bulky 5-[(*E*)-2-(aryl)-1-diazenyl]quinolin-8-olate ligand and agrees well with the value 1.99 mm s^{-1} reported for tribenzyltin(IV) complex $(C_6H_5CH_2)_3Sn(SPyO)$(HSPyO:2-mercaptopyridine) where a square pyramidal structure was reported [11]. The extent of distortion from *facial*-trigonal-bipyramidal geometry is clearly evident from the Mössbauer data and this has been clearly reflected from the results of diffraction studies (see Section 3.3.1.2) on some of the triphenyltin 5-[(*E*)-2-(aryl)-1-diazenyl]quinolin-8-olate (**1**, **2**, **5** and **6**).

3.3.1.2. X-ray crystallography

Crystals of the triphenyltin(IV) compounds $Ph_3SnL^1.0.5C_6H_6$ (**1**), Ph_3SnL^2 (**2**), $Ph_3SnL^7.C_6H_6$ (**5**) and $Ph_3SnL^8.0.5C_6H_6$ (**6**) suitable for single crystal X-ray structure determination were obtained from slow evaporation of benzene/hexane (1:1 v/v) solutions at room temperature. The crystal structures of four of the triphenyltin(IV) compounds **1**, **2**, **5** and **6** [15] have been determined. The data collection and refinement parameters are given in Table 3.2.

Compounds **1**, **2**, **5** and **6** represent the first examples of structurally characterized triphenyltin(IV) compounds containing the ligand quinolin-8-olate. In all the complexes, a single 5-[(*E*)-2-(aryl)-1-diazenyl]quinolin-8-olate ligand chelates the triphenyltin moiety, as illustrated in Figs. 3.1-3.4. Selected geometric parameters are collected in Tables 3.3-3.4.

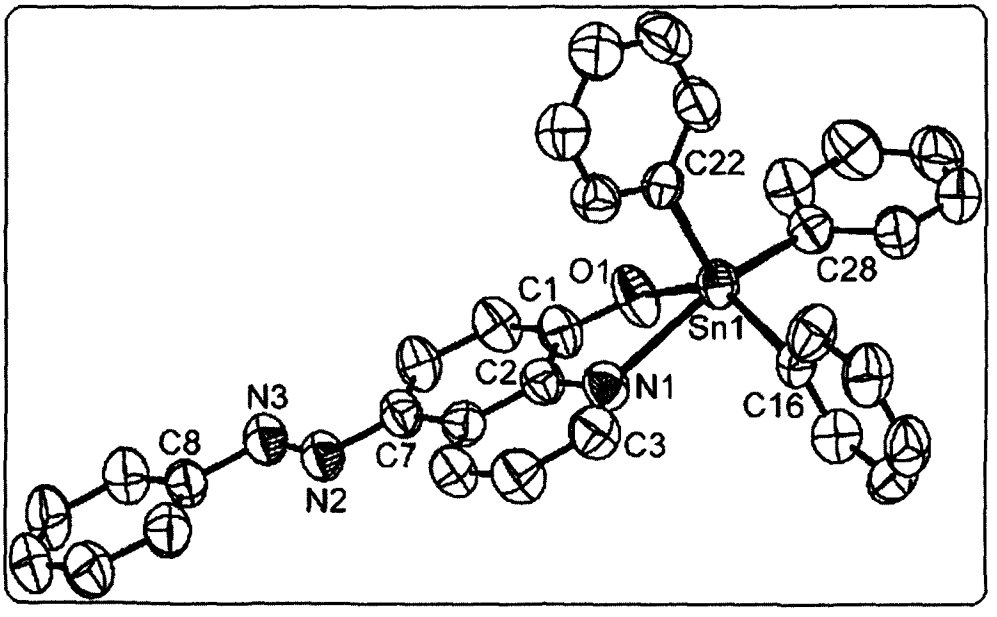

Fig. 3.1 Displacement ellipsoid plot (50% probability ellipsoids) of the molecular structure of $Ph_3SnL^1.0.5C_6H_6$ (**1**) showing the atom-labelling scheme. Hydrogen atoms and the solvent molecule have been omitted for clarity.

Table 3.2 Crystallographic data and structure refinement parameters for the triphenyltin(IV) complexes **1**, **2**, **5** and **6**

	1	**2**	**5**	**6**
Empirical formula	$C_{36}H_{28}N_3OSn$	$C_{34}H_{27}N_3OSn$	$C_{40}H_{33}N_3O_2Sn$	$C_{38}H_{32}N_3O_2Sn$
Formula weight	637.30	612.28	706.39	681.36
Crystal size (mm)	0.50 × 0.50 × 0.10	0.31× 0.14 × 0.12	0.34 × 0.25 × 0.04	0.52 × 0.26 × 0.04
Crystal shape	Plate	Rod	Plate	Plate
Temperature (K)	293(2)	293(2)	110(2)	203(2)
Crystal system	Triclinic	Monoclinic	Triclinic	Triclinic
Space group	$P\bar{1}$	$C2/c$	$P\bar{1}$	$P\bar{1}$
a (Å)	9.6623(9)	31.563(5)	8.873(8)	8.5573(8)
b (Å)	11.0909(11)	9.1928(13)	11.296(11)	9.1331(9)
c (Å)	14.3096(8)	22.763(3)	16.636(16)	20.895(2)
α (°)	79.645(6)		97.57(2)	99.741(2)
β (°)	86.971(6)	199.404(2)	99.25(2)	90.912(2)
γ (°)	82.161(8)		96.55(2)	103.737(2)
V (Å^3)	1493.8(2)	5753.9(14)	1616(3)	1560.8(3)
Z	2	8	2	2
Dx (g cm^{-3})	1.417	1.414	1.452	1.450
μ (mm^{-1})	0.888	0.919	0.831	0.857
Transmission factors (min, max)	0.665, 0.916	0.760, 0.900	0.765, 0.967	0.660, 0.970
$2\theta_{max}$ (°)	28.0	30.1	27.3	27.1
Reflections measured	14372	42002	25900	23907
Independent reflections (R_{int})	7189; 0.047	8288; 0.054	7211; 0.063	6792; 0.087
Reflection with $I > 2\sigma(I)$	5050	6766	6392	5145
Number of parameters	370	353	416	398
Number of restraints	0	0	0	1
$R(F)$ ($I > 2\sigma(I)$ reflns)	0.041	0.050	0.036	0.061
$wR(F^2)$ (all data)	0.083	0.114	0.088	0.133
$GOF(F^2)$	1.01	1.09	1.02	1.10
max, min $\Delta\rho$ (e/Å^3)	0.39, -0.30	0.88, -0.66	0.93, -0.42	0.74, -1.26

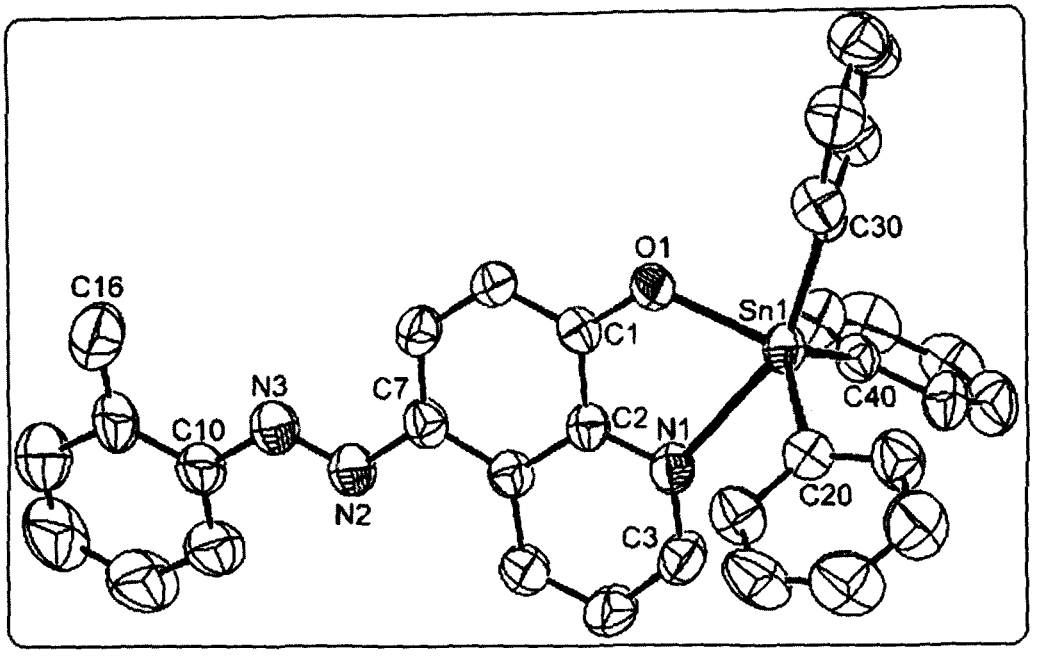

Fig. 3.2 The molecular structure of Ph_3SnL^2 (**2**) showing the atom-labelling scheme (50% probability ellipsoids). Hydrogen atoms and the solvent molecule have been omitted for clarity.

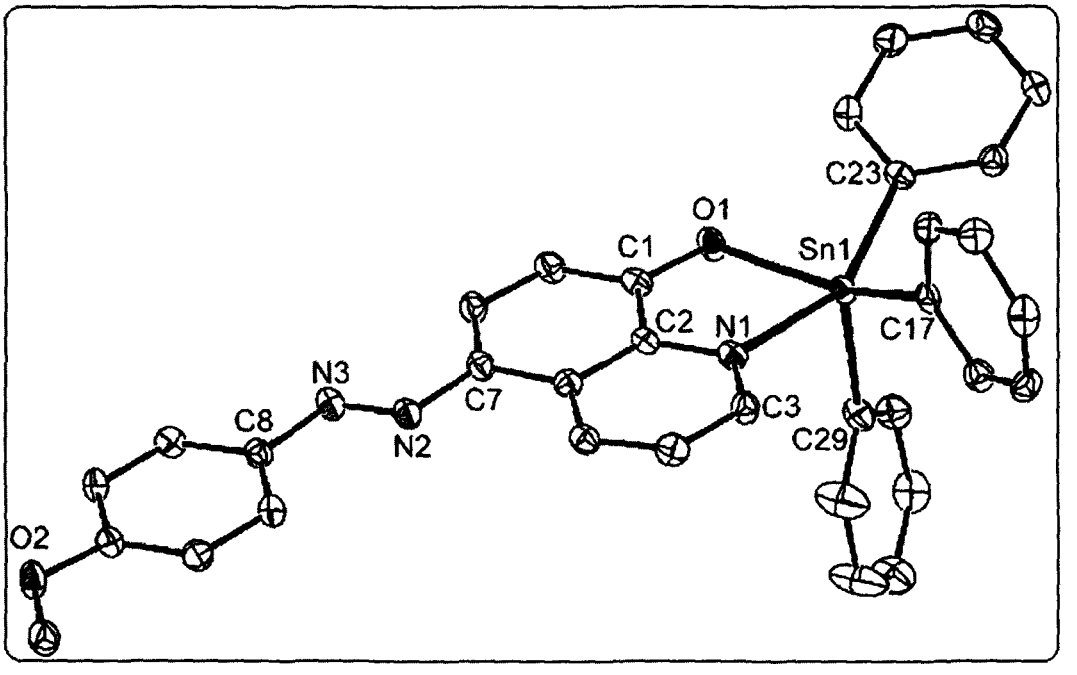

Fig. 3.3 The molecular structure of $Ph_3SnL^7.C_6H_6$ (**5**) showing the atom-labelling scheme (50% probability ellipsoids). Hydrogen atoms and the solvent molecule have been omitted for clarity.

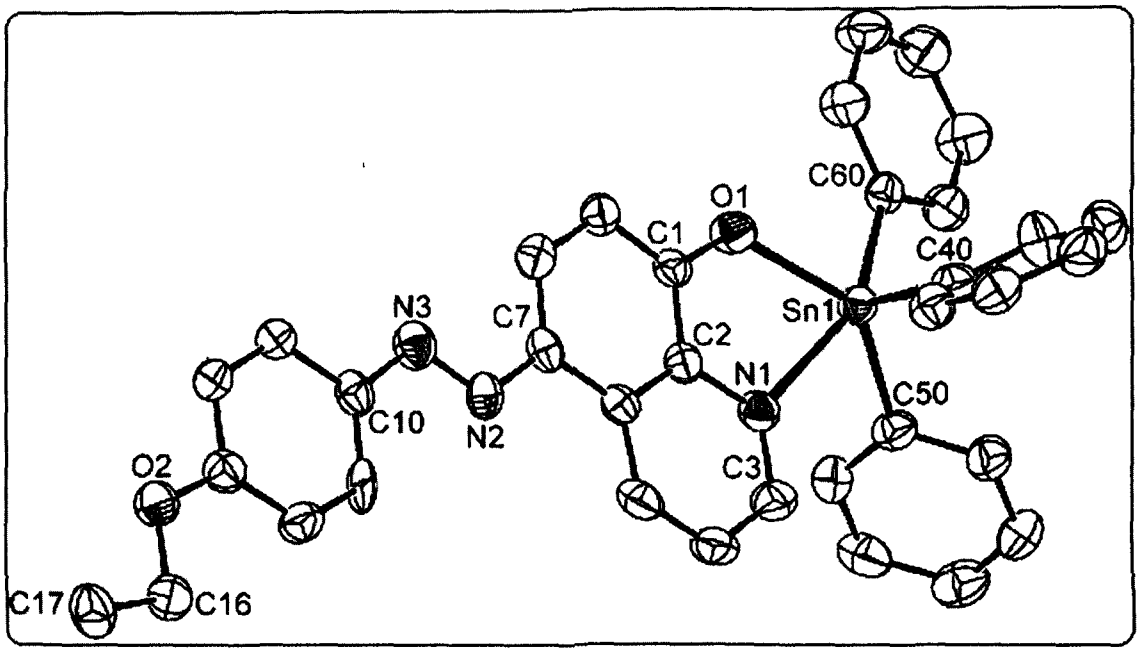

Fig. 3.4 The molecular structure of Ph_3SnL^8. $0.5C_6H_6$ (**6**) showing the atom-labelling scheme (50% probability ellipsoids). Hydrogen atoms and the solvent molecule have been omitted for clarity.

Table 3.3: Selected bond lengths (Å) and angles (°) for triphenyltin(IV) compounds **1** and **2**

1		**2**	
Sn(1)-O(1)	2.088(2)	Sn(1)-O(1)	2.063(2)
Sn(1)-N(1)	2.438(3)	Sn(1)-N(1)	2.528(2)
Sn(1)-C(22)	2.137(3)	Sn(1)-C(40)	2.130(3)
Sn(1)-C(28)	2.160(3)	Sn(1)-C(20)	2.134(3)
Sn(1)-C(16)	2.142(3)	Sn(1)-C(30)	2.170(3)
O(1)-C(1)	1.325(3)	O(1)-C(1)	1.329(3)
N(1)-C(2)	1.354(4)	N(1)-C(2)	1.357(4)
N(1)-C(3)	1.319(4)	N(1)-C(3)	1.321(4)
N(2)-N(3)	1.255(3)	N(2)-N(3)	1.251(4)
C(22)-Sn(1)-C(28)	109.17(12)	C(40)-Sn(1)-C(20)	119.84(11)
C(28)-Sn(1)-C(16)	102.30(12)	C(20)-Sn(1)-C(30)	103.67(11)
C(16)-Sn(1)-C(22)	108.46(11)	C(40)-Sn(1)-C(30)	107.99(11)
C(22)-Sn(1)-O(1)	104.36(10)	C(40)-Sn(1)-O(1)	111.44(10)
C(28)-Sn(1)-O(1)	87.82(10)	C(20)-Sn(1)-O(1)	120.22(10)
C(16)-Sn(1)-O(1)	139.87(12)	C(30)-Sn(1)-O(1)	86.82(9)
N(1)-Sn(1)-O(1)	71.23(8)	N(1)-Sn(1)-O(1)	70.47(8)
N(1)-Sn(1)-C(22)	92.90(11)	N(1)-Sn(1)-C(40)	84.92(9)
N(1)-Sn(1)-C(28)	152.94(11)	N(1)-Sn(1)-C(20)	85.09(10)
N(1)-Sn(1)-C(16)	84.54(10)	N(1)-Sn(1)-C(30)	156.92(9)
C(7)-N(2)-N(3)-C(8)	179.7(3)	C(7)-N(2)-N(3)-C(10)	175.3(3)

Table 3.4: Selected bond lengths (Å) and angles (°) for triphenyltin(IV) compounds **5** and **6**

5		**6**	
Sn(1)-O(1)	2.101(3)	Sn(1)-O(1)	2.072(4)
Sn(1)-N(1)	2.428(3)	Sn(1)-N(1)	2.409(4)
Sn(1)-C(23)	2.165(3)	Sn(1)-C(50)	2.159(6)
Sn(1)-C(17)	2.153(3)	Sn(1)-C(60)	2.160(6)
Sn(1)-C(29)	2.137(3)	Sn(1)-C(40)	2.153(6)
O(1)-C(1)	1.323(3)	O(1)-C(1)	1.338(6)
N(1)-C(2)	1.361(3)	N(1)-C(2)	1.360(7)
N(1)-C(3)	1.322(4)	N(1)-C(3)	1.319(7)
N(2)-N(3)	1.260(3)	N(2)-N(3)	1.268(6)
C(23)-Sn(1)-C(29)	110.39(12)	C(50)-Sn(1)-C(60)	101.1(2)
C(29)-Sn(1)-C(17)	108.70(12)	C(60)-Sn(1)-C(40)	106.80(2)
C(17)-Sn(1)-C(23)	103.03(12)	C(40)-Sn(1)-C(50)	112.0(2)
C(23)-Sn(1)-O(1)	88.79(10)	C(50)-Sn(1)-O(1)	136.65(19)
C(29)-Sn(1)-O(1)	103.62(11)	C(60)-Sn(1)-O(1)	87.36(18)
C(17)-Sn(1)-O(1)	138.66(9)	C(40)-Sn(1)-O(1)	105.71(18)
N(1)-Sn(1)-O(1)	71.39(8)	N(1)-Sn(1)-O(1)	71.90(15)
N(1)-Sn(1)-C(23)	151.79(9)	N(1)-Sn(1)-C(50)	85.90(18)
N(1)-Sn(1)-C(29)	94.06(11)	N(1)-Sn(1)-C(60)	155.22(18)
N(1)-Sn(1)-C(17)	81.16(11)	N(1)-Sn(1)-C(40)	92.10 (18)
C(7)-N(2)-N(3)-C(8)	179.7(2)	C(7)-N(2)-N(3)-C(10)	179.5(5)

Compounds **1** and **6** crystallize as benzene hemisolvates while **5** includes one molecule of benzene per complex. Five-coordination of the central Sn atom suggests structural variability which is indeed encountered. The results of the X-ray studies indicate that the benzene solvated compounds **1**, **5** and **6** are closely related with respect to the coordination of the central Sn atom. In these cases, the coordination polyhedron around Sn is best described as a distorted square pyramid, with one of the phenyl C atoms in the apex. In contrast, the ligand arrangement around central Sn atom in **2** is distorted trigonal-bipyramidal, with a phenyl C and the oxinato N in axial positions. A synopsis of the Sn coordination in all four compounds (**1**, **2**, **5** and **6**) is shown in Scheme 3.2.

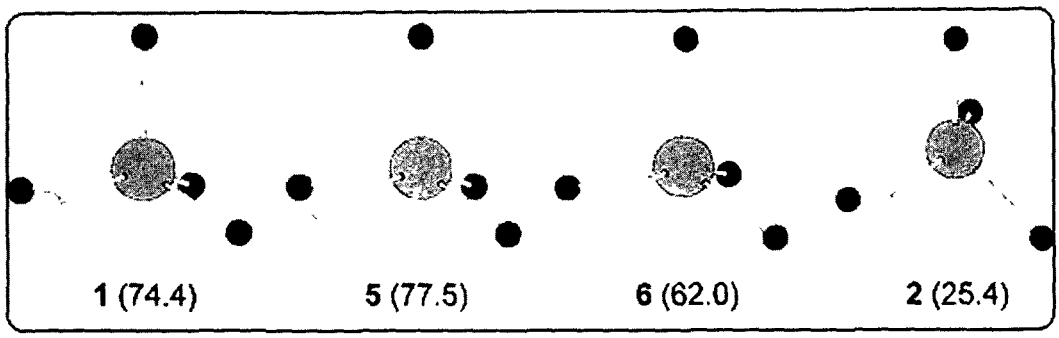

Scheme 3.2 Square-pyramidal (sp) Sn coordination in triphenyltin(IV) compounds **1**, **5** and **6** and trigonal-bipyramidal (tbp) coordination in **2**; the numbers in parentheses denote the percentage of Berry pseudorotation from tbp to sp. [16,17]. Color code: Sn, light grey; N, white; O, dark grey; C, black.

The above interpretation is corroborated by the fact that the Sn–N bond in **2**, the only compound with a N-bonded ligand in an axial position, amounts to 2.528(2) Å and is significantly longer than the Sn–N distances in the other three compounds **1**, **5** and **6** (min 2.409(4), max 2.438(3) Å). In line with this argument, the axial Sn–C bond in **2** (2.170(3) Å) is longer than the equatorial Sn–C bonds (2.130(3) and 2.134(3) Å). Distorted trigonal-bipyramidal coordination geometries have been described by Strutchkov *et al.* [18] for two symmetrically independent molecules of a thioxinate. In this report, the longest Sn–C bond is also associated with the ligand in axial position. With respect to intermolecular interactions, solid **1**, **2**, **5** and **6** represent typical molecular crystals without exceptionally short contacts. Intermolecular distances are significantly shorter than the sum of the van der Waals radii only occur between H and alkoxy O atoms in **5** and **6** and amount to ca. 2.45 Å.

3.3.1.3. NMR data (^1H, ^{13}C and ^{119}Sn)

Further characterization was accomplished from the NMR spectra of complexes **1–6** in order to obtain structural information in solution. The assignments of ^1H and ^{13}C NMR signals of L^1H–L^4H, L^7H and L^8H are described in Chapter 2. The conclusions drawn from the ligand assignments were then subsequently extrapolated to the complexes **1–6** owing to the data similarity. The ^1H NMR integration values were completely consistent with the formulation of the products. The ^1H and ^{13}C, NMR chemical shift assignment of the triphenyltin moiety is straight forward from the multiplicity pattern, resonance intensities and also by examining the $^nJ(^{13}C–^{119/117}Sn)$ coupling constants [19, 20]. In the ^1H and ^{13}C NMR spectra of the complexes, **1–6**, there is only one set of NMR signals for all the three phenyl groups (Sn–Ph) which provides evidence for the magnetic equivalence of the phenyls on the NMR time scale. This indicates that the predicted position of the phenyl groups in solid state (from ^{119}Sn Mössbauer and the X-ray crystallography discussion) is not retained in solution owing to axial-equatorial exchange. The chemical shifts $\delta(^{13}C,)$ of the carbon atoms of the phenyl substituents (Sn–Ph) are not very sensitive to changes in the coordination of central tin atom. Nevertheless, the values $\delta(^{13}C, (1^*))$, which are shifted mostly around 8–13 ppm downfield, in comparison with those in compounds having four-coordinate tin atom [21].

NMR spectral parameters (^{13}C, ^{15}N and ^{119}Sn (in solution) and ^{119}Sn CPMAS) of Ph_3SnOx have been investigated in great detail [22-25]. The results of ^{119}Sn CPMAS (in absence of X-ray diffraction) data of Ph_3SnOx and ^{119}Sn (solution) NMR spectra indicated that the solid state structure of triphenyltin(IV) quinolin-8-olate, i.e. five-coordinate structure, is retained in solution [25]. In view of this information, the results of ^{13}C and ^{119}Sn NMR have been utilized to provide structural evidence of the complexes (**1–6**) in solution. The value of the coupling constants $^nJ(^{119}Sn–^{13}C(Sn–Ph))$ matches closely with the data for penta-coordinated Ph_3SnOx complex in $CDCl_3$ solution (^1J = 633.1, ^2J = 47.8, ^3J = 62.5 (Hz)) [22]. The triphenyltin(IV) complexes **1–6**, all display a sharp singlet in the range –184 to –186 ppm and the $\delta(^{119}Sn)$ chemical shifts lie inside the range delimited for five-coordinate triphenyltin(IV) compounds [21]. The δ (^{119}Sn) values are comparable with the shift observed for Ph_3SnOx (–190.1 ppm in $CDCl_3$ solution [21,24]). Thus, ^{119}Sn NMR data indicate that the complexes (**1–6**) remain five-coordinated and retain their connectivity (see Mössbauer and X-ray discussion) in solution.

The basic ligand frame-work is shown in Chapter 2 (refer to Fig. 2.1) along with the abbreviations and numbering schemes for spectroscopic analyses. Numbering scheme for Sn-Ph skeleton as shown below:

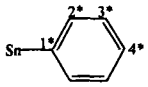

The detailed NMR spectral features for complexes **1-6** are given below:

3.3.1.3.1. $Ph_3SnL^1.0.5C_6H_6$ (1)

^{1}H NMR ($CDCl_3$, 400.13 MHz); δ_H: ligand skeleton: 9.45 [dd, 1H, H4], 8.26 [dd, 1H, H2], 8.22 [d, 1H, H6],7.95 [d, 2H, H2'and H6'], 7.66 [m, 1H, H3], 7.52 [m, 2H, H3'and H5'], 7.45 [d, 1H, H4'], 7.26 [d, 1H, H7]; Sn–Ph skeleton: 7.59 [m, 6H, H2*], 7.35 [m, 9H, H3* and H4*] ppm. ^{13}C NMR ($CDCl_3$, 100.62 MHz); δ_C: 160.3 [C8], 153.4 [C1'], 145.1 [C2], 137.5 [C5], 136.9 [C8a], 135.2 [C4],128.5 [C3'and C5'], 128.3 [C4'], 127.8 [C4a], 122.5 [C3, C2' and C6'], 118.2 [C6], 114.1 [C7]; Sn–Ph skeleton: 144.6 [C1*], 136.2 [C2*], 130.0 [C4*], 129.0 [C3*] ppm.

3.3.1.3.2. Ph_3SnL^2 (2)

^{1}H NMR ($CDCl_3$, 400.13 MHz) δ_H: Ligand skeleton: 9.45 [dd, 1H, H4], 8.26 [dd, 1H, H2], 8.18 [d, 1H, H6], 7.72 [d, 1H, H6'], 7.55 [m, 2H, H3 and H5'], 7.35 [m, 2H, H3'and H4'], 7.26 [d, 1H, and H7], 2.75 [s, 3H, CH_3]; Sn-Ph skeleton: 7.69 [m, 6H, H2*], 7.35 [m, 9H, H3* and H4*] ppm. ^{13}C NMR ($CDCl_3$, 100.62 MHz); δ_c: 160.0 [C8], 151.4 [C1'], 145.0 [C2], 137.5 [C5], 137.4 [C2'], 135.3 [C8a], 131.2 [C4], 130.0 [C3'], 128.4 [C4'], 127.7 [C4a], 126.3 [C5'], 122.5 [C3], 118.5 [C6'], 115.5 [C6], 114.0 [C7], 17.7 [CH_3]: Sn-Ph skeleton: 144.7 [C1*], 136.1 [C2*], 129.0 [C4*], 128.4 [C3*] ppm.

3.3.1.3.3. Ph_3SnL^3 (3)

^{1}H NMR ($CDCl_3$, 400.13 MHz) δ_H: Ligand skeleton: 9.47 [dd, 1H, H4], 8.28 [dd, 1H, H2], 8.18 [d, 1H, H6], 7.77 [m, 2H, H2'and H6'], 7.53 [m, 1H, H3], 7.35 [m, 2H, H4' and H5'], 7.27 [d, 1H, H7], 2.48 [s, 3H, CH_3]; Sn-Ph skeleton: 7.59 [m, 6H, H2*], 7.35 [m, 9H, H3* and H4*] ppm. ^{13}C NMR ($CDCl_3$ 100.62 MHz); δ_c: 160.1 [C8], 153.5 [C1'], 145.1 [C2], 138.9 [C5], 136.9 [C3'], 135.3 [C8a], 130.9 [C4], 128.8 [C4'], 128.1 [C5'], 127.7 [C4a], 123.0 [C2'], 122.4 [C3], 119.9 [C6'], 118.2 [C6], 114.1 [C7], 21.4 [CH_3]; Sn-Ph skeleton: 144.7 [C1*], 136.2 [C2*], 129.0 [C4*], 128.4 [C3*] ppm.

3.3.1.3.4. Ph_3SnL^4 (4)

^{1}H NMR ($CDCl_3$, 400.13 MHz) δ_H: Ligand skeleton: 9.43 [dd, 1H, H4], 8.26 [dd, 1H, H2], 8.19 [d, 1H, H6], 7.87 [d, 2H, H2' and H6'], 7.51 [m, 1H, H3], 7.35 [m, 2H, H3' and H5'], 7.25 [d, 1H, H7], 2.48 [s, 3H, CH_3]; Sn-Ph skeleton: 7.59 [m, 6H, H2*], 7.35 [m, 9H, H3* and H4*] ppm. ^{13}C NMR ($CDCl_3$ 100.62 MHz); δ_c: 159.9 [C8], 151.5 [C1'], 145.0 [C2], 143.4 [C4'], 140.5 [C5], 135.3 [C8a], 128.4 [C3' and C5'], 128.3 [C4], 127.7 [C4a], 122.5 [C2' and C6'], 122.4 [C3], 117.9 [C6], 114.1 [C7], 21.4 [CH_3]: Sn-Ph skeleton: 144.7 [C1*], 136.2 [C2*], 129.7 [C4*], 129.0 [C3*] ppm.

3.3.1.3.5. $Ph_3SnL^7.C_6H_6$ (5)

^{1}H NMR ($CDCl_3$, 400.13 MHz) δ_H: Ligand skeleton: 9.40 [dd, 1H, H4], 8.28 [dd, 1H, H2], 8.17 [d, 1H, H6], 7.85 [m, 2H, H2'and H6'], 7.55 [m, 2H, H3' and H5'], 7.51 [m, 1H, H3], 7.10 [m, 1H, H7], 3.95 [s, 3H, OCH_3]; Sn-Ph skeleton: 7.58 [m, 6H, H2*], 7.55 [m, 9H, H3* and H4*] ppm. ^{13}C NMR ($CDCl_3$, 100.62 MHz); δ_c: 160.1 [C8], 160.0 [C1'], 150.0 [C4'],146.6 [C2], 137.2 [C8a], 130.1 [C4], 129.9 [C4a], 129.6 [C3], 126.2 [C3' and C5'], 123.9 [C6], 119.6 [C7], 116.0 [C2' and C6'], 57.2 [OCH_3]: Sn-Ph skeleton: 146.6 [C1*], 136.1 [C2*], 130.6 [C4*], 130.3 [C3*] ppm.

3.3.1.3.6. $Ph_3SnL^8.0.5\ C_6H_6$ (6)

^{1}H NMR ($CDCl_3$, 400.13 MHz) δ_H: Ligand skeleton: 9.42 [dd, 1H, H4], 9.25 [dd, 1H, H2], 8.18 [d, 1H, H6], 7.92 [m, 2H, H2' and H6'], 7.51 [m, 1H, H3], 7.33 [m, 1H, H7], 7.10 [m, 2H, H3' and H5'], 4.10 [q, 2H, OCH_2CH_3], 1.5 [t, 3H ,OCH_2CH_3]; Sn-Ph skeleton: 7.55 [m, 6H, H2*], 7.33 [m, 9H, H3* and H4*] ppm. ^{13}C NMR ($CDCl_3$, 100.62 MHz); δ_c: 160.9 [C8], 159.7 [C1'], 147.7 [C2], 145.0 [C4'], 143.4 [C5], 136.5 [C8a], 135.3 [C4], 128.5 [C3' and C5'], 127.6 [C4a], 124.3 [C2' and C6'], 122.3 [C3], 117.6 [C6], 114.8 [C7], 63.8 [OCH_2CH_3], 14.8 [OCH_2CH_3]; Sn-Ph skeleton: 144.8 [C1*], 136.2 [C2*], 129.0 [C4*], 128.5 [C3*] ppm.

3.4 Structural précis of the triphenyltin(IV) complexes

The structures of the triphenyltin(IV) complexes which are characterized by single crystal X-ray crystallography, e.g., $Ph_3SnL^1.0.5C_6H_6$ (**1**), Ph_3SnL^2 (**2**), $Ph_3SnL^7.C_6H_6$ (**5**) and $Ph_3SnL^8.0.5C_6H_6$ (**6**), are summarized in Scheme 3.3.

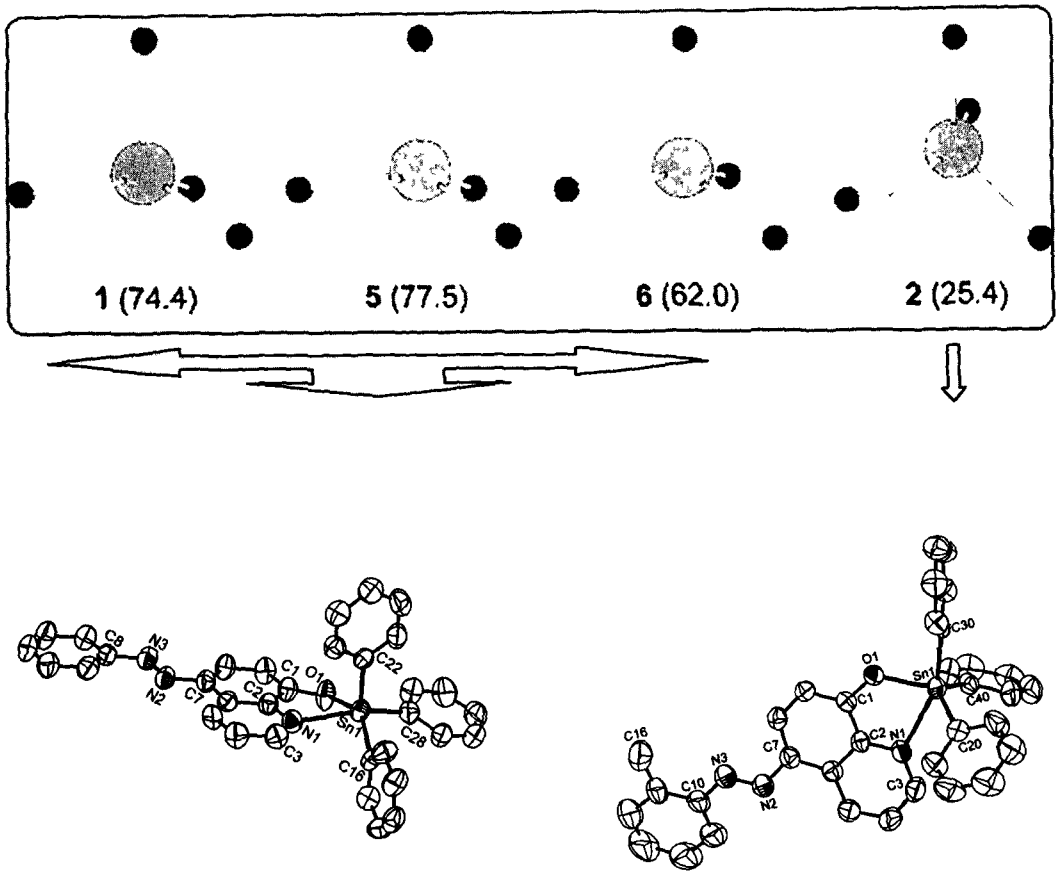

Scheme 3.3 The representations of the molecules (Ball and stick (upper) and Ortep (lower)) showing coordination geometries.

In complexes **1**, **5** and **6**, the coordination polyhedron around Sn is described as a distorted square pyramid, with one of the phenyl C atoms in the apex. In contrast, the ligand arrangement around central Sn atom in **2** is distorted trigonal-bipyramidal, with a phenyl C and the oxinato N in axial positions. The percentages of Berry pseudorotation from trigonal-bipyramidal to square pyramid are shown in parentheses.

3.5. Experimental

3.5.1. Synthesis of ligands

The ligands *viz.*, 5-[(*E*)-2-(phenyl)-1-diazenyl]quinolin-8-ol (L^1H), 5-[(*E*)-2-(2-methylphenyl)-1-diazenyl]-quinolin-8-ol (L^2H), 5-[(*E*)-2-(3-methylphenyl)-1-diazenyl]-quinolin-8-ol (L^3H), 5-[(*E*)-2-(4-methylphenyl)-1-diazenyl]quinolin-8-ol (L^4H), 5-[(*E*)-2-(4-methoxyphenyl)-1-diazenyl]-quinolin-8-ol (L^7H) and 5-[(*E*)-2-(4-ethoxyphenyl)-1-diazenyl]-

quinolin-8-ol (L^8H) used for synthesizing triphenyltin(IV) complexes are described in Chapter 2 (see Section 2.6).

3.5.2. Synthesis of triphenyltin(IV) complexes

A typical method for the synthesis of triphenyltin(IV) complexes is described below along with the characterization data.

3.5.2.1. Preparation of Ph_3SnL^1. 0.5 C_6H_6 (1) [15]

A methanolic solution of sodium methoxide (generated in situ from 0.046 g, 2.00 mmol of Na in 15 ml anhydrous methanol) was added drop-wise into a stirred hot anhydrous benzene solution (40 ml) containing L^1H (0.5g, 2.00 mmol). After complete addition, a precipitate appears and the stirring continued for 15 min. To this reaction mixture, an anhydrous benzene solution (15 ml) of Ph_3SnCl (0.77 g, 1.99 mmol) was added drop-wise which resulted in the disappearance of the precipitate. The reaction mixture was refluxed for 3 h and filtered to remove NaCl. The filtrate was collected and the solvent was removed under reduced pressure. The resultant residue was washed several times with hot hexane, dried *in vacuo*, dissolved in benzene and filtered to remove any suspended particles. The filtrate was concentrated and precipitated with hexane. The crude product was recrystallized from a mixture of benzene and hexane (v/v 1:1), which upon evaporation at room temperature afforded maroon colored crystalline product. Yield: 0.47 g (39.1%), M.p:. 115–116 °C. Anal. Found: C, 67.80; H, 4.32; N, 6.51. Calc. for $C_{36}H_{28}N_3OSn$: C, 67.84; H, 4.42; N, 6.59%.

The other triphenyltin complexes of 5-[(*E*)-2-(aryl)-1-diazenyl]quinolin-8-ol, were prepared analogously as mentioned above and their analytical data are presented below.

3.5.2.2. Preparation of Ph_3SnL^2 (2) [15]

Recrystallized from a mixture of benzene and hexane (v/v 1:1) to give orange crystalline product 0.57 g (49.1%). M.p.: 182-183 °C. Anal. Found: C, 66.60; H, 4.34; N, 6.79. Calc. for $C_{37}H_{27}N_3OSn$: C, 66.67; H, 4.44; N, 6.89%.

3.5.2.3. Preparation of Ph_3SnL^3 (3) [15]

Recrystallized from a mixture of benzene and hexane (v/v 1:1) to give orange crystalline product 0.33 g (28.1%); M.p.: 152-53 °C. Anal. Found: C, 66.57; H, 4.34; N, 7.10. Calc. for $C_{34}H_{27}N_3OSn$: C, 66.67; H, 4.44; N, 6.89%.

3.5.2.4. Preparation of Ph_3SnL^4 (4) [15]

Recrystallized from a mixture of benzene and hexane (v/v 2:1) to give maroon crystalline product 0.47 g (40.5%); M.p.: 154-55 °C. Anal Found: C, 66.66; H, 4.34; N, 6.80. Calc. for $C_{34}H_{27}N_3OSn$: C, 66.67; H, 4.44; N, 6.89%.

3.5.2.5. Preparation of Ph_3SnL^7. C_6H_6 (5) [15]

Recrystallized from a mixture of benzene and hexane (v/v 1:1) to give orange crystalline product 0.35 g (51.4%); M.p.: 96-97 °C. Anal. Found: C, 68.10; H, 4.16; N, 5.90. Calc. for $C_{40}H_{33}N_3O_2Sn$: C, 68.10; H, 4.71; N, 5.94%.

3.5.2.6. Preparation of Ph_3SnL^8. $0.5C_6H_6$ (6) [15]

Recrystallized from a mixture of benzene and hexane (v/v 1:1) to give orange crystalline product 0.45 g (54.1%); M.p.: 88-90 °C. Anal. Found: C, 67.10; H, 4.63; N, 6.15. Calc. for $C_{38}H_{32}N_3O_2Sn$: C, 67.00; H, 4.73; N, 6.16%.

3.5.3. Chemicals used for the preparations

Ph_3SnCl and Oxine (Merck) were used as such while the substituted anilines (reagent grade) were purified either by crystallization or distilled prior to use. The solvents used in the reactions were of AR grade and dried using standard procedures. Benzene was distilled from benzophenone ketyl.

3.5.4. Physical measurements

Carbon, hydrogen and nitrogen analyses were performed with a Perkin–Elmer 2400 series II instrument. The ^1H, ^{13}C and ^{119}Sn NMR spectra were recorded on a Bruker AMX 400 spectrometer and measured at 400.13, 100.62 and 149.18 MHz, respectively. The ^1H, ^{13}C and ^{119}Sn chemical shifts were referenced to Me_4Si set at 0.00 ppm, $CDCl_3$ set at 77.0 ppm and Me_4Sn set at 0.00 ppm, respectively. Mössbauer spectra were recorded on solid samples at liquid nitrogen temperature by using a conventional constant acceleration spectrometer, coupled with a multichannel analyser (a.e.n., Ponteranica (BG), Italy) equipped with a cryostat Cryo (RIAL, Parma, Italy). A $Ca^{119}SnO_3$ Mössbauer source, 10 mCi (from Ritverc, St. Petersburg, Russia) moving at room temperature with constant acceleration in a triangular waveform was used. The velocity calibration was made using a ^{57}Co Mössbauer source, 10 mCi, and an iron foil as absorber (from Ritverc, St Petersburg, Russia).

3.5.5. X-ray crystallography

Crystals of the triphenyltin(IV) compounds $Ph_3SnL^1.0.5C_6H_6$, Ph_3SnL^2, $Ph_3SnL^7.C_6H_6$ and $Ph_3SnL^8.0.5C_6H_6$ suitable for single crystal X-ray structure determination were obtained from slow evaporation of benzene/hexane (1:1 v/v) solutions. Intensity data were collected with graphite-monochromated MoKα radiation (λ = 0.71073 Å), either on a Nonius CAD4 diffractometer (for $Ph_3SnL^1.0.5\ C_6H_6$) or a Bruker D8 goniometer equipped with a SMART APEX CCD detector (for Ph_3SnL^2, $Ph_3SnL^7.C_6H_6$ and $Ph_3SnL^8.0.5C_6H_6$). Crystal data, data collection parameters and convergence results are listed in Table 3.2. Empirical absorption corrections based on a multiscan approach [26] or, for the CAD4 data, on azimuthal scans [27] were applied to the data sets before averaging over symmetry-related reflections. The structures were solved by direct methods with the help of the SHELXS-97 program [28] and refined on reflection intensities F^2 using SHELXL-97 [29]. In the final least-squares refinements, all non-hydrogen atoms were refined with anisotropic displacement parameters and hydrogen atoms were placed in idealized positions and included as riding on the corresponding atoms. Compounds $Ph_3SnL^1.0.5C_6H_6$ and $Ph_3SnL^8.0.5C_6H_6$ represent hemisolvates, both with a benzene molecule located on a crystallographic inversion center and the complex molecules in general position, whereas $Ph_3SnL^5.C_6H_6$ contains one benzene per complex molecule.

References

[1] M. Gielen, R. Willem, J. Holeček, A. Lyčka, Main Group Met. Chem. **16** (1993) 29.

[2] K.D. Ghuge, P. Umapathy, M.P. Gupta, D.N. Sen, Inorg. Nucl. Chem. **43** (1981) 653.

[3] T.S. Basu Baul, T.K. Chattopadhyay, B. Majee, Polyhedron **2** (1983) 635.

[4] B.K. Deb, A.K. Ghosh, Can. J. Chem. **65** (1987) 1241.

[5] T.S. Basu Baul, T.K. Chattopadhyay, B. Majee, Ind. J. Chem. A **23** (1984) 470.

[6] J. Ensling, P. Gutlich, K.M. Hassellbach, B.W. Fitzsimmons, J. Chem. Soc. (A) (1971) 1940.

[7] R.C. Poller, J.N.R. Ruddick, J. Organomet. Chem. **39** (1972) 121.

[8] H.C. Clark, V.K. Jain, I.J. McMahon, R.C. Mehrotra, J. Organomet. Chem. **243** (1983) 299.

[9] T.S. Basu Baul, A. Mizar, X. Song, G. Eng, R. Willem, M. Biesemans, I. Verbruggen, R. Butcher, J. Organomet. Chem. **691** (2006) 2605.

[10] T.S. Basu Baul, A. Mizar, A. Lyčka, E. Rivarola, R. Jirásko, M. Holčapek, D. de Vos, U. Englert, J. Organomet. Chem. **691** (2006) 3416.

[11] R. Barbieri, F. Huber, L. Pellerito, G. Ruisi, A. Silvestri, in: P.J. Smith (Ed.), Chemistry of Tin: ^{119}Sn Mössbauer Studies on Tin Compounds, Blackie, London, 1998, pp. 496-540.

[12] B.Y.K. Ho, J.J. Zuckerman, Inorg. Chem. **12** (1973) 1152.

[13] R.C. Poller, J.N.R. Ruddick, J. Chem. Soc. A (1969) 2273.

[14] J.N.R. Ruddick, J.R. Sams, J. Chem. Soc., Dalton Trans. (1974) 470.

[15] T.S. Basu Baul, A. Mizar, E. Rivarola, U. Englert, J. Organomet. Chem. **693** (2008) 1751

[16] A.L. Spek, J. Appl. Cryst. **36** (2003) 7.

[17] R.R. Holmes, Prog. Inorg. Chem. **32** (1984) 119.

[18] N.G. Furmanova, Yu.T. Strutchkov, E.M. Rokhlina, O.N. Kravtsov, Zh. Strukt. Khim. **21** (1980) 87.

[19] T.A.K. Al-allaf, J. Organomet. Chem. **306** (1986) 337.

[20] R. Willem, I. Verbruggen, M. Gielen, M. Biesemans, B. Mahieu, T.S. Basu Baul, E.R.T. Tiekink, Organometallics **17** (1998) 5758.

[21] J. Holeček, M. Nádvorník, K. Handlíř, A. Lyčka, J. Organomet. Chem. **241** (1983) 177.

[22] A Lyčka, J. Holeček, M. Nádvorník, K. Handlíř, J. Organomet. Chem. **280** (1985) 323.

[23] J. Holeček, A. Lyčka, R. Wagener, Collect. Czech. Chem. Commun. **51** (1986) 2116.

[24] A Lyčka, J. Holeček, M. Nádvorník, Main group Met. Chem. **12** (1989) 169.

[25] A Lyčka, J. Holeček, B. Schneider, J. Straka, J. Organomet. Chem. **389** (1990) 29.

[26] G.M. Sheldrick, SADABS, Program for Empirical Absorption Correction of Area Detector Data, University of Göttingen, Germany, 1996.

[27] A.C.T. North, D.C. Philips, F.S. Mathews, Acta Crystallogr. Sect. A **24** (1968) 351.

[28] G.M. Sheldrick, SHELXS97, Program for Structure Solution, University of Göttingen, Germany, 1997.

[29] G.M. Sheldrick, SHELXL97, Program for the Refinement of Crystal Structures, University of Göttingen, Germany, 1997.

Chapter 4

Diorganotin(IV) Complexes of 5-[(*E*)-2-(aryl)-1-diazenyl]quinolin-8-ol: Synthesis, Spectroscopic Characterization and X-ray Crystallography

CONTENTS

CHAPTER 4

DIORGANOTIN(IV) COMPLEXES OF 5-[(*E*)-2-(ARYL)-1-DIAZENYL]QUINOLIN-8-OL: SYNTHESIS, SPECTROSCOPIC CHARACTERIZATION AND X-RAY CRYSTALLOGRAPHY

4.1. Introduction	63-64
4.2. Synthesis of diorganotin(IV) complexes of 5-[(*E*)-2-(aryl)-1-diazenyl]-quinolin- 8-ol	64-65
4.3. Spectroscopic characterization and X-ray crystallography of diorganotin(IV) complexes	65-98
4.3.1. Di-n-butyltin(IV) complexes, $^{n}Bu_2Sn(L)_2$ (where L = L^{2-8})	
4.3.2. Diphenyltin(IV) complexes $Ph_2Sn(L)_2$ (where L = $L^{1-5,8}$)	
4.3.3. Dibenzyltin(IV) complexes $Bz_2Sn(L)_2$ (where L = L^{3-8})	
4.4. Structural précis of the diorganotin(IV) complexes	98-99
4.5. Experimental	100-107
References	108-110

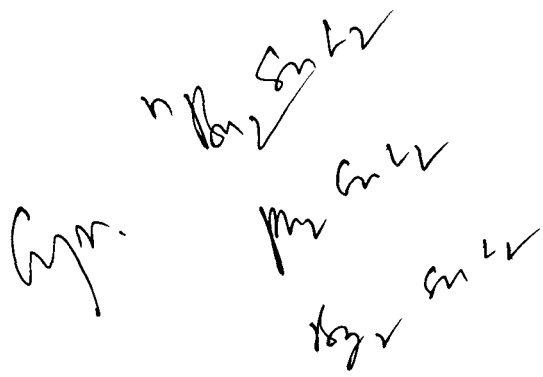

4.1. Introduction

In the preceding Chapter, the synthesis of a series of triphenyltin(IV) 5-[(*E*)-2-(aryl)-1-diazenyl]-quinolin-8-olate ligand system have been reported. The bonding mode(s) of the triphenyltin(IV) complexes were evaluated from a detailed analysis of their IR, NMR (^{1}H, ^{13}C, ^{119}Sn), ^{119}Sn Mössbauer spectra and finally the molecular structures were confirmed from the X-ray diffraction studies on some representative complexes *viz.*, $Ph_3SnL^1.0.5C_6H_6$ (**1**), Ph_3SnL^2 (**2**), $Ph_3SnL^5.C_6H_6$ (**5**), and $Ph_3SnL^6.0.5C_6H_6$ (**6**). Compounds **1**, **2**, **5** and **6** represented the first examples of structurally characterized triphenyltin(IV) compounds containing the ligand quinolin-8-olate where the coordination polyhedron around Sn is described as a distorted square pyramid for **1**, **5** and **6**, while the ligand arrangement around central Sn atom in **2** is distorted trigonal-bipyramidal.

Conversely, diorganotin(IV) oxinates and thiooxinates have been extensively studied [1] and the structures of this class of compounds have received considerable attention. The ability of organotin(IV) moieties to react with quinolin-8-ol is well established and classical examples with R_2SnLX (five-coordinate), R_2SnL_2 (six-coordinate), and $RSnL_3$ (seven-coordinate) (*R = alkyl or aryl, L = quinolin-8-olate and X = halogen or isothiocyanate*) are known [2-5]. Although most of the conventional techniques, namely ^{119}Sn Mössbauer [2,6], IR [2,3], UV [7], and NMR [3,8] spectroscopic techniques, have been employed as aids in structural investigations, the geometry of certain of these organotin(IV) quinolin-8-olate(s) was unclear. Consequently, a few organotin(IV) quinolin-8-olates have been investigated by X-ray crystallography. The diorganotin(IV) bis(quinolin-8-olate) group of compounds has received most attention and an X-ray crystal studies of R_2SnL_2, for e.g., R = Me [9], *p*-ClPh and *p*-MePh [10], ^{n}Bu and Cl [11], ^{n}Bu [12], ^{t}Bu [12] and Ph [13], showed a highly distorted octahedral molecule with bidentate quinolin-8-olate groups and essentially *cis*-organo groups. In addition, structural information on other two types, *viz.*, R_2SnLX (e.g. R = $EtCO_2Me$; X = Cl) [14] and $RSnL_3$ (R = p-ClPh) [15] are also available.

In view of this, a systematic approach was employed to determine the structures of several diorganoltin(IV) complexes of 5-[(*E*)-2-(aryl)-1-diazenyl)quinolin-8-ol ligand system, of the type R_2SnL_2 where R = ^{n}Bu, Ph and Bz, using ^{1}H-, ^{13}C-, ^{119}Sn- NMR, ESI-MS, IR and

^{119}Sn Mössbauer spectroscopic techniques in combination with X-ray diffraction. The results are presented in this Chapter.

4.2. Synthesis of diorganotin(IV) complexes of 5-[(*E*)-2-(aryl)-1-diazenyl]quinolin- 8-ol

Diorganotin(IV) complexes of 5-[(*E*)-2-(aryl)-1-diazenyl]quinolin-8-ol (LH = L^1H –L^8H) of the type $R_2Sn(L)_2$ (R = ^{n}Bu, Ph or Bz) can be prepared by the method described in Scheme 4.1. The di-*n*-butyltin(IV) complexes, $^nBu_2Sn(L)_2$ were prepared by reacting stoichiometric amounts of $^nBu_2SnCl_2$ and LNa (generated *in situ* from Na and anhydrous methanol) in anhydrous benzene (Reaction (i)). These complexes could also be prepared by reacting $^nBu_2SnO$ with LH in 1:2 molar ratios using a Dean–Stark apparatus in toluene (Reaction (ii)) and in some cases, the yields were better. The work-up convenience and purity considerations led to the choice of Reaction (i) [16].

On the other hand, the diphenyltin(IV) complexes, $Ph_2Sn(L)_2$ could be prepared by reacting stoichiometric amounts of Ph_2SnCl_2 and LH in a suitable solvent under conditions described by Blake *et al.* [17] and Ghuge *et al.* [18]. These reactions proceeded smoothly but results into a complex mixture in both the cases that could be separated with great difficulty. In view of this, an effort have been made to develop a new synthetic strategy using Ph_3SnCl via disproportionation dearylation reaction (Reaction (iii)) which proved to be convenient for synthesizing $Ph_2Sn(L)_2$ complexes [19]. The complexes could be isolated by fractional crystallization with high purity in moderate yield.

The dibenzyltin(IV) complexes, $Bz_2Sn(L)_2$ could easily be prepared [20] using the procedure described in reaction (i) for the $^nBu_2Sn(L)_2$ analogues [16]. These reactions proceeded smoothly and the pure products were obtained in yields ranging from 26% to 69%. Attempted preparation of $Bz_2Sn(L)_2$ complexes using Bz_3SnCl via a disproportionation debenzylation reaction (used for the preparation of $Ph_2Sn(L)_2$ analogue (Reaction (iii)) [19] resulted into a complex mixture that could be separated only with great difficulty. In addition, the yield was found to be much lower.

$$2LH + 2NaOMe + R_2SnCl_2 \xrightarrow[\text{Conditions: Stir / Reflux, 3 h}]{\text{Benzene}} R_2Sn(L)_2 + 2MeOH + 2NaCl \quad .....(i)$$

(R = ^{n}Bu or Bz)

$$2LH + {}^nBu_2SnO \xrightarrow[\text{Conditions: Stir / Reflux, 3 h}]{\text{Toluene}} {}^nBu_2Sn(L)_2 + H_2O \quad .....(ii)$$

$$2LH + 2Ph_3SnCl + 2Et_3N \xrightarrow[\text{Conditions: Reflux, 3 - 4 h}]{\text{Benzene}} Ph_2Sn\,(L)_2 + Ph_4Sn + 2Et_3N.HCl \quad .....(iii)$$

Scheme 4.1 Reaction proposals (**i-iii**) adopted for synthesizing $R_2Sn(L)_2$ complexes

The complexes are crystalline in nature, stable in air and soluble in all common organic solvents. The synthetic details and characterization data are presented in Section 4.4 while their spectroscopic data are summarized in Section 4.3.

4.3. Spectroscopic characterization and X-ray crystallography of diorganotin(IV) complexes

This Section deals with the spectroscopic characterization and X-ray crystallography of diorganotin(IV) complexes of the type $R_2Sn(L)_2$ (R = ^{n}Bu, Ph or Bz). For convenience of discussion, the di-*n*-butyltin(IV), diphenyltin(IV) and dibenzyltin(IV) complexes have been dealt separately.

4.3.1 Di-n-butyltin(IV) complexes, $^nBu_2Sn(L)_2$ (where $L = L^{2\text{-}8}$)

The di-*n*-butyltin(IV) complexes of 5-[(*E*)-2-(aryl)-1-diazenyl]quinolin-8-ol ($L^{2\text{-}8}H$) (**7-13**) have been characterized by IR, ^1H, ^{13}C, ^{119}Sn NMR, ^{119}Sn Mössbauer and electrospray mass spectrometry (ESI-MS) techniques. The crystal structures of four compounds, *viz.*, $^nBu_2Sn(L^4)_2$ (**9**), $^nBu_2Sn(L^5)_2 .0.5C_6H_6$ (**10**), $^nBu_2Sn(L^7)_2$ (**12**), and $^nBu_2Sn(L^8)_2$ (**13**) are reported.

4.3.1.1. Infrared and ^{119}Sn Mössbauer data

The ν(OH) in L^2H–L^8H occurs at around 3380 cm^{-1} as broad band which is assigned due to the presence of intermolecular H-bonding interactions involving the O–H–N bonds which is found to be absent in the di-*n*-butyltin (IV) complexes, $^nBu_2Sn(L^{2\text{-}8})_2$ **7–13,** confirming bonding through the O-atom of the ligand. A strong band at around 1250 cm^{-1} is assigned to the ν(C(aryl)O), i.e. C8-O-Sn linkage in the complexes [19-21].

The ^{119}Sn Mössbauer data for the $^{n}Bu_2Sn(L^{2-8})_2$ complexes (**7–13**) are given in Table 4.1. In general, the complexes displayed a doublet with δ and Δ values in the range 0.69–1.15 and 2.04–2.51 mm s^{-1}, respectively. The observed Δ values for complexes **7–13** lie within the range delimited for those diorganotin(IV) complexes which have a *cis*-R_2Sn octahedral geometry [22,23]. The values are in agreement with the data observed for the *cis*-octahedral $^{n}Bu_2Sn$(quinolin-8-olate)$_2$ complex (Δ = 2.04 [2]) [12]. The magnitudes of the δ and Δ values in the complexes **7–13** are similar to each other, which would indicate that they are isostructural. Thus, the Mössbauer spectroscopic data suggest a *cis*-R_2Sn octahedral geometry for complexes **7-13**.

Table 4.1: ^{119}Sn Mössbauer parameters (mm s^{-1}) and ^{119}Sn-NMR data (δ, ppm) for the di-*n*-butyltin(IV) complexes (**7-13**)

Complex[a]	^{119}Sn Mössbauer data[b]				^{119}Sn-NMR data[c]
	δ	Δ	Γ_1	Γ_2	
$^{n}Bu_2Sn(L^2)_2$ (**7**)	1.00	2.33	1.84	1.98	–249.8
$^{n}Bu_2Sn(L^3)_2$ (**8**)	0.99	2.43	2.00	2.00	–249.6
$^{n}Bu_2Sn(L^4)_2$ (**9**)	0.88	2.04	1.79	2.00	–249.8
$^{n}Bu_2Sn(L^5)_2$, $0.5C_6H_6$ (**10**)	0.69	2.07	2.00	2.00	–248.2
$^{n}Bu_2Sn(L^6)_2$ (**11**)	0.96	2.21	1.88	2.00	–248.5
$^{n}Bu_2Sn(L^7)_2$ (**12**)	0.93	2.04	2.00	1.85	–250.3
$^{n}Bu_2Sn(L^8)_2$ (**13**)	0.95	2.10	1.60	1.73	–250.6

[a]Complex numbers are in parentheses.
[b]Parameters: δ, isomer shifts; Δ, quadrupole splitting; Γ_1 and Γ_2: line widths.
[c]In $CDCl_3$ solution.

4.3.1.2. X-ray crystallography

Crystals of the di-*n*-butyltin(IV) compounds $^{n}Bu_2Sn(L^4)_2$ (**9**), $^{n}Bu_2Sn(L^5)_2$ $0.5C_6H_6$ (**10**), $^{n}Bu_2Sn(L^7)_2$ (**12**), and $^{n}Bu_2Sn(L^8)_2$ (**13**) suitable for single crystal X-ray structure determination were obtained from slow evaporation of benzene/hexane (1:1 v/v) solutions at room temperature. The crystal structures of four of the di-*n*-butyltin(IV) compounds **9**, **10**, **12**

and **13** [16] have been determined. The data collection and refinement parameters are given in Table 4.2.

Table 4.2 Crystallographic data and structure refinement parameters for the di-*n*-butyltin(IV) complexes **9**, **10**, **12** and **13**

	9	**10**	**12**	**13**
Empirical formula	$C_{40}H_{42}N_6O_2Sn$	$C_{41}H_{39}Br_2N_6O_2Sn$	$C_{40}H_{42}N_6O_4Sn$	$C_{42}H_{46}N_6O_4Sn$
Formula weight	757.41	926.21	789.41	817.46
Crystal size (mm)	0.17 × 0.20 × 0.25	0.10× 0.25 × 0.30	0.10× 0.25 × 0.30	0.17 × 0.20 × 0.35
Crystal shape	Prism	Tablet	Tablet	Prism
Temperature (K)	160 (1)	160 (1)	160 (1)	160 (1)
Crystal system	Monoclinic	Triclinic	Monoclinic	Triclinic
Space group	*C*2/c	$P\bar{1}$	*C*2/c	$P\bar{1}$
a (Å)	35.8749(4)	11.3778(2)	37.6805(5)	9.4380(2)
b (Å)	21.8444(3)	11.7967(2)	20.7797(3)	13.8486(3)
c (Å)	23.1536(3)	16.0362(2)	19.4559(3)	15.5419(2)
α (°)	90	87.3218(8)	90	99.069(1)
β (°)	126.1936(6)	76.9184(8)	106.7291(8)	97.614(1)
γ (°)	90	70.5888(7)	90	92.793(1)
V (Å^3)	14643.2(3)	1976.41(6)	14589.0(4)	1983.26(7)
Z	16	2	16	2
Dx (g cm^{-3})	1.374	1.556	1.438	1.369
μ (mm^{-1})	0.740	2.716	0.750	0.692
Transmission factors (min, max)	0.719, 0.823	0.602, 0.771	0.789, 0.930	0.748, 0.894
$2\theta_{max}$ (°)	60	55	55	60
Reflections measured	184867	46102	169908	60733
Independent reflections (R_{int})	21411 (0.079)	9054 (0.058)	16708 (0.092)	11577 (0.041)
Reflection with $I > 2\sigma(I)$	11070	7060	8881	10128
Number of parameters	968	462	993	565
Number of restraints	78	51	52	254
$R(F)$ ($I > 2\sigma(I)$ reflns)	0.053	0.042	0.045	0.033
$wR(F^2)$ (all data)	0.177	0.115	0.145	0.076
$GOF(F^2)$	1.05	1.06	1.04	1.03
max, min $\Delta\rho$ (e/Å^3)	1.29, -2.94	1.23, -1.52	1.70, -1.96	1.04, -0.90

The results of the X-ray crystallographic study on complexes **9**, **10**, **12** and **13** (Figs. 4.1–4.4) are fully consistent with the other spectroscopic evidence described elsewhere in Section 4.3.1. The selected geometric parameters of **9**, **10**, **12** and **13** are given in Table 4.3. The geometric parameters for the $^{n}Bu_2Sn(L)_2$ complexes are very similar. The asymmetric unit of **9** and **12** contains one molecule in a general position, plus two half molecules, each of which sits across a C_2-axis. The butyl groups in the C_2-symmetric molecules are disordered. These two complexes crystallize in the same space group, have quite similar unit cell dimensions, and are close to isostructural. The ethoxyphenyl group of one bidentate ligand in **13** is disordered over two positions, which result primarily from a reversal of the direction of the zig-zag conformation of the ethoxy group. In **10**, the asymmetric unit contains one molecule of the Sn-complex, plus one half of a molecule of benzene, which sits across a centre of inversion. One of the butyl groups in this complex is disordered over two conformations.

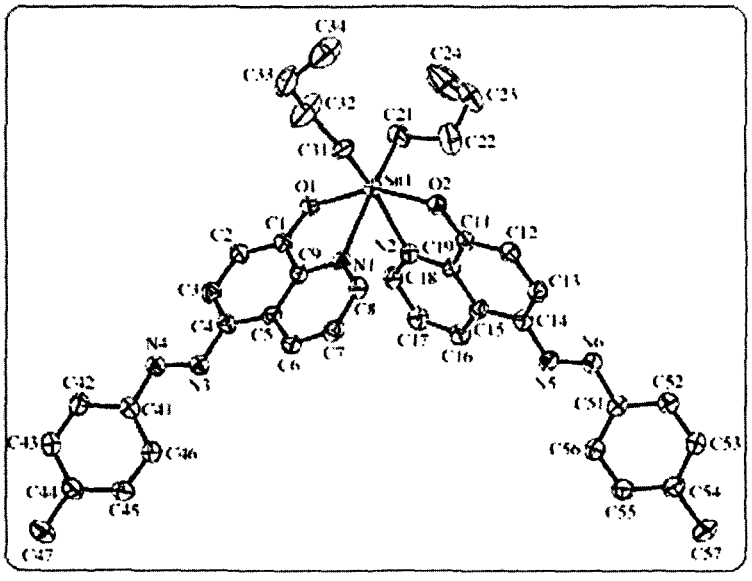

Fig. 4.1. The molecular structure of $^{n}Bu_2Sn(L^4)_2$ (**9**). Displacement ellipsoids are shown at the 50% probability level. Only one orientation of the disordered *n*-butyl group is shown.

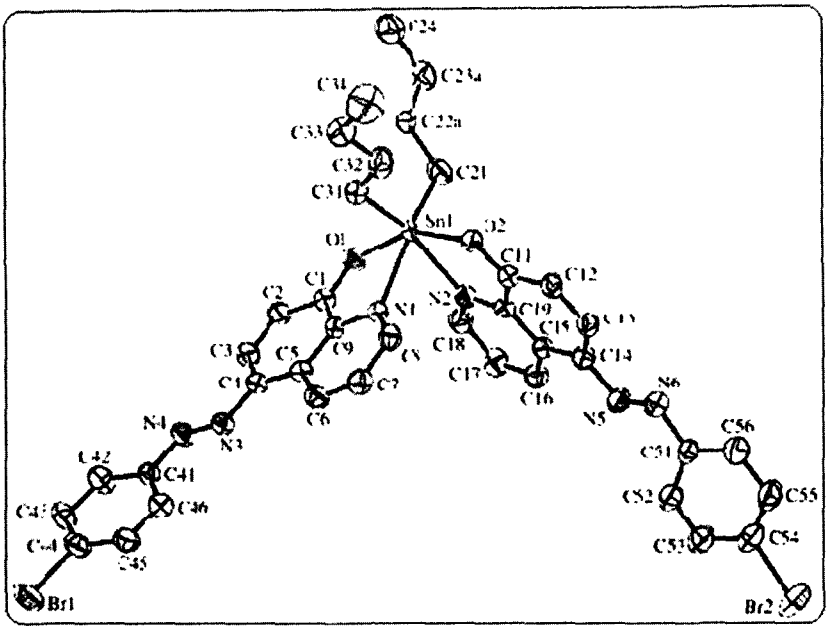

Fig. 4.2. The molecular structure of $^{n}Bu_2Sn(L^5)_2$ (**10**). Displacement ellipsoids are shown at the 50% probability level.

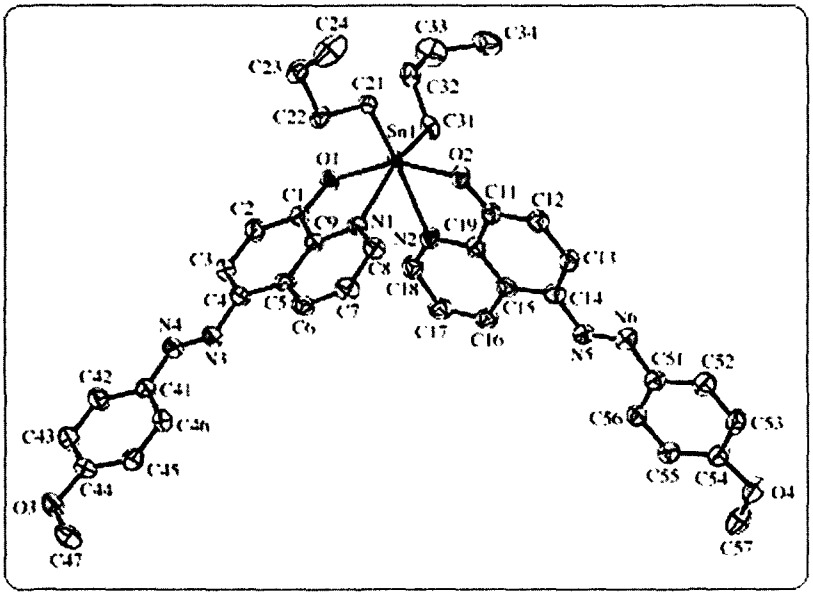

Fig. 4.3.The molecular structure of $^{n}Bu_2Sn(L^7)_2$ (**12**). Displacement ellipsoids are shown at the 50% probability level. Only one orientation of the disordered n-butyl group is shown.

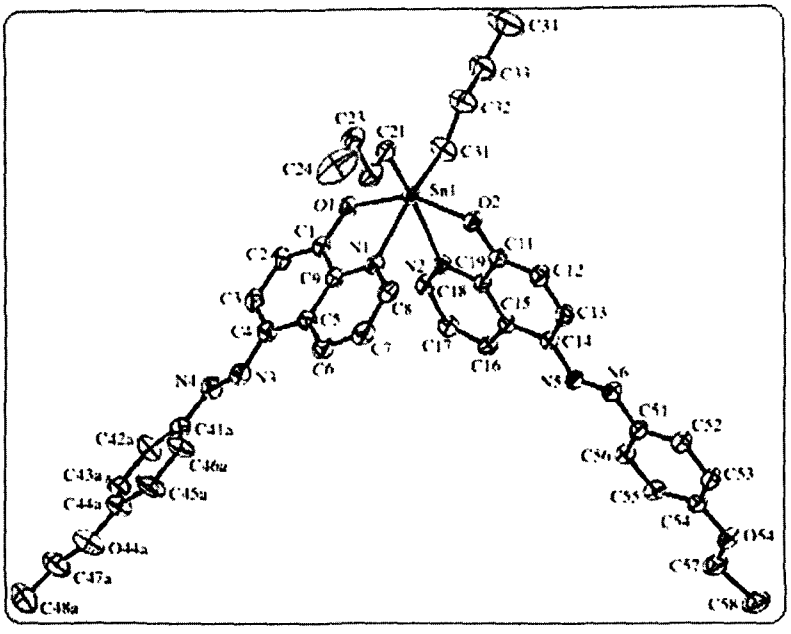

Fig. 4.4 The molecular structure of $^{n}Bu_2Sn(L^8)_2$ (**13**). Displacement ellipsoids are shown at the 50% probability level. Only one orientation of the disordered 4'-ethoxyphenyl group is shown.

The Sn-atom in all four complexes (**9**, **10**, **12** and **13**) has a distorted octahedral coordination geometry in which the O-atoms from the two bidentate ligands are approximately *trans* to one another, but *cis* to the two *n*-butyl ligands, while the quinolin-8-olate N-atoms are *trans* to the butyl groups. The small bite angle subtended by the donor atoms of the quinolin-8-olate moiety is the main reason for the distortion from a regular octahedral geometry. The metric parameters of these $^{n}Bu_2Sn(L)_2$ complex molecules closely match those of their $Ph_2Sn(L)_2$ and $Bz_2Sn(L)_2$ analogues (see Sections 4.3.2 and 4.3.3, respectively) [19,20]. The Sn-coordination geometry is also very similar to that found in $^{n}Bu_2Sn$(quinolin-8-olate)$_2$ and $^{t}Bu_2Sn$(quino-lin-8-olate)$_2$, which have more compact ligands [12]. Some variations are observed in the dihedral angle between the planes of the substituted phenyl ring and the quinolin-8-olate ring in each of the L ligands of **9**, **10**, **12** and **13**. Whereas these dihedral angles range from 37.0(2)° to 40.0(2)° among the four symmetry-independent L^4 ligands in **9**, the range across the four symmetry-independent L^5 ligands in **10** is only 6.0(2)° to 9.1(2)°, which indicates a much higher degree of coplanarity of these rings in **10**. In **10** and **13**, one L ligand is more twisted than the other, with the two dihedral angles being 11.2(1)° and 30.4(2)° for **13**, and 6.12(7)° and 21.9(2)° for **10**. In the related $Ph_2Sn(L)_2$ and $Bz_2Sn(L)_2$ analogues (see Sections 4.3.2 and 4.3.3, respectively) [19,20], both nearly planar and slightly twisted

arrangements of the L ligands were observed, with the dihedral angle between the planes of the substituted phenyl ring and the quinolin-8-olate ring.

Table 4.3: Selected bond lengths (Å) and angles (°) for di-*n*-butyltin(IV) complexes **9**, **10**, **12** and **13**

	9	**10**	**12**	**13**
Sn(1)-C(21)	2.140(4)	2.128(4)	2.158(3)	2.158(2)
Sn(1)-C(31)	2.148(4)	2.160(4)	2.141(3)	2.150(2)
Sn(1)-O(1)	2.104(3)	2.117(2)	2.114(3)	2.111(1)
Sn(1)-O(2)	2.112(3)	2.125(2)	2.120(4)	2.103(1)
Sn(1)-N(1)	2.376(3)	2.388(3)	2.333(4)	2.332(2)
Sn(1)-N(2)	2.343(3)	2.333(3)	2.356(4)	2.396(1)
N(1)-C(9)	1.365(5)	1.363(4)	1.368(6)	1.357(2)
N(2)-C(19)	1.371(5)	1.356 (4)	1.366(6)	1.365(2)
N(3)-N(4)	1.256(4)	1.265(4)	1.257(6)	1.251(3)
N(5)-N(6)	1.261(4)	1.254(4)	1.258(6)	1.264(2)
C(21)-Sn(1)-C(31)	109.0(2)	108.5(2)	110.1(1)	108.28(8)
O(1)-Sn(1)-N(1)	73.6(1)	72.99(8)	74.0(1)	73.74(5)
O(2)-Sn(1)-N(2)	73.8(1)	73.72(9)	73.7(1)	72.94(5)
N(1)-Sn(1)-N(2)	73.1(1)	75.07(9)	74.4(1)	73.05(5)
C(4)-N(3)-N(4)-C(41)	177.9(3)	-178.6(3)	178.7(4)	-178.0(7) -172.3(6)
C(14)-N(5)-N(6)-C(51)	176.9(3)	174.3(3)	-180.0(4)	-176.1(1)

4.3.1.3. NMR data (^1H, ^{13}C and ^{119}Sn)

Further characterization was accomplished from the NMR spectra of complexes **7–13** in order to obtain structural information in solution. The assignments of ^1H and ^{13}C NMR signals of L^2H–L^8H are described in Chapter 2. The conclusions drawn from the ligand assignments were then subsequently extrapolated to the complexes **7–13** owing to the data similarity and it was possible to detect all proton and carbon signals for $^nBu_2Sn(L)_2$ complexes **7–13** (see below). The ^1H NMR integration values and the number of ^{13}C signals correspond with the proposed formulations of the products. The ^1H and ^{13}C chemical shift assignment of the di-*n*-butyltin(IV) moiety is straight forward from the multiplicity patterns and resonance intensities. The coordination number in solution was determined from the ^{119}Sn chemical shift and the $^1J(^{119}Sn–^{13}C)$ coupling constants of the *n*-butyl ligands, since tin shielding and the coupling constant both increase with coordination number. The ^{119}Sn NMR spectrum of each of

the $^{n}Bu_2Sn(L)_2$ complexes studied displayed only one resonance signal for complexes **7–13** at around –250 ppm (see Table 4.1). The observed $\delta(^{119}Sn)$ chemical shifts for the chelated complexes **7–13** fall within the typical ranges for five (ca. –90 to –330 ppm) and six (ca. –125 to –515 ppm) coordinate derivatives [24]. The $\delta(^{119}Sn)$ values of complexes **7–13** are comparable with the shift observed for $^{n}Bu_2Sn$(quinolin-8-olate)$_2$ (–262 ppm in $CHCl_3$ solution [3,24] and –260 in $CDCl_3$ [25]).The solution ^{119}Sn NMR shift of $^{n}Bu_2Sn$(quinolin-8-olate)$_2$ was found to be comparable with that obtained from the solid state ^{119}Sn CP MAS NMR (–277 ppm), indicating that $^{n}Bu_2Sn$(quinolin 8-olate)$_2$ possesses the same structure in solution and in the solid state [26]. This conclusion was subsequently confirmed from $^{n}Bu_2Sn$(quinolin-8-olate)$_2$ by crystallography [12,27]. Furthermore, the $^{1}J(^{119}Sn–^{13}C)$ coupling constant values are around 625 Hz for $^{n}Bu_2Sn(L^{2-8})_2$ (**7–13**) which correspond well with the reported values [28,29]. On this basis, it is concluded that the $^{n}Bu_2Sn(L^{2-8})_2$ complexes (**7–13**) are six-coordinate in solution. Thus, the ^{119}Sn NMR data indicate that the complexes retain their solid-state structures in solution (see Sections 4.3.1.1 and 4.3.1.2 for Mössbauer and crystal structure discussions, respectively).

The basic ligand frame-work is shown in Chapter 2 (refer to Fig. 2.1) along with the abbreviations and numbering schemes for spectroscopic analyses. Numbering scheme for Sn-^{n}Bu skeleton as shown below:

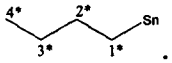

The detailed NMR spectral features for complexes **7–13** are given below:

4.3.1.3.1. $^{n}Bu_2Sn(L^2)_2$ (7)

^{1}H NMR ($CDCl_3$); δ_H: Ligand skeleton: 9.33 [dd, 1H, H4], 8.53"{{ [dd, 1H, H2], 8.22 [d, 1H, H6], 7.68 [d, 1H, H6'], 7.35 [m, 4H, H3, H3',H4'and H5'], 7.26 [d, 1H, H7] and 2.75 [s, 3H, CH_3]; Sn–^{n}Bu skeleton: 1.45 [m, 4H, H1*], 1.25 [m, 8H, H2*and H3*], 0.78 [t, 6H, H4*] ppm. ^{13}C NMR ($CDCl_3$); δ_C: 162.2 [C8], 151.4 [C1'], 143.0 [C2], 137.3 [C5], 136.5 [C8a], 135.6 [C2'], 131.2 [C4], 129.8 [C3'], 128.7 [C4a], 126.3 [C4'], 122.3 [C5'], 118.9 [C3'], 115.5 [C6 and C6'], 114.1 [C7], 17.6 [CH_3]; Sn–^{n}Bu skeleton: 27.7 [C2*], 26.7 [C3*], 26.1 [C1*], 13.6 [C4*] ppm.

4.3.1.3.2. $^{n}Bu_2Sn(L^3)_2$ (8)

^{1}H NMR ($CDCl_3$) δ_H: Ligand skeleton: 9.31 [dd,1H, H4], 8.54 [dd, 1H, H2], 8.23 [d, 1H, H6], 7.72 [m, 2H, H2'and H6'], 7.37 [m, 3H, H3, H4' and H5'], 7.24 [d, 1H, H7] and 2.45

[s, 3H, CH_3]; Sn–^{n}Bu skeleton: 1.44 [m, 4H, H1*], 1.24 [m, 8H, H2*and H3*], 0.77 [t, 6H, H4*] ppm. ^{13}C NMR ($CDCl_3$); δ_C: 162.3 [C8], 153.5 [C1'], 143.1 [C2], 138.8 [C5], 136.1 [C3'], 135.7 [C8a], 135.5 [C4], 130.7 [C4'], 128.8 [C5'], 123.3 [C4a], 122.9 [C2'], 122.3 [C3], 119.8 [C6'], 118.7 [C6], 114.1 [C7], 21.4 [CH_3]; Sn–^{n}Bu skeleton: 27.7 [C2*], 26.7 [C3*], 26.1 [C1*], 13.6 [C4*] ppm.

4.3.1.3.3. ^{n}Bu$_2$Sn(L^4)$_2$ (9)

^{1}H NMR($CDCl_3$) δ_H: Ligand skeleton: 9.28 [dd, 1H, H4], 8.54 [dd, 1H, H2], 8.21 [d, 1H, H6], 7.82 [d, 2H, H2'and H6'], 7.33 [m, 4H, H3, H3', H5'and H7], and 2.40 [s, 3H, CH_3]; Sn–^{n}Bu skeleton: 1.44 [m, 4H, H1*], 1.24 [m, 8H, H2* and H3*], 0.77 [t, 6H, H4*] ppm. ^{13}C NMR ($CDCl_3$); δ_C: 162.1 [C8], 151.5 [C1'], 143.0 [C2], 140.3 [C4'], 136.1 [C5], 135.7 [C8a], 135.5 [C4], 129.7 [C3'and C5'] 128.6 [C4a], 122.4 [C2'and C6'], 122.2 [C3], 118.4 [C6], 114.0 [C7], 21.4 [CH_3]; Sn-^{n}Bu skeleton: 27.7 [C2*], 26.8 [C3*], 26.1 [C1*], 13.6 [C4*] ppm.

4.3.1.3.4. ^{n}Bu$_2$Sn(L^5)$_2$. 0.5 C$_6$H$_6$ (10)

^{1}H NMR ($CDCl_3$) δ_H: Ligand skeleton: 9.25 [dd, 1H, H4], 8.53 [dd, 1H, H2], 8.24 [d, 1H, H6], 7.77 [d, 2H, H2'and H6'], 7.60 [m, 2H, H3'and H5'], 7.35 [d, 2H, H3 and H7]; Sn–^{n}Bu skeleton: 1.43 [m, 4H, H1*], 1.26 [m, 8H, H2*and H3*], 0.75 [t, 6H, H4*] ppm. ^{13}C NMR ($CDCl_3$); δ_C: 162.8 [C8], 152.2 [C1'], 143.2 [C2], 135.9 to 135.5 [C4', C5, C8a and C4],1 32.2 [C3' and C5'], 128.8 [C4a], 123.8 [C2' and C6'], 122.4 [C3], 119.1 [C6], 114.2 [C7]; Sn–^{n}Bu skeleton: 27.7 [C2*], 26.7 [C3*], 26.2 [C1*], 13.5 [C4*] ppm.

4.3.1.3.5. ^{n}Bu$_2$Sn(L^6)$_2$ (11)

^{1}H NMR ($CDCl_3$) δ_H: Ligand skeleton: 9.25 [dd, 1H, H4], 8.54 [dd, 1H, H2], 8.23 [d, 1H, H6], 7.82 [d, 2H, H2'and H6'], 7.45 [d, 2H, H3'and H5], 7.26 [m, 2H, H3 and H7]; Sn–^{n}Bu skeleton: 1.43 [m, 4H, H1*], 1.26 [m, 8H, H2*and H3*], 0.78 [t, 6H, H4*] ppm. ^{13}C NMR ($CDCl_3$); δ_C: 162.8 [C8], 151.8 [C1'], 143.1 [C2], 135.9 [C4'], 135.7 [C5], 135.6 [C8a], 135.5 [C4], 129.2 [C3'and C5'], 128.8 [C4a], 123.6 [C2' and C6'], 122.4 [C3], 119.0 [C6], 114.2 [C7], Sn–^{n}Bu skeleton: 27.7 [C2*], 26.7 [C3*], 26.2 [C1*], 13.5 [C4*] ppm.

4.3.1.3.6. ^{n}Bu$_2$Sn(L^7)$_2$ (12)

^{1}H NMR($CDCl_3$) δ_H: Ligand skeleton: 9.26 [dd, 1H, H4], 8.53 [d, 1H, H2], 8.19 [d, 1H, H6], 7.92 [d, 2H, H6'and H2'], 7.33 [m, 2H, H3 and H7], 7.03 [m, 2H, H3'and H5'] and 3.88 [s, 3H, OCH_3]; Sn–^{n}Bu skeleton: 1.43 [m, 4H, H1*], 1.26 [m, 8H, H2*and H3*], 0.78 [t, 6H,

H4*] ppm. ^{13}C NMR ($CDCl_3$); δ_C: 161.7 [C8], 161.3 [C1'], 147.8 [C4'], 142.9 [C2], 136.2 [C5], 135.5 [C8a], 135.5 [C4], 128.5 [C4a], 124.2 [C3'and C5'], 122.1 [C3], 118.1 [C6], 114.2 [C2'and C6'], 114.0 [C7], 55.5 [OCH_3]; Sn–^{n}Bu skeleton: 27.8 [C2*], 26.8 [C3*], 26.1[C1*], 13.6 [C4*] ppm.

4.3.1.3.7. $^nBu_2Sn(L^8)_2$ (13)

^1H NMR ($CDCl_3$) δ_H: Ligand skeleton: 9.25 [dd, 1H, H4], 8.52 [dd, 1H, H2], 8.17 [d, 1H, H6], 7.88 [m, 2H, H2'and H6'], 7.32 [m, 2H, H3 and H7], 6.97 [m, 2H, H3'and H5'], 4.09 [q, 2H, OCH_2CH_3] and 1.45 [t, 3H, OCH_2CH_3]; Sn–^{n}Bu skeleton: 1.45 [m, 4H, H1*], 1.24 [m, 8H, H2*and H3*], 0.76 [t, 6H, H4*] ppm. ^{13}C NMR ($CDCl_3$); δ_C: 161.6 [C8], 160.7 [C1'], 147.6 [C4'], 142.9 [C2], 136.1 [C5], 135.7 [C8a], 135.4 [C4], 128.5 [C4a], 124.1 [C3'and C5'], 122.0 [C3], 118.0 [C6], 114.6 [C2'and C6'], 113.9 [C7], 63.7 [OCH_2CH_3] and 14.7 [OCH_2CH_3]; Sn–^{n}Bu skeleton: 27.7 [C2*], 26.7 [C3*], 26.0 [C1*], 13.6 [C4*] ppm.

4.3.1.4. Electro-spray Ionization Mass spectrometry (ESI MS)

In the mass spectrometer, the main mechanism of ion formation is the cleavage of the most labile bond between tin and chloride or an organic ligand yielding two complementary ions, where the cationic part of the molecule is observed in the positive-ion mass spectra, i.e. $[M-L]^+$or $[M-Cl]^+$, and the anionic part in the negative-ion mass spectra, i.e. $[L]^-$ [30-32]. The ion $[Cl]^-$ cannot be observed in the spectra because the *m/z* value of 35 is outside the instrument scan range. When both chlorides and an organic ligand are coordinated to the tin atom, the loss of chlorine is preferred. Other ions observed in the first-order positive-ion mass spectra are sodium and potassium ion adducts and in some cases protonated molecules. It is also noteworthy that the position of the methyl group on the ligand in $^nBu_2Sn(L^{2\text{-}4})_2$ complexes (**7–9**) has no influence on the ion formation and the same mass spectra were obtained for these three complexes. The tandem mass spectra of some important ions were recorded in order to obtain more structural information. The neutral losses of butane or butene confirm the presence of a butyl substituent on the tin atom and the loss of 28 (N_2) confirms the presence of an azo group in the molecule. Moreover, the loss of alkyl is observed in the spectra of complexes (**10** and **11**), which contain an alkoxy group. The molecular weight of all studied complexes can be confirmed from the information obtained from both positive-ion and negative-ion first-order spectra.

The detailed mass spectral features for complexes **7–13** are given below:

4.3.1.4.1. $^{n}Bu_2Sn(L^2)_2$ (7)

MW = 758. Positive-ion ESI mass spectra: *m/z* 781 $[M+Na]^+$; *m/z* 496 $[M-L^2]^+$, 100%. MS/MS of 781: *m/z* 496 $[M-L^2]^+$; *m/z* 382 $[M-L^2-butene-butane]^+$. MS/MS of 496: *m/z* 438 $[M-L^2-butane]^+$; *m/z* 382 $[M-L^2-butene-butane]^+$. Negative-ion ESI mass spectra: *m/z* 262: *m/z* 234 $[L^2-N_2]^-$; *m/z* 143 $[L^2-CH_3C_6H_4N_2]^-$.

4.3.1.4.2. $^{n}Bu_2Sn(L^3)_2$ (8)

MW = 758. Positive and negative-ion ESI mass spectra are identical with $^{n}Bu_2Sn(L^2)_2$ *(7)*

4.3.1.4.3. $^{n}Bu_2Sn(L^4)_2$ (9)

MW = 758. Positive and negative-ion ESI mass spectra are identical with $^{n}Bu_2Sn(L^2)_2$ *(7)*

4.3.1.4.4. $^{n}Bu_2Sn(L^5)_2 . 0.5\ C_6H_6$ (10)

MW = 886. ESI mass spectrometric results are related to the unsolvated $^{n}Bu_2Sn(L^5)_2$ molecule. The presence of C_6H_6 is not observed in the mass spectra. Positive-ion ESI mass spectra: *m/z* 909 $[M+Na]^+$; *m/z* 560 $[M-L^5]$+, 100%; *m/z* 446 $[M-L^5-butene-butane]^+$. MS/MS of 909: m/z 560 $[M-L^5]^+$; *m/z* 446 $[M-L^5-butene-butane]^+$. MS/MS of 560: *m/z* 504 $[M-L^5-butane]^+$; *m/z* 446 $[M-L^5-butene-butane]^+$. Negative-ion ESI mass spectra: *m/z* 326 $[L^5]^-$, 100%.

4.3.1.4.5. $^{n}Bu_2Sn(L^6)_2$ (11)

MW = 798. Positive-ion ESI mass spectra: *m/z* 837 $[M+K]^+$; *m/z* 821 $[M+Na]^+$; *m/z* 516 $[M-L^6]^+$, 100%; *m/z* 402 $[M-L^6-butene-butane]^+$. MS/MS of 821: *m/z* 516 $[M-L^6]^+$; *m/z* 404 $[M-L^6-2*butene]^+$. MS/MS of 516: *m/z* 458 $[M-L^6-butane]^+$; *m/z* 402 $[M-L^6-butene-butane]^+$. Negative-ion ESI mass spectra: *m/z* 282 $[L^6]^-$, 100%.

4.3.1.4.6. $^{n}Bu_2Sn(L^7)_2$ (12)

MW = 790. Positive-ion ESI mass spectra: *m/z* 829 $[M+K]^+$; *m/z* 813 $[M+Na]^+$; *m/z* 512 $[M-L^7]^+$, 100%; *m/z* 398 $[M-L^7-butene-butane]^+$. MS/MS of 829: *m/z* 512 $[M-L^7]^+$; *m/z* 398 $[M-L^7-butene-butane]^+$. MS/MS of 813: *m/z* 512 $[M-L^7]^+$; m/z 398 $[M-L^7-butene-butane]^+$ MS/MS of 512: *m/z* 454$[M-L^7-butane]^+$; *m/z* 398 $[M-L^7-butene-butane]^+$. Negative-ion ESI mass spectra: *m/z* 278 $[L^7]^-$; *m/z* 263 $[L^7-CH_3]^-$ 100%. MS/MS of 278: *m/z* 263 $[L^7-CH_3]^-$; *m/z* 235 $[L^7-CH_3-N_2]^-$; *m/z* 209. MS/MS of 263: *m/z* 235 $[L^7-CH_3-N_2]^-$.

4.3.1.4.7. $^{n}Bu_2Sn(L^8)_2$ (13)

MW = 818. Positive-ion ESI mass spectra: *m/z* 857 $[M+K]^+$; *m/z* 841 $[M+Na]^+$; *m/z* 526 $[M\text{-}L^8]^+$, 100%; *m/z* 412 $[M\text{-}L^8\text{-butene-butane}]^+$. MS/MS of 857: *m/z* 526 $[M\text{-}L^8]^+$; *m/z* 412 $[M\text{-}L^8\text{-butene-butane}]^+$. MS/MS of 841: *m/z* 526 $[M\text{-}L^8]^+$; *m/z* 412 $[M\text{-}L^8\text{-butene-butane}]^+$. MS/MS of 526: *m/z* 412 $[M\text{-}L^8\text{-butene-butane}]^+$. MS/MS of 412: *m/z* 354 $[M\text{-}L^8\text{-butene-butane-ethane-}N_2]^+$. Negative-ion ESI mass spectra: *m/z* 292 $[L^8]^-$; *m/z* 263 $[L^8\text{-}C_2H_5]^-$, 100%. MS/MS of 292: *m/z* 263 $[L^8\text{-}C_2H_5]^-$; *m/z* 235 $[L^8\text{-}C_2H_5\text{-}N_2]^-$; *m/z* 209. MS/MS of 263: *m/z* 235 $[L^8\text{-}C_2H_5\text{-}N_2]^-$.

4.3.2. Diphenyltin(IV) complexes $Ph_2Sn(L)_2$ (where $L = L^{1\text{-}5,\ 8}$)

The diphenyltin(IV) complexes of 5-[(*E*)-2-(aryl)-1-diazenyl]quinolin-8-ol ($L^{1\text{-}5,\ 8}H$) (**14-19**) have been characterized by IR, ^1H, ^{13}C, ^{119}Sn NMR, ^{119m}Sn Mössbauer and electrospray mass spectrometry (ESI-MS) techniques. The crystal structures of three compounds, *viz.*, $Ph_2Sn(L^1)_2.C_3H_6O$ (**14**), $Ph_2Sn(L^4)_2$ (**17**) and $Ph_2Sn(L^5)_2$ (**18**) are reported.

4.3.2.1. Infrared and ^{119}Sn Mössbauer data

The ν(OH) in $L^{1\text{-}5}H$ and L^8H occurs at around 3380 cm^{-1} as broad band which is assigned due to the presence of intermolecular H-bonding interactions involving the O–H–N bonds. The ν(OH) band is found to be absent in the $Ph_2Sn(L)_2$ complexes, **14–19,** confirming bonding through the O-atom of the ligand as observed for its $^{n}Bu_2Sn(L)_2$ analogue (see Section 4.3.1.1). A strong band at around 1235 cm^{-1} in ligands is found to be shifted to around 1250 cm^{-1} in the complexes is assigned to the ν(C(aryl)O), (i.e. C8–O). An upward shift of the stretching frequency is expected in the complexes because the large polarity of $-O-SnR_2$ bond increases the conjugative interaction of the oxygen atom with the π-ring resulting in the increase of the C–O bond order [16,21]. The ν(C=N) vibration could not be assigned with certainty. Thus, IR spectroscopy provides only information of C8–O–Sn linkage in the complexes.

^{119}Sn Mössbauer spectroscopy has been performed on the $Ph_2Sn(L)_2$ complexes (**14–19**) in the solid state and are given in Table 4.4. Generally, δ values can differentiate between a *cis-* or a *trans*-R_2SnX_4 octahedral system. The *cis*-complexes have lower δ values than the *trans*-complexes [16,22,33], however, the δ values could not be utilized for characterizing the complexes **14–19** since there are no reference compounds of the type $[Ph_2Sn(Ox)_2]$ known having *trans*-R_2SnX_4 structure. On the other hand, Δ has proved useful in distinguishing between a *cis-* and a *trans*-configuration in the diphenyltin(IV) complexes. The Δ values in the range between 1.7–2.2 and 3.5–4.2 mm s^{-1} have been classified for a *cis-* and *trans*-octahedral

geometry, respectively [16,22,23]. The $Ph_2Sn(L)_2$ complexes **14–19** display a doublet nature of spectrum and Δ values are in the range 1.77–2.20 mm s^{-1}. The observed Δ values lie inside the range delimited for *cis*-R_2Sn octahedral geometry. The Δ values compare well with the data for $[Ph_2Sn(Ox)_2]$ complex (Δ = 1.70 mm s^{-1} [22]) having a *cis*-R_2Sn octahedral geometry [13]. Furthermore, the ratio ρ of the Δ to the δ has been found to be useful in determining the coordination number of tin [34] and in the complexes (**14–19**), ρ is ≥2.0, which indicate that the complexes have six-coordinate structure. Similar magnitude of δ and Δ values in all the complexes, further indicate that the complexes are isostructural. Thus, Mössbauer spectroscopic data suggest a *cis*-R_2Sn octahedral geometry where equatorial positions defined by two oxygen, a nitrogen and a phenyl group while axial site is occupied by a phenyl and a nitrogen atom.

Table 4.4 ^{119}Sn Mössbauer parameters (mm s^{-1}) and ^{119}Sn-NMR data (δ, ppm) for the diphenyltin(IV) complexes (**14–19**)

Complex[a]	^{119}Sn Mössbauer data[b]				^{119}Sn-NMR data[c]
	δ	Δ	Γ_1	Γ_2	
$Ph_2Sn(L^1)_2.C_3H_6O$ (14)	0.82	1.86	0.86	0.86	–385.9
$Ph_2Sn(L^2)_2$ (15)	0.81	1.77	0.83	0.84	–386.0
$Ph_2Sn(L^3)_2$ (16)	0.79	1.77	0.88	0.80	–386.4
$Ph_2Sn(L^4)_2$ (17)	0.81	1.77	1.00	1.00	–385.8
$Ph_2Sn(L^5)_2$ (18)	1.10	2.20	1.00	1.00	–385.0
$Ph_2Sn(L^8)_2$ (19)	0.80	1.82	0.91	0.91	–386.1

[a]Complex numbers are in parentheses.
[b]Parameters: δ, isomer shifts; Δ, quadrupole splitting; Γ_1 and Γ_2: line widths.
[c]In $CDCl_3$ solution.

4.3.2.2. X-ray crystallography

Crystals of diphenyltin(IV) compounds $Ph_2Sn(L^1)_2.C_3H_6O$ (**14**), $Ph_2Sn(L^4)_2$ (**17**) and $Ph_2Sn(L^5)_2$ (**18**) suitable for single crystal X-ray structure determination were obtained from acetone, hexane and benzene-hexane mixture (1:1 v/v), respectively. The crystal structures of three of the diphenyltin(IV) compounds **14**, **17** and **18** are depicted in Figs 4.5-4.7 have been

determined [19]. The data collection and refinement parameters are given in Table 4.5 and Table 4.6, respectively.

Table 4.5 Crystallographic data and structure refinement parameters for the diphenyltin(IV) complexes **14**, **17** and **18**

	14	**17**	**18**
Empirical formula	$C_{45}H_{36}N_6O_3Sn$	$C_{44}H_{34}N_6O_2Sn$	$C_{42}H_{28}Br_2N_6O_2Sn$
Formula weight	827.49	797.46	927.21
Crystal size (mm)	0.60 x 0.55 x 0.50	0.30 x 0.15 x 0.08	0.60 x 0.15 x 0.10
Crystal shape	Prism	Plate	Rod
Temperature (K)	110(2)	293(2)	228(2)
Crystal system	Monoclinic	Monoclinic	Monoclinic
Space group	$P2_1/c$	$C2/c$	$C2/c$
a (Å)	20.063(3)	19.880(3)	20.1514(17)
b (Å)	11.4413(19)	10.1913(10)	10.082(2)
c (Å)	16.417(3)	19.014(3)	18.785(3)
β (°)	91.096(3)	103.534(13)	104.340(12)
V (Å^3)	3767.8(11)	3745.3(9)	3697.6(10)
Z	4	4	4
D_x (g cm^{-3})	1.459	1.414	1.666
μ (mm^{-1})	0.729	0.728	2.898
Transmission factors (min, max)	0.67, 0.71	0.81, 0.94	0.76, 0.60
$2\theta_{max}$ (°)	28.3	26.0	27.0
Reflections measured	50915	14289	12596
Independent reflections (R_{int})	9374 (0.029)	3686 (0.193)	4026 (0.049)
Reflections with $I > 2\sigma(I)$	8626	1887	2970
Number of parameters	498	241	254
$R(F)$ ($I > 2\sigma(I)$ reflns)	0.0242	0.0689	0.0443
$wR2(F^2)$ (all data)	0.0622	0.1576	0.1025
$GOF(F^2)$	1.06	1.01	1.03
max, min $\Delta\rho$ (e/Å^3)	0.59, -0.33	0.84, -0.88	0.98, 1.02

The $Ph_2Sn(L)_2$ complexes of **14**, **17** and **18** represent van der Waals crystals without remarkably short intermolecular interactions. Shortest contacts are associated with C···H distances of 2.8 Å and CH···O distances of 2.5 Å. No short inter-halogen distances occur in the bromine containing compound **18**.

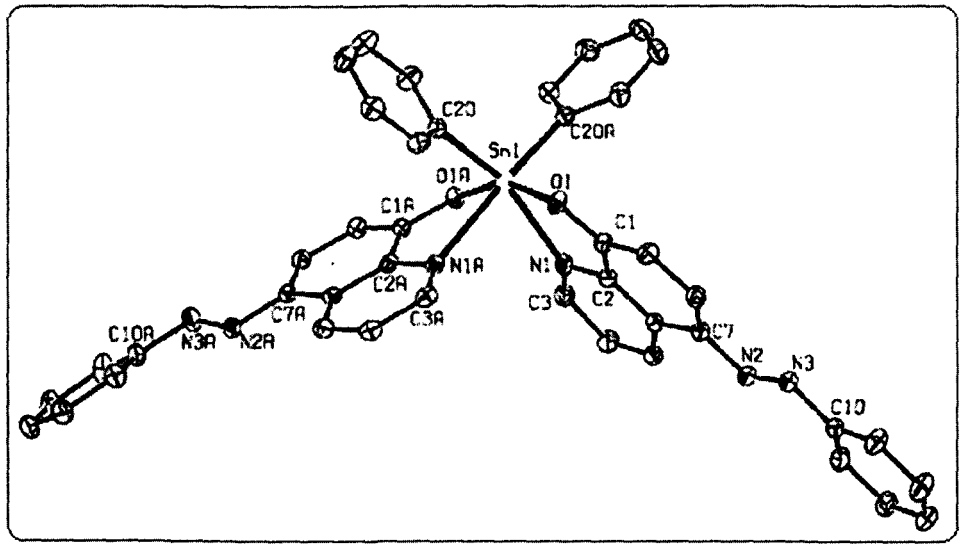

Fig.4.5: Structure of a molecule of $Ph_2Sn(L^1)_2.C_3H_6O$ (**14**) in the crystal **14**·$(CH_3)_2CO$. The solvent molecule in the crystal and the hydrogen atoms have been omitted for clarity.

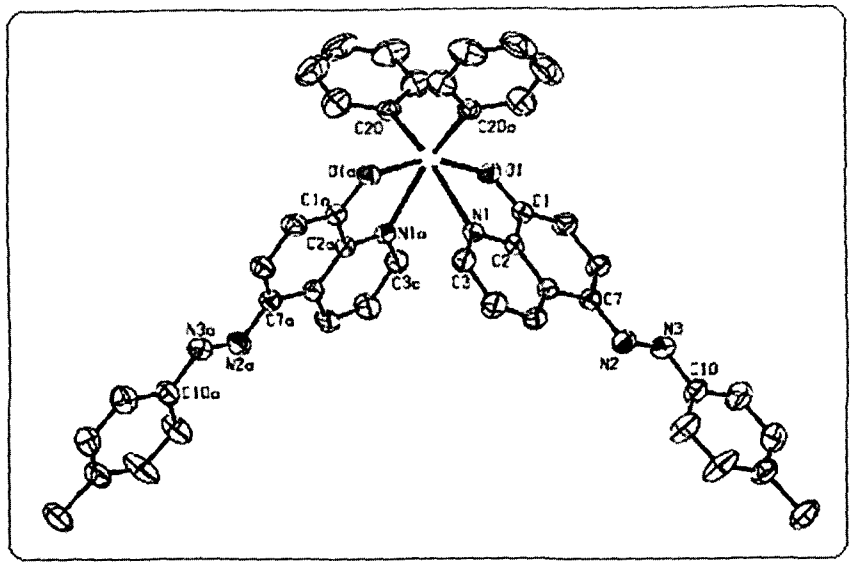

Fig. 4.6: Structure of a molecule of $Ph_2Sn(L^4)_2$ **(17)** in the crystal. The hydrogen atoms have been omitted for clarity.

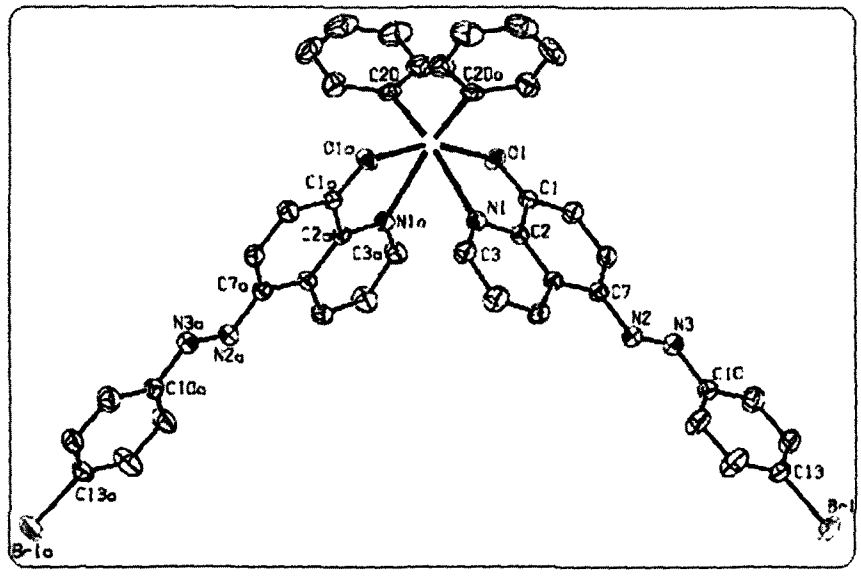

Fig.4.7 Structure of a molecule of $Ph_2Sn(L^5)_2$ **(18)** in the crystal. The hydrogen atoms have been omitted for clarity.

The $Ph_2Sn(L)_2$ complexes **17** and **18** show very similar lattice parameters and share all relevant packing features; they are most probably isomorphous. In both structures, the molecules are located on twofold crystallographic axes. In **14**, the diphenyltin complex and the solvent molecule are in general positions; the molecule of the former does not exhibit local C_2 symmetry. In the chelating ligand coordinated to tin via the atoms O1A and N1A, the 10 membered quinolinol ring N1A-C9A and the phenyl moiety C10A-C15A subtend a dihedral angle of 20° whereas the corresponding groups are significantly closer to coplanarity in the other ligand (O1/N1) as well as in **17** and **18** with dihedral angles in the range of 5-7°. Apart from these differences in conformation, all three $Ph_2Sn(L)_2$ complexes (**14**, **17** and **18**) show essentially the same arrangement of donor atoms found in $Ph_2Sn(Ox)_2$ [13]. The oxygen atoms of the two chelating ligands occupy *trans-* positions in a strongly distorted octahedron; the nitrogen donors are situated in *trans-* geometry with respect to the tin-coordinating phenyl C. Thus, so-formed O–Sn–O and N–Sn–C angles range between 157° and 164°. The *ipso-* carbon atoms of the phenyl ligands form angles of 107.48(5)° (**14**), 109.6(4)° (**17**) and 110.0(2)° (**18**) at the tin atom, in good agreement with the angle reported for $[Ph_2Sn(Ox)_2]$ (108.61(9)°) with *cis*-R_2Sn octahedral geometry [13].

Table 4.6: Selected bond lengths (Å) and angles (°) for diphenyltin complexes **14**, **17** and **18**

	14 (2 independent ligands)	**17**	**18**
Sn-C20	2.1463(14), 2.1509(15)	2.134(7)	2.149(4)
Sn-O1	2.0961(11), 2.0968(10)	2.093(5)	2.099(3)
Sn-N1	2.2833(13), 2.3868(13)	2.359(6)	2.345(3)
O1-C1	1.3240(17), 1.3185(17)	1.326(8)	1.313(5)
N1-C2	1.3662(19), 1.3680(18)	1.345(8)	1.361(5)
N1-C3	1.3218(19), 1.3198(19)	1.306(8)	1.315(5)
N2-N3	1.2619(18), 1.2596(18)	1.250(8)	1.253(5)
C20-Sn-C20A	107.48(5)	109.6(4)	110.0(2)
O1-Sn-N1	75.18(4), 73.53(4)	73.68(19)	73.66(11)
O1-Sn-O1A	157.19(4)	158.1(2)	159.04(16)
C20-Sn-N1	159.15(5), 164.06(5)	158.0(2)	157.06(14)
N1-Sn-N1A	79.99(4)	73.1(3)	73.02(17)
C7-N2-N3-C10	179.56(12), 178.43(12)	-179.6(6)	178.8(3)

4.3.2.3. NMR data (^1H, ^{13}C and ^{119}Sn)

As in the case of $^nBu_2Sn(L)_2$, further characterization of $Ph_2Sn(L)_2$ complexes (**14–19**) was also accomplished from the NMR spectra in order to obtain structural information in solution. The assignments of ^1H and ^{13}C NMR signals of $L^{1\text{-}5}H$ and L^8H are already described in Chapter 2. The conclusions drawn from the ligand assignments were then subsequently extrapolated to the diphenyltin complexes **14–19** owing to the data similarity. The ^1H NMR integration values were completely consistent with the formulation of the products. The ^1H and ^{13}C NMR chemical shift assignment of the diphenyltin moiety is straight forward from the multiplicity pattern, resonance intensities and also by examining the $^nJ(^{13}C\text{-}^{119/117}Sn)$ coupling constants [35]. In the ^1H and ^{13}C NMR spectra of the complexes, there is only one set of NMR signals for both the phenyl groups (Sn-Ph) and for the ligands, which provides evidence for the magnetic equivalence of both the phenyls attached to tin and both ligands on the NMR time scale. This indicates their relative symmetrical arrangement in the coordination sphere of the central tin atom in solution. The chemical shifts $\delta(^{13}C)$ of the carbon atoms of the phenyl substituents (Sn-Ph) are not very sensitive to changes in the coordination of central tin atom. Nevertheless, the values $\delta(^{13}C(1^*))$, which are shifted mostly by 5 ppm downfield, in comparison with those in compounds having four coordinate tin atom [36]. The value of the coupling constants $^nJ(^{119}Sn\text{-}^{13}C(Sn\text{-}Ph))$ (n = 1 to 4) matches closely with the data for hexa-coordinated $[Ph_2Sn(Ox)_2]$ complex in $CDCl_3$ solution [28]. In order to provide further structural evidence to establish the structure of the complexes in solution, we further recorded ^{119}Sn NMR spectra (Table 4.4). The complexes, all display a sharp singlet at around –386 ppm and the $\delta(^{119}Sn)$ chemical shifts lie inside the range (between –125 and –515 ppm) delimited for six coordinate diorganotin(IV) compounds [24]. The $\delta(^{119}Sn)$ values are comparable with the shift observed for $[Ph_2Sn(Ox)_2]$ complex (–397 ppm in $CHCl_3$ solution [28] and –394.2 in $CDCl_3$ [28]). Thus, ^{119}Sn NMR data indicate that the complexes retain their solid state structures (see Sections 4.3.2.1 and 4.3.2.2 for Mössbauer and X-ray discussions, respectively) in solution.

The basic ligand frame-work is shown in Chapter 2 (refer to Fig. 2.1) along with the abbreviations and numbering schemes for spectroscopic analyses. Numbering scheme for Sn-Ph skeleton as shown below:

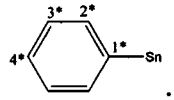

The detailed NMR spectral features for complexes **14–19** are given below:

4.3.2.3.1. $Ph_2Sn(L^1)_2.C_3H_6O$ **(14)**

^{1}H NMR ($CDCl_3$, 500.13 MHz); δ_H: 9.34 [dd, 2H, H4], 8.68 [d, 2H, H2], 8.26 [d, 2H, H6], 7.91 [d, 4H, H2'and H6'], 7.48 [m, 2H, H3], 7.60 [m, 4H, H3'and H5'], 7.43 [m, 2H, H4'], 7.36 [d, 2H, H7]; Sn–Ph skeleton: 7.48 [m, 4H, H2*], 7.25 [m, 6H, H3* and H4*] ppm. ^{13}C NMR ($CDCl_3$, 125.76 MHz); δ_C: 161.4 [C8], 153.3 [C1'], 143.4 [C2], 136.4 [C5], 136.2 [C8a], 135.4 [C4], 128.6 [C4'], 128.3 [C3'and C5'], 128.0 [C4a], 122.5 [C2'and C6'], 122.5 [C3], 118.8 [C6], 114.5 [C7]; Sn–Ph skeleton ($^nJ(^{119}Sn,^{13}C)$, Hz): 148.7 [C1*(920)], 135.0 [C2*(52)], 130.1 [C-4*(20)], 129.0 [C3*(80)] ppm.

4.3.2.3.2. $Ph_2Sn(L^2)_2$ **(15)**

^{1}H NMR ($CDCl_3$, 500.13 MHz) δ_H: 9.35 [dd, 2H, H4], 8.64 [dd, 2H, H2], 8.24 [d, 2H, H6], 7.66 [m, 2H, H6'], 7.49 [m, 2H, H3], 7.30-7.40 [m, 8H, H3', H4', H5' and H7], 2.75 [s, 6H, CH_3]; Sn-Ph skeleton: 7.59 [m, 4H, H2*], 7.24 [m, 6H, H3*and H4*] ppm. ^{13}C NMR ($CDCl_3$, 125.76 MHz); δ_C: 161.2 [C8], 151.3 [C1'], 143.3 [C2], 137.5 [C5], 137.0 [C2'], 136.2 [C8a], 136.1 [C4], 131.2 [C3'], 128.5 [C4'], 128.5 [C4a], 126.3 [C5'], 122.5 [C3], 119.1 [C6'], 115.5 [C6], 114.4 [C7], 17.6 [CH_3]; Sn-Ph skeleton ($^nJ(^{119}Sn, ^{13}C)$,Hz): 148.7 [C1*(925)], 135.2 [C2*(52)], 130.1 [C4*(20)], 128.2 [C3*(80)] ppm.

4.3.2.3.3. $Ph_2Sn(L^3)_2$ **(16)**

^{1}H NMR ($CDCl_3$, 500.13 MHz) δ_H: 9.32 [dd, 2H, H4], 8.63 [dd, 2H, H2], 8.26 [d, 2H, H6], 7.71 [m, 4H, H2' & H6'], 7.48 [m, 2H, H3], 7.32-7.42 [m, 4H, H4' and H5'], 7.25 [d, 2H, H7], 2.50 [s, 6H, CH_3]; Sn-Ph skeleton: 7.60 [m, 4H, H2*], 7.25 [m, 6H, H3*and H4*] ppm. ^{13}C NMR ($CDCl_3$, 125.76 MHz); δ_C: 161.4 [C8], 153.5 [C1'], 143.4 [C2], 138.9 [C5], 136.6 [C3'], 136.3 [C8a], 128.6 [C4 and C4'], 128.3 [C5'and C4a], 123.0 [C2'], 122.6 [C3], 119.9 [C6'], 118.9 [C6], 114.5 [C7], 21.4 [CH_3]; Sn-Ph skeleton ($^nJ(^{119}Sn, ^{13}C)$, Hz): 148.8 [C1*(920)], 134.9 [C2*(52)], 131.0 [C4*(18)], 128.9 [C3*(78)] ppm.

4.3.2.3.4. $Ph_2Sn(L^4)_2$ **(17)**

^{1}H NMR ($CDCl_3$, 500.13 MHz) δ_H: Ligand skeleton: 9.27 [dd, 2H, H4], 8.61 [dd, 2H, H2], 8.22 [d, 2H, H6], 7.80 [m, 4H, H2' and H6'], 7.24 [m, 2H, H3], 7.25 [m, 4H, H3' and H5'], 7.46 [d, 2H, H7], 2.41 [s, 6H, CH_3]; Sn-Ph skeleton: 7.59 [m, 4H, H2*], 7.23 [m, 6H, H3*and H4*] ppm. ^{13}C-NMR ($CDCl_3$, 125.76 MHz); δ_C: 161.1 [C8], 151.4 [C1'], 143.4 [C2], 140.6 [C4'], 136.5 [C5], 135.4 [C8a], 136.1 [C4], 129.7 [C3' & C5'], Not observed, possibly overlapped by a CH signal [C4a], 122.2 [C2', C6' and C3], 118.5 [C6], 114.5 [C7], 21.4 [CH_3];

Sn-Ph skeleton ($^{n}J(^{119}Sn,^{13}C)$, Hz): 148.7 [C1*(927)], 134.9 [C2* (55)], 128.5 [C4*(17)], 128.3 [C3*(81)] ppm.

4.3.2.3.5. $Ph_2Sn(L^5)_2$ (18)

^{1}H NMR ($CDCl_3$, 500.13 MHz) δ_H: 9.33 [dd, 2H, H4], 8.17 [dd, 2H, H2], 7.70 [d, 2H, H6], 7.54 [m, 4H, H2' and H6'], 7.22 [m, 4H, H3' and H5'], 7.34 [d, 2H, H3], 7.10 [d, 2H, H7]; Sn-Ph skeleton: 7.40 [m, 4H, H2*], 7.22 [m, 6H, H3* and H4*] ppm. ^{13}C NMR ($CDCl_3$, 125.76 MHz); δ_C: 161.8 [C8], 151.6 [C1'], 143.4 [C2],], 136.1 [C4], 135.9 [C5], 135.2 [C8a], 132.2 [C3' and C5'], 128.7 [C4a], 124.6 [C4'], 123.9 [C2' and C6'], 122.7[C3], 118.9 [C6], 114.6 [C7]; Sn-Ph skeleton ($^{n}J(^{119}Sn,^{13}C)$, Hz): 148.4 [C1*(925)], 134.8 [C2*(55)], 128.6 [C4*(17)], 128.3 [C-3*(82)] ppm.

4.3.2.3.6. $Ph_2Sn(L^8)_2$ (19)

^{1}H NMR ($CDCl_3$, 500.13 MHz) δ_H: 9.24 [dd, 2H, H4], 8.60 [dd, 2H, H2], 8.17 [d, 2H, H6], 7.86 [m, 4H, H2' & H6'], 7.27 [m, 2H, H3], 7.44 [m, 2H, H7], 6.95 [m, 4H, H3' and H5'], 3.97 [q, 4H, OCH_2CH_3], 1.31 [t, 6H, OCH_2CH_3]; Sn-Ph skeleton: 7.58 [m, 4H, H2*], 7.22 [m, 6H, H3*& H4*] ppm. ^{13}C NMR ($CDCl_3$, 125.76 MHz); δ_C: 160.9 [C4'], 160.7 [C8], 143.4 [C2], 143.3 [C1'], 136.5 [C5], 136.1 [C4], 135.4 [C8a], 128.4 [C4a], 124.3 [C2' and C6'], 122.3 [C3], 118.1 [C6], 114.7 [C3' and C5'], 114.4 [C7], 63.8 [OCH_2CH_3], 14.8 [OCH_2CH_3]; Sn-Ph skeleton ($^{n}J(^{119}Sn, ^{13}C)$, Hz): 148.8 [C1*(925)], 134.9 [C2*(55)], 128.5 [C4*(16)], 128.2 [C3*(82)] ppm.

4.3.2.4. Electro-spray Ionization Mass spectrometry (ESI MS)

The typical positive-ion ESI mass spectra of $Ph_2Sn(L)_2$ complexes (**14–19**) consist of molecular adducts with sodium and potassium ions, i.e., $[M+Na]^+$ and $[M+K]^+$ ions, together with the product of tin–oxygen bond cleavage $[M-L]^+$, which is the base peak of spectra for **14**, **15** and **17**. In the case of **14** and **17**, the product of tin–carbon cleavage is observed as well leading to the $[M-Ph]^+$ ion. The ligand ion $[L]^-$ is formed in the negative-ion ESI-MS as a complementary species to $[M-L]^+$ observed in the positive-ion mode, but the spectra of **15**, **18** and **19** are very noisy. All discussed mechanisms of the ion formation were already reported previously [30-32]. The molecular weight of complexes (**14–19**) can be confirmed from the information obtained from both positive-ion and negative-ion first-order spectra. Tandem mass spectra (MS/MS) provide the characteristic neutral losses, which can be correlated with

particular structural features, such as neutral losses of 90 or 92 (toluene) for **15**, **16** and **17**, 76 or 78 (benzene) for **14** and **18**, and 79 (HBr) for **18**, etc.

The detailed mass spectral features for complexes **14–19** are given below:

***4.3.2.4.1. $Ph_2Sn(L^1)_2.C_3H_6O$* (14)**

MW = 828. Positive-ion ESI mass spectra of unsolvated compound: *m/z* 809 $[M+K]^+$; *m/z* 793 $[M+Na]^+$; *m/z* 693 $[M-Ph]^+$; *m/z* 522 $[M-L^1]^+$, 100%. MS/MS of *m/z* 809: *m/z* 522 $[M-L^1]^+$. MS/MS of *m/z* 793: *m/z* 522 $[M-L^1]^+$. MS/MS of *m/z* 522: *m/z* 417 $[M-L^1\text{-benzene-}N_2]^+$; *m/z* 368 $[M-L^1\text{-benzene-}76]^+$. Negative-ion ESI masss spectra: *m/z* 248 $[L^1]^-$, 100%.

***4.3.2.4.2 $Ph_2Sn(L^2)_2$* (15)**

MW = 798. Positive-ion ESI mass spectra: *m/z* 837 $[M+K]^+$; *m/z* 821 $[M+Na]^+$; *m/z* 799 $[M+H]^+$; *m/z* 536 $[M-L^2]^+$, 100%. MS/MS of *m/z* 837: *m/z* 574 $[M+K-L^2H]^+$; *m/z* 536 $[M-L^2]^+$. MS/MS of *m/z* 821: *m/z* 558 $[M+ Na-L^2H]^+$; *m/z* 536 $[M-L^2]^+$. MS/MS of *m/z* 799: *m/z* 536 $[M-L^2]^+$. MS/MS of *m/z* 536: *m/z* 458 $[M-L^2\text{-benzene}]^+$; *m/z* 444 $[M-L^2\text{-toluene}]^+$; *m/z* 417 $[M-L^2\text{-toluene-}N_2]^+$; *m/z* 382 $[M-L^2\text{– benzene-}76]^+$.

***4.3.2.4.3. $Ph_2Sn(L^3)_2$* (16)**

MW = 798. Positive-ion ESI mass spectra: *m/z* 837 $[M+K]^+$; *m/z* 821 $[M+Na]^+$, 100%; *m/z* 536 $[M-L^3]^+$. MS/MS of *m/z* 837: *m/z* 574 $[M+K-L^3H]^+$; *m/z* 536 $[M-L^3]^+$. MS/MS of *m/z* 821: *m/z* 558 $[M+Na-L^3H]^+$; *m/z* 536 $[M-L^3]^+$. MS/MS of *m/z* 799: *m/z* 536 $[M-L^3]^+$. MS/MS of *m/z* 536: *m/z* 458 $[M-L^3\text{-benzene}]^+$; *m/z* 444 $[M-L^3\text{-toluene}]^+$; *m/z* 417 $[M-L^3\text{-toluene-}N_2]^+$; *m/z* 382 $[M-L^3\text{-benzene-}76]^+$. Negative-ion ESI mass spectra: *m/z* 262 $[L^3]^-$, 100%.

***4.3.2.4.4. $Ph_2Sn(L^4)_2$* (17)**

MW = 798. Positive-ion ESI mass spectra: *m/z* 837 $[M+K]^+$; *m/z* 821 $[M+Na]^+$; *m/z* 799 $[M+H]^+$; *m/z* 721 $[M-Ph]^+$; *m/z* 536 $[M-L^4]^+$, 100%. MS/MS of *m/z* 837: *m/z* 574 $[M+K-L^4H]^+$; *m/z* 536 $[M-L^4]^+$. MS/MS of *m/z* 821: *m/z* 558 $[M+Na-L^4H]^+$; *m/z* 536 $[M-L^4]^+$. MS/MS of *m/z* 799: *m/z* 536 $[M-L^4]^+$. MS/MS of *m/z* 721: *m/z* 645 $[M-76-Ph]^+$; *m/z* 603 $[M-Ph-N_2-90]^+$; *m/z* 525 $[M-Ph\text{-benzene-}N_2\text{-}90]^+$; *m/z* 458 $[M-L^4H-Ph]^+$; *m/z* 382 $[L^4Sn]^+$; *m/z* 263 $[L^4H]^+$. MS/MS of *m/z* 536: *m/z* 458 $[M-L^4\text{-benzene}]^+$; *m/z* 444 $[M-L^4\text{-toluene}]^+$; *m/z* 417 $[M-L^4\text{-toluene-}N_2]^+$; *m/z* 382 $[M-L^4\text{-benzene-}76]^+$. Negative-ion ESI mass spectra: *m/z* 262 $[L^4]^-$, 100%.

4.3.2.4.5. $Ph_2Sn(L^5)_2$ (18)

MW = 926. Positive-ion ESI mass spectra: *m/z* 965 $[M+K]^+$; *m/z* 949 $[M+Na]^+$; *m/z* 600 $[M\text{-}L^5]^+$; *m/z* 351 $[SnPh_3]^+$, 100%; *m/z* 197 $[SnPh]^+$. MS/MS of *m/z* 949: *m/z* 600 $[M\text{-}L^5]^+$. MS/MS of *m/z* 600: *m/z* 446 $[M\text{-}L^5\text{-}76\text{-benzene}]^+$; *m/z* 417 $[M\text{-}L^5\text{-}76\text{-HBr-}N_2]^+$.

4.3.2.4.6. $Ph_2Sn(L^8)_2$ (19)

MW = 858. Positive-ion ESI mass spectra: *m/z* 897 $[M+K]^+$; *m/z* 881 $[M+Na]^+$; *m/z* 566 $[M\text{-}L^8]^+$; *m/z* 351 $[SnPh_3]^+$. MS/MS of *m/z* 881: *m/z* 566 $[M\text{-}L^8]^+$. MS/MS of *m/z* 566: *m/z* 412 $[M\text{-}L^8\text{-}76\text{-benzene}]^+$.

4.3.3. Dibenzyltin(IV) complexes $Bz_2Sn(L)_2$ (where $L = L^{3\text{-}8}$)

The dibenzyltin(IV) complexes of 5-[(*E*)-2-(aryl)-1-diazenyl]quinolin-8-ol ($L^{3\text{-}8}H$) (**20-25**) have been characterized by IR, ^1H, ^{13}C, ^{119}Sn NMR, ^{119}Sn Mössbauer and electrospray mass spectrometry (ESI-MS) techniques. The crystal structures of three compounds, *viz.*, $Bz_2Sn(L^4)_2$ (**21**), $Bz_2Sn(L^5)_2$ (**22**) and $Bz_2Sn(L^7)_2$ (**24**) are reported.

4.3.3.1. Infrared and ^{119}Sn Mössbauer data

The ν(OH) in $L^{3\text{-}8}H$ occurs at around 3380 cm^{-1} as broad band which is assigned due to the presence of intermolecular H-bonding interactions involving the O–H–N bonds. The ν(OH) band is found to be absent in the $Bz_2Sn(L)_2$ complexes, **20-25,** confirming bonding through the O-atom of the ligand as observed for its $^nBu_2Sn(L)_2$ and $Ph_2Sn(L)_2$ analogues (see Sections 4.3.1.1 and 4.3.2.1). A strong band at around 1235 cm^{-1} in ligands is found to be shifted to around 1250 cm^{-1} in the complexes is assigned to the ν(C(aryl)O), (i.e. C8–O), which is in agreement with the earlier observation [19]. Attempts were not made to identify the bands due to ν(Sn-N) and ν(Sn-O) owing to the complex pattern of the spectra. Thus, IR spectroscopy provides only information of C8–O–Sn linkage in the complexes.

^{119}Sn Mössbauer spectroscopy has been performed on the $Bz_2Sn(L)_2$ complexes (**20-25**) in the solid state and are given in Table 4.7. In general, the complexes displayed a doublet with δ and Δ values in the range 0.84–0.93 and 1.58–1.77 mm s^{-1}, respectively. The observed Δ values lie within the range delimited for diorganotin(IV) complexes having a *cis*-R_2Sn octahedral geometry [22,23]. The values are in agreement with the data observed for $Ph_2Sn(L)_2$ complexes with cognate ligands also having a *cis*-R_2Sn octahedral geometry [19]. The magnitude of δ and Δ values in the $Bz_2Sn(L)_2$ complexes (**20-25**) are similar to each other which would indicate that they are isostructural. Thus, Mössbauer spectroscopic data suggest a

cis-R_2Sn octahedral geometry for the $Bz_2Sn(L)_2$ complexes (see X-ray discussion for further support).

Table 4.7 ^{119}Sn Mössbauer parameters (mm s^{-1}) for the dibenzyltin(IV) complexes (**20-25**)

Complex[a]	^{119}Sn Mössbauer data[b]			
	δ	Δ	Γ_1	Γ_2
$Bz_2Sn(L^3)_2$ (**20**)	0.81	1.77	1.00	1.00
$Bz_2Sn(L^4)_2$ (**21**)	0.91	1.69	1.67	1.79
$Bz_2Sn(L^5)_2$ (**22**)	0.87	1.58	2.00	2.00
$Bz_2Sn(L^6)_2$ (**23**)	0.87	1.58	2.00	2.00
$Bz_2Sn(L^7)_2$ (**24**)	0.91	1.73	2.00	2.00
$Bz_2Sn(L^8)_2$ (**25**)	0.93	1.64	1.66	1.69

[a]Complex numbers are in parentheses.
[b]Parameters: δ, isomer shifts; Δ, quadrupole splitting; Γ_1 and Γ_2: line widths.

4.3.3.2. X-ray crystallography

Crystals of dibenzyltin(IV) compounds $Bz_2Sn(L^4)_2$(**21**), $Bz_2Sn(L^5)_2$ (**22**) and $Bz_2Sn(L^7)_2$ (**24**) suitable for single crystal X-ray structure determination were obtained from benzene–hexane mixture (1:2 v/v), ethanol, chloroform–hexane mixture (1:1 v/v), respectively. The crystal structures of three of the dibenzyltin(IV) compounds **21**, **22** and **24** [20] have been determined. The data collection and refinement parameters are given in Table 4.8.

All three structures **21**, **22** and **24** are isostructural and contain a central tin atom that is octahedrally coordinated to two deprotonated 8-hydroxyquinoline derivatives and two benzyl ligands (see Figs. 4.8–4.9). Selected geometrical parameters are given in Table 4.9. The ligands are arranged about the central Sn such that the oxygen atoms are *trans* to each other while the benzyl carbon atoms and quinoline nitrogen atoms are mutually *cis* to each other. As indicated in the discussion above, these structures can best be thought of as a distorted octahedron with

Table 4.8. Crystallographic data and structure refinement parameters for the dibenzyltin(IV) complexes **21**, **22** and **24**

	21	**22**	**24**
Empirical formula	$C_{46}H_{38}N_6O_2Sn$	$C_{44}H_{32}Br_2N_6O_2Sn$	$C_{46}H_{38}N_6O_4Sn$
Formula weight	825.51	955.27	857.51
Crystal size (mm)	0.56 x 0.35 x 0.18	0.48 x 0.25 x 0.20	0.80 x 0.55 x 0.35
Crystal shape	plate	prism	prism
Temperature (K)	93(2)	296(2)	93(2)
Crystal system	Triclinic	Monoclinic	Triclinic
Space group	$P\bar{1}$	$P2_1/n$	$P\bar{1}$
a (Å)	10.1273(13)	15.341(18)	9.7212(15)
b (Å)	12.6410(16)	15.310(16)	13.714(2)
c (Å)	15.660(2)	17.49(2)	15.809(3)
β(°)	104.711(2)	95.29(4)	105.708(3)
V (Å^3)	1893.7(4)	4090(8)	1959.6(5)
Z	2	4	2
D_x (g cm^{-3})	1.448	1.551	1.453
μ (mm^{-1})	0.723	2.623	0.705
Transmission factors (min, max)	0.792, 1.000	0.0742, 1.000	0.808, 1.000
$2\theta_{max}$ (°)	28.19	20.81	28.29
Reflections measured	14640	15449	15445
Independent reflections (R_{int})	8868 (0.0440)	4283 (0.0999)	9206 (0.0376)
Indep. reflections with $I > 2\sigma(I)$	7292	2227	8420
Number of parameters	498	472	516
$R(F)$ ($I > 2\sigma(I)$ reflns)	0.0330	0.0749	0.0297
$wR_2(F^2)$ (all data)	0.0450	0.1550	0.0344
$GOF(F^2)$	0.974	1.038	1.038
max, min $\Delta\rho$ (e/Å^3)	0.926, -0.702	1.037, -0.977	0.433, -0.602

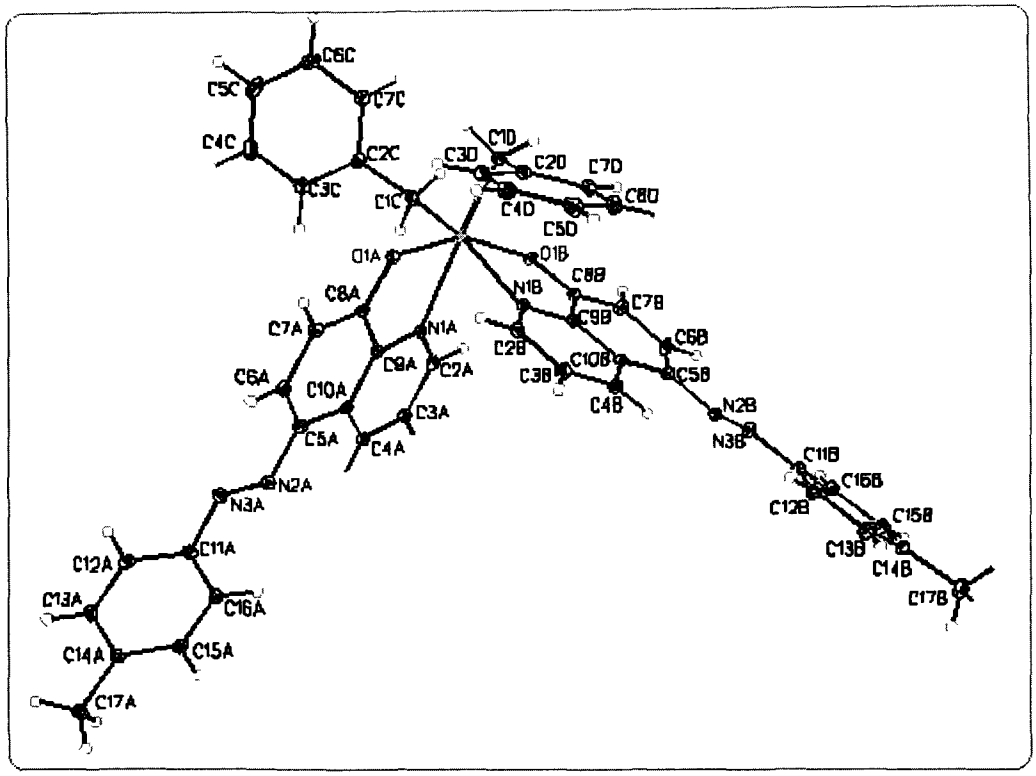

Fig.4.8. The molecular structure of $Bz_2Sn(L^4)_2$ (**21**) with the atom-labelling scheme.

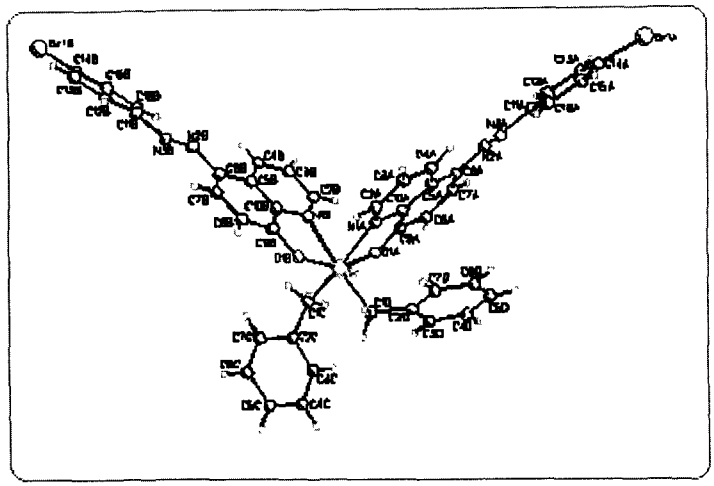

(a)

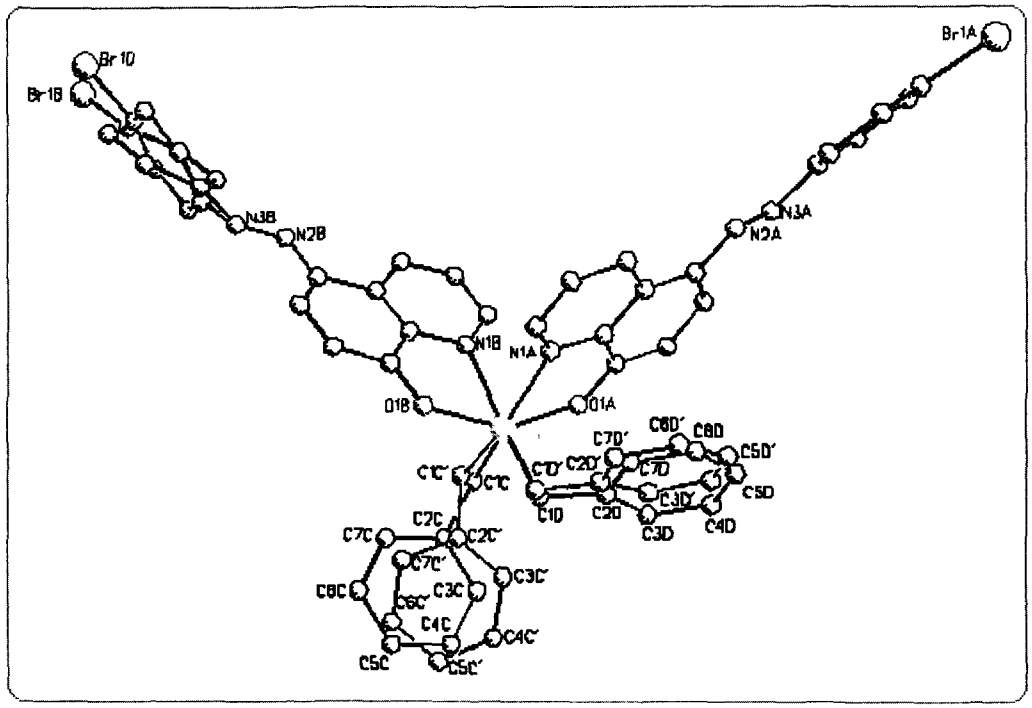

(b)

Fig.4.9. (a) The molecular structure of $Bz_2Sn(L^5)_2$ (**22**) with the atom-labelling scheme (b) The molecular structure of $Bz_2Sn(L^5)_2$ (**22**) showing disordered conformation.

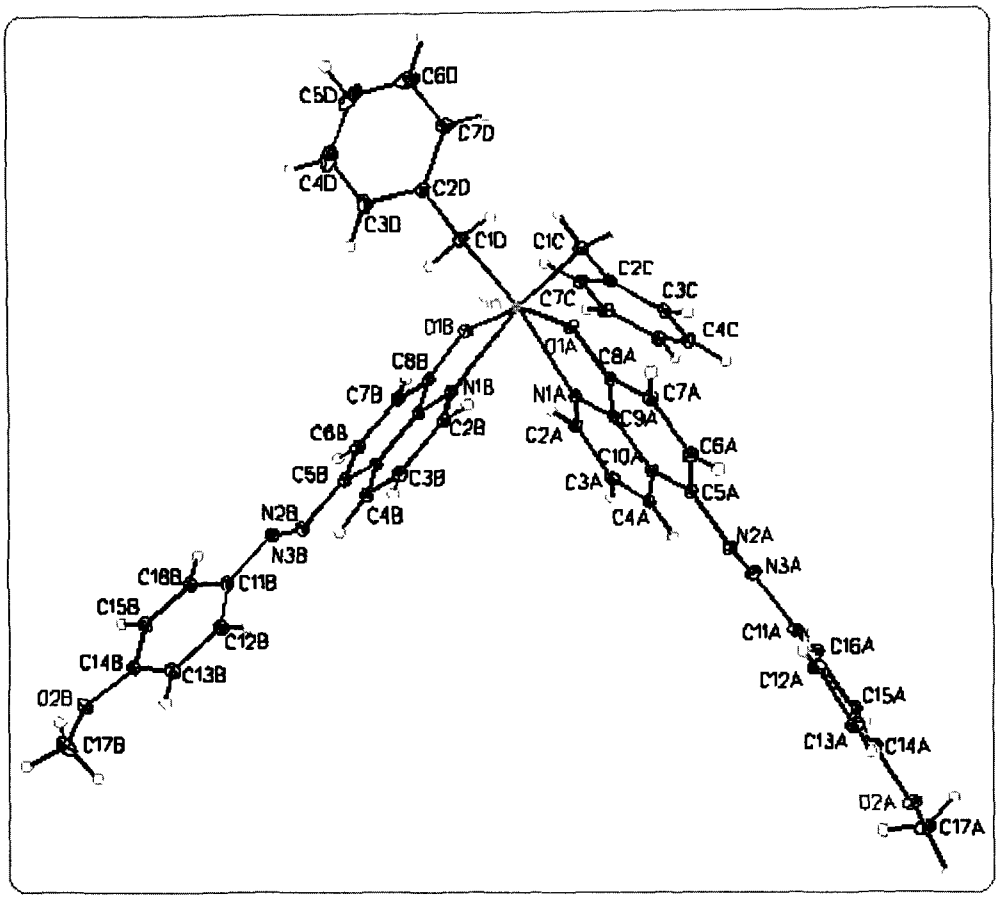

Fig. 4.10 The molecular structure of $Bz_2Sn(L^7)_2$ (**24**) with the atom-labelling scheme.

the two oxygen, nitrogen and benzyl carbon donors forming a plane and the remaining nitrogen and benzyl carbon donors being *trans* to each other. The small bite subtended by the oxygen and nitrogen of the 8-hydroxyquinoline moiety is the main reason for the distortion from a regular octahedral geometry. In summary, the metrical values for $Bz_2Sn(L)_2$ complexes (**21**, **22** and **24**) show a remarkable degree of self consistency in the coordination environment about the central tin atom for the three complexes. This, of course, is to be expected as the variations in the 8-hydroxyquinoline ligands occur at the periphery. A similar set of complexes containing phenyl substituents (compounds **17** and **18**) instead of benzyl substituents has been reported [19]. One point of interest concerns the structure of **22**. As indicated in the discussion of the solid-state ^{117}Sn NMR (see Section 4.3.3.3), there appears to be two slightly different environments for the central Sn atom. This is confirmed in the crystal structure as the two benzyl and one of the 8-hydroxyquinoline ligands are disordered over two conformations. This disorder is shown in Fig. 4.9.

Table 4.9: Selected bond lengths (Å) and angles (°) for the dibenzyltin(IV) complexes **21**, **22** and **24**

	21	**22**	**24**
Sn-C(benzyl)	2.166(2), 2.174(2)	2.155(13), 2.179(14)	2.176(2), 2.175(2)
Sn-O1	2.016(2), 2.114(2)	2.075(10), 2.086(10)	2.111(1), 2.096(1)
Sn-N1	2.306(2), 2.335(2)	2.305(11), 2.314(12)	2.301(2), 2.357(2)
O1-C1	1.320(3), 1.324(3)	1.313(15), 1.316(16)	1.321(2), 1.321(2)
N1-C2	1.320(3), 1.322(3)	1.290(15), 1.302(16)	1.324(2), 1.322(2)
N1-C3	1.361(3), 1.363(3)	1.376(15), 1.390(16)	1.362(2), 1.363(2)
N2-N3	1.265(3), 1.253(3)	1.178(15), 1.212(15)	1.259(3), 1.268(2)
C1C-Sn-C1D	105.87(9)	103.7(18), 113(2)	105.59(8)
O1-Sn-N1	74.16(6), 74.12(6)	75.2(4), 74.2(4)	74.34(5), 73.80(6)
O1A-Sn-O1B	154.68(6)	152.0(4)	154.00(5)
C1-Sn-N1(*trans)*	158.57(8), 162.81(8)	163.1(12), 165.6(14)	156.83(7), 163.18(6)
C1-Sn-N1(*cis*)	89.23(8), 91.08(8)	89.5(14), 88.7(12)	89.43(7), 91.86(7)
N1A-Sn-N1B	76.40(7)	79.6(4)	75.94(6)
C5-N2-N3-C11	179.04(18), 178.27(19)	-177.7(11), -176.2(17), -161(5)(minor comp)	-179.01(17), -178.59(16)

4.3.3.3. Solution NMR (^1H, ^{13}C and ^{119}Sn) and solid-state ^{117}Sn NMR data

As in the cases of $^nBu_2Sn(L)_2$ and $Ph_2Sn(L)_2$ complexes, further characterization of $Bz_2Sn(L)_2$ complexes (**20-25**) was also accomplished from the NMR spectra in order to obtain structural information in solution. The assignments of ^1H and ^{13}C NMR signals of $L^{3\text{-}8}H$ are already described in Chapter 2. The conclusions drawn from the ligand assignments were then subsequently extrapolated to the dibenzyltin complexes **20-25** owing to the data similarity. The ^1H NMR integration values were completely consistent with the formulation of the products. The ^1H and ^{13}C NMR chemical shift assignment of the dibenzyltin(IV) moiety is straight forward from the multiplicity pattern, resonance intensities and also by examining the $^nJ(^{13}C\text{-}^{119/117}Sn)$ coupling constants [37]. In the ^1H and ^{13}C NMR spectra of the complexes, there is only one set of NMR signals for both the benzyl groups (Sn-Bz) and for the ligands, which provides evidence for the magnetic equivalence of both the benzyls attached to tin and both

ligands on the NMR time scale. This indicates their relative symmetrical arrangement in the coordination sphere of the central tin atom in solution.

The basic ligand frame-work is shown in Chapter 2 (refer to Fig. 2.1) along with the abbreviations and numbering schemes for spectroscopic analyses. Numbering scheme for Sn-Ph skeleton as shown below:

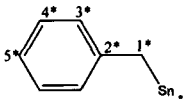

The detailed NMR spectral features for complexes **20-25** are given below:

4.3.3.3.1. $Bz_2Sn(L^3)_2$ (20)

^{1}H NMR ($CDCl_3$, 500.13 MHz)) δ_H: Ligand skeleton: 9.12 [dd, 2H, H4], 8.10 [m, 4H, H2 and H6], 7.63 [m, 4H, H2' and H6'], 7.31 [m, 2H, H3], 7.20 [m, 4H, H4'and H5'], 7.09 [d, 2H, H7], 2.37 [s, 6H, CH_3]; Sn–Bz Skeleton: 2.58 [d, 4H, H1*], 6.73 [m, 4H, H4*], 6.63 [m, 6H, H3*and H5*], ppm. ^{13}C NMR ($CDCl_3$ 125.76 MHz);); δ_c: 161.5 [C8], 153.3 [C1'], 142. 9 [C2], 138.9 [C5], 136.1 [C3'], 135.7 [C8a], 135.1 [C4], 130.9 [C4' and 5'], 128.5 [C4a], 123.1 [C2'], 122.1 [C3], 119.9 [C6'], 118.3 [C6], 113.8 [C7], 21.4 [CH_3]; Sn–Bz skeleton (^nJ(^{119}Sn,^{13}C), Hz): 33.5 [C1* (927)], 140.9 [C2*(55)], 128.8 [C3*(17)], 127.6 [C4*(81)], 122.8 [C5*(81)] ppm.

4.3.3.3.2. $Bz_2Sn(L^4)_2$ (21)

^{1}H NMR ($CDCl_3$500.13 MHz); δ_H: 9.09 [dd, 2H, H4], 8.09 [d, 2H, H2], 7.97 [d, 2H, H6], 7.65 [d,4H, H2' and H6'], 7.20 [m, 2H, H3], 7.13 [m, 4H, H3' and H5'], 7.00 [m, 2H, H7], 2.35 [d, 6H, CH_3]; Sn–Bz skeleton: 2.48 [d, 4H, H1*], 6.67 [m, 4H, H4*], 6.61 [m, 6H, H3*and H5*], ppm. ^{13}C NMR ($CDCl_3$125.76 MHz); δ_c: 161.1 [C8], 151.1 [C1'], 142.3 [C2], 139.4 [C4'], 135.5 [C5], 135.4 [C8a],134.9 [C4], 128.4 [C4a], 127.3 [C3'and C5'], 122.7 [C2'and C6'], 121.4 [C3], 118.1 [C6], 113.5 [C7], 21.4 [CH_3]; Sn–Bz skeleton (^nJ (^{119}Sn,^{13}C), Hz): 33.2 [C1*(927)], 140.7 [C2*(55)], 129.2 [C3*(17)], 127.2 [C4*(81)], 122.4 [C5*(81)] ppm.

4.3.3.3.3. $Bz_2Sn(L^5)_2$ (22)

^{1}H NMR ($CDCl_3$500.13 MHz) δ_H: 9.08 [dd, 2H, H4], 8.14 [dd, 2H, H2], 8.00 [d, 2H, H6], 7.68 [m, 4H, H2' and H6'], 7.52 [m, 4H, H3' and H5'], 7.17 [m, 2H, H3], 7.07 [m, 2H, H7]; Sn–Bz skeleton: 2.52 [d, 4H, H1*], 6.70 [m, 4H, H4*], 6.62 [m, 6H, H3* and H5*],ppm. ^{13} C NMR ($CDCl_3$125.76 MHz); δ_c: 162.0 [C8], 151.7 [C1'], 140.5 [C2], 135.3 [C5], 134.9

[C8a], 135.4 [C4], 131.9 [C3'and C5'], 127.3 [C4a], 123.9 [C4'], 122.9 [C2'and C6'], 121.8 [C3], 116.6 [C6], 113.8 [C7]; Sn–Bz skeleton ($^{n}J(^{119}Sn,^{13}C)$, Hz): 33.3 [C1*(927)], 142.6 [C2*(55)], 127.5 [C3*(17)], 127.4 [C4*(81)], 123.8 [C5*(81)] ppm.

4.3.3.3.4. $Bz_2Sn(L^6)_2$ (23)

^{1}H NMR ($CDCl_3$500.13 MHz) δ_H: 9.06 [dd, 2H, H4], 8.12 [dd, 2H, H2], 8.00 [d, 2H, H6], 7.71 [m, 4H, H2' and H6'], 7.32 [m, 4H, H3' and H5'], 7.15 [m, 2H, H3], 7.04 [m, 2H, H7]; Sn–Bz skeleton: 2.51 [d, 4H, H1*], 6.70 [m, 4H, H4*], 6.61 [m, 6H, H3* and H5*], ppm. ^{13}C NMR ($CDCl_3$125.76 MHz); δ_c: 161.9 [C8], 151.4 [C1'], 140.5 [C2'], 135.6 [C4'], 135.4 [C5], 135.3 [C8a], 134.9 [C4], 128.5 [C4a], 127.5 [C3'and C5'], 122.9 [C2'and C6'], 121.7 [C3], 118.7 [C6], 113.7 [C7]; Sn–Bz skeleton ($^{n}J(^{119}Sn,^{13}C)$, Hz): 33.3 [C1*(927)], 142.6 [C2*(55)], 128.9 [C3*(17)], 127.4 [C4*(81)], 123.5 [C5*(81)] ppm.

4.3.3.3.5. $Bz_2Sn(L^7)_2$ (24)

^{1}H NMR ($CDCl_3$500.13 MHz); δ_H: 9.14 [dd, 2H, H4], 8.12 [d, 4H, H2 and H6], 7.90 [d, 4H, H2' and H6'], 7.25 [m, 2H, H3], 7.12 [m, 2H, H7], 7.00 [m, 4H, H3'and H5'], 3.90 [d, 6H, OCH_3]; Sn–Bz skeleton: 2.64 [d, 4H, H1*], 6.81 [m, 4H, H4*], 6.73 [m, 6H, H3* and H5*], ppm. ^{13}C NMR ($CDCl_3$125.76 MHz); δ_c: 161.5 [C8], 161.1 [C1'], 147.9 [C2], 142.9 [C4'], 136.3 [C5], 135.7 [C8a],135.4 [C4], 128.3 [C4a], 124.2 [C3'and C5'], 123.1 [C3], 118.2 [C6], 114.3 [C2'and C6'], 113.9 [C7], 55.6 [OCH_3]; Sn–Bz skeleton ($^{n}J(^{119}Sn,^{13}C)$, Hz): 33.6 [C1*(927)], 141.1 [C2* (55)], 127.8 [C3*(17)], 127.6 [C4*(81)], 121.9 [C5*(81)] ppm.

4.3.3.3.6. $Bz_2Sn(L^8)_2$ (25)

^{1}H NMR ($CDCl_3$500.13 MHz); δ_H: 9.05 [dd, 2H, H4], 8.02 [dd, 2H, H2], 7.96 [d, 2H, H6], 7.66 [m, 4H, H2'and H6'], 7.12 [d, 2H, H3], 6.94 [d, 2H, H7], 6.72 [m, 4H, H3'and H5'], 3.89 [q, 4H, OCH_2CH_3], 1.30 [t, 6H, OCH_2CH_3]; Sn–Bz skeleton: 2.45 [d, 4H, H1*], 6.64 [m, 4H, H4*], 6.56 [m, 6H, H3* and H5*], ppm. ^{13}C NMR ($CDCl_3$125.76 MHz); δ_c: 160.7 [C8], 160.3 [C1'], 147.2 [C2], 142.3 [C4'], 135.5 [C5], 135.3 [C8a], 134.7 [C4], 128.2 [C4a], 123.9 [C3'and C5'], 121.2 [C3], 117.7 [C2' and C6'], 14.1 [C6], 113.5 [C7], 63.0 [OCH_2CH_3], 14.7 [OCH_2CH_3]; Sn–Bz skeleton ($^{n}J(^{119}Sn,^{13}C)$, Hz): 33.2 [C1*(927)], 140.8 [C2*(55)], 127.5 [C3*(17)], 127.3 [C4*(81)], 122.7 [C5*(81)] ppm.

Further structural conclusions have been extracted from the ^{119}Sn NMR spectra in solution (Table 4.10). The complexes **20-25**, all display a sharp singlet at –325.7 ± 1.5 ppm and

the $\delta(^{119}Sn)$ chemical shifts lie within the range –125 and –515 ppm. These values are in agreement with those reported for other six coordinate diorganotin compounds [24]. The $\delta(^{119}Sn)$ values are comparable with the shift observed for the $Bz_2Sn(Ox)_2$ complex (–335.2 ppm in $CDCl_3$ [28]). Thus, the ^{119}Sn NMR data indicate that the complexes in solution, retain their solid-state structures (see Mössbauer discussion, *vide supra*). ^{117}Sn-CP-MAS (Cross-polarization technique combined with magic angle spinning) NMR spectra were also recorded in the solid state, which is devoid of solvation and dynamic effects to further confirm the structures. The isotropic ^{117}Sn chemical shift and the data of the tensor analysis [38] for compounds **20-25** are reported in Table 4.10. The isotropic chemical shifts are all in the range –320 to –355 ppm and hardly different from the data in solution, implying that the same octahedral coordination is preserved. The dibenzyltin(IV) compounds, **22** and **23**, bearing a halogen substituent in the *para*-position have axial symmetry (η = 0.00 or 0.10). Compound **22** has two tin resonances with slightly different isotropic chemical shift suggesting minor differences in the C–Sn–C geometry in the crystals for this compound. This observation is confirmed by crystal structure analysis. The compound is shown to be disordered and adopts two slightly different conformations. Compounds **20** and **21**, with a methyl substituent in the *meta*- and *para*-positions, respectively, display an almost axial symmetry (η = 0.25) with the same isotropic chemical shift. The difference between the two compounds is reflected in the slightly different chemical shielding anisotropy (182 versus 203 ppm), with corresponding slightly different principal tensor components. The alkoxy-substituted compounds, **24** and **25**, have higher asymmetry parameters (η = 0.35 and 0.45), which are accompanied by a higher chemical shift anisotropy of ca. 50 ppm.

X-ray data for **21**, **22** and **24** clearly evidence that these compounds are essentially isostructural. The differences noted in the asymmetry parameters between these compounds can be traced back to varying deviations from a regular octahedral geometry, being stronger in **21** and **24** than in **22**. Especially the C1SnN1 bond angles are illustrative in this context, as the differences between these angles within one compound and the deviation from a regular octahedral increase in the order **22**< **21**<**24**, exactly the same order as the asymmetry parameter η.

Table 4.10. Solution ^{119}Sn-NMR data (δ, ppm) and Solid State ^{117}Sn NMR data for the dibenzyltin(IV) complexes (**20-25**)

Complex[a]	^{119}Sn-NMR data[b]	^{117}Sn MAS[c]					
		δ_{iso}	ζ	η	σ_{11}	σ_{22}	σ_{33}
$Bz_2Sn(L^3)_2$ (**20**)	–325.3	–339	182	0.25	225	271	521
$Bz_2Sn(L^4)_2$ (**21**)	–327.2	–338	203	0.25	212	262	541
$Bz_2Sn(L^5)_2$ (**22**)	–324.3	–336 –354	201 201	0.10 0.00	225 253	245 253	537 555
$Bz_2Sn(L^6)_2$ (**23**)	–324.5	–335	196	0.00	237	237	531
$Bz_2Sn(L^7)_2$ (**24**)	–326.4	–322	249	0.35	154	241	571
$Bz_2Sn(L^8)_2$ (**25**)	–326.4	–329	242	0.45	153	262	571

[a] Complex numbers are in parentheses.
[b] In $CDCl_3$ solution. [c] Parameters: δ_{iso}(ppm) $= -\sigma_{iso} - (\sigma_{11} + \sigma_{22} + \sigma_{33})/3$; ζ(ppm) $= \sigma_{33} - \sigma_{iso}$ and $\eta - |\sigma_{22} - \sigma_{11}|/|\sigma_{33} - \sigma_{iso}|$ where σ_{11}, σ_{22} and σ_{33} (ppm) are the principal tensor components of the chemical shielding anisotropy, sorted as follows:$|\sigma_{33} - \sigma_{iso}| \geq |\sigma_{11} - \sigma_{iso}| \geq |\sigma_{22} - \sigma_{iso}|$.

4.3.3.4. Electro-spray Ionization Mass spectrometry (ESI MS)

The typical ions in the first-order positive-ion ESI mass spectra of $Bz_2Sn(L)_2$ complexes (**20–25**) are sodium and potassium ion adducts with the molecule, which is used for the determination of molecular weights of the dibenzyltin(IV) compounds. In addition to these ions, the neutral loss of the ligand $[M\text{-}L]^+$ are observed as well as in the first-order spectra. The presence of the neutral losses of *m/z* 92 (toluene) or 90 in tandem mass spectra determine the presence of a benzyl group on tin atom. The neutral loss of LH (or LNa) confirms the presence of the corresponding ligand L. The deprotonated molecule of ligand $[L]^-$ is the base peak for all first-order negative-ion mass spectra except for compound **24**. The characteristic neutral losses in tandem mass spectra are 28 (N_2) and losses of ligand substituents (methane, toluene, chlorobenzene and bromobenzene) to form the radical ions.

The detailed mass spectral features for complexes **20–25** are given below:

4.3.3.4.1. $Bz_2Sn(L^3)_2$ **(20)**

MW = 826. Positive-ion MS: *m/z* 865 $[M+K]^+$; *m/z* 849 $[M+Na]^+$; *m/z* 564 $[M-L^3]^+$, 100%. MS/MS of *m/z* 849: *m/z* 665 [M+Na-2*toluene]$^+$; *m/z* 564 $[M-L^3]^+$; *m/z* 382 $[M-L^3$-toluene-90$]^+$. MS/MS of *m/z* 564: *m/z* 380 $[M-L^3$-2*toluene$]^+$. Negative-ion MS: *m/z* 262 $[L^3]^-$,100%. MS/MS of *m/z* 262: *m/z* 234 $[L^3-N_2]^-$; *m/z* 143 $[L^3-N_2$-toluene$]^-$.

4.3.3.4.2. $Bz_2Sn(L^4)_2$ **(21)**

MW = 826. Positive-ion MS: *m/z* 865 $[M+K]^+$; *m/z* 849 $[M+Na]^+$,100%; *m/z* 564 $[M-L^4]^+$. MS/MS of *m/z* 865: *m/z* 683 [M+K-toluene-90]$^+$; *m/z* 564 $[M-L^4]^+$; *m/z* 382$[L^4Sn]^+$. MS/MS of *m/z* 849: *m/z* 667 [M+Na-toluene-90]$^+$; *m/z* 564 $[M-L^4]$; *m/z* 382 $[L^4Sn]^+$. MS/MS of *m/z* 849: *m/z* 667 [M+Na-toluene-90]$^+$; *m/z* 564 $[M-L^4]^+$; *m/z* 382 $[L^4Sn]^+$. MS/MS of *m/z* 564: *m/z* 382 $[L^4Sn]^+$. Negative-ion MS: *m/z* 262 $[L^4]^-$, 100%. MS/MS of *m/z* 262: *m/z* 234 $[L^4-N_2]^-$; *m/z* 143 $[L^4$-toluene $-N_2]^-$.

4.3.3.4.3. $Bz_2Sn(L^5)_2$ **(22)**

MW = 954. Positive-ion MS: *m/z* 995 $[M+K]^+$; *m/z* 979 $[M+Na]^+$, 100%; *m/z* 628 $[M-L^5]^+$. MS/MS of *m/z* 995: *m/z* 813 [M+K-toluene-90]$^+$; *m/z* 446 $[L^5Sn]^+$. MS/MS of *m/z* 979: *m/z* 797 [M+Na-toluene-90]$^+$; *m/z* 627 $[M-L^5]^+$; *m/z* 446 $[L^5Sn]^+$. MS/MS of *m/z* 628: *m/z* 446 $[L^5Sn]^+$. Negative-ion MS: *m/z* 326 $[L^5]^-$, 100%. MS/MS of *m/z* 326: *m/z* 143 $[L^5$-brombenzene-$N_2]^-$.

4.3.3.4.4. $Bz_2Sn(L^6)_2$ **(23)**

MW = 866. Positive-ion MS: *m/z* 905 $[M+K]^+$; *m/z* 889 $[M+Na]^+$; *m/z* 584 $[M-L^6]^+$, 100%. MS/MS of *m/z* 889: *m/z* 707[M+Na-toluene-90]$^+$; *m/z* 584 $[M-L^6]^+$; *m/z* 402$[L^6Sn]^+$. MS/MS of *m/z* 564: *m/z* 402 $[L^6Sn]^+$. Negative-ion MS: *m/z* 282 $[L^6]^-$, 100%. MS/MS of *m/z* 282: *m/z* 143 $[L^6$-chlorbenzene-$N_2]^-$.

4.3.3.4.5. $Bz_2Sn(L^7)_2$ **(24)**

MW = 858. Positive-ion MS: *m/z* 897 $[M+K]^+$; *m/z* 881 $[M+Na]^+$, 100%; *m/z* 580 $[M-L^7]^+$. MS/MS of *m/z* 897: *m/z* 715 [M+K-toluene-90]$^+$; *m/z* 580 $[M-L^7]^+$; *m/z* 398 $[L^7Sn]^+$. MS/MS of *m/z* 881: *m/z* 699[M+Na-toluene-90]$^+$; *m/z* 580 $[M-L^7]^+$; *m/z* 398 $[L^7Sn]^+$. MS/MS of *m/z* 564: *m/z* 398 $[L^7Sn]^+$. Negative ion MS: *m/z* 278 $[L^7]^-$; *m/z* 263 $[L^7-CH_4]^-$, 100%. MS/MS of *m/z* 278: *m/z* 263 $[L^7-CH_4]^-$. MS/MS of *m/z* 263: *m/z* 234 $[L^7-CH_4-N_2]^-$; *m/z* 158 $[L^7$-toluene-$N_2]^-$.

4.3.3.4.6. $Bz_2Sn(L^8)_2$ (25)

MW = 886. Positive-ion MS: *m/z* 925 $[M+K]^+$; *m/z* 909 $[M+Na]^+$, 100%; *m/z* 594 $[M-L^8]^+$. MS/MS of *m/z* 925: *m/z* 743 [M+K-toluene-90]$^+$; *m/z* 594 $[M-L^8]^+$; *m/z* 412 $[L^8Sn]^+$. MS/MS of *m/z* 909: *m/z* 727 [M+Na-toluene-90]$^+$; *m/z* 594 $[M-L^8]^+$; *m/z* 412 $[L^8Sn]^+$. MS/MS of *m/z* 594: *m/z* 412 $[LSn]^+$. Negative-ion MS: *m/z* 292 $[L^8]^-$, 100%; *m/z* 263 $[L^8-C_2H_6]^-$. MS/MS of *m/z* 292: *m/z* 263 $[L^8-C_2H_6]^-$. MS/MS of *m/z* 263: *m/z* 234 $[L^8-C_2H_6-N_2]^-$.

4.4. Structural précis of the diorganotin(IV) complexes

A series of *cis*- bis{5-[(*E*)-2-(aryl)-1-diazenyl]quinolinolato}diorganotin(IV) complexes of the type $R_2Sn(L)_2$ (R = ^{n}Bu, Ph and Bz) have been prepared and their structures are characterized by single crystal X-ray crystallography. The crystal structures of four di-*n*-butyltin compounds, *viz.*, $^n Bu_2Sn(L^4)_2$ (**9**), $^n Bu_2Sn(L^5)_2 0.5C_6H_6$ (**10**), $^n Bu_2Sn(L^7)_2$ (**12**), and $^n Bu_2Sn(L^8)_2$ (**13**); three diphenyltin(IV) compounds, *viz.*, $Ph_2Sn(L^1)_2.C_3H_6O$ (**14**), $Ph_2Sn(L^4)_2$ (**17**) and $Ph_2Sn(L^5)_2$ (**18**) and three dibenzyltin(IV) compounds, *viz.*, $Bz_2Sn(L^4)_2$ (**21**), $Bz_2Sn(L^5)_2$ (**22**) and $Bz_2Sn(L^7)_2$ (**24**) are reported.

All the diorganotin(IV) complexes of the type $R_2Sn(L)_2$ (R = ^{n}Bu, Ph and Bz) are basically isostructural and contain a central tin atom that is octahedrally coordinated to two deprotonated 5-[(*E*)-2-(aryl)-1-diazenyl]quinolin-8-ol ligands and two R groups. The ligands are arranged about the central Sn such that the oxygen atoms are *trans* to each other while the carbon atoms of R and quinoline nitrogen atoms are mutually *cis* to each other. These structures can best be thought of as a distorted octahedron with the two oxygen, nitrogen and carbon (R group) forming a plane and the remaining nitrogen and carbon (R group) being *trans* to each other. The change in the ligand substituents or Sn-R substituents essentially does not effect in the geometry. A representative structure from each category is summarized in Scheme 4.2.

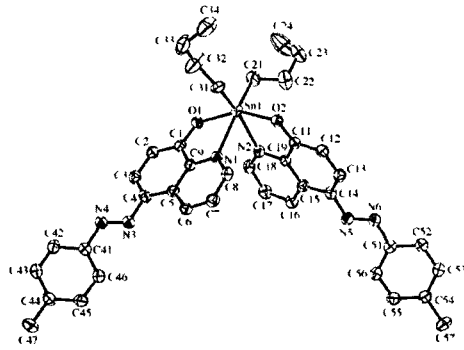

(9)

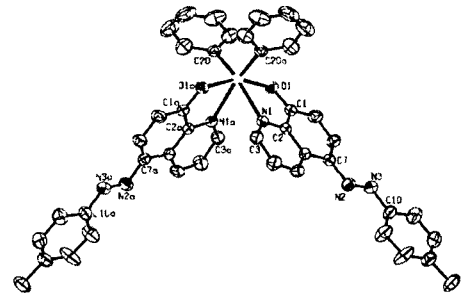

(17)

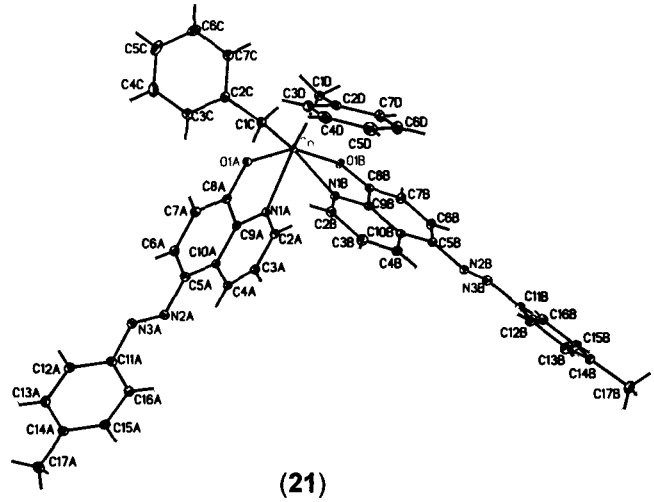

(21)

(a) distorted *cis*-octahedral arrangement in the molecules of $R_2Sn(L)_2$ around the tin atom

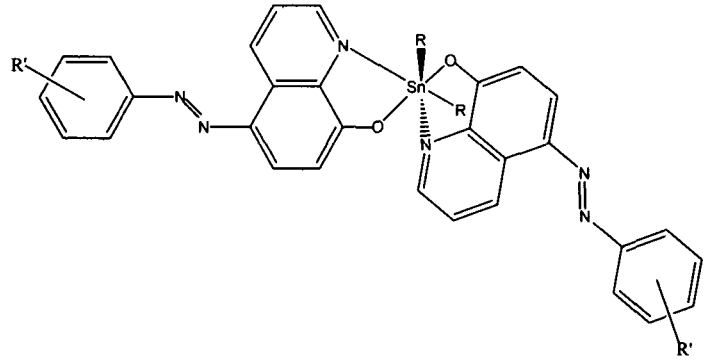

(R = ^{n}Bu, Ph or Bz; R' = various nuclear substituents)

(b) A chemdraw representation of the molecule of $R_2Sn(L)_2$ showing a distorted *cis*-octahedral arrangement around the tin atom

Scheme 4.2 The representative structures of the molecules of $^n Bu_2Sn(L^4)_2$ (**9**), $Ph_2Sn(L^4)_2$ (**17**) and $Bz_2Sn(L^4)_2$ (**21**) along with a chemdraw representation, showing coordination geometries.

4.5. Experimental

4.5.1. Synthesis of ligands

The ligands *viz.*, 5-[(*E*)-2-(phenyl)-1-diazenyl]quinolin-8-ol (L^1H), 5-[(*E*)-2-(2-methylphenyl)-1-diazenyl]-quinolin-8-ol (L^2H), 5-[(*E*)-2-(3-methylphenyl)-1-diazenyl]-quinolin-8-ol (L^3H), 5-[(*E*)-2-(4-methylphenyl)-1-diazenyl]quinolin-8-ol (L^4H), 5-[(*E*)-2-(4-bromophenyl)-1-diazenyl]quinolin-8-ol (L^5H), 5-[(*E*)-2-(4-chlorophenyl)-1-diazenyl]quinolin-8-ol (L^6H), 5-[(*E*)-2-(4-methoxyphenyl)-1-diazenyl]-quinolin-8-ol (L^7H) and 5-[(*E*)-2-(4-ethoxyphenyl)-1-diazenyl]quinolin-8-ol (L^8H) used for synthesizing diorganotin(IV) complexes are described in Chapter 2 (see Section 2.6).

4.5.2. Synthesis of diorganotin(IV) complexes

The synthesis of diorganotin(IV) complexes, *viz.*, di-*n*-butyltin(IV), diphenyltin(IV) and dibenzyltin(IV) complexes are described in sequel along with the characterization data.

4.5.2.1 Synthesis of di-n-butyltin(IV) complexes

A typical method is described below.

4.5.2.1.1. Preparation of $^nBu_2Sn(L^2)_2$ (7) [16]

A methanolic solution of sodium methoxide (generated *in situ* from 0.045 g, 1.95 mmol of Na in anhydrous methanol) was added drop-wise into a stirred hot anhydrous benzene solution (45 ml) containing L^2H (0.5 g, 1.90 mmol). After the addition, a precipitate appears and the stirring was continued for an additional 15 min. To this reaction mixture, an anhydrous benzene solution (15 ml) of $^nBu_2SnCl_2$ (0.26 g, 0.85 mmol) was added drop-wise which resulted in the formation of NaCl. The reaction mixture was refluxed for 3 h and filtered to remove the NaCl. The filtrate was collected and the solvent was removed under reduced pressure. The resultant residue was extracted with hexane. The crude product was recrystallized from hexane, which upon cooling afforded a maroon coloured crystalline product. Yield: 0.35 g (53.8%), M.p.: 64–65 °C. Anal. found: C, 63.32; H, 5.78; N, 10.89%. Calc. for $C_{40}H_{42}N_6O_2Sn$: C, 63.42; H, 5.58; N, 11.09%.

The other di-*n*-butyltin(IV) complexes of 5-[(*E*)-2-(aryl)-1-diazenyl]quinolin-8-ol, were prepared analogously and their analytical data are presented below.

4.5.2.1.2. Preparation of $^nBu_2Sn(L^3)_2$ (**8**) [16].

Recrystallized from hexane to give maroon crystalline product 0.33 g (50.7%). M.p.: 80-82 °C. Anal. Found: C, 63.40; H, 5.53; N, 11.01. Calc. for $C_{40}H_{42}N_6O_2Sn$: C, 63.42; H, 5.58; N, 11.09%.

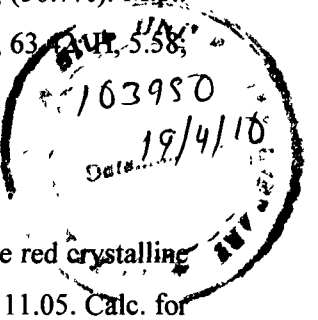

4.5.2.1.3. Preparation of $^nBu_2Sn(L^4)_2$ (**9**) [16]

Recrystallized from a mixture of benzene and hexane (v/v 1:1) to give red crystalline product 0.40 g (61.5%); M.p.: 171-172 °C. Anal. Found: C, 63.40; H, 5.56; N, 11.05. Calc. for $C_{40}H_{42}N_6O_2Sn$: C, 63.42; H, 5.58; N, 11.09%.

4.5.2.1.4. Preparation of $^nBu_2Sn(L^5)_2$ 0.5 C_6H_6 (**10**) [16]

Recrystallized from a mixture of benzene and hexane (v/v 2:1) to give red crystalline product 0.56 g (83.6%); M.p.: 154-56 °C. Anal Found: C, 53.13; H, 4.20; N, 9.07. Calc. for $C_{41}H_{39}Br_2N_6O_2Sn$: C, 53.16; H, 4.24; N, 9.07%.

4.5.2.1.5. Preparation of $^nBu_2Sn(L^6)_2$ (**11**) [16]

Recrystallized from hexane to give dark-red crystalline product 0.59g (85.3%); M.p.: 84-85 °C. Anal. Found: C, 57.13; H, 4.52; N, 10.45. Calc. for $C_{38}H_{36}N_6O_2Cl_2Sn$: C, 57.16; H, 4.54; N, 10.52%.

4.5.2.1.6. Preparation of $^nBu_2Sn(L^7)_2$ (**12**) [16]

Recrystallized from a mixture of benzene and hexane (v/v 1:1) to give orange crystalline product 0.47 g (69.6%); M.p.: 154-156°C. Anal. Found: C, 60.83; H, 5.33; N, 10.62%. Calc. for $C_{40}H_{42}N_6O_4Sn$: C, 60.85; H, 5.36; N, 10.64%.

4.5.2.1.7. Preparation of $^nBu_2Sn(L^8)_2$ (**13**) [16]

Recrystallized from a mixture of benzene and hexane (v/v 1:1) to give red crystalline product 0.57 g (82.7%); M.p.: 275-276°C. Anal. Found: C, 61.66; H, 5.63; N, 10.26%. Calc. for $C_{42}H_{46}N_6O_4Sn$: C, 61.70; H, 5.67; N, 10.28%.

•

4.5.2.2. Synthesis of diphenyltin(IV) complexes

A typical method is described below.

4.5.2.2.1. Preparation of $Ph_2Sn(L^4)_2$ (17) [19]

L^4H (1.0 g, 3.80 mmol) in hot anhydrous benzene (45 ml) was added drop-wise with continuous stirring to a hot anhydrous benzene solution (30 ml) containing Ph_3SnCl (1.46 g, 3.80 mmol). The reaction mixture was refluxed for 2h, then triethylamine (0.38 ml, 3.80 mmol) was added and reflux was continued for additional 1.5 h. The reaction mixture was cooled to room temperature and filtered to remove $Et_3N.HCl$. The filtrate was collected; volatiles were removed and dried *in vacuo*. The residue was extracted into hexane and filtered while hot. The crude product was obtained after evaporation of the hexane. This was then recrystallized from a mixture of benzene-hexane (1:1), which upon slow evaporation afforded red crystalline product. Yield: 1.02g (66.2 %), M.p.: 239-240 °C. Anal. Found: C, 66.35; H, 4.35; N, 10.60%. Calc. for $C_{44}H_{34}N_6O_2Sn$: C, 66.27; H, 4.30; N, 10.54%.

The other diphenyltin complexes of 5-[(*E*)-2-(aryl)-1-diazenyl]quinolin-8-ol, were prepared analogously as mentioned above and their analytical data are presented below:

4.5.2.2.2. Preparation of $Ph_2Sn(L^1)_2.C_3H_6O$ (14) [19].

Dark-red crystals were obtained from acetone. Yield: 0.74 g (74%), M.p:. 140-141 °C. Anal. Found: C, 65.34; H, 4.90; N, 11.09%. Calc. for $C_{45}H_{36}N_6O_3Sn$: C, 65.31; H, 3.85; N, 10.16%.

4.5.2.2.3. Preparation of $Ph_2Sn(L^2)_2$ (15) [19]

Red crystals were obtained from a mixture of benzene and hexane (v/v 1:1). Yield: 0.87g (56.5%), mp: 80-81 °C. Anal. Found: C, 66.30; H, 4.31; N, 10.50%. Calc. for $C_{44}H_{34}N_6O_2Sn$: C, 66.27; H, 4.30; N, 10.54%.

4.5.2.2.4. Preparation of $Ph_2Sn(L^3)_2$ (16) [19]

Maroon crystal were obtained from a mixture of benzene and hexane (v/v 1:1). Yield: 0.77 g (50%); M.p.: 194-195 °C. Anal. Found: C, 66.20; H, 4.38; N, 10.60. Calc. for $C_{44}H_{34}N_6O_2Sn$: C, 66.27; H, 4.30; N, 10.54%.

4.5.2.2.5. Preparation of $Ph_2Sn(L^5)_2$ (18) [19]

Orange crystals were obtained from a mixture of benzene and hexane (v/v 1:1). Yield: 0.28g (45.7%), M.p.: 275-276 °C. Anal. Found: C, 54.28; H, 3.33; N, 8.89%. Calc. for $C_{42}H_{28}Br_2N_6O_2Sn$: C, 54.40; H, 3.04; N, 9.06%.

4.5.2.2.6. Preparation of $Ph_2Sn(L^8)_2$ (19) [19]

Orange crystals were obtained from a mixture of benzene and hexane (v/v 1:1). Yield: 0.33g (45.8%), M.p.: 125-126 °C. Anal. Found: C, 64.43; H, 4.47; N, 9.80%. Calc. for $C_{46}H_{38}N_6O_4Sn$: C, 64.43; H, 4.47; N, 9.80%.

4.5.2.3. Synthesis of dibenzyltin(IV) complexes

A typical method is described below.

4.5.2.3.1. Preparation of $Bz_2Sn(L^3)_2$ (20) [20]

A methanolic solution of sodium methoxide (generated *in situ* from 0.045 g, 1.95 mmol of Na in 15 ml anhydrous methanol) was added drop-wise into a stirred hot anhydrous benzene solution (45 ml) containing L^1H (0.5 g, 1.90 mmol). After complete addition, a precipitate appears and the stirring was continued for 15 min. To this reaction mixture, an anhydrous benzene solution (15 ml) of Bz_2SnCl_2 (0.35 g, 0.94 mmol) was added drop-wise which resulted in the disappearance of the precipitate. The reaction mixture was refluxed for 3 h and filtered to remove NaCl. The filtrate was collected and the solvent was removed under reduce pressure. The resultant residue was extracted into hexane and filtered while hot. The crude product was obtained after evaporation of the hexane.This was then recrystallized from a mixture of benzene–hexane (1:1), which upon slow evaporation afforded dark-red crystalline product. Yield: 0.37 g (33.9 %), M.p.: 180–182 °C. Anal. Found: C, 66.92; H, 4.64; N, 10.18%. Calc. For $C_{46}H_{38}N_6O_2Sn$: C, 66.99; H, 4.60; N, 10.24%.

The other dibenzyltin complexes of 5-[(*E*)-2-(aryl)-1-diazenyl]quinolin-8-ol, were prepared analogously as mentioned above and their characterization an spectroscopic data of the complexes are presented below:

4.5.2.3.2. Preparation of $Bz_2Sn(L^4)_2$ (21) [20].

Orange crystals were obtained from a mixture of benzene and hexane (v/v 1:1). Yield: 0.58 g (26.5%), M.p.: 218–219 °C. Anal. Found: C, 67.04; H, 4.50; N, 10.29%. Calc. for $C_{46}H_{38}N_6O_2Sn$: C, 66.92; H, 4.64; N, 10.18 %.

4.5.2.3.3. Preparation of $Bz_2Sn(L^5)_2$ (22) [20]

Dark- red crystals were obtained from a mixture of benzene and hexane (v/v 1:1). Yield: 0.70 g (54.7%), M.p.: 215-216 °C. Anal. Found: C, 55.38; H, 3.30; N, 8.82%. Calc. for $C_{44}H_{32}Br_2N_6O_2Sn$: C, 55.32; H, 3.38; N, 8.79%.

4.5.2.3.4. Preparation of $Bz_2Sn(L^6)_2$ (23) [20]

Maroon crystals were obtained from a mixture of benzene and hexane (v/v 1:1). Yield: 0.50 g (69.4%), M.p: 141–142 °C. Anal. Found: C, 61.22; H, 3.50; N, 9.82%. Calc. for $C_{44}H_{32}Cl_2N_6O_2Sn$: C, 60.99; H, 3.72; N, 9.70%.

4.5.2.3.5. Preparation of $Bz_2Sn(L^7)_2$ (24) [20]

Orange crystals were obtained from a mixture of benzene and hexane (v/v 1:1). Yield: 0.48 g (31.8%), M.p.: 154-55 °C. Anal. Found: C, 64.50; H, 4.70; N, 9.88%. Calc. for $C_{46}H_{38}N_6O_4Sn$: C, 64.43; H, 4.47; N, 9.80%.

4.5.2.3.6. Preparation of $Bz_2Sn(L^8)_2$ (25) [20]

Orange crystals were obtained from a mixture of carbon tetrachloride and hexane (v/v 1:1). Yield: 0.58 g (37.4%), M.p.: 175-176 °C. Anal. Found: C, 65.01; H, 4.70; N, 9.60%. Calc. for $C_{48}H_{42}N_6O_4Sn$: C, 65.10; H, 4.78; N, 9.49%.

4.5.3. Chemicals used for the preparations

$^nBu_2SnCl_2$ (Merck), $^nBu_2SnO$, Ph_3SnCl (Fluka AG), Ph_2SnCl_2 (Aldrich) and 8-hydroxyquinoline (Merck) was used as such. Bz_2SnCl_2 was prepared by the reported method [37]. The substituted anilines (reagent grade) were used after purification. The solvents used in the reactions were of AR grade and dried using standard procedures. Benzene was distilled from sodium benzophenone ketyl.

4.5.3. Physical measurements

Carbon, hydrogen and nitrogen analyses were performed with a Perkin–Elmer 2400 series II instrument. IR spectra in the range 4000–400 cm^{-1} were obtained on a BOMEM DA-8 FT-IR spectrophotometer with samples investigated as KBr discs. The ^1H-, ^{13}C- and ^{119}Sn-NMR spectra were recorded either on a Bruker AMX 400 spectrometer and measured at 400.13, 100.62 and 149.18 MHz respectively or on a Bruker AMX 500 spectrometer and measured at 500.13, 125.76 and 186.18 MHz, respectively. The ^1H, ^{13}C and ^{119}Sn chemical shifts were referred to Me_4Si set at 0.00 ppm, $CDCl_3$ set at 77.0 ppm and Me_4Sn set at 0.00 ppm, respectively. Positive-ion and negative-ion electrospray ionization (ESI) mass spectra were measured on an ion trap analyzer Esquire 3000 (Bruker Daltonics, Bremen, Germany) in the range *m/z* 50–1500. The samples were dissolved in 100% acetonitrile and analyzed by

direct infusion at a flow rate of 5 μl/min. The selected precursor ions were further analyzed by MS/MS analyses under the following conditions: an isolation width of *m/z* = 8, a collision amplitude in the range 0.8–1.0V depending on the precursor ion stability, an ion source temperature of 300 °C, a tuning parameter for compound stability of 100%, while the flow rate and the pressure of nitrogen were 4 l/min and 10 psi, respectively [18,19]. The ^{119}Sn Mössbauer spectra of the diorganotin(IV) complexes ($^{n}Bu_2Sn(L)_2$: **7-13** and $Bz_2Sn(L)_2$: **20-25**) in the solid state were recorded using a Model MS-900 (Ranger Scientific Co., Burleson, TX) spectrometer in the acceleration mode with a moving source geometry. A 10 mCi $Ca^{119m}SnO_3$ source was used, and counts of 30,000 or more were accumulated for each spectrum. The spectra were measured at 80 K using a liquid-nitrogen cryostat (CRYO Industries of America, Inc., Salem, NH). The velocity was calibrated at ambient temperature using a composition of $BaSnO_3$ and tin foil (splitting 2.52 mm s^{-1}). The resultant spectra were analyzed using the Web Research software package (Web Research Co., Minneapolis, MN). On the other hand, ^{119}Sn Mössbauer spectra for the diphenyltin(IV) complexes ($Ph_2Sn(L)_2$: **14-19**) were recorded on solid samples at liquid nitrogen temperature by using a conventional constant acceleration spectrometer, coupled with a multichannel analyser (a.e.n., Ponteranica (BG), Italy) equipped with a cryostat Cryo (RIAL, Parma, Italy). A $Ca^{119}SnO_3$ Mössbauer source, 10 mCi (from Ritverc, St Petersburg, Russia) moving at room temperature with constant acceleration in a triangular waveform was used. The velocity calibration was made using a ^{57}Co Mössbauer source, 10 mCi, and an iron foil as absorber (from Ritverc, St Petesrburg, Russia)

4.5.4. X-ray crystallography

4.5.4.1. Di-n-butyltin(IV) complexes (**9**, **10**, **12** and **13**)

Crystals of compounds **9**, **10**, **12** and **13** suitable for an X-ray crystal structure determination were obtained from slow evaporation of benzene/hexane (v/v 1:1) solutions of the respective compounds. All measurements were made at 160 K on a Nonius KappaCCD diffractometer [39] with graphite-monochromated MoKα radiation (λ = 0.71073 Å) and an Oxford Cryosystems Cryostream 700 cooler. Data reduction was performed with HKL Denzo and Scalepack [40]. The intensities were corrected for *Lorentz* and polarization effects, and empirical absorption corrections based on the multi-scan method [41] were applied. Equivalent reflections were merged. The data collection and refinement parameters are given in Table **4.2**, and views of the molecules (**9**, **10**, **12** and **13**) are shown in Figs. 4.1–4.4. The structures were solved by direct-methods using SHELXS97 [42] for **9** and **12** and SIR92 [43] for **10** and **13**. The asymmetric unit in **9** and **13** contains one molecule in a general position, plus two half

molecules, each of which sits across a C_2-axis. In **9** and **13**, the butyl groups in each of the C_2-symmetric molecules are disordered. Two sets of equally occupied positions were defined for the atoms of each disordered symmetry-independent butyl group. Similarity restraints were applied to the chemically equivalent bond lengths and angles involving all disordered C-atoms, while neighbouring atoms within and between each conformation of the disordered butyl groups were restrained to have similar atomic displacement parameters.

The 4'-ethoxyphenyl group of one quinolinolato ligand in **8** is disordered over two conformations. Two sets of overlapping positions were defined for the atoms of the ethoxyphenyl group and the site occupation factor of the major conformation refined to 0.541(4). Similarity restraints analogous to those described for **3** were employed during the refinement.

In **10,** the asymmetric unit contains one molecule of the Sn-complex, plus one half of a molecule of benzene, which sits across a centre of inversion. The benzene molecule is highly disordered within its cavity and a reasonable model could not be developed. Therefore, the contribution of the solvent molecules to the intensity data was removed by using the *SQUEEZE* [44] routine of the *PLATON* [45] program. Omission of the solvent molecule from the model leaves one cavity of 212 $Å^3$ per unit cell, located at a centre of inversion. The number of electrons contributing to each void in the structure was calculated by the *SQUEEZE* routine to be approximately 38 e. This corresponds well with the electron count for one molecule of benzene per cavity (42 e), which is consistent with the crystallization solvent (benzene/hexane) and the residual electron density peaks initially observed for this region of the structure. The assumed solvent composition was used in the subsequent calculation of the empirical formula, formula weight, density, linear absorption coefficient and $F(000)$. One of the butyl groups in **10** is disordered over two conformations. Two sets of overlapping positions were defined for central two methylene groups of the disordered butyl group and the site occupation factor of the major conformation refined to 0.776(7). Similarity restraints analogous to those described for **9** were employed during the refinement.

For each structure, the non-hydrogen atoms were refined anisotropically. All of the H-atoms were placed in geometrically calculated positions and refined by using a riding model where each H-atom was assigned a fixed isotropic displacement parameter with a value equal to $1.2U_{eq}$ of its parent C atom ($1.5U_{eq}$ for the methyl groups). The refinement of each structure was carried out on F^2 using full-matrix least-squares procedures, which minimized the function $\Sigma w (F_o^2 - F_c^2)^2$. Corrections for secondary extinction were applied for **9** and **13**. Four reflections in **9**, six reflections in **13** and one reflection in **10,** whose intensities were considered to be

extreme outliers, were omitted from the final refinement. All calculations were performed using the SHELXL97 program [42].

4.5.4.2. Diphenyltin(IV) complexes (14, 17 and 18)

Crystals of diphenyltin(IV) compounds **14**, **17** and **18** suitable for an X-ray crystal structure determination were obtained from acetone, hexane and benzene/hexane mixture (1:1 v/v), respectively. Intensity data were collected with graphite-monochromated MoKα radiation (λ = 0.71073 Å), either on Nonius CAD4 diffractometers (**17** and **18**) or a Bruker SMART APEX (for **14**). For the tin complexes **14**, **17** and **18**, empirical absorption corrections based on a multiscan approach [46] or on azimuthal scans [47] were applied to the data sets before averaging over symmetry-related reflections. The structures were solved by direct methods with the help of the SHELXS-97 program [48] and refined on reflection intensities F^2 using the SHELXL-97 program [49]. In the final least-squares refinements, all non-hydrogen atoms were refined with anisotropic displacement parameters, and hydrogen atoms were placed in idealized positions and included as riding on the corresponding atoms.

4.5.3.3. Dibenzyltin(IV) complexes (21, 22 and 24)

Crystals of the dibenzyltin(IV) compounds $Bz_2Sn(L^4)_2$ (**21**), $Bz_2Sn(L^5)_2$ (**22**) and $Bz_2Sn(L^7)_2$ (**24**) suitable for an X-ray crystal structure determination were obtained from benzene/hexane mixture (1:2 v/v), ethanol, chloroform/hexane mixture (1:1 v/v), respectively. Intensity data were collected with graphite-mono-chromated MoKα radiation (λ = 0.71073 Å), on 1 K CCD diffractometer.

References

[1] M. Gielen, R. Willem, J. Holeček, A. Lyčka, Main Group Met. Chem. **16** (1993) 29.

[2] R.C. Poller, J.N.R. Ruddick, J. Chem. Soc. (A) (1969) 2273.

[3] K. Kawakami, R. Okawara, J. Organomet. Chem. **6** (1966) 249.

[4] K. Kawakami, U. Kawasaki, R. Okawara, Bull. Chem. Soc. Japan **40** (1967) 2693.

[5] T.N. Srivastava, M.P. Agarwal, K.L. Saxena, J. Inorg. Nucl. Chem. **35** (1973) 306.

[6] B. W. Fitzsimmons, N.J. Seeley, A.W. Smith, J. Chem. Soc. (A) (1969) 143.

[7] L. Roncucci, G. Faraglia, R. Barbieri, J. Organomet. Chem. **1** (1964) 427.

[8] W. Kitching, J. Organomet. Chem. **6** (1966) 586.

[9] E.O. Schlemper, Inorg. Chem. **6** (1967) 2012.

[10] W. Chen, W.K. Ng, V.G. Kumar Das, G.B. Jameson, R.J. Butcher, Acta Crystallogr. Sect. C **45** (1989) 861.

[11] E. Kellö, V. Vrábel, J. Holeček, J. Sivy, J. Organomet. Chem. **493** (1995) 13.

[12] A. Szorcsik, L. Nagy, M. Scopelliti, A. Deák, L. Pellerito, K. Hegetschweiler, J. Organomet. Chem. **690** (2005) 2243.

[13] A. Linden, T.S. Basu Baul, A. Mizar, Acta Crystallogr. Sect. E **61** (2005) m27.

[14] S.W. Ng, C. Wei, V.G. Kumar Das, J.P. Charland, F.E. Smith, J. Organomet. Chem. **364** (1989) 343.

[15] M. Schumann, R. Schmiedgen, F. Huber, A. Silvestri, G. Ruisi, A.B. Paulsen, R. Barbieri, J. Organomet. Chem. **584** (1999) 103.

[16] T.S. Basu Baul, A. Mizar, A.K. Chandra, X. Song, G. Eng, R. Jirásko, M. Holčapek, D. de Vos , A. Linden, J. Inorg. Biochem. **102** (2008) 1719.

[17] D. Blake, G.E. Coates, J.M. Tate, J. Chem. Soc. (1961) 756.

[18] K.D. Ghuge, P. Umapathy, M.P. Gupta, D.N. Sen, Inorg. Nucl. Chem. **43** (1981) 653.

[19] T.S. Basu Baul, A. Mizar, A. Lyčka, E. Rivarola, R. Jirásko, M. Holčapek, D. de Vos, U. Englert, J. Organomet. Chem. **691**(2006) 3416.

[20] T.S. Basu Baul, A. Mizar, X. Song, G. Eng, R. Willem, M. Biesemans, I. Verbruggen, R. Butcher, J. Organomet. Chem. **691** (2006) 2605.

[21] L. Pauling, The Nature of Chemical Bond, Cornell University Press, New York, 1960.

[22] R.V. Parish, in: L.S. Kothari, J.S. Baijal, S.P. Tewari (Eds.), Mössabauer Effect: Current Applications to Physical Sciences, Academic Publications, Delhi, India, 1984, p. 162.

[23] R. Barbieri, F. Huber, L. Pellerito, G. Ruisi, A. Silvestri, in: P.J.Smith (Eds.), Chemistry of Tin: ^{119}Sn Mössbauer Studies on Tin Compounds, Blackie, London, 1998, pp. 496–540.

[24] J. Otera, J. Organomet. Chem. **221** (1981) 57.

[25] J. Holeček, M. Nádvorník, K. Handlíř, A. Lyčka, J. Organomet. Chem. **315** (1986) 299.

[26] A. Lyčka, J. Holeček, B. Schneider, J. Straka, J. Organomet. Chem. **389** (1990) 29.

[27] D. Shi, S. Hu, Chin. J. Struct. Chem. 7 (1988) 111.

[28] A. Lyčka, J. Holeček, M. Nádvorník, Main Group Met. Chem. **12** (1989) 169.

[29] V.K. Jain, J. Mason, B.S. Saraswat, R.C. Mehrotra, Polyhedron **4** (1985) 2089.

[30] A. Růžička, L. Dostál, R. Jambor, V. Buchta, J. Brus, I. Císařová, M. Holčapek, J.Holeček, Appl. Organomet. Chem. **16** (2002) 315.

[31] A. Růžička, A. Lyčka, R. Jambor, P. Novák, I. Císařová, M. Holčapek, M. Erben, J. Holeček, Appl. Organomet. Chem. **17** (2003) 168.

[32] L. Kolářová, M. Holčapek, R. Jambor, L. Dostál, A, Růžička, M. Nádvorník, J. Mass Spectrom. **39** (2004) 621.

[33] R.V. Parish, in: S.J. Lippard (Eds.), Progress in Inorganic Chemistry, vol. 15, Wiley-Interscience, New York, 1972, p. 101.

[34] R.H. Herber, H.A. Stockler, W.T. Reichle, J. Chem. Phys. **42** (1965) 2447.

[35] T.A.K. Al-allaf, J. Organomet. Chem. **306** (1986) 337.

[36] J. Holeček, M. Nádvorník, K. Handlíř, A. Lyčka, J. Organomet. Chem. **241** (1983) 177.

[37] K. Sisido, T. Takeda, J. Kinigawa, J. Am. Chem. Soc. **83** (1961) 538.

[38] J. Herzfeld, A.E. Berger, J. Chem. Phys. **73** (1980) 6021.

[39] R. Hooft, KappaCCD Collect Software, Nonius BV, Delft, The Netherlands, 1999.

[40] Z. Otwinowski, W. Minor, in: C.W. Carter Jr., R.M. Sweet (Eds.), Methods in Enzymology, vol. 276, Macromolecular Crystallography, Part A, Academic Press, New York, 1997, pp. 307–326.

[41] R.H. Blessing, Acta Crystallogr. Sect. **A 51** (1995) 33.

[42] G.M. Sheldrick, SHELXS97, Program for the Solution of Crystal Structures, University of Göttingen, Germany, 1997.

[43] A. Altomare, G. Cascarano, C. Giacovazzo, A. Guagliardi, M.C. Burla, G. Polidori, M. Camalli, SIR92, J. Appl. Crystallogr. **27** (1994) 435.

[44] P. van der Sluis, A.L. Spek, Acta Crystallogr. Sect. **A 46** (1990) 194.

[45] A.L. Spek, PLATON, Program for the Analysis of Molecular Geometry, University of Utrecht, The Netherlands, 2005.

[46] G.M. Sheldrick, SADABS, Program for Empirical Absorption Correction of Area Detector Data, University of Göttingen, Germany, 1996.

[47] A.C.T. North, D.C. Philips, F.S. Mathews, Acta Crystallogr. Sect. **A 24** (1968) 351

[48] G.M. Sheldrick, SHELXL97, Program for Structure Solution, University of Göttingen, Germany, 1997.

[49] G.M. Sheldrick, SHELXL97, Program for the Refinement of Crystal Structures, University of Göttingen, Germany, 1997.

Chapter 5

Synthesis, Spectroscopic and X-ray Characterization of Di-*n*-butyltin(IV) Complexes of 5-[(*E*)-2-(4-methoxyphenyl)-1-diazenyl]quinolin-8-ol and Benzoic Acid Derivatives: En Route to Elegant Self-Assembly via Modulation of the Tin Coordination Geometry

CONTENTS

CHAPTER 5

SYNTHESIS, SPECTROSCOPIC AND X-RAY CHARACTERIZATION OF DI-*n*-BUTYLTIN(IV) COMPLEXES OF 5-[(*E*)-2-(4-METHOXYPHENYL)-1-DIAZENYL]-QUINOLIN-8-OL AND BENZOIC ACID DERIVATIVES: EN ROUTE TO ELEGANT SELF-ASSEMBLY VIA MODULATION OF THE TIN COORDINATION GEOMETRY

5.1. Introduction	111-112
5.2. Synthesis of mixed ligand di-*n*-butyltin(IV) complexes	112
5.3. Spectroscopic characterization and X-ray crystallography of chlorobutyltin(IV) complex $^{n}Bu_2SnCl(L^7)$ and mixed ligand di-*n*-butyltin(IV) complexes $[^{n}Bu_2Sn(L^7)(L^{10\text{-}14})]_2$	112-134
5.4. Structural précis of the di-*n*-butyltin(IV) complexes of 5-[(*E*)-2-(4-methoxyphenyl)- 1-diazenyl]quinolin-8-ol and benzoic acid derivatives	134-139
5.5. Experimental	139-143
References	144-145

5.1. Introduction

The chemistry of organotin(IV) quinolin-8-olates has been known for a long time, even though the coordination number of the tin atom and the type of distortion of the coordination polyhedron in the solid state are still open issues. Consequently, the structures of only a few organotin(IV) quinolin-8-olate(s) have been investigated so far, and among these, the diorganotin(IV) *bis*(quinolin-8-olate) group of compounds has received most of the attention as desribed in preceding Chapter. The crystal structures of R_2SnL_2 complexes, where R = Me [1], *p*-ClPh and *p*-MePh [2], ^{n}Bu and Cl [3], ^{n}Bu [4,5], ^{t}Bu [4], Ph [6,7] and Bz [8] revealed molecules with a highly distorted octahedral coordination of the tin atom by bidentate quinolin-8-olate groups and essentially *cis*-R groups. Structural information on $R_2SnX(L)$ type complexes (e.g. R = $EtCO_2Me$; X = Cl) [9] is also available.

On the other hand, the chemistry and structural properties of organotin(IV) carboxylates have been studied extensively; however, their potential for the construction of new mixed ligand complexes has not been explored so widely, with known examples involving the $^-O_2CC_6H_4(N{=}C(H)C_6H_4NMe_2\text{-}4)\text{-}2$, $^-O_2CC_6H_4NH_2\text{-}2$ and $^-O_2CC_6H_4N^+H_3\text{-}2$ [10] 2,6-($^-O_2C)_2C_5H_3N$ and $^-O_2C\text{-}CO_2^-$ [11], $^-O_2CC_6H_4(OH\text{-}2)(N{=}NC_6H_4(Cl\text{-}4)\text{-}5)$, $^-O_2CC_6H_4(OH\text{-}2)(N{=}NC_6H_4(Me\text{-}4)\text{-}5)$ and $^-O_2CC_6H_4(OH\text{-}2)(N{=}NC_6H_4(Br\text{-}4)\text{-}5)$ [12], and $2\text{-}ClC_6H_4CO_2^-$ and $^-O_2CC_5H_4N\text{-}2$ [13] ligands. They display distorted trigonal bipyramidal, skew-trapezoidal bipyramidal and pentagonal bipyramidal coordination geometries around the tin atom. In order to fill this void, given the synthetic and structural importance and the potential biological activity of organotin(IV) complexes in general [7,8,14], and di-*n*-butyltin(IV) complexes with 5-[(*E*)-2-(aryl)-1-diazenyl)quinolin-8-olates in particular [5], we initiated the exploration of the reaction products of $^nBu_2SnCl(L^7)$ (**26**) with various substituted benzoic acids. Besides the conventional spectroscopic analysis (IR, NMR (^1H, ^{13}C, ^{119}Sn) and ^{119}Sn Mössbauer) of the resulting mixed ligand complexes **27-31** (see Section 5.3), this work evaluates the impact of the electronic and steric influence of the carboxylate residue attached to the tin atom on the structural characteristics of these complexes, as determined by X-ray crystallography and further complemented by ^{117}Sn CP-MAS NMR spectroscopy in the solid state and, for one of the complexes, by variable temperature NMR in solution. The results reveal a strong

modulation of the tin coordination geometry as a function of the substituent pattern on the L^{10-14} ligand (refer to Chapter 2 for the structures of the ligands).

5.2. Synthesis of mixed ligand di-*n*-butyltin(IV) complexes

The mixed ligand di-*n*-butyltin(IV) complexes of composition $[^{n}Bu_2Sn(L^7)(L^{10-14})]_2$ (refer to Chapter 2 for specific ligands) were prepared in two steps. Firstly, the chloro butyltin(IV) complex $^{n}Bu_2SnCl(L^7)$ (**26**) was obtain by the reaction of $^{n}Bu_2SnCl_2$ and L^7Na (generated *in situ* using sodium methoxide in anhydrous methanol) in an equimolar ratio in anhydrous benzene. Further, the reactions of **26** with the appropriate substituted benzoic acid (1:1 molar rato) in refluxing toluene yielded mixed ligand di-*n*-butyltin(IV) complexes $[^{n}Bu_2Sn(L^7)(L^{10-14})]_2$ (**27-31**) upon neutralization with Et_3N (see Scheme 5.1). The synthetic details and characterization data for the complexes are presented in Section 5.5.2 while their spectroscopic data are summarized in Section 5.3. All the complexes have well defined melting points, are stable in the air and soluble in common organic solvents.

$$L^7H + NaOMe + {}^{n}Bu_2SnCl_2 \xrightarrow[\text{Conditions: Reflux, 3 h}]{\text{Benzene}} {}^{n}Bu_2SnCl(L^7) + MeOH + NaCl \quad .....(i)$$

$$^{n}Bu_2SnCl(L^7) + L^{n}H' + Et_3N \xrightarrow[\text{Conditions: Reflux, 3 - 4 h}]{\text{Toluene}} [^{n}Bu_2Sn(L^7)(L^{n})]_2 + Et_3N.HCl \quad .....(ii)$$

$(L^{n} = L^{10-14})$

Scheme 5.1. Reaction proposals (**i-ii**) adopted for synthesizing $[^{n}Bu_2Sn(L^7)(L^{10-14})]_2$ complexes

5.3. Spectroscopic characterization and X-ray crystallography of chlorobutyltin(IV) complex $^{n}Bu_2SnCl(L^7)$ and mixed ligand di-*n*-butyltin(IV) complexes $[^{n}Bu_2Sn(L^7)(L^{10-14})]_2$

This Section deals with the di-*n*-butyltin(IV) complexes of the types $^{n}Bu_2SnCl(L^7)$ and $[^{n}Bu_2Sn(L^7)(L^{10-14})]_2$ which have been characterized by IR, ^1H, ^{13}C, ^{119}Sn NMR and ^{119}Sn Mössbauer spectroscopic techniques. The specific ligands used herein are described in Chapter 2. The crystal structures of six compounds, *viz.*, $^{n}Bu_2SnCl(L^7)$ (**26**), $[^{n}Bu_2Sn(L^7)(L^{10})]_2.0.33(C_6H_{12})$ (**27**), $[^{n}Bu_2Sn(L^7)(L^{11})]_2$ (**28**), $[^{n}Bu_2Sn(L^7)(L^{12})]_2$ (**29**), $[^{n}Bu_2Sn(L^7)(L^{13})]_2$ (**30**) and $[^{n}Bu_2Sn(L^7)(L^{14})]_2$ (**31**) are reported.

5.3.1. Infrared spectra

The IR spectrum of the ligand L^7H is already described in earlier Chapters. The ν(OH) band at around 3380 cm^{-1} is found to be absent in the IR spectrum of chloro di-*n*-butyltin(IV) complex **26** confirming bonding through the O-atom of the ligand. A strong band at around 1259 cm^{-1}, is assigned to the ν(C(aryl)-O), i.e. C_8-O-Sn linkage in the complex **26** [5,7,8,15] which does not shift appreciably upon complexation with the benzoates [5,16] (**27-31**, see below). By contrast, the infrared band associated with the antisymmetric [ν_{asym}(OCO)] stretching shows a substantial shift (around 50-110 cm^{-1}; the specific values are 1603, 1598, 1600, 1613 and 1653 cm^{-1} for complexes **27-31**, respectively.) in mixed ligand complexes **27-31**, when compared with the respective benzoic acids ($L^{10}H'$: 1693, $L^{11}H'$: 1701, $L^{12}H'$: 1653, $L^{13}H'$: 1725, $L^{14}H'$: 1733 cm^{-1}). The shift of the [ν_{asym}(OCO)] band to lower wave number is ascribed to carboxylate coordination, as reported earlier [17-19], supporting the formulation of the mixed ligand complexes.

5.3.2. X-ray crystallography

Crystals of compounds suitable for X-ray crystal-structure determination were obtained from benzene/hexane ($^nBu_2SnCl(L^7)$ **26** and $[^nBu_2Sn(L^7)(L^{11})]_2$ **28**), chloroform/cyclohexane ($[^nBu_2Sn(L^7)(L^{10})]_2.0.33(C_6H_{12})$ **27**), toluene/chloroform ($[^nBu_2Sn(L^7)(L^{12})]_2$ **29**), ethanol/acetone ($[^nBu_2Sn(L^7)(L^{13})]_2$ **30**) and benzene/cyclohexane ($[^nBu_2Sn(L^7)(L^{14})]_2$ **31**) solutions of the respective compounds. The crystal structures of six of the di-*n*-butyltin(IV) compounds **26-31** [16] have been determined. The data collection and refinement parameters are given in Table 5.1.

Compound $^nBu_2SnCl(L^7)$ (**26**) is a mononuclear complex in which the tin atom is five-coordinate (Fig. 5.1). The coordination geometry is best described as distorted *cis*-trigonal bipyramidal. The bidentate quinolin-8-olate ligand coordinates such that the N- and O-atoms are in axial and equatorial positions, respectively. The other axial position is occupied by the Cl-atom and the *n*-butyl groups complete the equatorial plane [5]. The distortions from perfect trigonal bipyramidal geometry cause an opening of the C–Sn–C angle and a deviation of the axial Cl–Sn–N bond angle by ca. 20° from linearity and in a direction that allows the axial atoms to release steric strain from the *n*-butyl groups (Table 5.2). The five-membered chelate ring has a slight envelope puckering with the tin atom lying 0.3294(1) Å from the plane of the other four atoms. The steric strain in the small chelate ring is manifested in the significantly distorted bond angles at N(1); much more so than at C(1).

Table 5.1: Crystallographic data and structure refinement parameters for di-*n*-butyltin(IV) compounds **26-31**

	26	**27**	**28**	**29**	**30**	**31**
Empirical formula	$C_{24}H_{30}ClN_3O_2Sn$	$C_{62}H_{70}N_6O_8Sn_2 \cdot 0.33C_6H_{12}$	$C_{76}H_{82}N_{10}O_{10}Sn_2$	$C_{76}H_{82}N_{10}O_{10}Sn_2$	$C_{88}H_{86}Cl_2N_{12}O_{10}Sn_2$	$C_{76}H_{78}N_{10}O_{12}Sn_2$
Molecular weight	546.57	1292.52	1532.74	1532.74	1779.82	1560.71
Crystal size (mm)	0.05 × 0.17 × 0.28	0.18 × 0.20 × 0.25	0.05 × 0.15 × 0.23	0.10 × 0.15 × 0.25	0.15 × 0.22 × 0.32	0.25×0.25 × 0.35
Crystal system	Triclinic	Trigonal	Triclinic	Triclinic	Monoclinic	Triclinic
Space group	$P\bar{1}$	$R\bar{3}$	$P\bar{1}$	$P\bar{1}$	$P2_1/c$	$P\bar{1}$
a (Å)	7.1363(1)	34.5459(3)	10.2516(3)	10.3634(2)	10.8834(1)	12.2249(3)
b (Å)	7.8377(1)	34.5459(3)	13.6965(5)	10.7030(2)	20.8341(2)	12.2740(2)
c (Å)	21.8378(4)	12.9981(1)	13.7049(5)	17.0291(4)	18.3434(2)	25.2903(4)
α (°)	79.9572(9)	90	65.084(2)	100.164(1)	90	97.105(1)
β (°)	85.616(1)	90	89.347(2)	100.587(1)	106.5608(7)	94.069(1)
γ (°)	83.558(1)	120	87.401(2)	104.604(1)	90	107.000(1)
V (Å^3)	1193.11(3)	13433.9(2)	1743.4(1)	1746.74(6)	3986.75(7)	3578.1(1)
Z	2	9	1	1	2	2
D_x [g cm^{-3}]	1.521	1.438	1.460	1.457	1.483	1.448
μ [mm^{-1}]	1.207	0.896	0.783	0.782	0.762	0.767
Transmission factors (min./max)	0.822, 0.947	0.784, 0.866	0.896, 0.962	0.626, 0.945	0.810, 0.893	0.748, 0.826
$2\theta_{max}$ (°)	60	60	55	60	60	60
Reflections measured	30870	76280	40005	47144	95357	61859
Independent reflections /R_{int}	6915 /0.053	8733 /0.081	7969 /0.072	10207 /0.088	11645 /0.074	20626 /0.065
Independent reflections with $I > 2\sigma(I)$	6171	6505	6554	8372	8940	14549
Number of parameters/ restraints	283/ 0	439/ 246	451/ 0	479/ 52	521/ 0	954/ 123
$R(F)$ ($I > 2\sigma(I)$ reflections)	0.0333	0.0406	0.0415	0.0489	0.0441	0.0457
$wR(F^2)$ (all data)	0.0814	0.1060	0.0978	0.1303	0.1155	0.1202
Goodness-of-fit (F^2)	1.108	1.092	1.097	1.042	1.077	1.047
Max, min $\Delta\rho$ [e/Å^3]	1.16, -1.35	2.38, -1.08	1.15, -1.35	0.92, -1.06	0.91, -0.87	1.68, -0.99

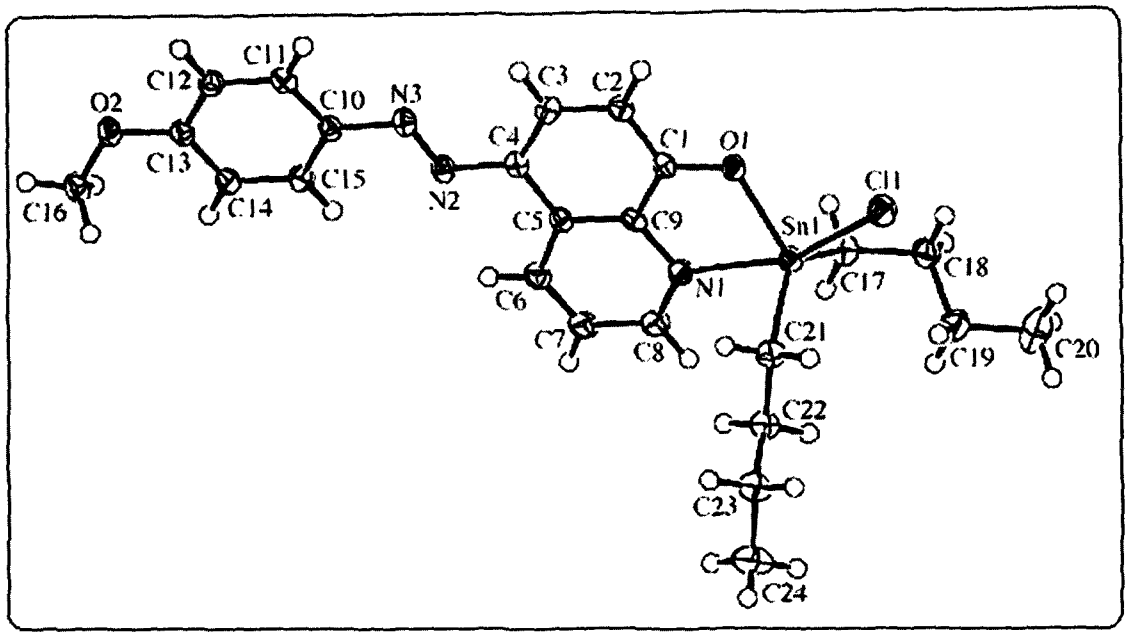

Fig. 5.1. The molecular structure of $^{n}Bu_2SnCl(L^7)$ (**26**). Displacement ellipsoids are shown at the 50% probability level.

The structure of the corresponding diethyl analogue of **26** has been reported [20]. That compound is a one-dimensional zig-zag *cis*-Cl-bridged polymer resulting from an additional long intermolecular Sn–Cl contact of 3.69 Å, which completes a distorted octahedral coordination sphere about each tin atom. It would seem that the bulk of the *n*-butyl groups in **26** blocks the approach of another atom from a second molecule and thereby precludes the formation of a similar polymeric structure. In all other respects, the geometric parameters and distortions involving the bidentate quinolin-8-olate ligand in the di-*n*-butyl and diethyl derivatives are very similar. The Cambridge Structural Database (CSD; version 4.29 with January 2008 updates) [21] contains atomic coordinate data for just 20 quinolin-8-olato-Sn(IV) complexes which do not contain another metal. Of these, 18 have six-coordinate tin atoms and 17 are bis(quinolin-8-olate) complexes. The Sn–N bond lengths range from 2.20-2.60 Å, mean 2.35 Å, with most entries lying in the range 2.30-2.43 Å. The Sn–O bond lengths range from 2.03-2.12 Å, mean 2.09 Å, and the intraring C–N–Sn angle is in the range 107.4-113.3°, mean 110.6°. The corresponding parameters for **26** lie well within these ranges and, except for the somewhat shorter Sn–O bond, close to the mean values.

Table 5.2: Selected interatomic distances (Å) and angles (°) for compound **26**

Sn(1)-O(1)	2.044(2)
Sn(1)-N(1)	2.364(2)
Sn(1)-Cl(1)	2.4514(6)
Sn(1)-C(17)	2.139(2)
Sn(1)-C(21)	2.137(2)
O(1)-C(1)	1.339(3)
N(1)-C(8)	1.328(3)
N(1)-C(9)	1.364(3)
O(1)-Sn(1)-C(17)	111.06(8)
O(1)-Sn(1)-C(21)	118.38(8)
C(17)-Sn(1)-C(21)	128.8(1)
O(1)-Sn(1)-N(1)	74.51(6)
C(17)-Sn(1)-N(1)	89.03(8)
C(21)-Sn(1)-N(1)	91.83(8)
O(1)-Sn(1)-Cl(1)	85.55(5)
C(17)-Sn(1)-Cl(1)	101.47(7)
C(21)-Sn(1)-Cl(1)	94.79(7)
N(1)-Sn(1)-Cl(1)	159.79(5)
C(1)-O(1)-Sn(1)	119.3(1)
C(8)-N(1)-Sn(1)	131.6(2)
C(9)-N(1)-Sn(1)	109.3(1)

The molecular structures of complexes **27-30** are centrosymmetric dinuclear Sn-complexes in which the monomeric [^{n}Bu$_2$Sn(L^7)(L^x)] entity found in solution (see Section 5.3.4 for discussion of the solution ^{117}Sn NMR) has dimerized *via* two symmetry-equivalent, but highly asymmetric μ-O bridges involving the quinolin-8-olate O-atom to give a cyclic Sn_2O_2 core (Figs. 5.2-5.5) [16]. The shorter Sn(1)–O(1) bonds in the bridge range from 2.176(2) Å in **29** to 2.275(2) Å in **30**, while the longer Sn(1')–O(1) bonds range from 2.555(2) Å in **30** to 2.678(2) Å in **27**, giving a difference in these distances of 0.40-0.48 Å for **27-29** and 0.28 Å for

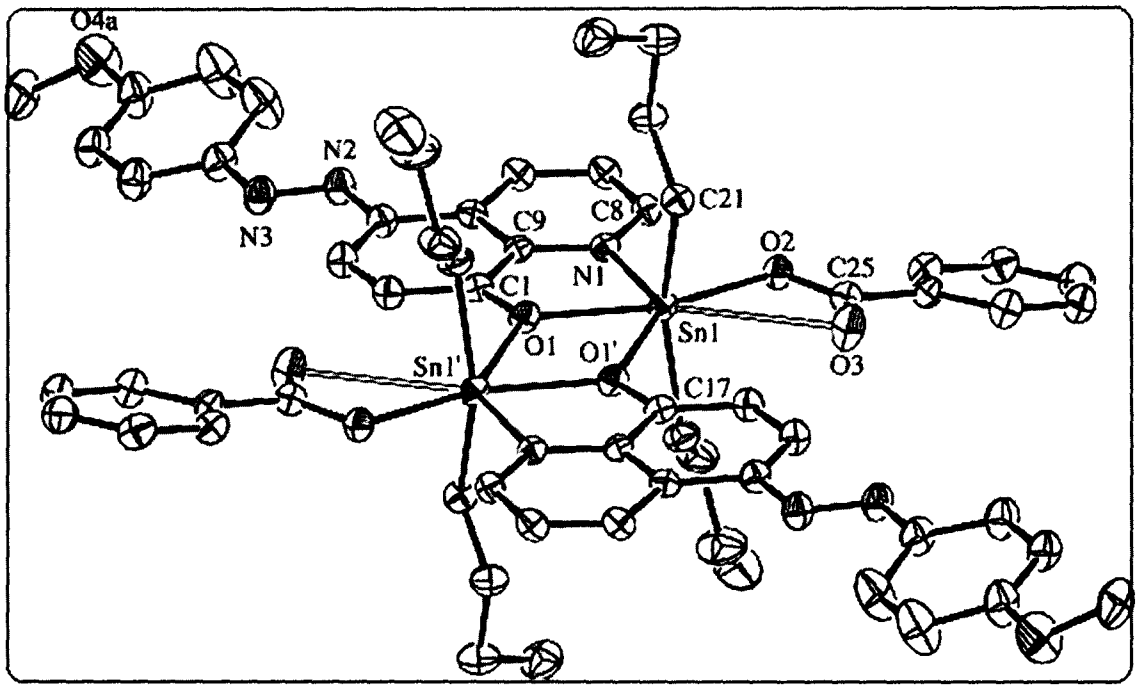

Fig. 5.2. The molecular structure of [^{n}Bu$_2$Sn(L^7)(L^{10})]$_2$ (**27**). Displacement ellipsoids are shown at the 40% probability level. H-atoms omitted for clarity. Only one orientation of the disordered terminal methoxyphenyl group is shown.

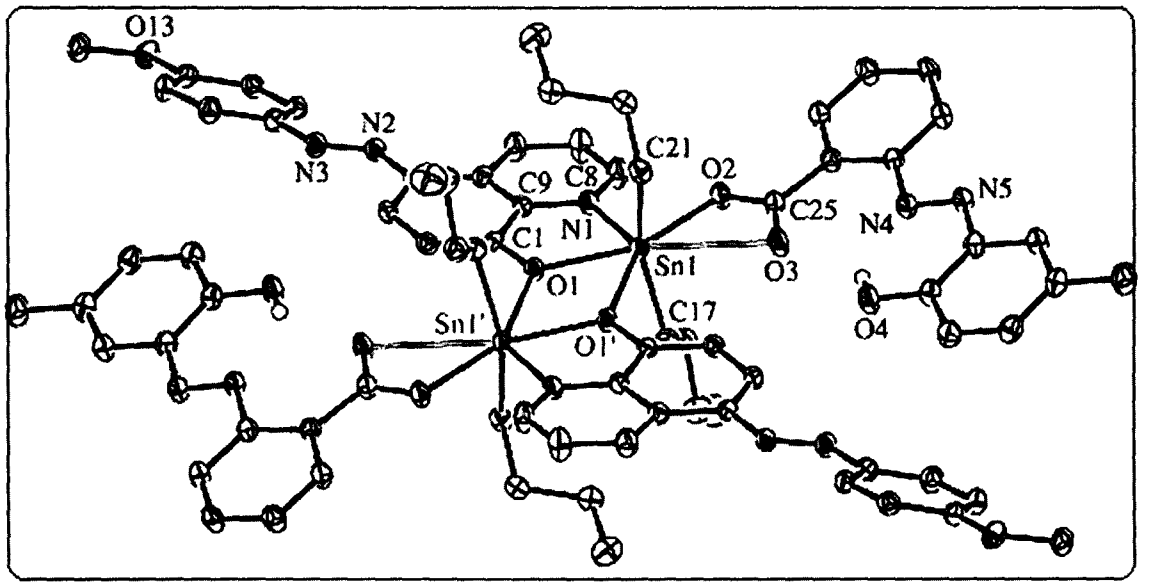

Fig. 5.3. The molecular structure of [^{n}Bu$_2$Sn(L^7)(L^{11})]$_2$ (**28**). Displacement ellipsoids are shown at the 40% probability level. Most H-atoms omitted for clarity.

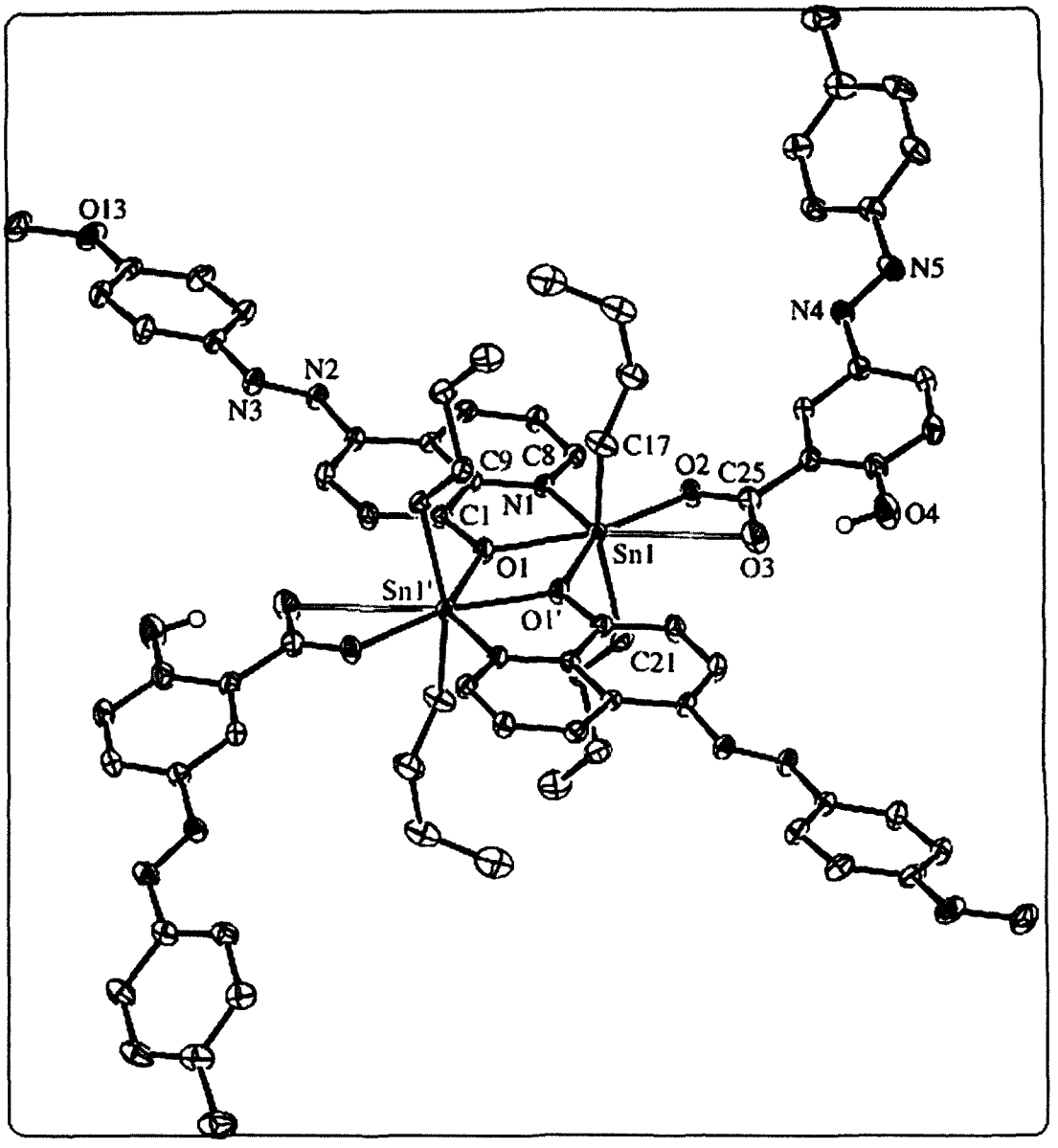

Fig. 5.4. The molecular structure of $[^{n}Bu_2Sn(L^{7})(L^{12})]_2$ (**29**). Displacement ellipsoids are shown at the 40% probability level. Most H-atoms omitted for clarity. Only one orientation of the disordered *n*-butyl groups is shown.

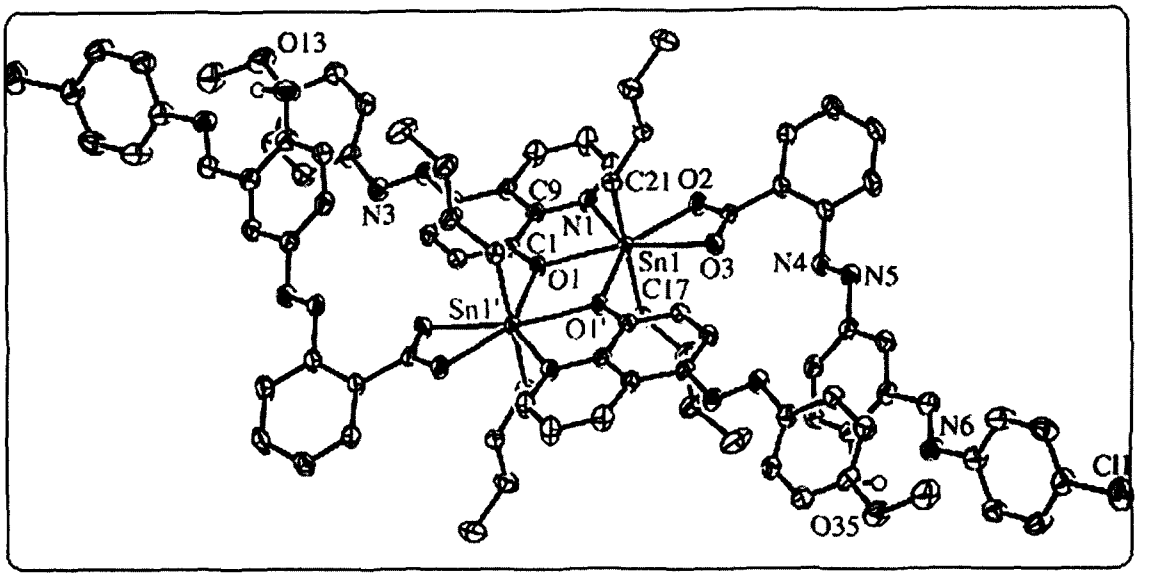

Fig. 5.5. The molecular structure of [^{n}Bu$_2$Sn(L^7)(L^{13})]$_2$ (**30**). Displacement ellipsoids are shown at the 50% probability level. Most H-atoms omitted for clarity.

30 (Table 5.3). The most symmetric bridges are found in **30**. Essentially, the two longer Sn(1')–O(1) interactions provide weak links between the formal monomeric units and explain the absence of significant quantities of the dinuclear species in solution. The Sn···Sn distances within the Sn_2O_2 cores of **27-30** are 4.1035(3), 4.0660(3), 4.0695(3) and 3.9723(2) Å, respectively.

Each tin atom is coordinated by the bidentate quinolin-8-olate ligand, the longer bridging interaction from the centrosymmetrically-related quinolin-8-olate O-atom, the two *n*-butyl groups and by the carboxylate O-atoms of the benzoate ligand. In complexes **27-29**, the benzoate ligand O-atoms coordinate highly asymmetrically to the tin atom with the distance to the carboxylate carbonyl O-atom, Sn(1)–O(3), lying in the range 2.915(2)- 3.030(2) Å and the shorter Sn(1)–O(2) distance in the range 2.218(2)-2.247(2) Å (Table 5.3). When all interactions are considered, the coordination geometry about each tin atom may be described as a distorted pentagonal bipyramid where the *n*-butyl groups occupy the axial positions. The equatorially coordinated atoms, the tin atoms and the entire quinolin-8-olate moiety form a highly planar system. The main deviations from pentagonal bipyramid geometry arise from the bite angles of the three chelating rings in the complex plus the significant deviation from linearity of the C–Sn–C angles involving the *n*-butyl groups by 26-30°. This latter distortion bends the *n*-butyl

Table 5.3: Selected interatomic distances (Å) and angles (°) for compounds **27-30**

Bond length or angle[a]	**27**	**28**	**29**	**30**
Sn(1)-O(1)	2.201(2)	2.202(2)	2.176(2)	2.275(2)
O(1)-Sn(1')	2.678(2)	2.610(2)	2.647(2)	2.555(2)
Sn(1)-O(2) [**Sn–O–C=O**]	2.218(2)	2.232(2)	2.247(2)	2.327(2)
Sn(1)-O(3) [**Sn–O=C–O**]	2.976(2)	2.915(2)	3.030(2)	2.441(2)
Sn(1)-N(1)	2.259(2)	2.278(2)	2.256(2)	2.323(2)
Sn(1)-C(17)	2.116(3)	2.120(3)	2.115(3)	2.126(3)
Sn(1)-C(21)	2.117(3)	2.132(3)	2.119(3)	2.129(3)
O(1)-C(1)	1.317(3)	1.318(3)	1.334(3)	1.330(3)
O(2)-C(25)	1.274(3)	1.291(3)	1.277(4)	1.267(3)
O(3)-C(25)	1.238(3)	1.235(3)	1.252(4)	1.250(3)
N(1)-C(8)	1.329(3)	1.329(4)	1.332(4)	1.329(3)
N(1)-C(9)	1.371(3)	1.369(3)	1.370(3)	1.373(3)
C(17)-Sn(1)-C(21)	152.0(1)	153.6(1)	150.4(1)	168.1(1)
C(17)-Sn(1)-O(1)	95.21(9)	96.38(9)	96.1(1)	90.19(8)
C(21)-Sn(1)-O(1)	96.05(9)	96.15(9)	96.4(1)	91.51(8)
C(17)-Sn(1)-O(2)	89.80(9)	92.66(9)	89.6(1)	90.90(9)
C(21)-Sn(1)-O(2)	92.24(9)	87.79(9)	91.6(1)	93.64(8)
O(1)-Sn(1)-O(2)	151.82(6)	150.31(7)	152.43(8)	149.17(6)
C(17)-Sn(1)-N(1)	105.4(1)	100.7(1)	101.9(1)	95.83(9)
C(21)-Sn(1)-N(1)	102.36(9)	105.2(1)	107.4(1)	95.87(9)
O(1)-Sn(1)-N(1)	73.41(7)	72.91(7)	73.80(8)	71.92(7)
O(2)-Sn(1)-N(1)	78.51(7)	77.65(7)	78.63(8)	77.32(7)
C(17)-Sn(1)-O(1')	79.74(8)	81.76(9)	79.5(1)	86.22(8)
C(21)-Sn(1)-O(1')	81.65(8)	82.72(9)	81.5(1)	83.38(8)
O(1)-Sn(1)-O(1')	65.85(6)	64.93(7)	65.28(8)	69.47(6)
O(2)-Sn(1)-O(1')	142.22(6)	144.61(6)	142.21(7)	141.33(6)
N(1)-Sn(1)-O(1')	139.25(6)	137.74(7)	138.91(7)	141.35(6)
Sn(1)-O(1)-Sn(1')	114.15(6)	115.07(7)	114.72(8)	110.53(6)

[a] Primed atoms are moved through the molecular centre of inversion by the symmetry operator 1-*x*, -*y*, 1-*z* for **27** and **29**, 1-*x*, -*y*, 2-*z* for **28**, and -*x*, -*y*, 2-*z* for **30**.

groups slightly away from the quinolin-8-olate ligand. If one was to consider the very long Sn(1)–O(3) distance as being an insignificant, or at least a very weak interaction, the coordination environment might be described as distorted octahedral, and this is consistent with the solid state ^{117}Sn NMR data, as discussed in more detail later (see Section 5.3.4). Nonetheless, the steric constraints enforced by the coplanar coordination of the benzoate and quinolin-8-olate ligands to the tin atom mean that atom O(3) has a significant influence on the overall distribution of the ligands about the metal centre.

The molecular structure of complex **30** is essentially the same as those of **27-29**, but the μ-O bridge is more symmetric and the benzoate ligand coordinates almost symmetrically to the tin atom with the Sn(1)–O(3) distance now being much shorter at 2.441(2)° (Table 5.3). In this case, the tin atom is formally seven-coordinate and a more regular pentagonal bipyramidal geometry results, in which the deviation of the C–Sn–C angle from linearity is only 11.9(1)°.

The five-membered chelate ring involving the quinolin-8-olate moiety has a slight envelope conformation puckered on the tin atom in the structure of **29**, but is virtually planar in the other structures. The Sn–O bond lengths involving the quinolin-8-olate moiety are about 0.10-0.15 Å longer in **27-29** than in **26** and in the related quinolin-8-olate structures in the CSD and as much as 0.23 Å longer in **30** than in **26**. The Sn–N bond lengths are correspondingly shorter than in **26** and related structures, although the difference is much smaller in **30**. Unlike in **26**, the bond angles at N(1) do not show significant distortion in any of complexes **27-30**.

Dinuclear Sn-complexes involving the quinolin-8-olate ligand have not been reported previously. The CSD contains data for 124 dinuclear Sn(IV) structures with an Sn_2O_2 core and the bridging O-atom bonded to a C-atom. Over 80% of these structures have centrosymmetric cores. There is a cluster of 40 structures with almost perfectly symmetrical μ-O bridges having a difference between the longer and shorter of the Sn–O bonds of less than 0.04 Å and another 13 up to a difference of 0.10 Å. There are 66 structures with their bond length difference scattered fairly evenly over the range of 0.10-0.44Å, with five structures in the 0.45-0.64 Å range. Thus, the observed asymmetry of the μ-O bridges in **27-30** is consistent with other observations, but the differences in the bridging Sn–O bond lengths of 0.40-0.48 Å in the cases of **27-29** tend toward the upper end of the observed range. The absolute values of the Sn–O bond lengths in these literature structures vary widely from 2.0 to 2.9 Å and are clearly related to the coordination environment and nature of the ligands involved, so a direct comparison with the current structures is less enlightening. However, there is a tendency for the Sn–O bonds on each side of the O-atom to be either both quite long (> 2.3 Å) or both much shorter (2.0-2.3 Å), with relatively few examples of one very long and one very short bond.

The molecule of **31** is also a centrosymmetric dinuclear Sn-complex, but the core motif is different. Instead of the μ-O bridges *via* the quinolin-8-olate O-atom observed in **27-30**, the carboxylate groups of two benzoate ligands bridge the two tin atoms to give a cyclic $Sn_2C_2O_4$ core motif [16](Fig. 5.6).

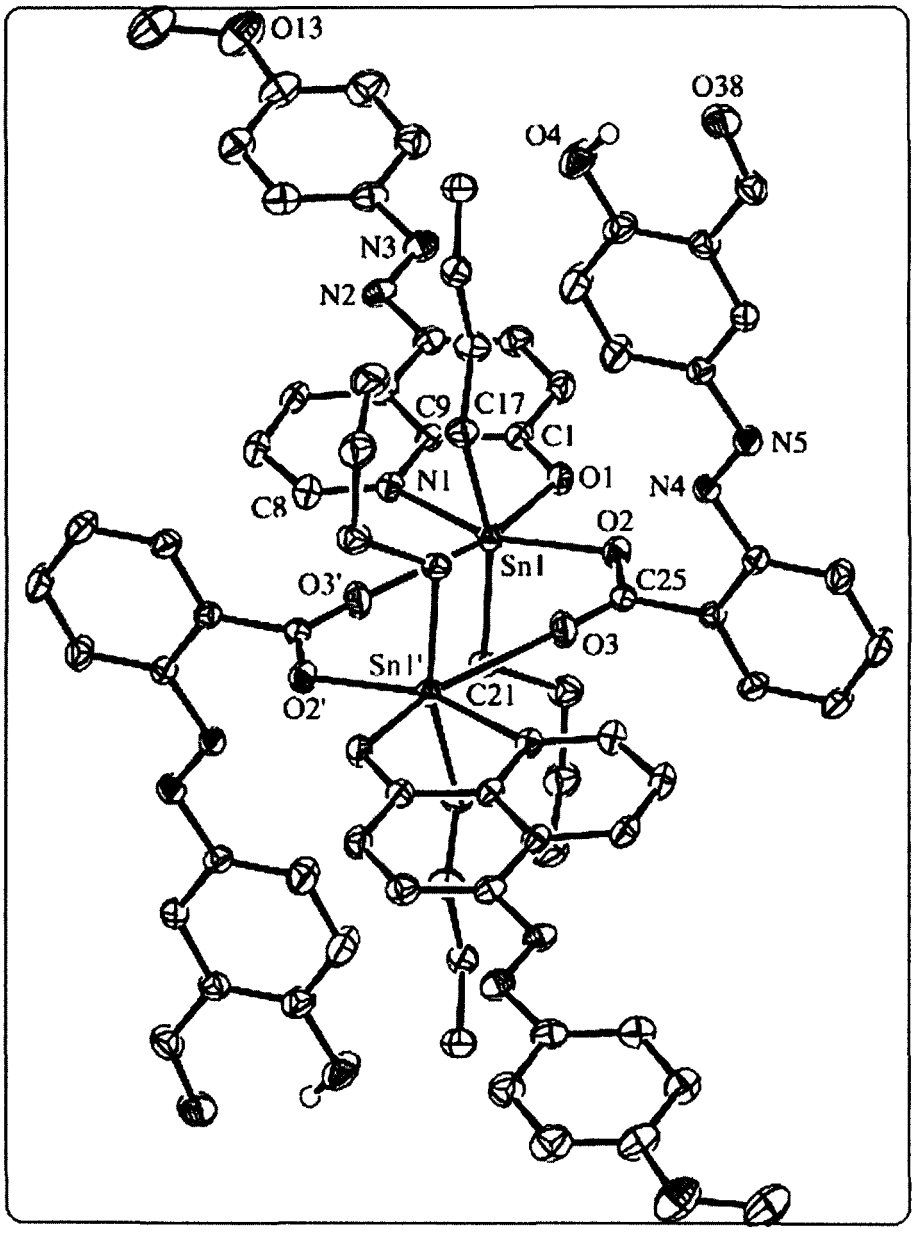

Fig. 5.6a. The molecular structure of one of the two symmetry-independent molecules of $[^nBu_2Sn(L^7)(L^{14})]_2$ (**31**). Displacement ellipsoids are shown at the 40% probability level. Most H-atoms omitted for clarity.

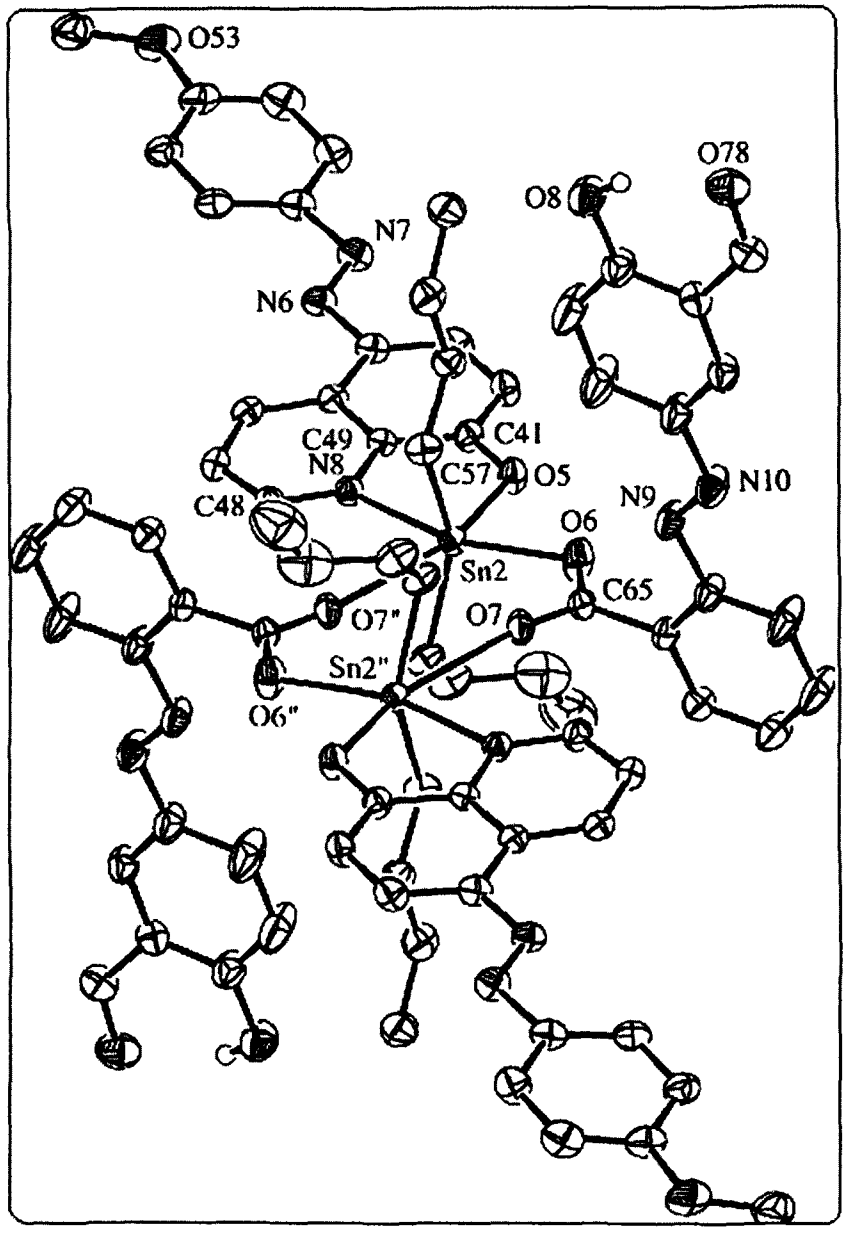

Fig. 5.6b. The molecular structure of molecule B of $[^{n}Bu_2Sn(L^7)(L^{14})]_2$ (**31**). Displacement ellipsoids are shown at the 40% probability level. Most H-atoms omitted for clarity. Only one orientation of the disordered *n*-butyl groups is shown.

Each tin atom in **31** is coordinated by a bidentate quinolin-8-olate ligand, two O-atoms from the two carboxylate bridges and two *n*-butyl groups. This results in a distorted octahedral coordination geometry about each tin atom with the *n*-butyl groups in the *trans* positions. The asymmetric unit of the crystal structure of **31** contains one half of each of two molecules, where

these molecules sit across crystallographic centres of inversion. Most of the geometric parameters of the two independent molecules are quite similar, with the major differences being in the conformation of one *n*-butyl group and in the length of the longer of the bridging Sn–O bonds which differs by about 0.12 Å (Table 5.4). The solid state ^{117}Sn NMR measurements also detect two distinct structures, as discussed later (see Section 5.3.4). Once again, the bridges are quite asymmetric, with the Sn–O bond lengths in the bridge differing by 0.51 and 0.64 Å in molecules A and B, respectively. The longer Sn–O distance involves the carboxylate carbonyl O-atom in each molecule. Despite the bridge in **31** being a carboxylate group, the short and long Sn–O bonds in the bridge are very similar in length to those involving the μ-O atom in complexes **27-30**. However, the distances between the tin atom and the carboxylate carbonyl O-atom of 2.683(2) and 2.798(2) Å for molecules A and B, respectively, are now significantly shorter than the corresponding long distances of 2.92-3.03 Å in complexes **27-29**. The Sn···Sn distance within the core of **31** is 4.6165(3) and 4.6831(3) Å for molecule A and B, respectively, which reflects the additional spacing between these atoms introduced by the three-atom carboxylate bridge when compared with the single-atom μ-O bridges in **27-30**. Now that the quinolin-8-olate O-atom is not involved in a bridge in **31**, the quinolin-8-olate Sn–O bond is 0.1-0.2 Å shorter than in the other dinuclear complexes, but comparable with that in **26**. The Sn–N bonds are also more similar to that in **26** than in the other dinuclear complexes, which are shorter. The carboxylate carbonyl O-atom is also within a contact distance of the tin atom to which carboxylate group is primarily coordinated, with these Sn···O distances being 3.085(2) and 2.898(2) Å for molecules A and B, respectively. If all interactions with the tin atoms are considered, as in **27-30**, the geometric arrangement about each tin atom in **31** is a distorted pentagonal bipyramid with the *n*-butyl groups in the axial positions.

The CSD records data for 26 structures containing an $Sn_2C_2O_4$ core involving bridging carboxylate ligands. Ten of these are dinuclear Sn(IV) complexes, of which nine have centrosymmetric cores and most have reasonably symmetric Sn–O distances in the bridges in which the longest Sn–O distance is less than 2.35 Å. The only dinuclear Sn(IV) structure with asymmetric bridge dimensions similar to those in **31** is bis(tetrakis(triphenylphosphine-P)-silver(I)) bis(μ_2-trifluoroacetato-O,O')-tetrakis(trifluoroacetato-O)-tetramethyl-di-tin(IV) [22], where the longer Sn–O distance is 2.82 Å.

The hydroxy group in each carboxylate ligand in **28-31** forms an intraligand hydrogen bond with the nearest adjacent heteroatom, thereby completing a six-membered loop. In **28**, the hydroxy H-atom is involved in a bifurcated interaction with the second acceptor being the carboxylate carbonyl O-atom of the same ligand. In **27-30**, a very short intramolecular

Table 5.4: Selected interatomic distances (Å) and angles (°) for the two symmetry-independent molecules of **31**

Bond length or angle[a]	**molecule A**	bond length or angle	**molecule B**
Sn(1)-O(1)	2.086(2)	Sn(2) -O(5)	2.083(2)
Sn(1)-O(2) [**Sn–O–C=O**]	2.171(2)	Sn(2)-O(6)	2.167(2)
O(3)-Sn(1') [**Sn–O=C–O**]	2.683(2)	Sn(2)-O(7")	2.798(2)
Sn(1)-O(3)	3.085(2)	Sn(2)-O(7)	2.898(2)
Sn(1)-N(1)	2.345(2)	Sn(2)-N(8)	2.343(2)
Sn(1)-C(17)	2.133(3)	Sn(2)-C(57)	2.121(3)
Sn(1)-C(21)	2.120(3)	Sn(2)-C(61a)	2.119(4)
O(1)-C(1)	1.321(3)	O(5)-C(41)	1.328(3)
O(2)-C(25)	1.282(3)	O(6)-C(65)	1.266(3)
O(3)-C(25)	1.227(3)	O(7)-C(65)	1.225(4)
N(1)-C(8)	1.319(4)	N(8)-C(48)	1.317(4)
N(1)-C(9)	1.361(3)	N(8)-C(49)	1.360(4)
O(1)-Sn(1)-C(21)	101.4(1)	O(5)-Sn(2)-C(61a)	107.0(2)
O(1)-Sn(1)-C(17)	101.7(1)	O(5)-Sn(2)-C(57)	103.4(1)
C(21)-Sn(1)-C(17)	156.8(1)	C(61a)-Sn(2)-C(57)	147.7(2)
O(1)-Sn(1)-O(2)	79.87(8)	O(5)-Sn(2)-O(6)	80.40(8)
C(21)-Sn(1)-O(2)	93.3(1)	C(61a)-Sn(2)-O(6)	99.4(3)
C(17)-Sn(1)-O(2)	93.2(1)	C(57)-Sn(2)-O(6)	96.1(1)
O(1)-Sn(1)-N(1)	74.68(8)	O(5)-Sn(2)-N(8)	74.39(8)
C(21)-Sn(1)-N(1)	94.1(1)	C(61a)-Sn(2)-N(8)	87.1(3)
C(17)-Sn(1)-N(1)	89.7(1)	C(57) -Sn(2) -N(8)	90.8(1)
O(2)-Sn(1)-N(1)	154.44(8)	O(6)-Sn(2)-N(8)	154.77(9)
O(1)-Sn(1)-O(3')	160.27(7)	O(5)-Sn(2)-O(7")	161.66(8)
C(21)-Sn(1)- O(3')	77.37(9)	C(61a)-Sn(2)-O(7")	71.8(2)
C(17)-Sn(1)-O(3')	80.03(9)	C(57)-Sn(2)-O(7")	75.9(1)
O(2)-Sn(1)-O(3')	119.79(7)	O(6)-Sn(2)-O(7")	117.93(7)
C(25)-O(3)-Sn(1')	177.5(2)	C(65)-O(7)-Sn(2")	171.6(2)

[a]Primed atoms are moved through the molecular centre of inversion by the symmetry operator *-x*, 1-*y*, 1-*z* for molecule A and *-x*, *-y*, *-z* for molecule B.

C(8)-H···O(2) interaction (H···O distances and C-H···O angles in the ranges 2.24-2.29 Å and 118-123°, respectively) consistently appears between the quinolin-8-olate and carboxylate ligands coordinated to the same tin atom in the dinuclear molecule. In addition, an intramolecular C(2)-H···O(3) interaction between the quinolin-8-olate and carboxylate ligands coordinated to different tin atoms may be helping to stabilize the μ-O bridging mode in the dinuclear molecules. The H···O distances and C-H···O angles for this interaction are in the ranges 2.40-2.43 Å and 167-180°, respectively, for **27-29**, but for **30**, the H···O distance is extremely short at 2.09 Å (angle 159°). Interestingly, neither of these C-H···O interactions, nor any others, occur in the structure of **31**, which has a different mode of bridging between the tin atoms. It is therefore concluded that the C-H···O interactions are not the sole driving force controlling the bridging mode developed during the assembly of the dinuclear molecule. Other factors may be the steric arrangement necessary to accommodate the ligands about a tin atom or to efficiently pack the molecules in the crystal, given that the steric bulk of the carboxylate ligands is the main variable in these compounds.

5.3.3. ^{119}Sn Mössbauer data

The ^{119}Sn Mössbauer data, i.e. isomer shift (δ), quadrupole splittings (Δ) and the line widths at half-peak height (Γ) for the chloro di-*n*-butyltin(IV) complex (**26**) and mixed ligand complexes (**27-31**) are given in Table 5.5.

The observed Δ value for $^{n}Bu_2SnCl(L^7)$ (**26**) is 2.51 mm s^{-1}, which falls within the value, 4.17 mm s^{-1}, is typical of *trans*-R_2 octahedral structures with a linear C–Sn–C fragment. On the other hand, by using the same equation, the experimental value of the C–Sn–C bond angle, 168.1°, would give a calculated Δ value of 4.05 mm s^{-1}, in ± 0.1 mm s^{-1} error in comparison with the observed value, well within the ± 0.4 mm s^{-1} range accepted by the point-charge method. Such a deviation may be due to a variation of the bonding nature of the ligands and to a more negative pqs of the alkyl group, as a consequence of the much shorter Sn–O(3) distance, which effectively increases the coordination number of the tin atom, and results in a chemical environment with a much more regular pentagonal bipyramidal geometry, and consequently a more linear C–Sn–C bond angle, compared with that in compounds **27-29** and **31**. This assumption is supported by the large Δ values observed for pentagonal bipyramidal complexes with C-Sn-C bond angles similar to that found in compound **30** [26]. However, the variations observed in the C–Sn–C bond angles determined from Mössbauer parameters and single crystal analysis by X-ray diffraction (see Tables 5.3 and 5.4) can not be put side by side

Table 5.5: ^{119}Sn Mössbauer parameters (mm s^{-1}) for the di-n-butyltin(IV) complexes **(26-31)**

Complex[a]	^{119}Sn Mössbauer data[b]			
	δ	Δ	Γ_1	Γ_2
^{n}Bu$_2$SnCl(L^7) **(26)**	1.15	2.51	1.80	1.96
[^{n}Bu$_2$Sn(L^7)(L^{10})]$_2$.0.33(C$_6$H$_{12}$) **(27)**	1.46	3.79	0.82	0.83
[^{n}Bu$_2$Sn(L^7)(L^{11})]$_2$ **(28)**	1.44	3.79	0.76	0.77
[^{n}Bu$_2$Sn(L^7)(L^{12})]$_2$ **(29)**	1.47	3.85	0.82	0.83
[^{n}Bu$_2$Sn(L^7)(L^{13})]$_2$ **(30)**	1.50	4.17	0.80	0.79
[^{n}Bu$_2$Sn(L^7)(L^{14})]$_2$ **(31)**	1.40	3.60	0.79	0.78

[a]Complex numbers are in parentheses. [b]Parameters: δ, isomer shifts; Δ, quadrupole splitting; Γ_1 and Γ_2: line widths. [c]In $CDCl_3$ solution.

owing to the dissimilar sampling techniques, for instance, bulk powder and single crystal, respectively.

5.3.4. Solution and solid-state ^{117}Sn NMR

The basic ligand frame-work is shown in Chapter 2 (refer to Figs. 2.1 and 2.2) along with the abbreviations and numbering schemes for spectroscopic analyses. Numbering scheme for Sn-^{n}Bu skeleton as shown below:

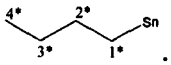

Characterization of complexes **26-31** in a $CDCl_3$ solution (approx. 10 mg in 0.7 ml) was performed by ^{1}H, ^{13}C and ^{117}Sn NMR. A combination of 1D ^{1}H, ^{13}C (proton decoupled and DEPT) and 2D ^{1}H-^{13}C correlation spectra (HSQC and HMBC), assisted in some cases by ^{1}H-^{1}H COSY spectra, allowed complete assignment of all ^{1}H and ^{13}C resonances. Only one set of resonances is observed at room temperature, but some resonances are broad, suggesting some dynamic process might be operative in solution. The detailed NMR spectral features for complexes **26–31** are given below:

5.3.4.1. $^{n}Bu_2SnCl(L^7)$ **(26)**

^{1}H NMR ($CDCl_3$, 400.13 MHz); δ_H: Ligand skeleton: 9.65 [dd, 1H, H4], 8.20 [d, 1H, H2], 7.95 [d, 3H, H6', H6 and H2'], 7.74 [m, 1H, H3], 7.25 [m, 1H, H7], 7.03 [m, 2H, H3' and H5'] and 3.92 [s, 3H, OCH_3]; Sn-^{n}Bu skeleton: 1.72 [m, 4H, H1*], 1.35 [m, 8H, H2* and H3*], 0.85 [t, 6H, H4*] ppm. ^{13}C NMR ($CDCl_3$, 100.62 MHz); δ_C: Ligand skeleton: 161.7 [C8], 160.8 [C1'], 147.6 [C2], 145.9 [C4'], 138.1 [C4], 136.5 [C5], 136.3 [C8a], 128.4 [C4a], 124.4 [C3' and C5'], 122.3 [C3], 118.4 [C6], 115.6 [C7], 114.3 [C2' and C6'], 55.6 [OCH_3]; Sn-^{n}Bu skeleton: 28.2 [C-2*], 26.9 [C-3*], 26.3 [C-1*], 13.4 [C-4*] ppm.

5.3.4.2. $[^{n}Bu_2Sn(L^7)(L^{10})]_2.0.33(C_6H_{12})$ **(27)**

^{1}H NMR ($CDCl_3$); δ_H: Ligand skeleton (Coupling constants in Hz): 9.48 [s, 1H, H4], 8.80 [s, 1H, H2], 8.14 [d, 1H, H6 (8.6)], 8.12 [d, 1H, H2'' and H6'' (7.0)], 7.90 [d, 2H, H2'and H6' (8.9)], 7.66 [s, 1H, H3], 7.51 [t, 1H, H4'' (7.3)], 7.27 [d, 1H, H7 (8.6)], 6.98 [d, 2H, H3'and H5' (8.9)], 3.85 [s, 3H, -OCH_3]; Sn–^{n}Bu skeleton: 1.64 [m, 4H, H2*], 1.52 [m, 4H, H1*], 1.25 [m, 4H, H3*], 0.73 [t, 6H, H4* (7.0)] ppm. ^{13}C NMR ($CDCl_3$); δ_C: 174.6 [COO], 161.4 [C8 and C4'], 147.6 [C1'], 144.8 [C2], 137 [C8a], 136.7 [C4], 136.4 [C5], 132.3 [C4''], 131.8 [C1''], 130.2 [C2'' and C6''], 128.4 [C4a], 128.1 [C5'' and C3''], 124.3 [C2' and C6'], 122.2 [C3], 118 [C6], 115.0 [C7], 114.2 [C3'and C5'], 55.5 [OCH_3]; Sn–^{n}Bu skeleton ($^{n}J(^{117/119}Sn, ^{13}C)$, Hz): 26.9 [C2* (42)], 26.4 [C1*(630/658)], 26.4 [C3* (102)], 13.5 [C4*] ppm.

5.3.4.3. $[^{n}Bu_2Sn(L^7)(L^{11})]_2$ **(28)**

^{1}H NMR ($CDCl_3$); δ_H: Ligand skeleton (Coupling constants in Hz): 12.3 [s, 1H, ArOH], 9.46 [d, 1H, H4 (8.3)], 8.77 [s, 1H, H2], 8.17 [dd, 1H, H2'' (7.5, 1.5)], 8.11 [d, 1H, H6 (8.7)], 7.89 [d, 2H, H2'and H6' (8.9)], 7.86 [d, 1H, H5'' (7.5)], 7.69 [d, 1H, H12'' (1.5)], 7.55 [td, 1H, H4'' (7.5, 1.5)], 7.5 [s, 1H, H3], 7.47 [td, 1H, H3'' (7.5, 1.5)], 7.23 [d, 1H, H7 (8.7)], 7.08 [dd, 1H, H10'' (8.6, 1.5)], 6.96 [d, 2H, H3' and H5' (8.9)], 3.83 [s, 3H, -OCH_3], 2.44 [s, 3H, $ArCH_3$]; Sn–^{n}Bu skeleton: 1.70 [m, 4H, H2*], 1.53 [m, 4H, H1*], 1.24 [m, 4H, H3*], 0.70 [t, 6H, H4* (7.0)] ppm. ^{13}C NMR ($CDCl_3$); δ_C: 174.6 [COO], 161.4 [C8 and C4'], 150.5 [C8''], 149.4 [C6''], 147.6 [C1'], 145.2 [C2], 137.9 [C7''], 130.2 [C3''], 129.9 [C1''], 128.6 [C11''], 128.4 [C4a], 124.3 [C2' and C6'], 122.1 [C3], 118.4 [C9''], 118.0 [C6], 114.8 [C7], 114.2 [C3' and C5'], 55.5 [OCH_3], 20.3 [$ArCH_3$]; Sn–^{n}Bu skeleton ($^{n}J(^{117/119}Sn, ^{13}C)$, Hz): 26.9 [C2* (38)], 26.5 [C1* (619/643)], 26.3 [C3* (106)], 13.5 [C4*] ppm.

5.3.4.4. [^{n}Bu$_2$Sn(L^7)(L^{12})]$_2$ (29)

^{1}H NMR ($CDCl_3$); δ_H: Ligand skeleton (Coupling constants in Hz): 12.09 [s, 1H, ArOH], 9.55 [d, 1H, H4 (8.3)], 8.90 [s, 1H, H2], 8.60 [d, 1H, H6''(2.5)], 8.14 [d, 1H, H6 (8.7)], 7.99 [dd, 1H, H6''(8.9, 2.5)], 7.90 [d, 2H, H2' and H6' (8.9)], 7.75 [d, 1H, H8'' and H12'' (8.2)], 7.7 [s, 1H, H3], 7.27 [d, 1H, H7 (8.7)], 7.02 [d, 1H, H3'' (8.9)], 6.97 [d, 2H, H3'and H5' (8.9)], 6.96 [d, 2H H3' and H5' (8.9)], 3.84 [s, 3H, -OCH_3]; Sn–^{n}Bu skeleton: 1.69 [m, 4H, H2*], 1.53 [m, 4H, H1*], 1.26 [m, 4H, H3*], 0.70 [t, 6H, H4* (7.2)] ppm. ^{13}C NMR ($CDCl_3$); δ_C: 175.6 [COO], 164.1 [C2''], 161.6 [C4'], 160.9 [C8], 150.8 [C7''], 147.6 [C1'], 145.2 [C2 and C5''], 140.8 [C10''], 137.5 [C4], 137 [C8a], 136.6 [C5], 128.4 [C4a], 129.7 [C9'' and C11''], 127.9 [C6''], 127.7 [C4''], 124.4 [C2' and C6'], 122.6 [C8'' and C12''], 122.3 [C3], 118.1 [C6], 115.2 [C7 and C1''], 114.3 [C3' and C5'], 55.5 [OCH_3], 21.4 [$ArCH_3$]; Sn–^{n}Bu skeleton (^nJ($^{117/119}$Sn, ^{13}C): 27.2 [C2* (38)], 26.6 [C1* (619/643)], 26.4 [C3* (100/104)], 13.8 [C4*] ppm.

5.3.4.5. [^{n}Bu$_2$Sn(L^7)(L^{13})]$_2$ (30)

^{1}H NMR ($CDCl_3$); δ_H: Ligand skeleton (Coupling constants in Hz): 13.52 [s, 1H, ArOH], 9.44 [d, 1H, H4 (7.4)], 8.76 [s, 1H, H2], 8.47 [s, 1H, H13''], 8.03 [d, 1H, H6 (8.7)], 7.97 [d, 1H, H2''], 7.97 [d, 1H, H12'' (7.1)], 7.96 [s, 1H, H8''], 7.87 [d, 2H, H2' and H6' (8.8)], 7.59 [d, 1H, H5'' (7.5)], 7.5 [s, 1H, H3], 7.49 [dd, 1H, H4'' (7.5, 1.5)], 7.43 [dd, 1H, H3'' (7.5, 1.5)], 7.20 [d, 2H, H16''and H18'' (8.4)], 7.13 [d, 1H, H7 (8.7)], 6.96 [d, 2H, H3' and H5'(8.8)], 3.83 [s, 3H, -OCH_3]; Sn–^{n}Bu skeleton: 1.70 [m, 4H, H2*], 1.53 [m, 4H, H1*], 1.21 [m, 4H, H3*], 0.69 [t, 6H, H4*] ppm. ^{13}C NMR ($CDCl_3$); δ_C: 173.9 [COO], 164.1 [C10''], 162.2 [C13''], 161.5 [C4'], 161.3 [C8], 151.4 [C6''], 146.0 [C14''], 145.8 [C7''], 145.5 [C2], 137.6 [C4], 137.0 [C8a], 136.2 [C5], 132.9 [C17''], 131.5 [C3''], 131.4 [C1''], 130.6 [C2''], 129.9 [C4''], 129.5 [C16'' and C18''], 129.0 [C8''], 128.4 [C4a], 127.7 [C12''], 124.3 [C2' and C6'], 122.2 [C15'' and C19''], 118.7 [C11''], 118.1 [C6], 118.0 [C9''], 114.8 [C7], 114.2 [C3' and C5'], 55.5 [OCH_3]; Sn–^{n}Bu skeleton (^nJ($^{117/119}$Sn, ^{13}C): 27.1 [C2* (34)], 26.5 [C3* (102)], 26.3 [C1* (618/650)], 13.5 [C4*] ppm.

5.3.4.6. [^{n}Bu$_2$Sn(L^7)(L^{14})]$_2$ (31)

^{1}H NMR ($CDCl_3$); δ_H: Ligand skeleton (Coupling constants in Hz): 11.28 [s, 1H, ArOH], 9.48 [d, 1H, H4], 8.78 [s, 1H, H2], 8.16 [d, 1H, H12'' (9.88)], 8.11 [d, 1H, H6 (8.7)], 8.09 [dd, 1H, H8'' (8.9, 2.5)], 7.98 [dd, 1H, H2'' (7.1, 1.8)], 7.88 [d, 1H, H2' and H6' (8.7)], 7.59 [dd, 1H, H5'' (7.1, 1.8)], 7.52 [td, 1H, H4'' (7.1, 1)], 7.19 [d, 1H, H7 (8.7)], 6.99 [d, 1H,

H9'' (8.9)], 6.96 [d, 2H, H3' and H5' (8.7)], 3.89 [s, 3H, -OCH_3]; Sn–^{n}Bu skeleton: 1.67 [m, 4H, H2*], 1.52 [m, 4H, H1*], 1.23 [m, 4H, H3*], 0.70 [t, 6H, H4* (7.2)] ppm. ^{13}C NMR ($CDCl_3$); δ_C: 196.3 [C13''], 163.9 [C10''], 161.4 [C4'], 161.3 [C8], 151.2 [C6''], 147.6 [C1'], 146.1 [C7''], 145.0 [C2], 137.0 [C4 and C8a], 136.3 [C5], 131.8 [C1''], 131.4 [C3''], 130.8 [C8''], 130.4 [C4''], 130.2 [C12''], 128.4 [C4a], 122.1 [C3], 120.2 [C11''], 118.5 [C9''], 118.3 [C6], 116.7 [C5''], 114.8 [C7], 114.2 [C3' and C5'], 55.5 [OCH_3]; Sn–^{n}Bu skeleton ($^nJ(^{117/119}Sn, ^{13}C)$: 27.0 [C2* (38)], 26.4 [C3* (102)], 26.3 [C1* (623/651)], 13.5 [C4*] ppm.

The $\delta(^{119}Sn)$ value of −104.1 ppm for the chloro di-*n*-butyltin(IV) complex **26** corresponds well with that of $^nBu_2SnCl(Ox)$ (-112 ppm in $CHCl_3$ solution [27,28]). On the other hand, the solution ^{117}Sn spectrum at 303K reveals three resonances for compounds **27**, **30** and **31**, two resonances for **28** and a single resonance for **29** (Table 5.6) with a chemical shift of −170 ppm. The major resonance of the compounds **27**, **28**, **30** and **31** has a chemical shift ranging from −185 to −188 ppm. Compounds **27**, **30** and **31** also display a smaller resonance between −143 and −150 ppm, while all (except **29**) also show the presence of a species with a chemical shift around −252 ppm. All these resonances are broad (between 200 and 700 Hz), especially the one around −185 ppm, supporting the previous assumption of a dynamic process

Table 5.6: Solution ($CDCl_3$) and solid State ^{117}Sn NMR data for compounds **27-31**

Compound	$\delta(^{117}Sn)^a$	^{117}Sn MAS[b]					
		δ_{iso}	ζ	η	δ_{11}	δ_{22}	δ_{33}
27	−150.3 (230, 15%), −187.7 (450, 72%), −251.9 (190, 13%)	−268	−675	0.35	188	−48	−943
28	−187.9 (700, 95%), −251.8 (250, 5%)	−292	−705	0.40	202	−80	−997
29	−170.4 (375, 100%)	−258	−612	0.45	185	−90	−870
30	−145.9 (210, 8%), −186.1 (265, 80%), −251.1 (280, 12%)	−368	−714	0.00	−11	−11	−1082
31	−143.3 (360, 8%), −185.2 (430, 82%), −251.4 (250, 10%)	−245 −261	−653 −622	0.25 0.30	163 143	0 −43	−897 −883

[a] In $CDCl_3$ solution. The numbers in parentheses are the widths at half height (in Hz) and the percentage amplitudes of the resonances.

[b] δ_{iso} (ppm) = $(\delta_{11}+\delta_{22}+\delta_{33})/3$; ζ(ppm) = $\delta_{33} - \delta_{iso}$ and $\eta = |\delta_{22} - \delta_{11}| / |\delta_{33} - \delta_{iso}|$ were δ_{11}, δ_{22} and δ_{33} (ppm) are the principal tensor components of the chemical shielding anisotropy, sorted as follows $|\delta_{33} - \delta_{iso}| > |\delta_{11} - \delta_{iso}| > |\delta_{22} - \delta_{iso}|$.

being present in solution. The different chemical shifts reflect different modes of coordination of the tin atom, to be ascribed to complexes in which some bonds are broken, when compared to the tin coordination in the solid state (*vide infra*).

In order to get some insight into this dynamic process and to characterize the nature of the different species in equilibrium, a more concentrated sample of **27** was subjected to a variable temperature study. Fig. 5.7a displays a selection of the ^{117}Sn spectra at low temperature. As the temperature is lowered, the resonance at −188 ppm sharpens and shifts slightly to lower frequency, while the resonance at −252 ppm diminishes in intensity and finally disappears into the noise while a new resonance appears at −100 ppm.

At 233 K, most of the ^{1}H resonances are sharpened up when compared to 303 K, and additional small resonances appear (Fig. 5.7b). A ^{1}H-^{117}Sn correlation spectrum at 233 K reveals that the major tin resonance at −188 ppm correlates with the H-2 proton (at 8.80 ppm)

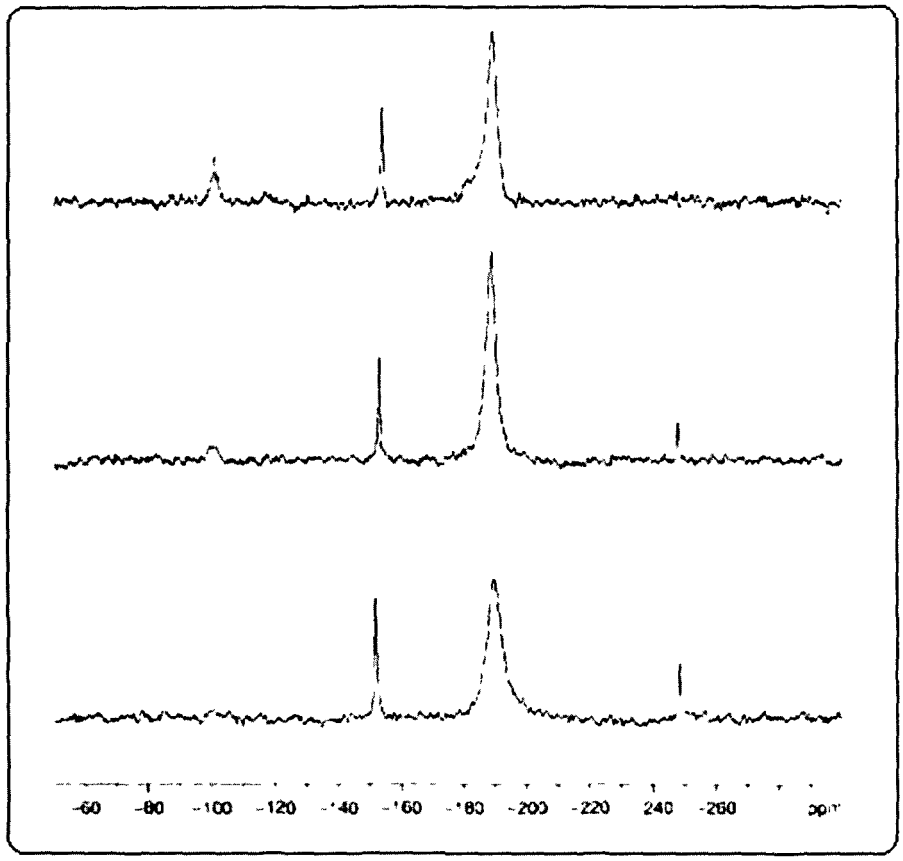

Fig. 5.7a. The ^{117}Sn NMR spectra of **27** in $CDCl_3$ from bottom to top (a) at 253K, (b) at 233K and (c) at 213K.

of the quinolin-8-ol ligand, while the small resonance at –252 ppm correlates with the small new resonance at 8.52 ppm, which is assigned to the H-2 proton in a less abundant species.

All these observations are rationalized as follows. In solution at room temperature, the major species consists of a six-coordinate monomeric species with the Sn atom bound to the two *n*-butyl groups, chelated by the oxygen and nitrogen atoms of the quinolin-8-ol moiety as well as by both oxygen atoms of the carboxylate group. The resonance at –252 ppm is assigned to the dimeric species composed of the μ-O Sn_2O_2 core, involving the oxygen atom of the quinolin-8-ol moiety, as observed in the crystal structure. That this dimer does not appear as the dominant species in solution is quite acceptable, since, in spite of probable packing effects in the crystalline state, the Sn–O–Sn bridges giving rise to the dimers systematically contain one quite long Sn–O distance, and are thus not expected to be so particularly strong. The resonance at –150 ppm is due to a structure in which the coordination with N-1 is lost, as demonstrated by the absence of correlation with the H-2 proton, and finally the resonance at –101 ppm, only visible at very low temperature (213 K), is assigned to a species in which the Sn←O=C–O– bond is also broken, leaving a four-coordinate species. The generation of a four-coordinate tin species at low temperature in solution may appear surprising at first glance, but is also

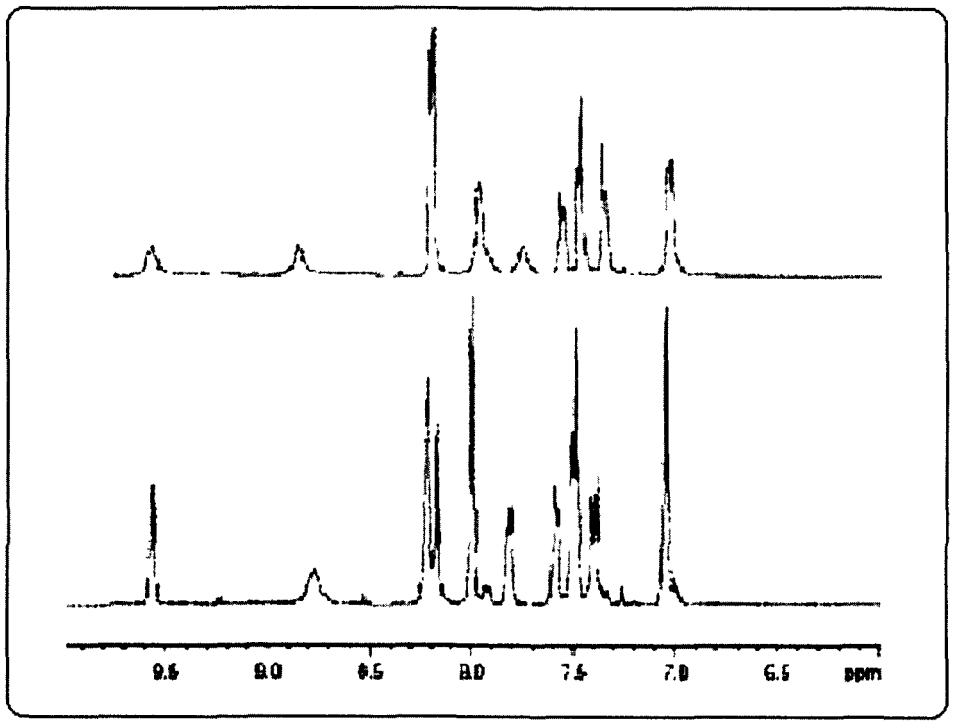

Fig. 5.7b. The Aromatic region of the ^{1}H NMR spectra of **27** in $CDCl_3$ at 303K (top) and 233K (bottom).

acceptable in view of the expected reinforcement of the covalent Sn–O bond upon formation of a stronger monodentate carboxylate coordination at low temperature.

The solid-state ^{117}Sn NMR data (Table 5.6) are in agreement with the crystal structures. The isotropic chemical shifts for all compounds, except **30**, range roughly from –250 to –290 ppm, typical for six-coordination, thus reflecting the mostly rather loose seven-coordination of the tin atom in the dimeric species, as revealed by the crystal structures. The more negative chemical shift of compound **30** (–368 ppm) can be traced back to the ca. 0.47 Å shorter distance between the tin atom and the C=O(3) carboxylate oxygen atom than in the other compounds, as discussed earlier (Tables 5.3 and 5.4). The stronger coordination with this oxygen atom results in a low frequency shift while the principal tensor components are also affected. Compound **30** has axial symmetry (η = 0.0), while all others are nearly axially symmetric (η = 0.30-0.45). A special situation is encountered for compound **31**, since two isotropic chemical shifts can be discerned, with a distinctively different set of principal tensor components. One set is comparable to that of **27-29**, while the other set is somewhat different with a slightly higher frequency and a δ22 of 0, whereas the other compounds have δ22 values between –43 and –90 ppm. These solid state NMR features can be correlated with the crystal structure of **31**, in which a different type of dimeric motif is observed, at least for the crystal analyzed. Unlike **27**, **28**, **29** and **30**, the $Sn_2C_2O_4$ core of **31**, as found from X-ray diffraction data, involves the carboxylate oxygen atoms instead of the quinolin-8-ol oxygen atom. The presence of two isotropic chemical shifts in the solid state tin NMR spectrum of **31** is in agreement with the observation by X-ray diffraction where two molecules are present in the asymmetric unit (see Table 5.4). However, as solid state NMR analyses the bulk sample, by contrast with single crystal analysis by X-ray diffraction, it could also be that compound **31** consists of constitutionally isomeric coordination motifs: the unique one found by X-ray diffraction, and another one in line with those of the other compounds, in particular **27** and **29**, in view of their more similar solid state ^{117}Sn NMR data to those of **31**.

Thus, the NMR data altogether indicate that the different types of coordination are involved in a kind of dissociation-association competition depending in a complex way on crystal packing, the electronic and/or steric nature of the substituted benzoate ligand $L^{10\text{-}14}$, and, in solution, also on the temperature and the concentration; globally, however, it appears that intermolecular coordination giving rise to dimeric structures in the crystalline state are not the dominant factor, and occur with very versatile but weak coordination modalities, since the

typical chemical shifts they give rise to in the crystalline state are not dominant in any of the complexes in solution.

5.4 Structural précis of the di-*n*-butyltin(IV) complexes of 5-[(*E*)-2-(4-methoxyphenyl)-1-diazenyl]quinolin-8-ol and benzoic acid derivatives

The structures of the di-*n*-butyltin(IV) complexes which are characterized by single crystal X-ray crystallography, e.g., $^{n}Bu_2SnCl(L^7)$ (**26**), $[^{n}Bu_2Sn(L^7)(L^{10})]_2.0.33(C_6H_{12})$ (**27**), $[^{n}Bu_2Sn(L^7)(L^{11})]_2$ (**28**), $[^{n}Bu_2Sn(L^7)(L^{12})]_2$ (**29**), $[^{n}Bu_2Sn(L^7)(L^{13})]_2$ (**30**) and $[^{n}Bu_2Sn(L^7)(L^{14})]_2$ (**31**) are summarized in Scheme 5.2.

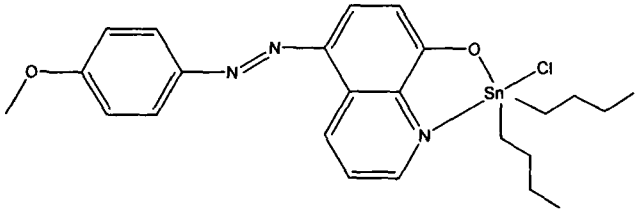

(**26**)

distorted *cis*-trigonal bipyramidal Sn coordination

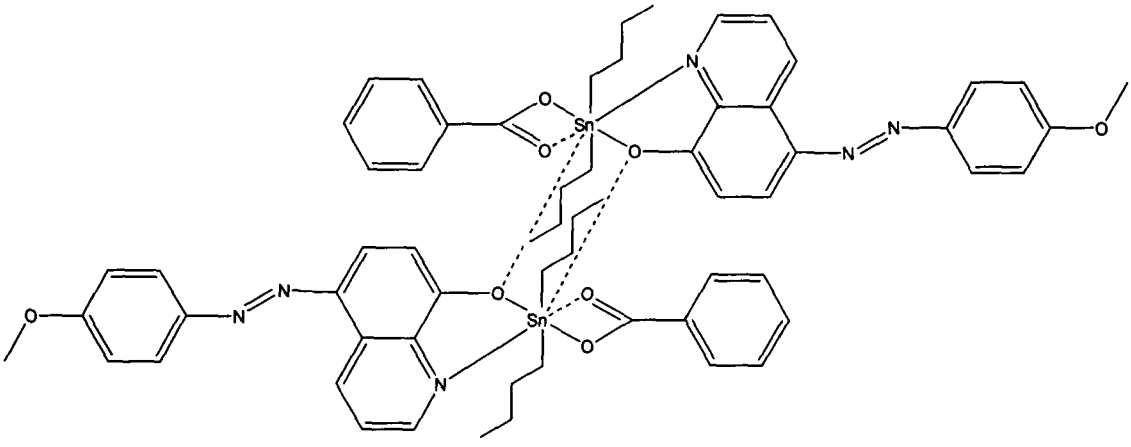

(**27**)

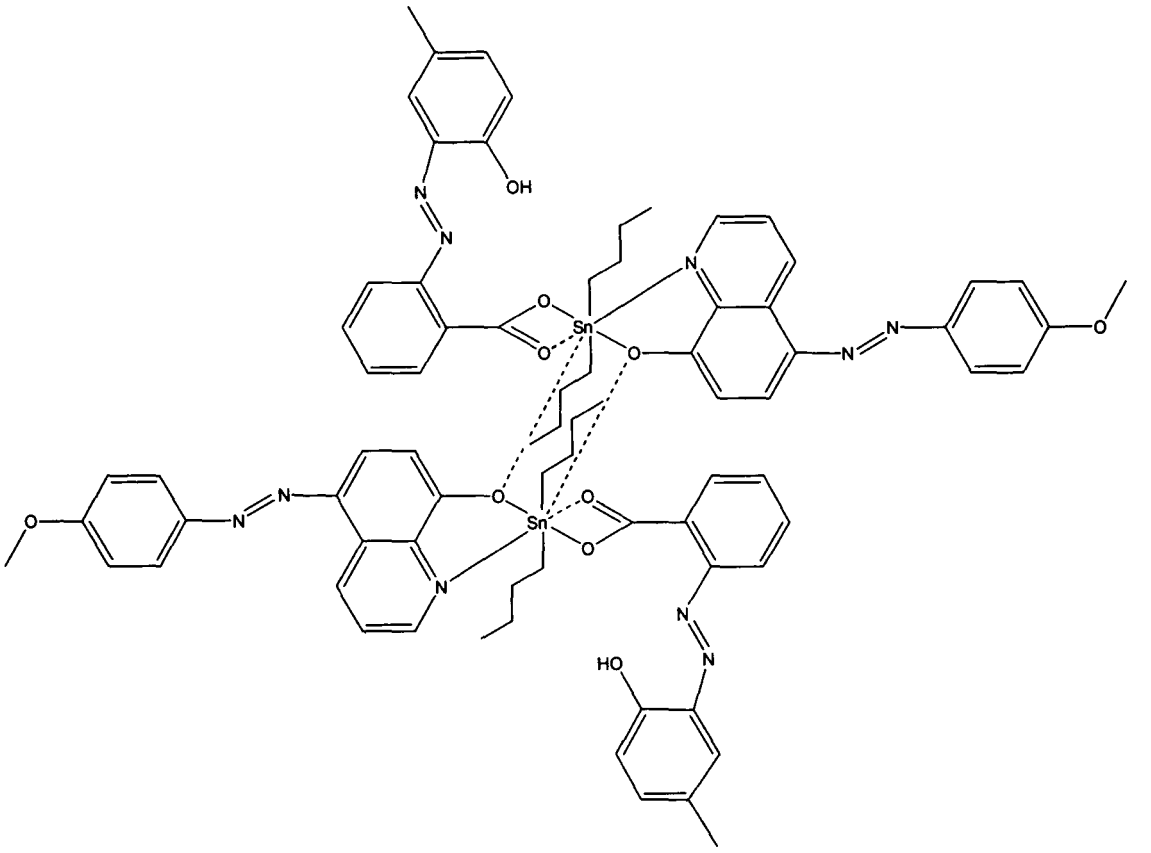

(28)

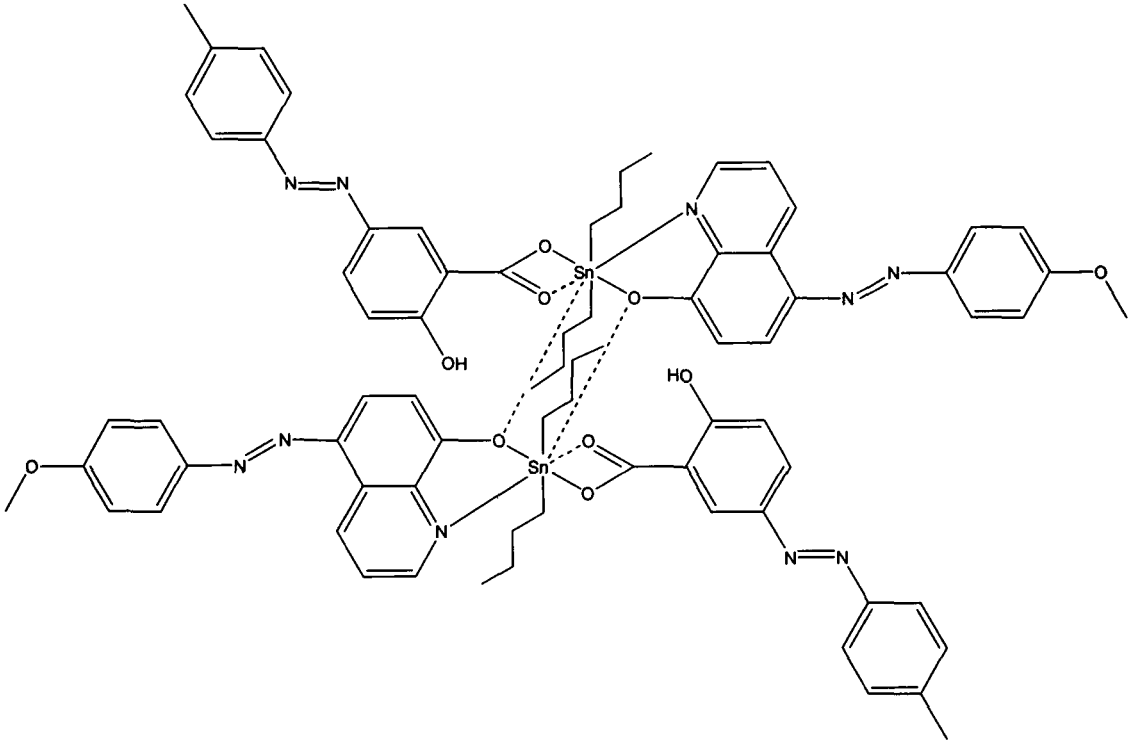

(29)

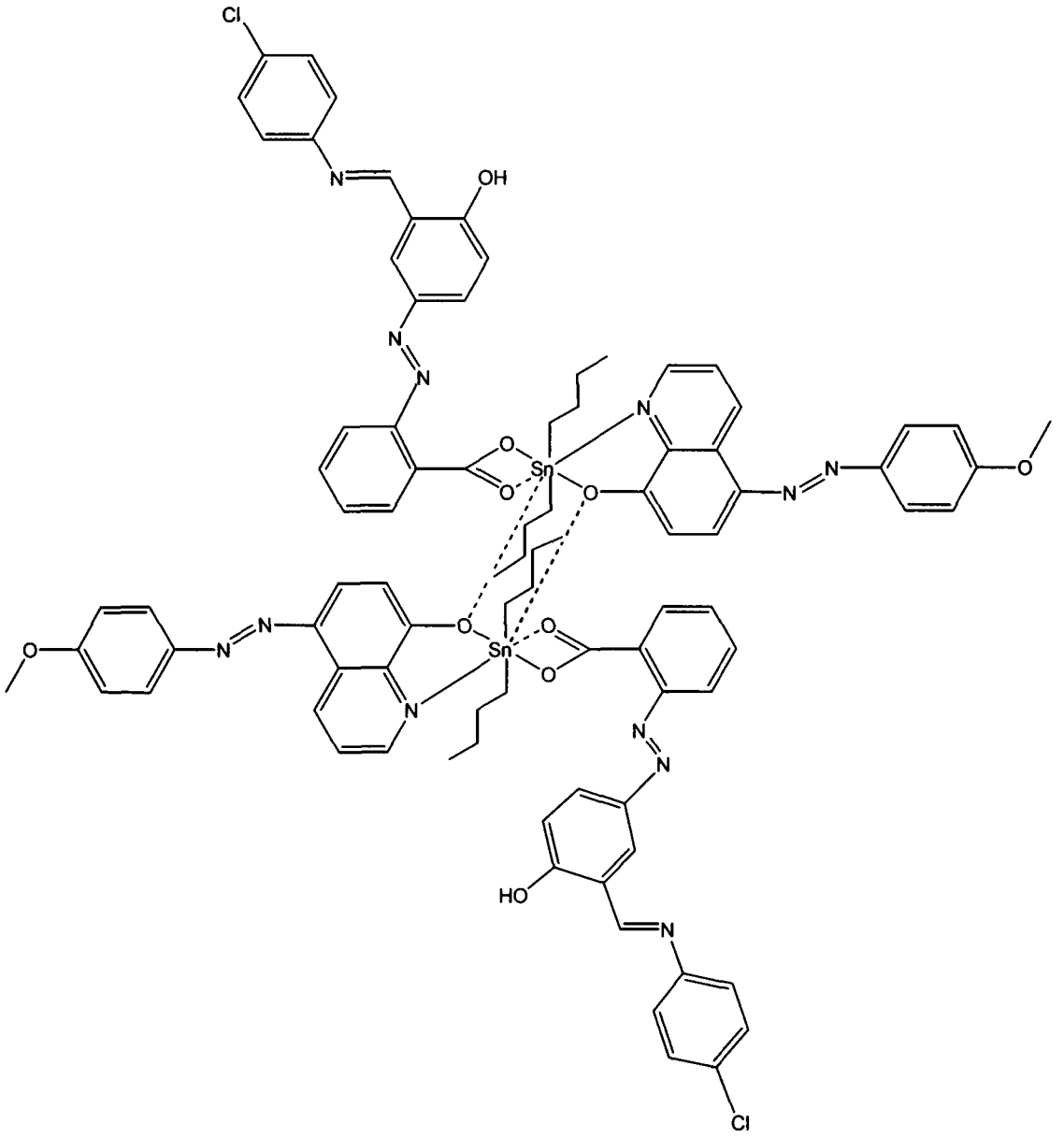

(30)

Centrosymmetric dinuclear Sn-complexes with a cyclic Sn_2O_2 core motif where the O-atoms of two quinolin-8-olate ligands bridge the two tin atoms (27-30) in a distorted pentagonal bipyramidal Sn coordination

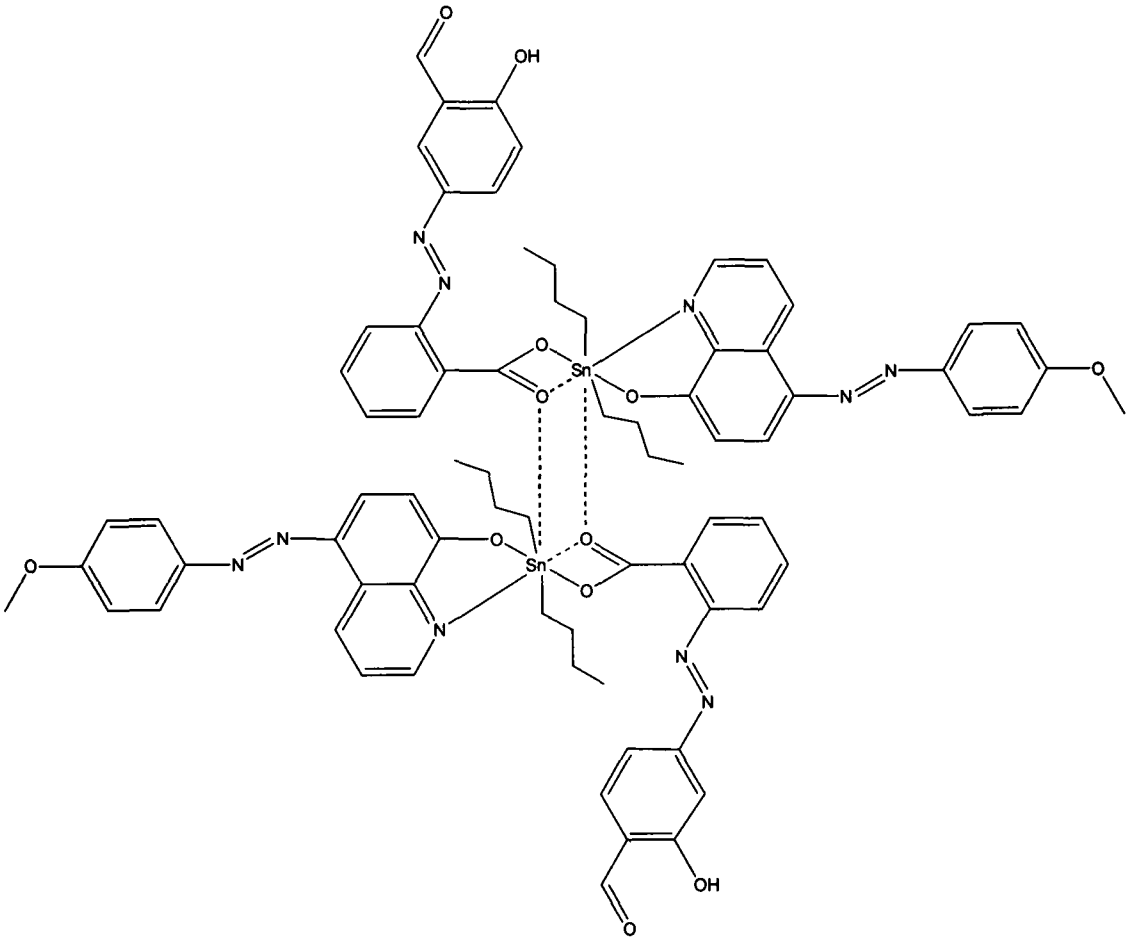

(31)

Centrosymmetric dinuclear Sn-complexes with a cyclic $Sn_2C_2O_4$ core motif where the carboxylate groups of two benzoate ligands bridge the two tin atoms (31) in a distorted pentagonal bipyramidal Sn coordination

Scheme 5.2. The chemdraw representations of the molecules (**26-31**) showing coordination geometries.

Complex $^{n}Bu_2SnCl(L^7)$ (**26**) is a mononuclear complex where the coordination geometry is distorted *cis*-trigonal bipyramidal. The bidentate quinolin-8-olate ligand coordinates such that the N- and O-atoms are in axial and equatorial positions, respectively. The other axial position is occupied by the Cl-atom and the *n*-butyl groups complete the equatorial plane.

On the other hand, the molecular structures of complexes **27-30** are centrosymmetric dinuclear Sn-complexes where a highly asymmetric μ-O bridges involving the quinolin-8-olate O-atom to give a cyclic Sn_2O_2 core. Each tin atom is coordinated by the bidentate quinolin-8-

olate ligand, the longer bridging interaction from the centrosymmetrically-related quinolin-8-olate O-atom, the two *n*-butyl groups and by the carboxylate O-atoms of the benzoate ligand. The coordination geometry about each tin atom is distorted pentagonal bipyramid where the *n*-butyl groups occupy the axial positions. In contrast to the μ-O bridges *via* the quinolin-8-olate O-atom observed in **27-30**, the molecule of **31** is comprised of carboxylate groups of two benzoate ligands which bridge the two tin atoms to give a cyclic $Sn_2C_2O_4$ core motif in a centrosymmetric dinuclear Sn-complex.

5.5. Experimental

5.5.1. Synthesis of ligands

The ligands *viz.*, 5-[(*E*)-2-(4-methoxyphenyl)-1-diazenyl]quinolin-8-ol (L^7H), 2-[(*E*)-2-(2-hydroxy-5-methylphenyl)-1-diazenyl]benzoic acid ($L^{11}H'$), 5-[(*E*)-2-(4-methylphenyl)-1-diazenyl]-2-hydroxybenzoic acid ($L^{12}H'$), 2-{(*E*)-4-hydroxy-3-[(*E*)-4-chlorophenyliminomethyl]phenyldiazenyl}benzoic acid ($L^{13}H'$) and 2-[(*E*)-2-(3-formyl-4-hydroxyphenyl)-1-diazenyl]benzoic acid ($L^{14}H'$) were prepared and characterized by methods described in earlier reports [8,17-19,29] used for synthesizing di-*n*-butyltin(IV) complexes are described in Chapter 2 (see Section 2.6). Note: H and H' refer to the replaceable protons in the ligands L^7 and L^{11-14}, respectively.

5.5.2. Synthesis of di-n-butyltin(IV) complexes

The synthesis of two di-*n*-butyltin(IV) complexes (a chlorobutyltin(IV) derivative $^nBu_2SnCl(L^1)$) and a mixed ligands complex $[^nBu_2Sn(L^7)(L^{10})]_2.0.33(C_6H_{12})$) are described below.

5.5.2.1. Preparation of $^nBu_2SnCl(L^7)$ (**26**) [5]

The chloro di-*n*-butyltin(IV) complex (**26**) was prepared by drop-wise addition of sodium methoxide (generated *in situ* from 0.04g, 1.75 mmol of Na in 15 ml anhydrous methanol) into a stirred hot anhydrous benzene solution (45 ml) of the ligand L^7H (0.5g, 1.79 mmol). Immediate precipitation of the sodium salt occurred and then the reaction mixture was stirred vigorously for an additional 15 min. To this reaction mixture, an anhydrous benzene solution (15 ml) of $^nBu_2SnCl_2$ (0.52 g, 1.71 mmol) was added drop-wise. The reaction mixture was refluxed for 3 h and filtered to remove the NaCl. The filtrate was collected and the solvent was removed under reduced pressure. The resultant mass was washed several times with ice cold hexane. The crude product was recrystallized from a mixture of benzene and hexane (v/v 1:2) which afforded

orange crystals of **26**. Yield: 0.48g (48.45%), mp: 72-74 °C. Anal. Found: C, 52.71; H, 5.45; N, 7.3%. Calc. for $C_{24}H_{30}N_3O_2ClSn$: C, 52.73; H, 5.53; N, 7.69%. M. W. = 547. Positive-ion ESI mass spectra: m/z 586 $[M+K]^+$; m/z 570 $[M+Na]^+$; m/z 548 $[M+H]^+$; m/z 512 $[M-Cl]^+$, 100%. MS/MS of586: m/z 512 $[M-Cl]^+$; m/z 548 $[M+H]^+$. MS/MS of 570: m/z 512 $[M-Cl]^+$. MS/MS of 548: m/z 512 $[M-Cl]^+$; m/z 490 $[M+H\text{-butane}]^+$; m/z 434 $[M+H\text{-butene-butane}]^+$. MS/MS of 512: m/z 454 $[M\text{-Cl-butane}]^+$; m/z 398 $[M\text{-Cl-butene-butane}]^+$. Negative-ion ESI mass spectra: m/z 278 $[L^4]^-$; m/z 263 $[L^4\text{-}CH_3]^-$, 100%. MS/MS of 278: m/z 263 $[L^4\text{-}CH_3]^-$; m/z 235 $[L^4\text{-}CH_3\text{-}N_2]^-$; m/z 209. MS/MS of 263: m/z 235 $[L^4\text{-}CH_3\text{-}N_2]^-$.

5.5.2.2. Preparation of $[^nBu_2Sn(L^7)(L^{10})]_2.0.33(C_6H_{12})$ (27) [16]

$L^{10}H'$ (0.13 g, 1.06 mmol) in hot anhydrous toluene (40 mL) was added to a hot anhydrous toluene solution (30 mL) of $^nBu_2SnCl(L^7)$ (**26**) (0.50 g, 1.08 mmol). The reaction mixture was refluxed for one hour; triethylamine (0.11 g, 1.08 mmol) was then added drop-wise and reflux was continued for additional 3 h. The reaction mixture was cooled to room temperature and filtered in order to remove $Et_3N.HCl$. The filtrate was evaporated and the residue dried *in vacuo*. The residue was extracted into a benzene and hexane mixture (v/v 1:1) and filtered to remove any suspended particles. The filtrate was concentrated and allowed to evaporate slowly at room temperature until the solid material precipitated. The solid was filtered, dried *in vacuo* and then recrystallized from a mixture of chloroform-cyclohexane (v/v 1:1), which upon slow evaporation afforded pure red crystals. Yield: 0.38g (55.8%), M.p. 102-103 °C. Anal. Calc. for $C_{64}H_{74}N_6O_8Sn_2$: C, 59.46; H, 5.77; N, 6.50. Found: C, 60.01; H, 5.80; N, 6.31%.

The other mixed ligand complexes ($^nBu_2Sn(L^7)(L^{11\text{-}14})$ (**28-31**) were prepared by reacting **26** with the appropriate conjugated acids of the ligands ($L^{11}H'$-$L^{14}H'$) using analogous procedures and their analytical data are presented below.

5.5.2.3. Preparation of $[^nBu_2Sn(L^7)(L^{11})]_2$ (28) [16]

Red plates of **28** were obtained from benzene-hexane (v/v 1:1). Yield: 0.56 g (68.3%), M.p. 103-104 °C. Anal. Calc. for $C_{76}H_{82}N_{10}O_{10}Sn_2$: C, 59.55; H, 5.39; N, 9.14. Found: C, 60.12; H, 5.50; N, 8.96%.

5.5.2.4. Preparation of $[^nBu_2Sn(L^7)(L^{12})]_2$ (**29**) [16]

Orange crystals of **29** were obtained from toluene-chloroform (v/v 1:1). Yield: 0.43 g (52.4%), M.p. 155-157 °C. Anal. Calc. for $C_{76}H_{82}N_{10}O_{10}Sn_2$: C, 59.55; H, 5.39; N, 9.14. Found: C, 60.01; H, 5.57; N, 8.96%.

5.5.2.5. Preparation of $[^nBu_2Sn(L^7)(L^{13})]_2$ (**30**) [16]

Orange crystals of **30** were obtained from ethanol-acetone (v/v 1:1). Yield: 0.39 g (40.6%), M.p. 161-162 °C. Anal. Calc. for $C_{88}H_{86}$ $Cl_2N_{12}O_{10}Sn_2$: C, 59.38; H, 4.87; N, 9.44. Found: C, 60.01; H, 4.57; N, 9.46%.

5.5.2.6. Preparation of $[^nBu_2Sn(L^7)(L^{14})]_2$ (**31**) [16]

Orange crystals of **31** were obtained from benzene-cyclohexane (v/v 1:2). Yield: 0.50 g (59.5%), M.p. 130-132 °C. Anal. Calc. for $C_{76}H_{78}N_{10}O_{12}Sn_2$: C, 58.48; H, 5.04; N, 8.97. Found: C, 58.50; H, 4.87; N, 8.76%.

5.5.3. Chemicals used for the preparations

$^nBu_2SnCl_2$ and oxine were of Merck products while benzoic acid was obtained from Aldrich and were used as such. The substituted anilines (reagent grade) were purified either by crystallization or distilled prior to use. The solvents used in the reactions were of AR grade and dried using standard procedures. Benzene was distilled from benzophenone ketyl.

5.5.4. Physical measurements

Carbon, hydrogen and nitrogen analyses were performed with a Perkin Elmer 2400 series II instrument. IR spectra in the range 4000-400 cm^{-1} were obtained on a Perkin Elmer Spectrum BX series FT-IR spectrophotometer with samples investigated as KBr discs. ^1H-, ^{13}C- and ^{117}Sn-NMR spectra of the organotin(IV) compounds were recorded on a Bruker Avance 250 spectrometer and measured at 250.53, 63.00 and 89.27 MHz, respectively. The ^1H, ^{13}C and ^{117}Sn chemical shifts were referenced to Me_4Si set at 0.00 ppm, $CDCl_3$ set at 77.0 ppm and Me_4Sn set at 0.00 ppm respectively. ^1H and ^{13}C NMR assignments have been achieved using standard 1D ^1H and ^{13}C NMR and gradient-assisted 2D ^1H-^{13}C heteronuclear multiple-quantum correlation (HMQC) and heteronuclear multiple-bond correlation (HMBC) spectroscopy, on the basis of the numbering scheme shown in Figs. 2.1 and 2.2 (refer to Chapter 2). CP-MAS ^{117}Sn NMR spectra were recorded on the same instrument, equipped with a 4 mm MAS broad-band probe. ^{117}Sn was chosen instead of the more common ^{119}Sn nucleus, because of RF

intereferences from a local radio station. Spinning frequencies are chosen between 7 and 9 kHz. A contact time of 1 ms and a recycling delay of 2 s were used. The chemical shift reference was set using (cyclo-$C_6H_{11})_4Sn$ (–97.35 ppm relative to $(CH_3)_4Sn$). The principal values of the ^{117}Sn chemical shielding tensors were determined by fitting the anisotropy pattern of the spinning side bands according to the Herzfeld-Berger formalism, using the 'dmfit' program (Massiot D. *dmfit program*; available at http://crmht-europe.cnrs-orleans.fr). The Mössbauer spectra were recorded with a conventional spectrometer operating in the transmission mode. The source was $Ca^{119}SnO_3$ (Ritverc GmbH, St. Petersburg, Russia; 10 mCi), moving at room temperature with constant acceleration in a triangular waveform. The driving system was obtained from Halder (Seehausen, Germany), and the NaI (Tl) detector from Harshaw (De Meern, The Netherlands). The multi-channel analyser and the related electronics were purchased from Takes (Bergamo, Italy). The solid absorber samples, containing *ca.* 0.5 mg cm^{-2} of ^{119}Sn, were held at 77.3 K in a MNC 200 liquid-nitrogen cryostat (AERE, Harwell, UK). The velocity was calibrated using a ^{57}Co Mössbauer source (Ritverc GmbH, St. Petersburg, Russia, 10 mCi), and an iron foil as absorber. The isomer shifts are relative to room temperature $Ca^{119}SnO_3$. C-Sn-C angles determined from the Mössbauer spectra were calculated with p.q.s. [alkyl] = -1.30 mm s^{-1} [25].

5.5.5. X-ray crystallography

Crystals of compounds suitable for X-ray crystal-structure determination were obtained from benzene/hexane ($^nBu_2SnCl(L^7)$ **26** and $[^nBu_2Sn(L^7)(L^{11})]_2$ **28**), chloroform/cyclohexane ($[^nBu_2Sn(L^7)(L^{10})]_2.0.33(C_6H_{12})$ **27**), toluene/chloroform ($[^nBu_2Sn(L^7)(L^{12})]_2$ **29**), ethanol/acetone ($[^nBu_2Sn(L^7)(L^{13})]_2$ **30**) and benzene/cyclohexane ($[^nBu_2Sn(L^7)(L^{14})]_2$ **31**) solutions of the respective compounds. All measurements were made at 160 K on a Nonius Kappa-CCD diffractometer [30] with graphite-monochromated MoKα radiation (λ = 0.71073 Å) and an Oxford Cryosystems Cryostream 700 cooler. Data reduction was performed with HKL Denzo and Scalepack [31]. The intensities were corrected for *Lorentz* and polarization effects, and an empirical absorption correction based on the multi-scan method [32] was applied. A summary of crystal data, data collection and structure refinement parameters are given in Table 5.1. The structures were solved by direct methods using SIR92 [33] or SHELXS97 [34] and refined against F^2 for all reflections using the SHELXL97 [35] software.

The Sn-complexes **27-31** are centrosymmetric dinuclear molecules with one half of the molecule in the asymmetric unit. In **31**, the asymmetric unit contains one half of each of two centrosymmetric molecules. The atomic coordinates of the two molecules were tested carefully

for a relationship from a higher symmetry space group using the program *PLATON* [36], but none was found.

The structure of **27** also contains cyclohexane molecules which are located about threefold inversion centres, giving a solvent:complex ratio of 1:3. The terminal methoxyphenyl group of the azo ligand in **27** is disordered, while one of the *n*-butyl groups is disordered in one of the independent molecules of **29** and in **31**. The disorder was modelled in each case by defining two positions for each disordered atom, refining an overall site occupation factor for each conformation and applying similarity restraints to the chemically equivalent bond lengths and angles involving all disordered atoms, while neighbouring atoms within and between each conformation of the disordered group were restrained to have similar atomic displacement parameters. The non-hydrogen atoms were refined anisotropically. The hydroxy H-atoms were placed in the positions indicated by a difference electron density map and their positions were allowed to refine together with individual isotropic displacement parameters. All other H-atoms were placed in geometrically calculated positions and refined using a riding model where each H-atom was assigned a fixed isotropic displacement parameter with a value equal to $1.2U_{eq}$ of its parent atom ($1.5U_{eq}$ for the methyl groups).

References

[1] E.O. Schlemper, Inorg. Chem. **6** (1967) 2012.

[2] W. Chen, W.K. Ng, V.G. Kumar Das, G.B. Jameson, R.J. Butcher, Acta Crystallogr. Sect. C **45** (1989) 861.

[3] E. Kellö, V. Vrábel, J. Holeček, J. Sivy, J. Organomet. Chem. **493** (1995) 13.

[4] A. Szorcsik, L. Nagy, M. Scopelliti, A. Deák, L. Pellerito, K. Hegetschweiler, J. Organomet. Chem. **690** (2005) 2243.

[5] T.S. Basu Baul, A. Mizar, A.K. Chandra, X. Song, G. Eng, R. Jirásko, M. Holčapek, D. de Vos, A. Linden, J. Inorg. Biochem. **102** (2008) 1719.

[6] A. Linden, T.S. Basu Baul, A. Mizar, Acta Crystallogr. Sect. E **61** (2005) m27.

[7] T.S. Basu Baul, A. Mizar, A. Lyčka, E. Rivarola, R. Jirásko, M. Holčapek, D. de Vos, U. Englert, J. Organomet. Chem. **691** (2006) 3416.

[8] T.S. Basu Baul, A. Mizar, X. Song, G. Eng, R. Willem, M. Biesemans, I. Verbruggen, R. Butcher, J. Organomet. Chem. **691** (2006) 2605.

[9] S.W. Ng, C. Wei, V.G. Kumar Das, J.P. Charland, F.E. Smith, J. Organomet. Chem. **364** (1989) 343.

[10] T.S. Basu Baul, E.R.T. Tiekink, J. Chem. Crystallogr. **26** (1996) 393.

[11] S.W. Ng, J. Organomet. Chem. **585** (1999) 12.

[12] T.S. Basu Baul, W. Rynjah, E. Rivarola, C. Pettinari, A. Linden, J. Organomet. Chem. **690** (2005) 1413.

[13] H.L. Xu, H.D. Yin, Z.J. Gao, G. Li, J. Organomet. Chem. **691** (2006) 3331.

[14] T.S. Basu Baul, A. Mizar, E. Rivarola, U. Englert, J. Organomet. Chem. **693** (2008) 1751.

[15] L. Pauling, The Nature of Chemical Bond, 3rd Ed., Cornell University Press, New York, 1960.

[16] T.S. Basu Baul, A. Mizar, A. Paul, G. Ruisi, R. Willem, M. Biesemans, A. Linden, J. Organomet. Chem. In press. doi:10.1016/j.jorganchem.2009.02.021

[17] T.S. Basu Baul, S.M. Pyke, K.K. Sarma, E.R.T. Tiekink, Main Group Met. Chem. **19** (1996) 807.

[18] T.S. Basu Baul, S. Dhar, S.M. Pyke, E.R.T. Tiekink, E. Rivarola, R. Butcher, F.E. Smith, J. Organomet. Chem. **633** (2001) 7.

[19] T.S. Basu Baul, K.S. Singh, X. Song, A. Zapata, G. Eng, A. Lycka, A. Linden, J. Organomet. Chem. **689** (2004) 4702.

[20] S. Dashuang, H. Shengzhi, Chin. J. Struct. Chem. **6** (1987) 193.

[21] F.H. Allen, Acta Crystallogr. Sect. B **58** (2002) 380.

[22] P.F.R. Ewings, P.G. Harrison, T.J. Morris, J. Chem. Soc., Dalton trans. (1976) 1602.

[23] R.C. Poller, J.N.R. Ruddick, J. Chem. Soc. (A) (1969) 2273.

[24] R.V. Parish, in: G.J. Long (Eds.), Mössbauer Spectroscopy Applied to Inorganic Chemistry Plenum Press, New York, 1984, Chapter 16, pp. 527-575.

[25] T.K. Sham, G.M. Bancroft, Inorg. Chem. **14** (1975) 2281.

[26] C. Di Nicola, A. Galindo, J.V. Hanna, F. Marchetti, C. Pettinari, R. Pettinari, E. Rivarola, B.W. Skelton, A.H. White, Inorg. Chem. **44** (2005) 3094.

[27] J. Otera, J. Organomet. Chem. **221** (1981) 57.

[28] F. Huber, R. Kaiser, J. Organomet. Chem. **6** (1966) 126.

[29] R. Willem, I. Verbruggen, M. Gielen, M. Biesemans, B. Mahieu, T.S. Basu Baul, E.R.T. Tiekink, Organometallics **17** (1998) 5758.

[30] R. Hooft, KappaCCD Collect Software, Nonius BV, Delft, The Netherlands, 1999.

[31] Z. Otwinowski, W. Minor, in: C.W. Carter Jr., R.M. Sweet (Eds.), Methods in Enzymology, Macromolecular Crystallography, Part A, vol. 276, Academic Press, New York, 1997, pp. 307-326.

[32] R.H. Blessing, Acta Crystallogr. Sect A **51** (1995) 33.

[33] A. Altomare, G. Cascarano, C. Giacovazzo, A. Guagliardi, M.C. Burla, G. Polidori, M. Camalli, SIR92, J. Appl. Crystallogr. **27** (1994) 435.

[34] G.M. Sheldrick, SHELXS-97, Program for the Solution of Crystal Structures, University of Göttingen, Göttingen, Germany, 1997.

[35] G.M. Sheldrick, SHELXL-97, Program for the Refinement of Crystal Structures, University of Göttingen, Göttingen, Germany, 1997.

[36] A.L. Spek, PLATON, Program for the Analysis of Molecular Geometry, University of Utrecht, The Netherlands, 2007.

Chapter 6

Evaluation of *in vitro* Cytotoxic Activity of Di-*n*-butyltin(IV) 5-[(*E*)-2-(aryl)-1-diazenyl]quinolin-8-olates against Human Tumour Cell Lines

CONTENTS

CHAPTER 6

EVALUATION OF *IN VITRO* CYTOTOXIC ACTIVITY OF DI-n-BUTYLTIN(IV) 5-[(*E*)-2-(ARYL)-1-DIAZENYL]QUINOLIN- 8-OLATES AGAINST HUMAN TUMOUR CELL LINES

6.1. Introduction 146-147

6.2. Synthesis and characterization of di-*n*-butyltin(IV) complexes 147

6.3. Quantum chemical calculations and Biological applications 147-151

6.4. Experimental 152-153

References 154-155

List of Publications

6.1. Introduction

Organotin(IV) complexes of 5-[(*E*)-2-(aryl)-1-diazenyl]quinolin-8-ols (see Fig. 6.1 for ligand skeleton) have been studied in great detail due to their various structural motifs as well as for their important role in understanding Sn(IV) coordination chemistry in solution as well as in the solid state (refer to Chapters 3-5) [1-5].

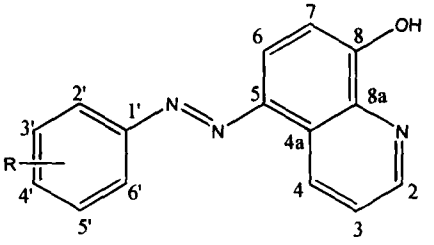

[Abbreviations: L^1H: X = H; L^2H: 2'-CH_3; L^3H: 3'-CH_3; L^4H: 4'-CH_3; L^5H: 4'-Br; L^6H: 4'-Cl; L^7H: 4'-OCH_3; L^8H: 4'-OCH_2CH_3 (see Chapter 2 for details)]

Fig. 6.1 Structure of the ligand, $L^{1\text{-}8}HH'$

In addition, organotin(IV) compounds are currently one of the most studied organometallic systems in terms of industrial and agricultural applications, which involve such widely divergent fields as stabilizers for poly(vinylchloride), industrial catalysts and agricultural agents [6-8]. Further, tri-n-butyltin(IV) compounds display a large array of biocidal properties and are used in wood preservatives and in marine anti-fouling paints [9]. Due to their wide range of biocidal activities, triorganotin(IV) compounds have also been screened as possible larvicides against various species of mosquitoes [10,11]. For example, tri-n-butyltin(IV) complexes were screened against the fourth larval instar stage of the *Aedes aegypti* mosquito and were found to be more effective than the triphenyltin(IV) derivatives [12]. Consequently, a series of tri-n-butyltin(IV) 5-[(*E*)-2-(aryl)-1-diazenyl]-2-hydroxybenzoates have been investigated and have shown moderate [13] activities.

Furthermore, an area of current interest involves the screening of organotin(IV) compounds for potential antitumour activity and focuses upon results obtained in the past decade or so, as well as upon other therapeutic applications of tin(IV) compounds [14]. In this context, a few organotin(IV) complexes of azo-ligands of the types $^nBu_2Sn(LH)_2$ and $\{[^nBu_2Sn(LH)_2O]_2\}$

(where LH is 5-[(*E*)-2-(aryl)-1-diazenyl]-2-hydroxybenzoate) were investigated for their cytotoxic potential and $\{[^nBu_2Sn(LH)_2O]_2\}$ type complexes have shown promising antitumour activity *in vitro* [15].

In view of the overall effectiveness of the organotin(IV) compounds and in search of better candidates for the cytotoxic potential, the present Chapter reports the *in vitro* cytotoxicity of a series of di-*n*-butyltin(IV) complexes, *viz.*, $^nBu_2Sn(L^4)_2$ (**9**), $^nBu_2Sn(L^5)_2.0.5C_6H_6$ (**10**), $^nBu_2Sn(L^6)_2$ (**11**), $^nBu_2Sn(L^7)_2$ (**12**), $^nBu_2Sn(L^8)_2$ (**13**), $^nBu_2SnCl(L^7)$ (**26**) against seven well characterized human tumour cell lines and the results were compared with one diphenyltin(IV) analogue $Ph_2Sn(L^1)_2.C_3H_6O$ (**14**). The basicity of the two quinolinolato donor N and O atoms of the ligands are discussed in relation to the cytotoxicity data.

Note: The compound numbers used in this Chapter refer to the compound numbers used in Chapters. Refer to Chapter 2 for ligand substitutions.

6.2. Synthesis and characterization of di-*n*-butyltin(IV) complexes

The 5-[(*E*)-2-(aryl)-1-diazenyl]quinolin-8-ols (Fig. 6.1) [1,2] used for synthesizing the di-*n*-butyltin(IV)- and diphenyltin(IV) complexes are described in Chapter 2. The synthetic details for di-*n*-butyltin(IV) complexes, *viz.*, $^nBu_2Sn(L^4)_2$ (**9**) [4], $^nBu_2Sn(L^5)_2.0.5C_6H_6$ (**10**) [4], $^nBu_2Sn(L^6)_2$ (**11**) [4], $^nBu_2Sn(L^7)_2$ (**12**) [4], $^nBu_2Sn(L^8)_2$ (**13**) [4], $^nBu_2SnCl(L^7)$ (**26**) [5] and diphenyltin(IV) analogue $Ph_2Sn(L^1)_2.C_3H_6O$ (**14**) [2] are described in Chapters 4 and 5.

6.3. Quantum chemical calculations and Biological applications

6.3.1. Proton affinity for the N(1) atom of L-H and O(1)$^-$ atom of LO$^-$ anion

The optimized structures for the ligands (L^1H and L^2H- L^8H) are shown in Fig. 2.7 while the geometrical parameters for L^1H, L^2H–L^8H are listed in Table 2.5 (Chapter 2). The calculated proton affinity for the N(1) atom of L–H and the O(1)$^-$ atom of the LO$^-$ anion are listed in Table 6.1.

Table 6.1: The proton affinity (PA in kcal/mol) values of ligands (L^1H, L^4H–L^8H) for the N(1) atom of L–H and O(1)$^-$ atom of LO^- anion

Ligands (Substituents)	**L^1H (H)**	**L^4H (4-Me)**	**L^5H (4-Br)**	**L^6H (4-Cl)**	**L^7H (4-OMe)**	**L^8H (4-OEt)**
PA(N(1))	237.1	238.5	235.5	235.5	240.6	241.0
PA (O(1)–)	342.2	343.3	344.9	345.0	338.6	338.5

Most of the geometric parameters (Table 2.5; Chapter 2) are found to be insensitive to the nature of the substitutents but the substitutents can have a strong effect on the basicity of donor atoms. Since the basic structures of the di-*n*-butyltin(IV) complexes (**9-13**) are similar for the differently substituted ligands, it can be expected that the ligand properties will have direct influences on the stability of the corresponding di-*n*-butyltin(IV) complexes, as well as on their cytotoxic activity (see Section 6.3.2). As the O(1) and N(1) atoms of the ligands act as donor atoms to bind with the Sn-atom, we further investigated how the basicity of these two atoms changes with the change in substituents. The proton affinity values (Table 6.1) for both the N(1) and O(1) atoms increase for the electron donor substituents (such as Me (in L^4H), OMe (in L^7H), and OEt (in L^8H)), while it decreases for the electron withdrawing substituents when compared with the unsubstituted ligand (L^1H). A good correlation is observed between the proton affinities for the N(1) atom of the ligands and the O(1) atom of the corresponding anions and Hammett's parameters (σ_P) [16] for different remote substituents. A correlation between PA(N(1)) and σ_P are shown in Fig. 6.2. Ligands with the -NH_2, -CN and -CF_3 substituents are also included in the correlation to increase the breadth of this comparison.

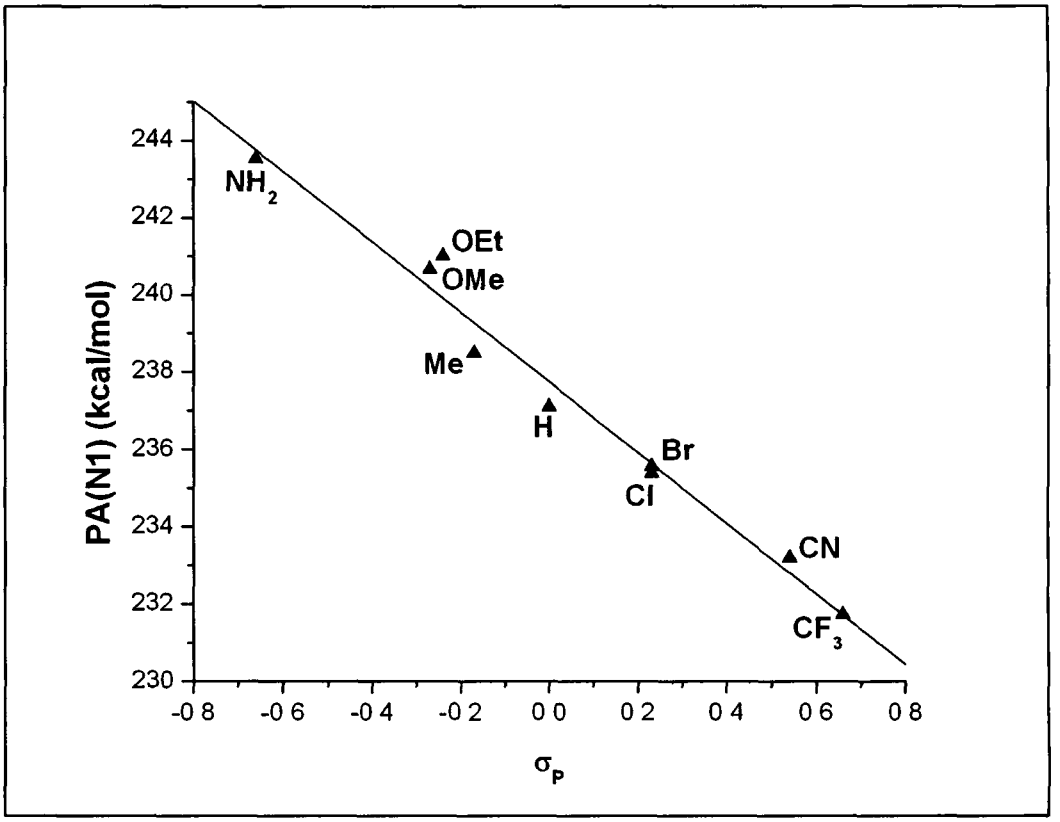

Fig. 6.2. A plot of proton affinity (PA) of the N(1) atom of the ligands (para-substituents) against Hammett's substituent constants (σ_P).

6.3.2. In vitro cytotoxicity of the organotin(IV) complexes against human tumour cell lines

The results of the *in vitro* cytotoxicity test in human tumour cell lines on $^{n}Bu_2Sn(L^4)_2$ (**9**), $^{n}Bu_2Sn(L^5)_2.0.5C_6H_6$ (**10**), $^{n}Bu_2Sn(L^6)_2$ (**11**), $^{n}Bu_2Sn(L^7)_2$ (**12**), $^{n}Bu_2Sn(L^8)_2$ (**13**), $^{n}Bu_2SnCl(L^7)$ (**26**) along with a diphenyltin(IV) complex $Ph_2Sn(L^1)_2.C_3H_6O$ (**14**) are given as ID_{50} values in Table 6.2, and compared with the data for some compounds that are in current clinical use as antitumour agents.

Table 6.2: The ID_{50} values (ng/ml) of test compounds (**9-14, 26**) *in vitro* (using as cell viability test) in seven human tumour cell lines

Test compound[a]	Cell lines						
	A498	**EVSA-T**	**H226**	**IGROV**	**M19**	**MCF-7**	**WIDR**
$^{n}Bu_2Sn(L^4)_2$ (**9**)	90	38	113	65	59	48	233
$^{n}Bu_2Sn(L^5)_2.0.5C_6H_6$ (**10**)	136	46	224	111	65	95	451
$^{n}Bu_2Sn(L^6)_2$ (**11**)	589	167	864	351	268	374	2064
$^{n}Bu_2Sn(L^7)_2$ (**12**)	248	85	407	395	72	143	1190
$^{n}Bu_2Sn(L^8)_2$ (**13**)	112	32	147	44	64	51	330
$^{n}Bu_2SnCl(L^7)$ (**26**)	1605	527	1721	440	374	968	3680
$Ph_2Sn(L^1)_2.C_3H_6O$ (**14**)	16902	8677	8950	4774	10104	7332	8441
DOX	90	8	199	60	16	10	11
CPT	2253	422	3269	169	558	699	967
5-FU	143	475	340	297	442	750	225
MTX	37	5	2287	7	23	18	<3.2
ETO	1314	317	3934	580	505	2594	150
TAX	<3.2	<3.2	<3.2	<3.2	<3.2	<3.2	<3.2

[a]Abbreviation for the reference drugs: DOX = doxorubicin, CPT = cisplatin, 5-FU = 5-fluorouracil, MTX = methotrexate, ETO = etoposide and TAX = paclitaxel.

The table clearly shows that di-*n*-butyltin(IV) complexes (**9-13**) are overall, but not for every cell line, more active than cisplatin. The compounds **9**, **10** and **13** display the highest activity, even higher than several of the standard cytotoxic agents. All di-*n*-butyltin(IV) compounds show a dramatic increase in *in vitro* cytotoxicity compared with the related diphenyltin(IV) compound, $Ph_2Sn(L^1)_2.C_3H_6O$ (**14**). However, the exact reasons for increased activity could not be inferred from the present data. A reverse trend i.e. an increase in activity from *n*-butyl to phenyl substitutents has also been found (see ref. 14, also for more information on structure-activity relationship).

Further, di-*n*-butyltin(IV) compounds (**9-13**) allow calculations on the structure activity relationship with respect to the substituents at the *para-* position of the diazo forming moiety of the ligand ($L^{4-8}H$). The ID_{50} values given in Table 6.2 show that the activity of the $^{n}Bu_2Sn(L^{4-8})_2$ compounds (**9-13**) decrease in the order **9** < **12** < **13** (Me, OMe and OEt substituents in L^4H, L^7H and L^8H, respectively), whereas the ID_{50} value for **11** (Cl-substituted compound) for all cell lines

is higher than that of **9**, the ID_{50} value for **10** (Br-substituted compound) is found to be less than that of **9** for EVSA-T, IGROV and MCF-7 cell lines and slightly higher for other cell lines.

In general, the activity seems to depend upon the basicity of the donor atoms of the ligand employed [17]. The compounds become less active as the basicity increases and this correlation is depicted in Fig. 6.3.

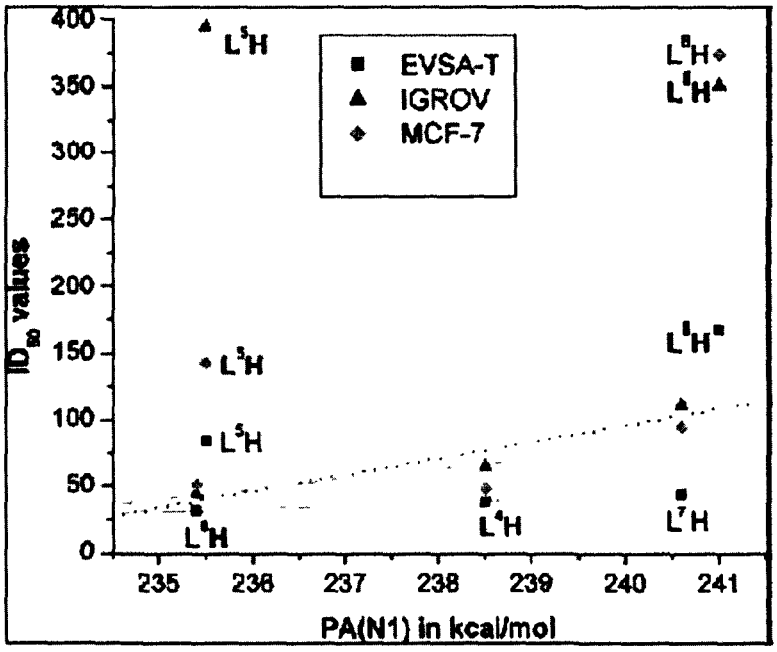

Fig. 6.3. The correlation between ID_{50} values and the proton affinity (PA) of the N(1) atom of the ligands.

Compounds **10** and **13** with -Br and -OEt substituents (L^5H and L^8H) deviate from the correlation possibly due the solubility problem in DMSO (see Section 6.4.2 for details). It can be anticipated from this trend that the incorporation of electron withdrawing substituent (such as CF_3) at the ligand moiety of di-*n*-butyltin(IV) compound will possibly enhance the cytotoxic activity. Thus, the test results of the di-*n*-butyltin(IV) compounds (**9-13**) led to important structure activity information. This encouraging cytotoxic effect may be predictive of *in vivo* antitumour activity. Compounds **9**, **10** and **13** may be suitable candidates for modification in order to improve cytotoxic and dissolution properties and related work in this area is in progress.

6.4 Experimental

6.4.1. Proton affinity for the N(1) atom of L-H and O(1)$^-$ atom of LO$^-$ anion (Quantum chemical calculations)

The basicity of the N(1) atom of the ligand and the O(1) atom of the corresponding anion generated after removal of the H-atom of the O(1)H group is estimated from the proton affinity of the N(1) atom [PA (N(1))] and the O(1) atom [PA (O(1))]. The PA for a base (B) is defined as the negative of the enthalpy (H) change for the reaction:

$B + H^+ \rightarrow BH^+$

Therefore, at any finite temperature (T) the PA can be estimated from the expression:

$PA = H(B) + H(H^+) - H(BH^+)$

At 0 K, $H(H^+)$ can be taken as zero and H(B) = E(B), where E(B) is the energy of base B at 0 K. In the present calculations, the PA values at 0 K were estimated simply from the total energies calculated at the B3LYP/6-311G(d,p)//6-31G(d) level: PA(N(1)) = E(L-H) – $E(L\text{-}H\text{-}NH^+)$ and PA(O(1)) = $E(L\text{-}O^-)$ – E(L-H). In the present study, the main aim is to calculate relative PA values for the ligands and for this purpose, the B3LYP method [18,19] was used which is known to produce reliable PA values. Gaussian-03 program was used for all the electronic structure calculations [20].

6.4.2. Biological tests

The *in vitro* cytotoxicity test of di-n-butyltin(IV) compounds, *viz.*, $^nBu_2Sn(L^4)_2$ (**9**), $^nBu_2Sn(L^5)_2.0.5C_6H_6$ (**10**), $^nBu_2Sn(L^6)_2$ (**11**), $^nBu_2Sn(L^7)_2$ (**12**), $^nBu_2Sn(L^8)_2$ (**13**), $^nBu_2SnCl(L^7)$ (**26**) and a diphenyltin(IV) compound $Ph_2Sn(L^1)_2.C_3H_6O$ (**14**) were performed using the SRB test for the estimation of cell viability. The cell lines WIDR (colon cancer), M19 MEL (melanoma), A498 (renal cancer), IGROV (ovarian cancer) and H226 (non-small cell lung cancer) are currently used in the anticancer screening panel at the National Cancer Institute of the National Institutes of Health, USA [21]. The MCF7 (breast cancer) cell line is estrogen receptor (ER)+/ progesterone receptor (PgR)+ and the cell line EVSA-T (breast cancer) is (ER)-/(Pgr)-. Prior to the experiments, a mycoplasma test was carried out on all cell lines and found to be negative. All cell lines were maintained in a continuous logarithmic culture in RPMI 1640 medium with Hepes and phenol red. The medium was supplemented with 10% FCS, penicillin 100 μg/ml and streptomycin 100 μg/ml. The cells were mildly trypsinized for passage and for use in the experiments. RPMI and FCS were obtained from Life technologies (Paisley, Scotland). SRB,

DMSO, Penicillin and streptomycin were obtained from Sigma (St. Louis MO, USA), TCA and acetic acid from Baker BV (Deventer, NL) and PBS from NPBI BV (Emmer-Compascuum, NL).

The test compounds **9-14** and **26** and reference compounds were dissolved to a concentration of 250000 ng/ml in full medium, by 20 fold dilution of a stock solution which contained 1 mg of compounds / 200 µl. Compounds **9**, **10** and **12** were dissolved in DMSO (dimethylsulfoxide) while compounds **11**, **13** and **26** did not dissolve completely in DMSO, and the suspension of the test compound in DMSO was used to make the appropriate dilutions in medium. Cytotoxicity was estimated by the microculture sulforhodamine B (SRB) test [22].

6.4.2.1. Experimental protocol and cytotoxicity tests

The experiment was started on day 0. On day 0, 10000 cells per well were seeded into 96-wells flatbottom microtiter plates (falcon 3072, DB). The plates were incubated overnight at 37 °C, 5 % CO_2 to allow the cells to adhere to the bottom. On day 1, a three-fold dilution sequence of ten steps was made in full medium, starting with the 250 000 ng/ml stock solution. Every dilution was used in quadruplicate by adding 200 µl to a column of four wells. This procedure results in the highest concentration of 625000 ng/ml being present in column 12. Column 2 was used for the blank. After incubation for 3 days, the plates were washed with PBS twice. Fluorescein diacetate (FDA) stock solution was diluted to 2 µg/ml with PBS and 200 µl of this solution was added to each of the control, experimental and blank wells. The plates were incubated for 30 min at 37 °C and the fluorescence generated from each well was measured at an excitation wavelength of 485 nm and an emission wavelength of 535 nm using an automated microplate reader (Labsystems Multiskan MS). The data were used for the construction of concentration-response curves and the determination of the ID_{50} value by use of the Deltasoft 3 software. ID_{50} value represents the inhibitory dose in ng/ml measured from the fluorescence indicating a cell kill of 50%.

The variability of the *in vitro* cytotoxicity test depends on the cell lines used and the serum applied. With the same batch of cell lines and the same batch of serum the interexperimental CV (coefficient of variation) is 1-11% depending on the cell line and the intraexperimental CV is 2-4%. These values may be higher with other batches of cell lines and/or serum.

References

[1] T.S. Basu Baul, A. Mizar, X. Song, G. Eng, R. Jirásko, M. Holčapek, R. Willem, M. Biesemans, I. Verbruggen, R. Butcher, J. Organomet. Chem., **691** (2006) 2605.

[2] T.S. Basu Baul, A. Mizar, A. Lyčka, E. Rivarola, R. Jirásko, M. Holčapek, D. de Vos, U. Englert, J. Organomet. Chem. **691**(2006) 3416.

[3] T.S. Basu Baul, A. Mizar, E. Rivarola, U. Englert, J. Organomet. Chem. **693** (2008) 1751

[4] T.S. Basu Baul, A. Mizar, A.K. Chandra, X. Song, G. Eng, R. Jirásko, M. Holčapek, D. de Vos , A. Linden, J. Inorg. Biochem. **102** (2008) 1719.

[5] T.S. Basu Baul, A. Mizar, A. Paul, G. Ruisi, R. Willem, M. Biesemans, A. Linden, J. Organomet. Chem. In press. doi:10.1016/j.jorganchem.2009.02.021

[6] R.C.Poller, The Chemistry of Organotin Compounds, Logos Press, London, UK, 1970.

[7] A.G.Davis, P.J.Smith, in: Comprehensive Organometallic Chemistry, Vol. 2, Wilkinson G, F.G.A.Stone, E.W. Abel (Eds.), Pergamon Press, New York, 1982, pp 519-627.

[8] C.J.Evans, in: The Chemistry of Tin, P.J. Smith (Eds.), Blackie Academic & Professional, London, 1998, pp 442-474.

[9] S.J. De Mora, in: Tributyltin Case Study of an Environmental Contaminant, S.J. De Mora (Eds.), Cambridge University Press, London, 1996, pp 1-20.

[10] G. François, M.V. Looveren, G. Timperman, B. Chimanuka, L.A. Assi, J. Holenz, G. Bringmann, J. Ethnopharmacol. **54** (1996) 125.

[11] V.G. Kumar Das, L.Y. Kuan, K.I. Sudderuddin, C.K. Chang, Y. Thomas, C.K. Yap, M.K. Lo, Y.Hoi-sen, Toxicology **32** (1984) 57.

[12] T.T. Nguyen, N. Ogwuru, G. Eng, Appl. Organomet. Chem. **14** (2000) 345.

[13] T.S. Basu Baul, S. Dhar, E. Rivarola, F.E. Smith, R. Butcher, X. Song, M. McCain, G. Eng, Appl.Organomet.Chem. **17** (2003) 261.

[14] M. Gielen, E.R.T. Tiekink, in: M. Gielen, E.R.T. Tiekink (Eds.), Metallotherapeutic Drug and Metal-Based Diagnostic Agents: ^{50}Sn Tin Compounds and Their Therapeutic Potential, Wiley, 2005, pp. 421-439.

[15] T.S. Basu Baul, W. Rynjah, E. Rivarola, A. Lyčka, M. Holčapek, R. Jirásko, D. de Vos, R. J. Butcher, A. Linden, J. Organomet. Chem. **691** (2006) 4850.

[16] C. Hansch, A. Leo, R.W. Taft, Chem. Rev. **91** (1991) 165.

[17] H. Li, C.S. Lai, J. Wu, P.C. Ho, D. De Vos, E.R.T. Tiekink, J. Inorg. Biochem. **101** (2007) 809.

[18] A.K. Chandra, D. Michalska, R. Wysokinsky, T. Zeegers-Huyskens, J. Phys. Chem. Section A **108** (2004) 9593.

[19] A.K. Chandra, T. Zeegers-Huyskens, J. Org. Chem. **68** (2003) 3618.

[20] Gaussian 03, Revision D.01, M.J. Frisch et al., Gaussian, Inc., Wallingford CT, 2004.

[21] M.R. Boyd, Principles and Practice Oncol. **3** (1989) 1.

[22] M.N. Shuaibu, H. Kanbara, T. Yanagi, A. Ichinose, D.A. Ameh, J.J. Bonire, A.J. Nok, Jpn. Parasitolog. Res. **91** (2003) 5.

List of Publications

(1) Dibenzyltin(IV) complexes of the 5-[(E)-2-(aryl)-1-diazenyl]quinolin-8-olates: Synthesis and an investigation of structures by X-ray diffraction, solution and solid-state tin NMR, ^{119}Sn Mössbauer and electrospray ionization MS, T.S. Basu Baul, **A. Mizar**, X. Song, G. Eng, R. Willem, M. Biesemans, I. Verbruggen, R. Butcher, **J. Organomet. Chem.** 691(2006) 2605-2613.

(2) Diphenyltin(IV) complexes of the 5-[(E)-2-(aryl)-1-diazenyl]quinolin-8-olates: Synthesis and multinuclear NMR, ^{119}Sn Mössbauer, electrospray ionization MS, X-ray characterization and assessment of in vitro cytotoxicity, T.S. Basu Baul, **A. Mizar**, A. Lyčka, E. Rivarola, R. Jirásko, M.Holčapek, D. de Vos, U. Englert, **J. Organomet. Chem**.691 (2006) 3416-3425.

(3) Methyl-2-{[(E)-8-oxo-5,8-dihydroquinolin-5-ylidene]hydrazino}benzoate, T.S. Basu Baul, **A. Mizar**, E. R. T. Tiekink, **Acta Crystallogr**. E 63 (2007) o4256

(4) cis-Bis(8-hydroxyquinolinato-k2N, O)diphenyltin(IV), A. Linden, T.S. Basu Baul, **A. Mizar**, **Acta Crystallogr. Sect. E 61** (2005) m27-m29.

(5) Re-visiting of 5-[(E)-2-(aryl)-1-diazenyl]quinolin-8-ol with tweaking of Sn-Ph groups, Synthesis, Spectroscopic Characterization and X-ray crystallography, T.S. Basu Baul, **A. Mizar**, E. Rivarola, U. Englert, **J. Organomet. Chem.** 693 (2008) 1751-1758.

(6) Syntheis, crystal structure, cytoxicity and qualitative Structure -activity relationship (QSAR) of Cis-bis{5-(E)-2-(aryl)-1-diazenyl]quinolinolato} di-n-butyltin(IV)complexes, T.S. Basu Baul, **A. Mizar**, A. K. Chandra, X. Song, G. Eng, R. Jirásko, M. Holčapek, D. de Vos , A. Linden, **J. Inorg. Biochem.** 102 (2008) 1719-1730.

(7) ^{119}Sn Mossbauer characterization of self assembled Organotin(IV) complexes with Sciff bases containing amino acetate skeleton, S. Basu, **A. Mizar**, T.S. Basu Baul, E. Rivarola, **Hyperfine Interaction,** 185 (2008) 95-102.

(8) Crystal and solution structures of di-n-butyltin(IV) complexes of 5-[(E)-2-(4-methoxyphenyl)-1-diazenyl]quinolin-8-ol and benzoic acid derivatives: En route to elegant self-assembly via modulation of the tin coordination geometry, T. S. Basu Baul, **A. Mizar**, A. Paul, G. Ruisi, R. Willem, M. Biesemans, and A. Linden, **J. Organomet. Chem.**, doi.10.1016/j.jorganchem.2009.02.021.

BIODATA

Name: Archana Mizar

Date of Birth: Dec 20.

Marital Status: Unmarried

Nationality: Indian

Sex: Female

2002 : M. Sc. in Chemistry, 72% (First Class, 2nd Rank in the University), North-Eastern Hill University, Shillong, India

2000: B. Sc. (Chemistry), 72% (First Class, 3rd Rank in the University), St Mary's College, Shillong, India

2007-2008: Awarded Financial Assistantship in non-EU category by the University of Camerino, Italy for pursuing research for one year in Indo-Italian Exchange programme under the supervision of Prof. Claudio Pettinari, University of Camerino, Italy.